Fakultät für Medizin

HOX genes in pathogenesis of Ewing sarcoma

Miriam Verena Manuela Ertl

Vollständiger Abdruck der von der Fakultät für Medizin der Technischen Universität München zur Erlangung des akademischen Grades eines

Doktors der Medizin

genehmigten Dissertation.

Vorsitzender:		Prof. Dr. Ernst J. Rummeny
Prüfer der Dissertation:	1.	Prof. Dr. Stephanie Elisabeth Combs
	2.	Prof. Dr. Stefan Burdach

Die Dissertation wurde am 25.09.2017 bei der Technischen Universität München eingereicht und durch die Fakultät für Medizin am 02.05.2018 angenommen.

meiner Mutter

Table of contents

List of abbreviations

Abd-A	Abdominal A; component of Bithorax complex
Abd-B	Abdominal B; component of Bithorax complex
ACTB	β-actin
AGC1	Aggrecan 1
ALL	Acute lymphoid leukemia
ALP	Alkalic phosphatase
ALPL	Alkalic phosphatase
AMH	Anti-Muellerian hormone
AML	Acute myeloid leukemia
Antp	Antennapedia; component of Antennapedia complex
Arg	Arginine
Asn	Asparagine
ATRX	α thalassamia/mental retardation syndrome x-linked; also known as XNP
B3GAT1	β-1,3-glucuronyltransferase 1; also known as CD57, LEU7 and HNK1
BAMBI	BMP and activin membrane bound inhibitor
BCP	1-bromo-3-chloropropane
BGLAP	Bone γ-carboxyglutamate protein; also known as osteocalcin
BHA	Butylated hydroxyanisole
BMI1	BMI1 proto-oncogene, polycomb ring finger protein; also known as PCGF4; component of PRC1
BMP	Bone morphogenetic protein
BMP2	Bone morphogenetic protein 2
BMP4	Bone morphogenetic protein 4
BMP7	Bone morphogenetic protein 7
BMPs	Bone morphogenetic proteins
bp	Base pair
BSA	Bovine serum albumine
BSP	Bone sialoprotein
CBFα1	Core binding factor α1; also known as RUNX2
CBX	Component of PRC1
CCD	Cleidocranial dysplasia
CD49	Certain cell surface glycoprotein; lymphoid marker
CD57	β-1,3-glucuronyltransferase 1; also known as B3GAT1, LEU7 and HNK1

CD99	Certain cell surface glycoprotein; also known as MIC2
cDNA	Complementary DNA
CHM1	Chondromodulin 1
CNS	Central nervous system
COL10A1	Collagen type X alpha 1
COL1A1	Collagen type I alpha 1
COL2A1	Collagen type II alpha 1
CpG site	Certain DNA region where cytosine and guanine are separated by only one phosphate
CT	Computed tomography
CTEV	Congenital talipes equinovarus
DEPC	Diethylpyrocarbonate
Dfd	Deformed; component of Antennapedia complex
DKK2	Dickkopf 2
DMSO	Dimethyl sulfoxide
DNA	Deoxyribonucleic acid
dNTPs	Deoxynucleotides; nucleoside triphosphates
DPBS	Dulbecco's phosphate-buffered saline
ds	Double strand
ECM	Extracellular matrix
EDTA	Ethylenediaminetetraacetic acid
EED	Embryonic ectoderm development
EEF1D	Eukaryotic translation elongation factor 1 delta
EFT	Ewing family of tumors
EGF	Epidermal growth factor
EHS	Engelbreth-Holm-Swarm; name of a mouse tumor with abundant extracellular matrix
ENT	Ear, nose and throat
ERG	ETS-related gene; full name: v-ets avian erythroblastosis virus E26 oncogene homolog
ERK	Extracellular signal-regulated kinase
ES	Ewing sarcoma
ETS	E26 family of transcription factors
ETS	E26 transformation-specific gene; encodes transcription factor
ETV1	ETS variant 1
ETV4	ETS variant 4, also called E1AF

EWS	Ewing sarcoma gene
EWS-FLI1	Fusion protein which characterizes Ewing sarcomas
EWSR1	Ewing sarcoma breakpoint region 1
EWSR2	Ewing sarcoma breakpoint region 2
EZH1	Enhancer of zeste homolog 1; polycomb repressive complex 2 subunit
EZH2	Enhancer of zeste homolog 2; polycomb repressive complex 2 subunit
FAM™	6-carboxyfluorescein
FDG-PET	fluorine-18 fluorodeoxyglucose positron emission tomography
FEV	Gene in fifth Ewing sarcoma variant
FGF	Fibroblast growth factor
FISH	Fluorescence in situ hybridization
FLI1	Friend leukemia virus integration site 1
GDF	Growth differentiation factor
gDNA	Genomic DNA
GPR64	G protein-coupled receptor 64
GTP	Guanosine triphosphate
HAUS6	HAUS augmin-like complex, subunit 6
HCl	Hydrogen chloride
HNK1	β-1,3-glucuronyltransferase 1; also known as B3GAT1, LEU7 and CD57
HOTAIR	Acronym of a certain RNA called **HO**X **A**ntisense **I**ntergenic **R**NA
HOX genes	Homeotic genes
HOXA13	Homeobox A13
HOXD10	Homeobox D10
HOXD11	Homeobox D11
HOXD13	Homeobox D13
HPH	Component of PRC1
IBSP	Integrin binding sialoprotein; also known as BSP
IGF	Insulin-like growth factor
IGFBP3	Insulin-like growth factor binding protein 3
IHH	Indian hedgehog
I-SMAD	Inhibitory SMAD
JNK	c-Jun NH_2-terminal kinase
kb	Kilobase
Lab	Labial; component of Antennapedia complex
LEU7	β-1,3-glucuronyltransferase 1; also known as B3GAT1, HNK1 and CD57

MAP2K	MAPK kinase
MAP3K	MAPK kinase kinase
MAPK	Mitogen-activated protein kinase
MDS	Myelodysplastic syndrome
MEIS	Family of proteins; group of homeobox genes
MGB	Minor groove binder; name of a certain quencher
MIC2	Certain cell surface glycoprotein which is also known as CD99
min	Minutes
miR	MicroRNA
miR-10b	MicroRNA 10b
miR-224	MicroRNA 224
miR-23a	MicroRNA 23a
miR-7	MicroRNA 7
miRNA	MicroRNA
MMP	Matrix metalloproteinase
MMP13	Matrix metallopeptidase 13
MRI	Magnetic resonance imaging
mRNA	Messenger RNA
MSC	Mesenchymal stem cell
n.d.	Not detectable
n.s.	Not significant
NHL	Non-Hodgkin lymphoma
NMR	Nuclear magnetic resonance
NSE	Neuron-specific enolase
NTC	Non-template control
ON	Osteonectin
OP1	Also known as BMP7
OSX	Also known as SP7
PAK1	p21-activated kinase 1
Pb	Proboscipedia; component of Antennapedia complex
PBS	Phosphate-buffered saline
PBX	PBX homeobox protein
PcG	Polycomb-group
PCGF	Certain polycomb group protein; component of PRC1
PCGF4	Also known as BMI1; polycomb ring finger protein; component of PRC1

pPNET	Peripheral primitive neuroectodermal tumor
PRC	Polycomb repressor complex
PRC1	Polycomb repressor complex 1
PRC2	Polycomb repressor complex 2
PTHR1	Parathyroid hormone-related peptide receptor
PTHrP	Parathyroid hormone-related peptide
qRT-PCR	Quantitative Real-Time PCR
RAC1	RAS-related C3 botulinum substrate 1
RAC2	RAS-related C3 botulinum substrate 2
RAC3	RAS-related C3 botulinum substrate 3
RANKL	Receptor activator of nuclear factor kappa B ligand
RING1	ring finger protein 1; component of PRC1
RNA	Ribonucleic acid
rpm	Revolutions per minute
R-SMAD	Receptor-regulated SMAD
RTCA	Real-Time Cell Analyzer
RT-PCR	reverse transcription-polymerase chain reaction
RUNX2	Runt-related transcription factor 2, also known as CBFα1
s	Seconds
S100	S100 protein
Scr	Sex combs reduced; component of Antennapedia complex
SEM	Standard error of the mean
Ser	Serine
shRNA	small hairpin RNA
siRNA	short interfering RNA
SMAD	Family of proteins
SMAD4	SMAD family member 4
SMURF	SMAD ubiquitin regulatory factor
SMURF1	SMAD specific E3 ubiquitin protein ligase 1
SOX5	SRY (sex determining region Y)-box 5
SOX6	SRY (sex determining region Y)-box 6
SOX9	SRY (sex determining region Y)-box 9
SP7	Also known as OSX (osterix)
SPD	Synpolydactyly
SPDH	Synpolydactyly homolog

SPP1	Secreted phosphoprotein 1; also known as osteopontin
STEAP1	Six transmembrane epithelial antigen of the prostate 1
SUZ12	Suppressor of zeste 12; polycomb repressive complex 2 subunit
SWI2/SNF2	Switch 2, sucrose non-fermenting 2. Family of chromatin remodelers
TALE	Three amino-acid-loop extension proteins; family of proteins
TAMRA	Tetramethylrhodamine
TGFβ	Transforming growth factor β
tPA	Tissue plasminogen activator
Ubx	Ultrabithorax; component of Bithorax complex
VACTERL	Certain disorder which is characterized by **v**ertebral defects, **a**nal atresia, **c**ardiac defects, **t**racheo-**e**sophageal fistula, **r**enal anomalies and **l**imb abnormalities
WNT	Family of genes; certain signaling pathway
XNP	X-linked nuclear protein gene; also known as ATRX

1 Introduction

1.1 HOX genes

1.1.1 Definition, classification and structure of HOX genes

HOX genes form a subgroup of the family of homeobox genes. Members of this gene family share a common DNA sequence of 180 bp called “homeobox”. The homeobox was first discovered in the Drosophila melanogaster genome; since then it was detected in all multicellular organisms that were analyzed, such as plants, fungi, sponges, but also vertebrates including humans. (Gehring *et al.* 1994; McGinnis *et al.* 1984) Sequences of analysed homeoboxes were very similar to the drosophila homeobox; changes of particular nucleotides still resulted in identical amino acids. Thus, it was soon established that the homeobox encodes a certain 60-amino-acid long polypeptide segment which was designated as the “homeodomain”. (Duboule 1994; Gehring *et al.* 1994)

HOX genes are “small” genes with a genomic length of 5-10 kb compared to the mean size for protein-coding genes of 27 kb. The mean number of exons per gene amounts 10.4. HOX genes, however, consist of only two exons separated by one intron. The exon near to the 3’ end contains the 180 bp homeobox encoding the homeodomain of the HOX protein. (Alberts *et al.* 2014, p. 184; Grier *et al.* 2005; Kappen *et al.* 1989)

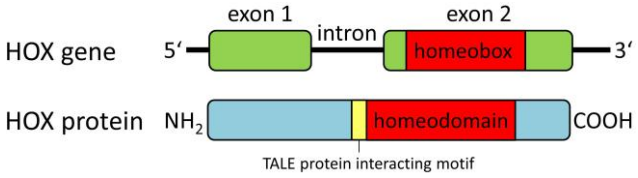

Figure 1: Structure of HOX genes and proteins.
HOX genes consist of two exons separated from each other by one intron. Exon near 3’end contains homeobox which encodes homeodomain of HOX proteins. Adjacent to the homeodomain, there is a binding site for cofactors. Modified from Grier *et al.* (2005). Reproduced by permission of John Wiley & Sons.

Homeodomains of many different organisms were analyzed and compared with each other to elucidate its function. Sequence conformities between the homeodomain and gene regulatory proteins were detected and suggested a similar function for all homeodomain proteins. Suspicion was raised that the homeodomain contained a helix-turn-helix DNA-binding motif, a common structural motif in transcription

regulators, and that HOX genes encoded transcription factors with the homeodomain acting as the DNA-binding domain. (Alberts *et al.* 2014, p. 376; Duboule 1994; Shepherd *et al.* 1984) The homeodomain was demonstrated to bind to DNA *in vitro* and soon the three-dimensional structure of the homeodomain was revealed by NMR spectroscopy. The assumption that homeobox proteins acted as transcription factors with the homeodomain as the DNA-binding motif was later functionally confirmed. (Muller *et al.* 1988) In most HOX proteins, a certain sequence of six amino acids can be found near by the homeodomain. This domain was discovered to function as binding site for cofactors. Cofactors mainly involve TALE proteins such as PBX and MEIS. Some HOX proteins were documented to lack this hexapeptide. (Erselius *et al.* 1990; Grier *et al.* 2005)

Common structures of a HOX gene and its gene product, the HOX protein, are illustrated in Figure 1. Figure 2 in turn shows three-dimensional structure of homeodomain containing three α-helices and a more flexible fourth helix. Two α-helices form a helix-turn-helix motif. The third α-helix corresponds to the DNA-recognition site. The N-terminal arm is elongated by a fourth helix which stabilizes contact to DNA. (Duboule 1994; Otting *et al.* 1988).

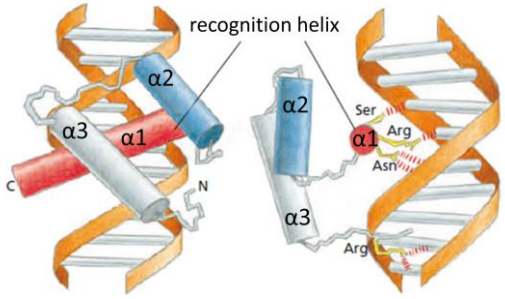

Figure 2: Binding of homeodomain to DNA. Same structure is shown from two different angles. Homeodomain is folded into three α-helices which are held together by hydrophobic interactions. Structure is similar to a helix-turn-helix-motif. α1 is the recognition helix and forms contacts with major groove of DNA. α3 is elongated by a flexible arm which binds nucleotide pairs in the minor groove of DNA. Serine (Ser), arginine (Arg), asparagine (Asn). Modified from (Alberts *et al.* 2014, p. 376). © 2015 from Molecular Biology of the Cell. by Alberts *et al.* Reproduced by permission of Garland Science/Taylor & Francis Group LLC.

Analysis of amino acid sequences and three-dimensional structures of homeodomains of different organisms revealed high evolutionary conservation of the homeobox and its gene product, the homeodomain. This conservation suggested an important function in organism. Three-dimensional structure of the homeodomain seems to have been more highly conserved than its amino acid sequence. Despite 25% identity in amino acid sequences only, three-dimensional structures of two homeodomains are more or less the same. (Alberts *et al.* 2014, p. 120)

HOX genes were originally called “homeotic selector genes” due to the discovery of specific mutations observed in Drosophila. These “homeotic mutations” cause bizarre deformities of the adult fly where one body structure has been replaced by another which is normally located elsewhere. The term “homeosis” (Greek “homoios” meaning similar) was coined by the English geneticist William Bateson who had already described two biological variations in 1894. He reported on the antennapedia mutant in which legs grew at the top of the head instead of antennae; the bithorax mutant, on the other hand, was characterized by an additional pair of wings instead of the smaller appendages called halteres. Later on, the bithorax mutant turned out to be part of a cluster of genes called the bithorax complex, consisting of the three homeobox genes Ubx, Abd-A and Abd-B. The antennapedia complex, on the other hand, was shown to consist of the five homeobox genes Lab, Pb, Dfd, Scr and Antp. (Alberts *et al.* 2014, p. 235; Grier *et al.* 2005; McGinnis 1994) HOX genes in vertebrates correspond to the bithorax and antennapedia cluster in Drosophila. HOX genes were discovered to control patterning along the anterior-posterior axis during embryonic development of all animals. They ensure development of correct structures appropriate to respective body part. Thus, HOX genes are regarded as master regulators of development. (Lewis 1978; McGinnis & Krumlauf 1992)

In humans, there are 39 HOX genes arranged in four HOX clusters A-D which are located on four different chromosomes. Each cluster is about 100 kb in length and consists of 9 to 11 genes. (Alberts *et al.* 2014, p. 235; Scott 1992; Zeltser *et al.* 1996) HOXA is located at 7p15, HOXB at 17q21, HOXC at 12q13 and HOXD at 2q31. (Apiou *et al.* 1996) Within each cluster HOX genes are subdivided into 13 paralogous groups according to their similarity in the homeobox region and position within the cluster. The most 5’ group of each cluster was designated as number 13 and the most 3’ group as number 1. According to this, paralogs, i.e. genes sharing the same number but from different clusters, are more related to each other than HOX genes within one cluster. (Duboule 1994; Lewis 1978; Maconochie *et al.* 1996)

As mentioned in the beginning, homeobox genes are defined by sharing a common DNA sequence which encodes the homeodomain. In mammals, there are more than 200 different homeobox-containing genes. According to the sequence of their homeodomains but also according to other criteria such as similarity in other protein

domains and organization in clusters, they can be subdivided into many different classes and even more subgroups. For reasons of simplification, homeobox genes can be classified into HOX genes and non-HOX genes. Only those genes which are located within the HOX cluster, i.e. the 13 paralogs of cluster A-D respectively, are HOX genes. Non-HOX genes lie outside the HOX clusters and represent the larger proportion of homeobox genes. (Duboule 1994; Gehring *et al.* 1994; Holland 2013)

HOX clusters in mammals and insects are assumed to have evolved from an ancestral HOX complex by divergence and duplication. The ancestral HOX complex is also thought to have arisen from one single HOX gene by repeated duplication. Cluster duplication in mammals is suggested to have taken place after the 13 paralogous HOX genes had been formed. During or after the duplication events, several genes got lost. (Alberts *et al.* 2014, p. 1170; Duboule 1994; Krumlauf 1992; Lewis 1978) The hypothesis of development from an ancestral homeobox cluster was solidified when

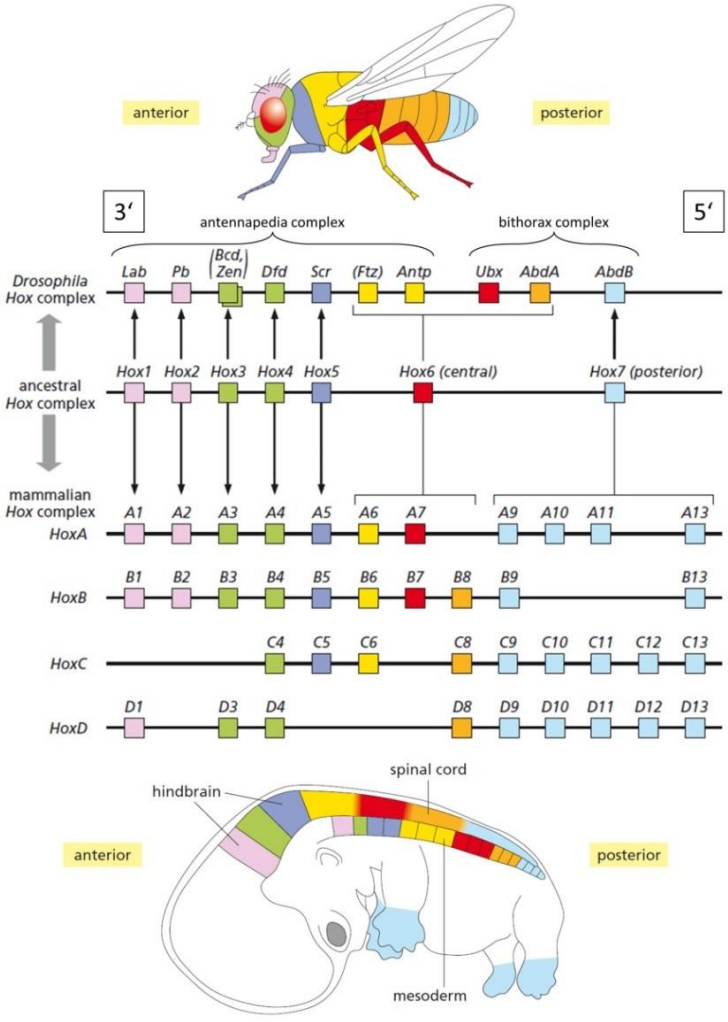

Figure 3: HOX complexes of an insect and a mammal in relation to body parts. Genes of HOX complexes are shown in chromosomal order (3'-5'). Genes and respective expression domains in the body are indicated in same colors. HOX complexes of insects and mammals are considered to have evolved from an ancestral HOX complex by duplication and divergence. The ancestral HOX complex is thought to have developed from one single HOX gene by repeated duplication. (Alberts *et al.* 2014, p. 1170).
Illustration was modified from Alberts *et al.* (2014, p. 1170) and is based on a diagram courtesy of William McGinnis. Reproduced by personal permission of William McGinnis.

sequences of mammalian homeoboxes were compared with their drosophila counterparts and a high degree of homology was determined. Nucleotide sequences of mammalian homeoboxes of the 3' end were similar to those of the 3' end of the drosophila; the same applied to homeoboxes of the 5' end, respectively. (Duboule 1994) Mammalian paralogs 9-13 were identified to be closely related to the drosophila bithorax complex; human paralogs with lower numbers rather corresponded to the drosophila antennapedia complex. The position of HOX genes within their clusters or rather their position on the chromosome from 3'-5' was revealed to correspond to their expression along the anterior-posterior axis in the animal. 3' HOX genes are expressed in the anterior parts of the body such as the head and upper thorax whereas 5' HOX genes are expressed in more caudal and distal body structures. This is known as "spatial collinearity". Furthermore, HOX clusters are expressed temporally from 3' to 5' in development. This results in 3' HOX genes, i.e. low-number HOX genes, being expressed earlier than higher-number HOX genes. This phenomenon is called "temporal collinearity". Moreover, a "posterior prevalence" was observed: being simultaneously expressed in the same domain, 5' HOX genes are functionally dominant over 3' genes. (Duboule 1994; Duboule & Morata 1994; Izpisua-Belmonte *et al.* 1991; Krumlauf 1994; McGinnis & Krumlauf 1992).

Figure 3 illustrates HOX clusters of drosophila and mammals and their assumed origin from an ancestral HOX complex. Homologs are indicated by same colors, just as respective gene expression domains in the body.

As already mentioned, HOX proteins function as transcription factors with the homeodomain binding to the DNA. (Duboule 1994; Shepherd *et al.* 1984) They are thought to control axial patterning in development by activation and repression of specific sets of target genes. Biochemical analyses, however, revealed that isolated HOX proteins bind to DNA with very low affinity and specificity because respective DNA domains are all rich in adenine-thymine base pairs. HOX proteins were subsequently identified to exert specificity by interaction with cofactors in complexes. (Ladam & Sagerstrom 2014; Levine & Hoey 1988; Lewis 1978; McGinnis & Krumlauf 1992) More and more, HOX-interacting proteins are being discovered. These cofactors involve members of signaling pathways and various other proteins. TALE proteins, chromatin-modifying enzymes, RNA polymerases and SMAD proteins which mediate

BMP signaling (see 1.3) are just a few examples. (Foronda *et al.* 2009; Ladam & Sagerstrom 2014; Williams *et al.* 2005) Downstream HOX targets are just as diverse. They don't only include transcription factors and members of signaling pathways such as BMPs but also genes which directly regulate cellular processes. That way, HOX genes intervene in cell proliferation, differentiation, apoptosis, cell adhesion and migration. (Foronda *et al.* 2009; Pearson *et al.* 2005; Suzuki *et al.* 2003)

1.1.2 Regulation and function of HOX genes

HOX genes are master regulators of embryonic development which are responsible for patterning along the anterior-posterior axis. (Lewis 1978; McGinnis & Krumlauf 1992) Due to this critical function, pattern and timing of HOX expression have to be strictly controlled. Spatially and temporally collinear expression is especially provided by organization of HOX genes in clusters; expression of each gene depends on its relative position within the cluster. HOX genes are assumed to be mostly regulated at the transcriptional level. Their extraordinary genomic organization, among other things, enables them to share chromatin structure and common regulatory elements. Non-coding sequences within the clusters and flanking genomic regions turned out to be cis-regulatory elements which are known to control transcription of nearby genes. (Lee *et al.* 2006; Montavon & Soshnikova 2014; Tschopp & Duboule 2011; van der Hoeven *et al.* 1996) Collinear expression of HOX genes is also coordinated by trans-regulatory elements. These DNA sequences encode transcription factors. Among others, retinoic acid, fibroblast growth factors and WNT signals were demonstrated to activate HOX expression. (Montavon & Soshnikova 2014) Chromatin structure was also identified to maintain an important role in transcriptional control of HOX genes. Polycomb repressive complexes PRC1 and PRC2 were revealed to silence HOX genes. These multiprotein complexes contain several histone-modifying enzymes such as methyltransferases and demethylases and that way, maintain a stable gene inactivation. (Montavon & Soshnikova 2014) Alterations of HOX expression are associated with malformations and malignant tumors. (Grier *et al.* 2005)

1.1.3 Posterior HOXD genes

Particular functions of HOX genes have been elucidated by means of gain- and

loss-of-function experiments in animals. Posterior HOXA and HOXD genes are especially involved in limb development. HOXD genes do not only affect chondrogenesis but also bone condensation and growth. (Goff & Tabin 1997; Jung & Tsonis 1998) HOX genes are known to control patterning along the anterior-posterior axis during embryonic development. During this process, among other things, our digits are differently shaped. The thumb, for example, is shorter and more mobile than other fingers. Posterior HOXD genes are especially involved in limb anterior-posterior asymmetry. (Lewis 1978; McGinnis & Krumlauf 1992; Zakany *et al.* 2004)

Various limb malformations can be referred to alterations of HOX expression and interestingly, localization of limb defects corresponds to collinearity of HOX genes. According to this, disruption of more 3' HOX genes results in a more proximal phenotype whereas disruption of 5' HOX genes especially causes defects of distal limb elements.

The vertebrate limb is subdivided into three morphogenetic domains from proximal to distal: the stylopod, the zeugopod and the autopod (see Figure 4).

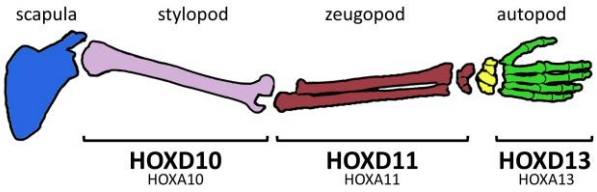

Figure 4: Functional domains of HOXD10, HOXD11 and HOXD13 in limb development.
Simplified illustration according to Zakany and Duboule (1999). Overlaps have been ignored. Paralogous HOXA and HOXD genes represent same functional domains. Carpal bones (yellow) are also affected by HOXD12.

HOXD10, HOXD11 and HOXD13 were identified to have distinct functional domains in limb development. HOXD10 represents the proximal limb segment, i.e. the stylopod which gives rise to the humerus and the femur, respectively. HOXD11 is responsible for the middle skeletal segment, i.e. the zeugopod which contains radius and ulna in the forelimb and tibia and fibula in the hindlimb. The autopod mainly corresponds to HOXD13. This domain gives rise to carpal bones, metacarpals and digits in the forelimb and to tarsal bones, metatarsals and toes in the hindlimb, respectively. (Long & Ornitz 2013; Zakany & Duboule 1999) Figure 4 illustrates functional domains of HOXD10, HOXD11 and HOXD13 in a simplified way because domains usually overlap. HOXD10-HOXD12 were discovered to play a role in digit development as well, though less substantiated than HOXD13. (Delpretti *et al.* 2012) Phenotypes due to targeted disruption of HOXD10, HOXD11 and HOXD13, respectively, are described in detail in

the following chapters.

Besides their involvement in limb development, posterior HOXD genes are also expressed during skin development and in neuroblastoma where they seem to control growth and neuronal differentiation. (Kanzler *et al.* 1994; Zha *et al.* 2012)

1.1.3.1 Current knowledge on HOXD10

Mice with targeted disruption of HOXD10 have abnormal hindlimbs. Skeletal and neural defects were observed whereas muscles were not substantially altered. Animals carrying a double mutation of HOXD9 and HOXD10, however, showed alterations in axial and appendicular skeletal structures, hindlimb peripheral nerve and distal hindlimb musculature. (Carpenter *et al.* 1997; de la Cruz *et al.* 1999) In humans, HOXD10 was also shown to be associated with limb malformations. In detail, mutations of HOXD10 were detected in families with isolated congenital vertical talus, a severe form of a congenital rigid flatfoot with dislocation of the talonavicular joint and near-vertical orientation of the talus. One family also suffered from Charcot-Marie-Tooth disease, a hereditary motor and sensory neuropathy. In this condition a genetically heterogeneous group of disorders share the same clinical phenotype: distal limb muscles are wasting and weak, distal sensory can be affected, skeletal deformities are possible and tendon reflexes are sluggish or even missing. (Dobbs *et al.* 2006; McKie & Radomisli 2010; Pareyson 1999; Shrimpton *et al.* 2004) Recently, HOXD10 was also shown to maintain a role in the pathogenesis of intervertebral disc degeneration. (Yu *et al.* 2013) All these findings indicate an important role of HOXD10 in skeletal and neural structures in humans. HOXD10 is also expressed in the developing lumbosacral spinal cord, however, not in the thoracic cord (Lance-Jones *et al.* 2001). Together with HOXA10, it was shown to control lumbar motor neuron pattering (Lin & Carpenter 2003) Ectopic expression of HOXD10 in thoracic segments in chick embryos induced motoneurons with a lumbosacral molecular profile and axon projections to the limb. (Shah *et al.* 2004) HOXD10 expression was also observed in malignancies of skeletal and neural structures, such as osteosarcoma (Han *et al.* 2014), neuroblastoma (Merrill *et al.* 2004) and brain tumors like astrocytoma and glioblastoma (Abdel-Fattah *et al.* 2006).

Furthermore, HOXD10 expression was not only detected during kidney development

(Fu *et al.* 2014) but also in renal malignancies such as Wilm's Tumor (Redline *et al.* 1994). HOXD10 is also expressed in postnatal developing uterines of mice and is assumed to regulate endometrial receptivity (Hu *et al.* 2004; Xu *et al.* 2014). In endometrial carcinoma an alteration of HOXD10 expression was detected, varying with the histologic grade of differentiation. (Osborne *et al.* 1998) In this case HOXD10 seems to maintain a role in angiogenesis because its overexpression in endometrial cancer impaired endothelial cell migration and blocked angiogenesis *in vivo*. Furthermore, human endothelial cells with HOXD10-overexpression were not able to form new vessels after implantation into immunocompromised mice. (Myers *et al.* 2002) A potential role for HOXD10 was also proposed in development of hemangiomas. (Hansen *et al.* 2006)

Several data suggest HOXD10 can function as a tumor suppressor. In both breast and endometrial tumors HOXD10 expression in epithelial cells seemed to conserve a non-malignant phenotype. Progression of malignancy was associated with a decrease of HOXD10 expression whereas sustained HOXD10 expression impaired endothelial cell migration and inhibited tumor growth *in vivo*. (Carrio *et al.* 2005) Lower HOXD10 mRNA levels in breast cancer samples were significantly associated with higher histological grade of the tumor (Sekar *et al.* 2014; Vardhini *et al.* 2014)

HOXD10 was also found to positively regulate a microRNA called miR-7 in breast cancer. HOXD10 expression resulted in increased miR-7 expression and miR-7 expression in turn suppressed motility, invasiveness, anchorage-independent growth, and tumorigenic potential of breast cancer cells. (Reddy *et al.* 2008) Several results suggest that HOXD10 also functions as a tumor suppressor in gastric cancer because HOXD10 expression is commonly downregulated in gastric cancer tissues and cell lines compared to normal stomach tissues. Re-expression caused inhibition of cell survival, induction of apoptosis, impairment of migration and invasion and suppression of tumor growth in a mouse xenograft. (Wang *et al.* 2012) Insulin-like growth factor binding protein 3 was revealed as transcriptional HOXD10 target in gastric cancer. Like HOXD10, it is frequently downregulated in gastric cancer tissues. Since IGFBP3 expression is related to overall survival and it was already shown to influence proliferation, apoptosis, invasion in other tumor entities, an important role in gastric cancer progression is probable. (Xue *et al.* 2013)

Interestingly, hypermethylation indicating inactivation of HOXD10 was also observed in follicular lymphoma. (Bennett *et al.* 2009) All these findings substantiate the hypothesis of HOXD10 acting as a tumor suppressor in these malignomas.

In another very important finding HOXD10 was shown to be a direct and functional target of miR-10b. In breast cancer this microRNA promotes tumor invasion and metastasis. (Ma *et al.* 2007) Overexpression of miR-10b was also observed in bladder transitional cell cancer metastases whereas HOXD10 expression was downregulated in metastases compared to its expression in matched primary tumors. (Baffa *et al.* 2009) It was shown that miRNA-10b promoted migration and invasion through HOXD10 in human bladder cancer. (Xiao *et al.* 2014) miR-10b was similarly overexpressed in glioma samples and directly associated with the glioma's pathological grade and malignancy. The microRNA directly targeted HOXD10 in this tumor as well and thereby induced glioma cell invasion by modulating tumor invasion factors expression. (Sun *et al.* 2011) Similar results, i.e. miR-10b promoting invasion and metastasis via HOXD10, were obtained in many more tumor entities, involving gastric carcinoma (Liu *et al.* 2012), colorectal cancer (Wang *et al.* 2015), brain tumors such as glioblastoma multiforme (Lin *et al.* 2012), other gynecologic tumors such as ovarian cancer (Nakayama *et al.* 2013), and hepatocellular carcinoma (Liao *et al.* 2014). In hepatocellular carcinoma, HOXD10 can also be targeted by another microRNA (miR-224) to promote cell proliferation, migration and invasion. (Li *et al.* 2014) Generally, HOXD10 seems to be a common target of microRNAs. In gliomas, HOXD10 was also detected to be a target of miR-23a. (Hu *et al.* 2013)

HOXD10 expression was also observed in several ENT (ear, nose and throat) tumors. In oral squamous cell carcinoma HOXD10 belongs to the three most upregulated homeobox genes. (Rodini *et al.* 2012) Its expression can also be observed in several esophageal cancer cell lines. (Gu *et al.* 2007) In head and neck squamous cell carcinoma, HOXD10 is overexpressed and its knockdown caused decreased proliferation and invasion. (Sharpe *et al.* 2014) HOXD10 was also discovered to be overexpressed in colon carcinoma. (Bhatlekar *et al.* 2014)

Summing up, HOXD10 maintains an important role in skeletal and neural development and its expression was observed in many different tumors. It seems to have a dual role in pathogenesis of tumors since in some tumors there is an overexpression promoting

proliferation and invasion whereas in other tumor entities, HOXD10 seems to function as a tumor suppressor being expressed at very low levels only or even being inactivated by hypermethylation. However, little is known about the detailed function of HOXD10 or its targets.

1.1.3.2 Current knowledge on HOXD11

Doing literature research on HOXD11, most works deal with limb development. Double disruption of HOXD11 and its paralog HOXA11 causes a severe malformation of the zeugopod in mice. Mesenchymal condensations which, later on, form the basic structure of the zeugopod (i.e. containing the two bones respectively: radius and ulna, tibia and fibula), are started normally but ultimately they remain smaller in size; radius and ulna end up shortened and misshapen. (Boulet & Capecchi 2004) In a different work radius and ulna in HOXA11/HOXD11 double mutant mice are even described as “almost entirely absent”. Furthermore, a malformation of the wrist with affection of the proximal carpal bones is mentioned. (Davis *et al.* 1995; Kjosness *et al.* 2014) Disruption of HOXD11 in mice leads to additional lumbar vertebrae, shortened metacarpals and second phalanges. (Davis & Capecchi 1994; Zakany *et al.* 1997) HOXA11/HOXD11 double mutant mice have eight lumbar vertebrae (normal mice have six lumbar vertebrae). Number of lumbar vertebrae was reduced to only five by increasing the number of HOXD11 transcripts in particular cells. In the autopod increased HOXD11 copy number causes an increase of bone length. (Boulet & Capecchi 2002) Interestingly, it’s not only quantity of HOXD11 transcripts that matters but also the point in time when HOXD11 is expressed. If it is expressed too early, lumbar vertebrae might be missing, if HOXD11 is expressed too late, additional lumbar vertebrae can be found. (Gerard *et al.* 1997) All three HOX11 paralogs (there is no HOXB11, see p. 4) are involved in joint formation of the zeugopod, i.e. elbow and knee joint formation. In triple mutants, the ulna lacks the olecranon, instead there is a sort of sesamoid bone; knee joints are remodeled with fibula and tibia being equally involved in articulation with the femur. Interestingly, organization of elbow and knee joints can be largely restored if one of the three HOX11 genes is functional. (Koyama *et al.* 2010)

In mice HOXA11 and HOXD11 were shown to control early steps of chondrocyte

differentiation. In HOXA11/HOXD11 double mutants chondrogenic differentiation in the zeugopod was generally delayed and chondrocytes were not competent to undergo hypertrophic differentiation. (Gross *et al.* 2012)

Beyond their involvement in limb development, HOXD11 and its paralog HOXA11 are known to maintain a complex and important role in kidney development. They control certain programs in metanephric kidney induction, parts of which later persist as the adult kidney. Mutations cause, among others, an abnormal pattern of ureteric bud branching. Mice with homozygous null mutation of HOXD11 or HOXA11 have normal kidneys whereas animals carrying a double mutation of HOXD11 and HOXA11 have rudimentary or absent kidneys. (Mugford *et al.* 2008; Patterson *et al.* 2001; Wellik *et al.* 2002) Congenital renal malformations in children, however, can also emerge without mutations of HOXA11 and HOXD11. (Bouba *et al.* 2009) Deregulation of HOXD11 expression was also observed in clear cell renal cancer tissues. (Cantile *et al.* 2011)

HOXD11 also seems to maintain a role in genital development because altered methylation of its CpG site was associated with hypospadia (Choudhry *et al.* 2012). HOXD11 is also expressed in the endometrium. HOXD11 expression seems to be dependent on menstrual cycle-stage since it can be detected throughout the cycle but levels decrease severely in the secretory phase compared to the proliferative phase. (Akbas & Taylor 2004)

HOXD11 also appears in context of several malignancies. In human breast cancer and ovarian cancer tissue samples, just as in human malignant melanoma cells, HOXD11 was often shown to be aberrantly methylated. (Cai *et al.* 2007; Furuta *et al.* 2006; Miyamoto *et al.* 2005) In one ovarian cancer cell line HOXD11 was shown to be overexpressed. (Morgan *et al.* 2010) By the side of HOXD10 and HOXA5, HOXD11 belongs to the three most upregulated homeobox genes in oral squamous cell carcinoma (Rodini *et al.* 2012). Little is known about its function though. Strong HOXD11 expression was observed in head and neck cancer tissues where its knockdown impaired invasion (Sharpe *et al.* 2014). In gastric cancer tissue samples HOXD11 expression was associated with altered integrin expression profiles compared to normal mucosa. (Rossi Degl'Innocenti *et al.* 2007)

HOXD11 also appears in the context of hematological malignancies. NUP98 gene was

shown to be fused to several different partner genes in hematological malignancies, such as MDS and AML with certain translocations. In a 15-year-old boy with acute myeloid leukemia a certain translocation t (2; 11) (q31; p15) was detected which caused a fusion of NUP98 to HOXD11. (Taketani *et al.* 2002)

Like HOXD10, HOXD11 was shown to influence motoneuron subtype specification in the developing lumbosacral spinal cord of chick embryos. HOXD11 is only expressed in caudal segments of the lumbosacral spinal cord; ectopic HOXD11 expression lead to a change of the number of motoneurons and new axonal projections from rostral segments to thigh muscles. (Misra *et al.* 2009)

Altogether, little is known about HOXD11 and its functions. Studies mainly concentrate on its role in development of skeletal, urogenital and neural structures. Comparing to HOXD10, only few works described aberrant HOXD11 expression in different tumor entities. Its role in pathology of cancer remains widely unclear.

1.1.3.3 Current knowledge on HOXD13

As previously mentioned, HOXD10, HOXD11 and HOXD13 are involved in limb formation with each of them representing a certain portion of the limb (see Figure 4 on p. 7). Paralogs HOXA13 and HOXD13 especially correspond to the autopod.

A certain HOXD13 mutation is especially associated with synpolydactyly (SPD). This rare limb deformity is characterized by a clinically very heterogenous combination of syndactyly and polydactyly. Main features of SPD are the webbing of digits III/IV and toes IV/V with partial or complete digit duplication within the syndactylous web. SPD is inherited in an autosomal dominant manner with incomplete penetrance. Three genetically distinct SPD malformations are known, SPD1, SPD2 and SPD3. SPD1 is linked to a HOXD13 mutation (locus: 2q31). SPD2 and SPD3 are mapped on chromosome 22 and 14, respectively. (Malik & Grzeschik 2008)

In humans, expansions of a polyalanine stretch in the amino-terminal region of HOXD13 were revealed to cause synpolydactyly. (Muragaki *et al.* 1996) The polyalanine expansion was found to cause misfolding, degradation and cytoplasmic aggregation of the mutant proteins. (Albrecht *et al.* 2004) Synpolydactyly phenotypes were discovered to correlate with size of expansions in HOXD13 polyalanine tract (Goodman *et al.* 1997). The polyalanine expansion itself is thought to result from unequal

crossing-over of HOXD13. (Warren 1997)

A similar mutation was found in mice. The phenotype of the mouse mutant synpolydactyly homolog (spdh) corresponds to the human phenotype with polydactyly, syndactyly and brachydactyly and is also caused by a polyalanine expansion in the HOXD13 gene. (Albrecht *et al.* 2002) In these mice, supernumerary digits were shown to be induced by mutant HOXD13 directly and indirectly, via a decrease of retinoic acid. Retinoic acid was demonstrated to have an antichondrogenic effect on mesenchymal cells. (Kuss *et al.* 2009)

Homozygous mice with a targeted deletion of HOXD11-HOXD13 exhibit several defects in their distal limbs which are similar to human synpolydactyly. (Zakany & Duboule 1996)

Missense mutations of HOXD13 were also revealed to be associated with brachydactyly, partially in combination with syndactyly. (Johnson *et al.* 2003; Zhao *et al.* 2007) Furthermore, HOXD13 is suggested to play a role in foot malformations such as the congenital clubfoot, also known as congenital talipes equinovarus (CTEV). (Cao *et al.* 2009; L. L. Wang *et al.* 2008)

Besides their involvement in limb formation, paralogs HOXA13 and HOXD13 control development of the terminal parts of the urogenital and digestive tracts. Mice lacking these genes, for example, exhibit hypogenetic male accessory sex glands, malpositioning of the vaginal, urethral and anal openings, anomalies of the rectum and defective morphogenesis of the anal sphincter. (Kondo *et al.* 1996; Warot *et al.* 1997) Specific HOXD13 mutations are linked with both synpolydactyly and hypospadias. (Tuzel *et al.* 2007)

A certain deletion of HOXD13 was linked to VACTERL syndrome which is characterized by an association of multiple malformations. Patients exhibit vertebral defects, anal atresia, cardiac anomalies, tracheoesophageal fistula with esophageal atresia, renal dysplasia and limb lesions. (Garcia-Barcelo *et al.* 2008)

HOXD13 expression was examined across 79 different tumor tissue types. Tissues of different origins such as adrenal gland, brain, gynecologic organs, digestive tract, lymphoid tissue and skin were tested. HOXD13 expression varied quantitatively and qualitatively between normal tissue and tumor types of the same organ. Majority of cancers showed an increase of HOXD13 expression. Within particular tissue groups,

HOXD13 expression varied between distinct histological subtypes. For example, invasive lobular and tubular carcinomas of the breast showed different HOXD13 expression than mucinous, medullar and ductal invasive carcinomas. Pancreas and stomach tumor subtypes represent an exception because they displayed negative HOXD13 expression. In pancreatic cancer, HOXD13 expression was associated with better prognosis and higher 12-month survival rates. (Cantile *et al.* 2009)

Certain gene fusions of HOXD13 to NUP98 were detected in myelodysplastic syndromes and acute myelogenous leukemia. (Raza-Egilmez *et al.* 1998; Slape *et al.* 2008) The fusion gene was discovered to cause ineffective hematopoiesis. On the one hand it increases self-renewal of hematopoietic stem or progenitor cells; on the other hand, it inhibits differentiation of precursors and increases apoptosis in other lineages in the bone marrow. (Gough *et al.* 2011; Slape *et al.* 2007) NUP98 fusion oncoproteins were revealed to lead to mitotic spindle defects and chromosome missegregation. (Salsi *et al.* 2014) In mice NUP98-HOXD13 fusion also leads to myelodysplastic syndrome progressing to acute leukemia. (Lin *et al.* 2005) Impaired DNA break and repair mechanisms were detected in NUP98-HOXD13 transgenic mice. (Puthiyaveetil *et al.* 2013)

1.2 Skeletogenesis and bone formation

The skeleton is composed of cartilage and bone and generally formed in two different phases. During the first phase which is called skeletal patterning, mesenchymal cells migrate to putative sites of skeletogenesis, aggregate and form condensations. These condensations assume the shape of the future skeletal element. Cells of mesenchymal condensations produce an extracellular matrix which is abundant in type I collagen. The second phase comprises differentiation of the three specific cell types of skeleton, chondrocyte in cartilage, osteoclast and osteoblast in bone. (Karsenty *et al.* 2009; Lefebvre & Smits 2005)

Bone formation in mammals occurs via two different mechanisms in embryonic development: intramembranous ossification and endochondral ossification. In process of intramembranous ossification, cells of mesenchymal condensations directly differentiate into osteoblasts and osteocytes. Osteoblasts produce bone extracellular matrix (ECM) and are also responsible for mineralization of this ECM; thus they are

considered as bone-forming cells. Mechanism of intramembranous ossification, however, applies to few bones in mammal skeleton only, more precisely only to the clavicle and parts of the skull. (Ducy *et al.* 1997; Karsenty *et al.* 2009) After commitment into osteoblast lineage, skeletal precursor cells differentiate towards osteoprogenitor cells, pre-osteoblasts, osteoblasts and finally osteocytes. Each stage of osteogenic differentiation is characterized by a certain gene expression profile (see Figure 5).

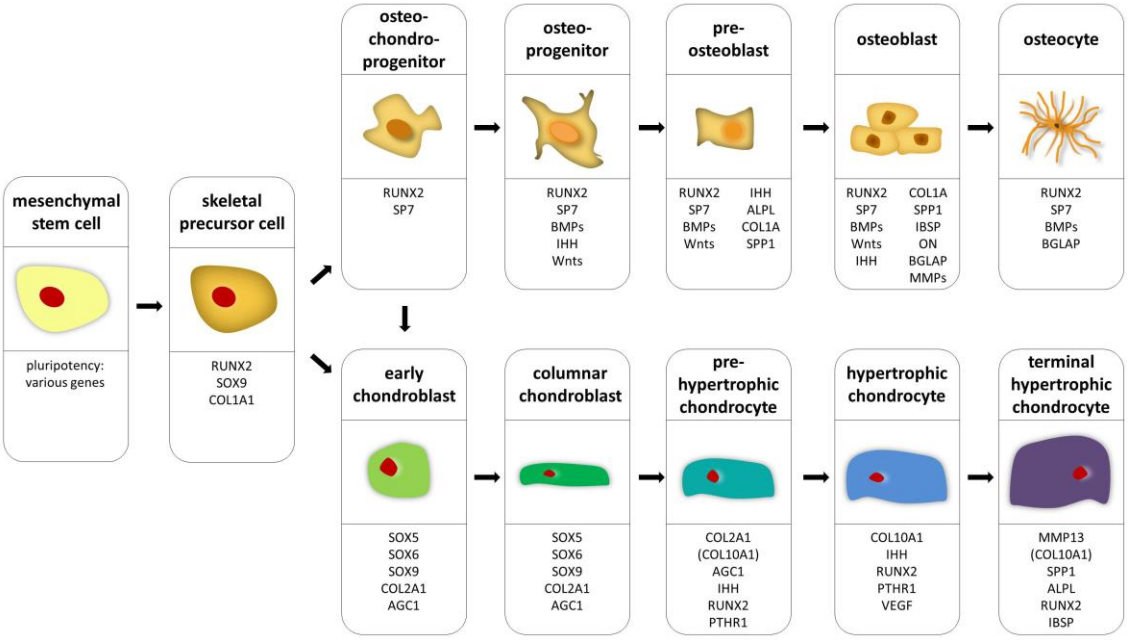

Figure 5: Osteogenic and chondrogenic differentiation of MSC.
Stages of osteogenic and chondrogenic differentiation from pluripotent mesenchymal stem cells are shown. Characteristic cell morphology and selected marker genes of respective developmental stage are illustrated. Full names of genes can be found in list of abbreviations on p. III. A mesenchymal progenitor cell is assumed to be the original cell of Ewing sarcoma. (Kauer *et al.* 2009; Tirode *et al.* 2007) Created according to Lefebvre and Smits (2005), Javed *et al.* (2010) and Zuscik *et al.* (2008). Reproduced by permission of John Wiley & Sons, Elsevier and the American Society for Clinical Investigation.

Osteoblastogenesis is controlled by various growth factors such as IHH, WNT proteins, BMPs, Notch signaling and FGFs but also transcription factors such as RUNX2 and Osterix (also known as SP7). (Long & Ornitz 2013) RUNX2 expression can already be observed in skeletal precursor cells which are capable of both osteogenic and chondrogenic differentiation. (Ducy *et al.* 1997) However, RUNX2 is the master regulator of osteoblast differentiation. Among other things, RUNX2 was demonstrated to activate bone matrix protein genes such as osteocalcin (BGLAP), osteopontin (SPP1), bone sialoprotein (IBSP) and type I collagen (COL1A1). (Ducy *et al.* 1997) RUNX2 null mice completely lack bone formation throughout the body. Immediate death at birth

due to respiratory failure is probably caused by absent ossification of the ribs. (Komori *et al.* 1997) RUNX2 haploinsufficiency is associated with cleidocranial dysplasia, an autosomal dominant inherited syndrome which is, among other things, characterized by failed closure of the fontanelles, abortive clavicles and short stature. Both intramembranous and endochondral bone formation seem to be defective. (Mundlos *et al.* 1997) Heterozygous mice exhibit similar skeletal abnormalities. (Otto *et al.* 1997)

In process of endochondral ossification, an intermediate template made of cartilage is formed. The cartilaginous template prefigures the future skeletal element and is then gradually replaced by bone tissue. This mechanism applies to most skeletal elements of the body, especially long bones. (Karsenty *et al.* 2009; Wuelling & Vortkamp 2011) For endochondral ossification, cells of mesenchymal condensation mature into chondrocytes. Immature chondrocytes produce an ECM which is rich in type II, type IX and XI collagen, glycoproteins and proteoglycans such as aggrecan. (Karsenty *et al.* 2009; Long & Ornitz 2013) In central diaphyseal regions of long bones cells rapidly undergo differentiation process towards pre-hypertrophy, hypertrophy and terminal maturation. Pre-hypertrophic and hypertrophic chondrocytes produce collagen type X in abundance before they die by apoptosis. (Karsenty *et al.* 2009; Lefebvre & Smits 2005)

In the meanwhile, peripheral cells of mesenchymal condensations keep producing type I collagen and become fibroblast-like cells. Those arrange in a layer and surround the cartilage elements (perichondrium). During hypertrophic maturation of chondrocytes, inner cells of the perichondrium start expressing RUNX2, the master gene of osteoblastogenesis which was already mentioned earlier. Those cells differentiate into osteoblasts and form the periosteum. (Ducy *et al.* 1997; Karsenty *et al.* 2009; Wuelling & Vortkamp 2011) Periosteal osteoblasts produce bone matrix of the bone collar. This structure prefigures the future cortical bone, in other words the outer bone layer. Apoptotic terminal hypertrophic chondrocytes have generated a type X collagen-rich ECM which promotes vascular invasion from the bone collar. (Karsenty *et al.* 2009) Cartilage is usually avascular. Coupled with terminal maturation of chondrocytes, however, blood vessel invasion from the bone collar brings cells of the osteoblast lineage and osteoclasts into the middle of the hypertrophic cartilage of the central diaphysis. Osteoblasts establish primary ossification centers. They generate

trabecular bone and replace the cartilaginous ECM with osseous, type I collagen-rich ECM. This ossification occurs centrifugally, i.e. ossification starts in the center and spreads to the periphery. (Karsenty *et al.* 2009; Lefebvre & Smits 2005; Long & Ornitz 2013) Osteoclasts, the second bone-specific cell type, are multinuclear cells which derive from the same hematopoietic progenitors in the bone marrow like monocytes and macrophages by fusion. Being responsible for bone resorption and remodeling, they control bone integrity and calcium metabolism. (Bar-Shavit 2007)

Early chondroblasts at each end of a long bone flatten, organize into columns and thus, form the growth plates. After a phase of proliferation, they mature into hypertrophic and terminal hypertrophic chondrocytes in the growth plate as well. Systematic maturation of chondrocytes in the growth plate generates zones of proliferation, hypertrophy and bone formation which continuously proceed from epiphyseal to diaphyseal. This is critical for longitudinal growth. (Karsenty *et al.* 2009; Lefebvre & Smits 2005; Long & Ornitz 2013) In contrast to primary ossification centers in embryonic development, secondary ossification centers in the epiphysis don't develop until days or weeks after birth. (Lefebvre & Smits 2005)

Formation of respective chondrocyte populations is, just as osteogenic differentiation, controlled by multiple pathways. Regulation mechanisms involve growth factors such as IHH, PTHrP, BMPs, FGFs, WNT proteins and NOTCH. (Long & Ornitz 2013; Wuelling & Vortkamp 2011) Analogically, individual steps of chondrogenic differentiation are also characterized by specific gene expression profiles (see Figure 5).

Especially SOX9 expression is critical for commitment and differentiation of mesenchymal cells toward the chondrogenic lineage. SOX9 expression can already be observed in the common skeletal precursor cell of osteogenic and chondrogenic differentiation. (Akiyama *et al.* 2002; Akiyama *et al.* 2005) However, sustained SOX9 expression and co-expression of two additional SOX family members, SOX5 and SOX6, are crucial for initiation and early stages of chondrocyte maturation. (Lefebvre *et al.* 1998; Lefebvre & Smits 2005) SOX5, SOX6 and SOX9 double null mutant mice exhibit similar phenotypes. Animals suffer from severe generalized chondrodysplasia and die early. Heterozygous mutations of SOX9 are associated with campomelic dysplasia, a skeletal malformation syndrome with congenital bowing and angulation of long bones and defective cartilage formation. SOX5 and SOX6 single null mutants have limited

skeletal abnormalities. (Akiyama *et al.* 2002; Foster *et al.* 1994; Smits *et al.* 2001) SOX5, SOX6 and SOX9 were shown to activate markers for early chondrogenesis (COL2A1 and AGC) and suppress markers for hypertrophic chondrocytes and osteoblasts at the same time. (Lefebvre *et al.* 2001; Lefebvre & Smits 2005) Expression of the three SOX genes decreases when cells undergo further differentiation. Pre-hypertrophic and hypertrophic chondrocytes express RUNX2 and COL10A1 among others. (Lefebvre & Smits 2005) RUNX2 maintains a major role in terminal chondrocyte differentiation. It was revealed to control COL10A1 expression in hypertrophic chondrocytes and the expression of SPP1, IBSP and MMP13 in terminal hypertrophic chondrocytes. (Komori 2010) RUNX2-deficient mice also exhibit impaired chondrocyte differentiation besides their lack of bone formation. (Komori *et al.* 1997)

Majority of bones in skeleton is formed via endochondral bone formation. This basically means that chondrogenesis is the first and most important step of bone formation in mammals, not osteogenesis. (Karsenty *et al.* 2009) Recently, hypertrophic chondrocytes were even reported to be competent to transdifferentiate into osteoblasts during endochondral bone formation. (Yang *et al.* 2014; Zhou *et al.* 2014)

Involvement of HOX genes in limb formation was already mentioned in 1.1. Interestingly, it has almost been 20 years that HOXD gene expression was revealed to be required for mesenchymal condensation and chondrogenic differentiation. (Jung & Tsonis 1998)

Besides its involvement in initial cartilage condensation, posterior HOXD genes were also demonstrated to affect later growth phase of bones. (Goff & Tabin 1997)

1.3 Bone morphogenetic proteins and the TGF β pathway

Bone morphogenetic proteins (BMPs) belong to the transforming growth factor β (TGFβ) superfamily of proteins, a large family of cytokines which cause multiple biological effects in multiple different cell types, such as cell growth, differentiation, migration, adhesion or apoptosis. The family comprises 42 members in the human genome; the prototype is transforming growth factor β. Other members are nodals, activins, myostatins and anti-Muellerian hormone (AMH). (Massague *et al.* 2005)

The active form of a TGFβ ligand is a homodimer. In BMPs monomers are linked by a disulfide bridge. More than 15 BMPs have been identified in mammals, they can be

further classified in several subgroups by their amino acid sequence similarity: BMP 2/4 group, BMP 5/6/7/8 group which is also called OP1 group (osteogenic protein 1 group), GDF (growth and differentiation factor) 5/6/7 group and BMP 9/10 group. Most of these proteins induce formation of bone and cartilage tissues *in vivo*, except the members of the GDF group which induce cartilage and tendon-like, but no bone-like tissues. (Kawabata *et al.* 1998; Miyazono *et al.* 2010) Analysis of osteogenic activity of 14 different BMPs and GDFs resulted in a hierarchical model in which especially BMP2, BMP6 and BMP9 showed biggest potential in induction of osteoblast differentiation of mesenchymal stem cells, most BMPs, however, were able to stimulate osteogenesis in mature osteoblasts. Most studies on BMPs and their biological activities were carried out using homodimeric proteins, heterodimeric

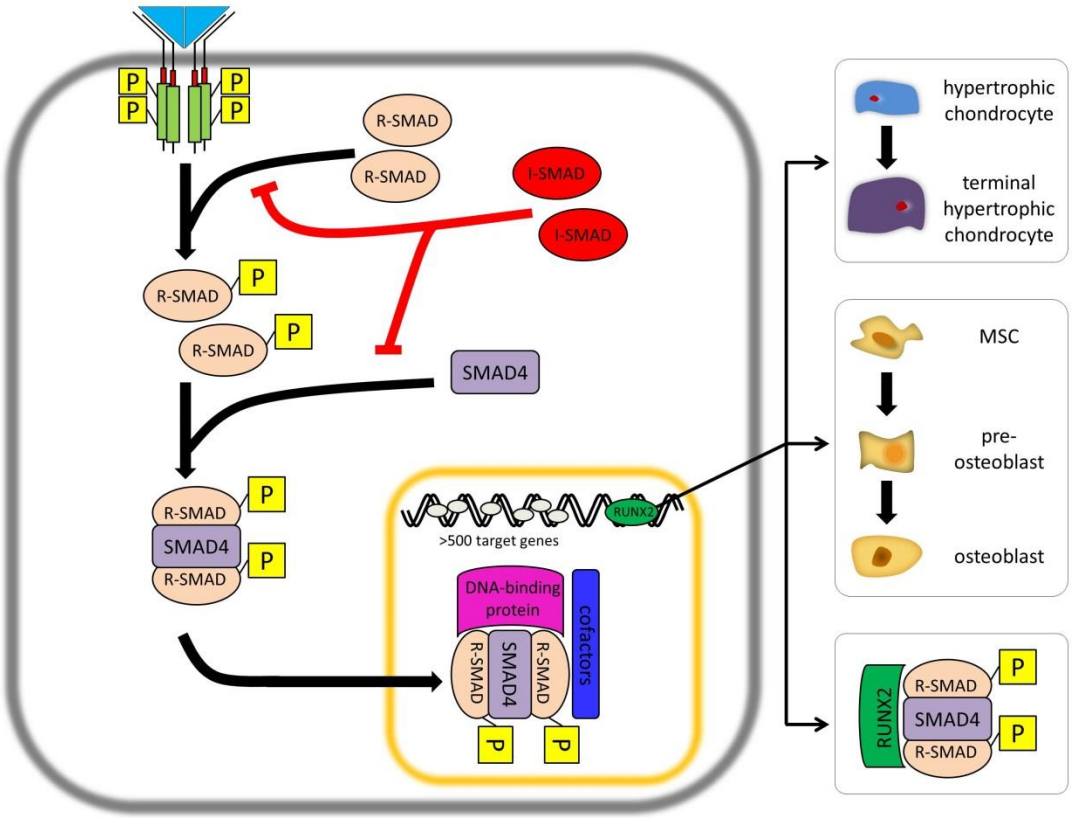

Figure 6: BMP signaling through SMAD proteins in bone formation.
Homodimeric ligand (blue triangle) binds to receptor with serine/threonine kinase activity. After activation receptor phosphorylates R-SMADs, those in turn form a complex with SMAD4. Process is inhibited by I-SMADs. SMAD-complex transfers into the nucleus. Together with cofactors and DNA-binding proteins, the complex functions as a transcription factor and activates various target genes, RUNX2 being one of them. RUNX2 in turn induces mesenchymal stem cells (MSC) to commit into osteogenic lineage and promotes the final step in chondrogenic differentiation. Furthermore RUNX2 is known to interact with SMAD proteins. (Ducy *et al.* 1997; Komori 2010; Zhang *et al.* 2000) Created in the style of Chen *et al.* (2012) and Miyazono *et al.* (2005).

proteins, however, such as BMP2/BMP4 showed even enhanced activities than corresponding homodimers. (Aono *et al.* 1995; Cheng *et al.* 2003; Israel *et al.* 1996; Kawabata *et al.* 1998)

TGFβ signaling initiates when a TGFβ ligand binds to specific cell membrane-associated receptors with serine/threonine kinase activity. There are two types of these receptors, type I and type II, which are structurally very similar. So far, seven type I and five type II receptors have been identified in mammals. (Heldin *et al.* 1997; Miyazono *et al.* 2010)

After receptor activation, signals are transduced via SMAD and non-SMAD signaling pathways. Receptor I kinase propagates the signal by phosphorylating SMAD proteins. There are three functional classes of SMAD proteins: receptor-regulated SMADs (R-SMAD), Co-mediator SMAD (in our case SMAD4) and inhibitory SMADs (I-SMADs). R-SMADs, which SMADs 1, 2, 3, 5 and 8 belong to, are directly activated through phosphorylation by receptor I kinase. SMADs 1, 5 and 8 are principally substrates for BMP and anti-Muellerian receptors, SMADs 2 and 3 for TGFβ, activin and nodal receptors. R-SMADs form complexes with Co-SMAD SMAD4 which transfer into the nucleus where they, along with cofactors, control transcription of various target genes. These target genes involve, among others, transcription factors important for bone formation such as RUNX2 and collagens. I-SMADs, i.e. SMAD 6 and 7, inhibit TGFβ signaling. On the one hand they compete with R-SMADs for binding sites; on the other hand they target receptors and cause their degradation. (Chen *et al.* 2012; Lee *et al.* 2000; Massague *et al.* 2005; Shi & Massague 2003; Volk *et al.* 1998)

BMP signaling pathway is also controlled via other inhibitory mechanisms. Extracellular antagonists such as noggin bind BMPs and prevent them from binding to the receptor. Transmembrane proteins such as BAMBI associate with type I and type II receptors and inhibit BMP signaling at the cell membrane level. SMURFs (SMAD ubiquitin regulatory factors) initiate ubiquitination and degradation of R-SMADs and inhibit type I receptors. (Tsumaki & Yoshikawa 2005)

Non-SMAD signaling pathways involve MAPK (mitogen-activated protein kinase) cascades. In mammals, the MAPK family comprises ERK (extracellular signal-regulated kinase), p38 and JNK (c-Jun NH_2-terminal kinase). Each signaling axis consists of at least three components: a MAPK is phosphorylated by a MAP2K (MAPK kinase) which was

phosphorylated by a MAP3K (MAPK kinase kinase) before. Activated MAP kinases, in turn, phosphorylate various proteins, for example transcription factors. That way, they influence multiple cellular processes such as proliferation, differentiation, migration, inflammatory responses and cell death. (Chen *et al.* 2012; Kim & Choi 2010)

Both, SMAD and non-SMAD pathway were identified to converge at the RUNX2 gene to control mesenchymal precursor cell differentiation. (Chen *et al.* 2012; Lee *et al.* 2002) RUNX2 was already mentioned in chapter 1.2. It is not only the master regulator of osteoblast differentiation but also maintains a major role in terminal chondrocyte differentiation. (Ducy *et al.* 1997; Komori 2010) Furthermore, RUNX2 is not only a common BMP target but also an important cofactor in BMP signaling. It was identified to physically interact with R-SMADs and thus cooperatively induce target genes. (Lee *et al.* 2000; Zhang *et al.* 2000) Other common targets of BMP signaling involve genes which encode type I and type X collagen, in detail COL1A1 and COL10A1. (Ducy *et al.* 1997; Lee *et al.* 2000; Volk *et al.* 1998)

1.4 Ewing sarcoma

Ewing sarcoma is the second most frequent primary bone tumor. (Bernstein *et al.* 2006) In comparison to other pediatric malignancies, however, Ewing sarcomas are rather rare. According to numbers of the German Childhood Cancer Registry, the three most frequent malignancies in children under 18 years, leukemias, CNS tumors and lymphomas (in this order) constitute more than two thirds of pediatric malignomas. Malignant bone tumors represent only a small number of 5%. In children, malignant bone tumors basically comprise osteosarcomas and Ewing sarcomas; chondrosarcomas and other bone tumors are considered as rarities at this age. (Deutsches Kinderkrebsregister, p. 4; Niemeyer & Rössler 2013) Most common age of diagnosis is the second decade of life with peaks at 15 years of age. 20-30% of patients, respectively, are younger than 10 or older than 20 years at diagnosis. Ewing sarcoma in children younger than 5 years is very uncommon. In general, boys are afflicted a little more often than girls (sex ratio male/female: 1.3). (Bernstein *et al.* 2006; Deutsches Kinderkrebsregister, p. 48) Interestingly, Caucasians are much more often affected than Asians and Africans and prevalences, age at time of diagnosis, tumor characteristics and overall survival differ depending on ethnic background. (Worch *et*

al. 2010)

Classic Ewing sarcoma was first described as “Diffuse endothelioma of bone” by James Ewing in 1921. (Ewing 1972) These days the term “Ewing sarcoma” represents a whole family of tumors with same histological appearance and certain immunohistochemical features. (Bernstein *et al.* 2006) According to their degree of neuroglial differentiation, members of the Ewing family of tumors (EFT) are further classified. Classical Ewing sarcoma, for example, is poorly differentiated while peripheral neuroectodermal tumors (pPNETs) are more mature. Ewing sarcoma of the chest wall is also called Askin’s tumor. (Bernstein *et al.* 2006; Potratz *et al.* 2012) James Ewing originally described the tumor as “endothelioma”, a mesenchymal tumor. (Ewing 1972; Staege *et al.* 2004) Today, Ewing sarcoma is assumed to originate from a primitive neural crest-derived progenitor at the transition to mesenchymal and endothelial differentiation because induction of EWS/FLI1 in mesenchymal progenitor cells caused a transformation and generated Ewing sarcoma-like tumors. (Riggi *et al.* 2005; Staege *et al.* 2004)

Tumors consist of small round blue cells with large nuclei and narrow rims of cytoplasm. Cells strongly express cell-surface glycoprotein CD99, also known as MIC2. More differentiated tumors (pPNETs) may express markers of neural differentiation such as S100, NSE and LEU7. Immunoreactivity for vimentin and cytokeratins is possible as well. However, microscopical and immunophenotypic characteristics of Ewing sarcoma partially coincide with other small round cell tumors of the childhood such as NHL, rhabdomyosarcoma, neuroblastoma, medulloblastoma and ALL. Therefore, further immunohistochemical investigations are required. Molecular genetic studies such as FISH and RT-PCR allow for definitive diagnosis since members of the Ewing family of tumors are characterized by certain chromosome translocations. (Bernstein *et al.* 2006; Dockhorn-Dworniczak *et al.* 1994) Chromosome translocations in Ewing sarcomas were already described in the early 1980s. (Turc-Carel *et al.* 1984) Soon reciprocal chromosomal translocation t (11; 22), which involves EWS (Ewing sarcoma gene) and FLI1 (Friend leukemia virus integration site 1), was identified to be responsible for oncogenic gene fusion in Ewing sarcoma. Resulting fusion protein EWS-FLI1 alone was revealed to transform mesenchymal progenitor cells and thus, to induce Ewing sarcoma. There are two different breakpoint regions called EWSR1 and

EWSR2: EWSR1 relates to the breakpoint region of the EWS gene, EWSR2 relates to different breakpoint regions of the FLI1 gene. EWSR1 can be fused to two different FLI1 exons. Resulting gene fusions were considered as type 1 and type 2 translocations and can be observed in more than 85% of all cases. Since then, other fusion partners of EWS were detected. Just as FLI1, they belong to the ETS family of transcription factors. In 5% of cases EWS is fused to ERG (chromosome 21). Very infrequent fusion partners involve ETV1, ETV4 or FEV. Compared to EWS/FLI1, all these translocations are rather rare though. (Bernstein *et al.* 2006; Delattre *et al.* 1994; Delattre *et al.* 1992; Riggi *et al.* 2005; Sankar & Lessnick 2011)

About one in two Ewing sarcomas is located in long bones of limbs, preferably in bones of the lower limb. Around 20% of Ewing sarcomas arise from the femur, another 18% from tibia or fibula. In these cases, proximal diaphyseal parts of the bones are predominantly affected. In another 40% of cases Ewing sarcoma is located in flat bones of the trunk such as the pelvis and chest wall. Affection of the spine and upper limb is possible but less frequent. Affection of the hand, foot or skull is rather rare. Generally, Ewing sarcoma can arise from any bone of the body. (Bernstein *et al.* 2006; Freyschmidt *et al.* 2010) In a smaller amount of cases Ewing sarcoma emerges as a soft tissue tumor beyond the skeletal system. Interestingly, prevalences of soft tissue tumors differ depending on ethnic background; they range from 20% in Caucasians to around 40% in Asians and African Americans, respectively. (Worch *et al.* 2010)

Patients with Ewing sarcoma may report on intermittent pain of the affected bone in the beginning, especially nocturnal pain is very common. Within weeks or months, afflictions persist and increase in intensity, a swelling of the affected area may emerge due to tumor growth. At this point of time patients often develop accompanying symptoms which remind of a septic clinical picture. Leukocytosis, fever, elevated blood sedimentation rate as well as anemia can be observed. Elevations of levels of serum lactate dehydrogenase correlate with tumor burden. These symptoms as well as loss of weight often indicate an advanced tumor stage. Since most patients are in their second decade of life at time of diagnosis, intermittent pain of the bone at early stage of disease is sometimes misinterpreted as pain due to “bone growth” or sports injury. Accompanying symptoms such as fever and fatigue may also remind of osteomyelitis at first. As a result, the malignant bone tumor might unfortunately have reached

advanced stages at time of diagnosis. Ewing sarcoma mainly metastasizes hematogenously into lung, bone and bone marrow. Lymph node metastases or metastases to other sites such as liver or central nervous system can be found but are rather rare. In about 25% of patients, primary metastases can already be detected at time of diagnosis. (Bernstein *et al.* 2006; Freyschmidt *et al.* 2010)

Specific symptoms occur according to localization of primary tumor or metastases. A tumor of the spine can cause paraplegia whereas a tumor of the ribs and pulmonary metastases might trigger respiratory ailments. Depending on localization of tumor bulk, urinary retention and intestinal obstruction are possible. In case of pelvic or thoracic tumor localization patients may develop symptoms only at a very late stage. Differential diagnoses comprise a wide range of diseases. Osteomyelitis and other small round cell tumors, both of which were already mentioned earlier, Langerhans cell histiocytosis, juvenile bone cyst, as well as other malignant bone tumors or metastases have to be excluded. There is no blood or urine test which can prove Ewing sarcoma. It may be helpful, however, to determine serum and urine catecholamine levels to exclude neuroblastoma. An x-ray in two planes may show the typical diaphyseal location of Ewing sarcoma (unlike osteosarcoma) and certain indications of malignancy. The latter involve pathologic fractures, osteolysis as well as periosteal reactions such as detachment, a lamellar onion skin-like reaction or formation of spiculae. These radiological features are not specific for Ewing sarcoma though. Cases were described in which osteomyelitis looked quite similar in the x-ray. Indeed, magnetic resonance imaging allows most precise characterization of the tumor regarding extent and neighboring structures, it doesn't give a hundred percent proof either. Definitive diagnosis can be made by biopsy only. Fine needle aspiration biopsy and core needle biopsy can be considered; diagnostic gold standard, however, is the open biopsy which provides more material for further investigations. Immunohistochemistry suggests the diagnosis of a Ewing sarcoma if tumor cells are CD99-positive and negative for markers of other small round cell tumors such as CD49 (lymphoid), myogenin/desmin/actin (rhabdomyosarcoma) and neurofilament protein (neuroblastoma). Diagnosis is ultimately proven by detection of the typical Ewing translocation mentioned earlier. (Bernstein *et al.* 2006; Freyschmidt *et al.* 2010)

Once diagnose of Ewing sarcoma is secured, patients should be staged for metastases,

which can be detected in a quarter of patients. As already mentioned, most common sites are lung, bone and bone marrow. Thoracic CT, bone marrow biopsy and aspirates as well as whole body 99m-technetium bone scan are appropriate investigations. FDG-PET can be indicated if available. Suspicious lesions at other sites have to be further examined. (Bernstein *et al.* 2006)

Ewing sarcoma therapy includes combination chemotherapy, surgery and radiotherapy. Current therapeutic regimens intend induction chemotherapy before appropriate tumor resection by orthopedic surgery, either alone or combined with radiotherapy. In general, R0 resection with negative margins should be aimed at. If possible, limbs and joints should be preserved, otherwise reconstruction by means of allografts or endoprosthetics is required. Since Ewing sarcoma is radiosensitive in contrast to osteosarcoma, radiotherapy should be considered in case of inoperability. Local therapy is followed by adjuvant chemotherapy. Applied chemotherapeutics involve vincristine, doxorubicin, cyclophosphamide, etoposide, ifosfamide and occasionally actinomycin D and topotecan. High risk patients, i.e. those with primary metastasis at diagnosis or with recurrent disease, receive remission induction chemotherapy and local treatment before they undergo myeloablative therapy. (Bernstein *et al.* 2006; Burdach & Jurgens 2002; Burdach *et al.* 2000; Potratz *et al.* 2012) Myeloablative therapy involves high-dose chemotherapy with autologous hematopoietic stem cell rescue as well as irradiation of metastases, for example total bone marrow irradiation or irradiation of the lung. Melphalan, etoposide and carboplatin are examples of applied high-dose chemotherapeutics. (Burdach & Jurgens 2002; Burdach *et al.* 1993; Burdach *et al.* 1996)

Several prognostic factors were revealed to be unfavorable for patients with Ewing sarcoma. Those involve age > 10 years, tumor size > 200 ml and pelvic tumor location in general. Moreover, prognosis differs depending on exact type of translocation and potential cytogenetic changes. (Bernstein *et al.* 2006) Presence of metastasis, however, is the most unfavorable prognostic feature for patients and reduces survival probabilities massively. In the 1980s, survival probability ten years after diagnosis amounted to less than 55% in Germany. Since then numbers have been improving a little; altogether, they are still frustrating though. These days, patients with localized disease have survival rates between 65-70%. In case of metastasis, however, survival

rates decrease severely and only amount to 28%. (Bernstein *et al.* 2006; Deutsches Kinderkrebsregister, p. 48; Duchman *et al.* 2015) In contrast to this, survival probability ten years after diagnosis of an acute lymphoid leukemia, the most frequent pediatric malignoma, is more than 90%. (Deutsches Kinderkrebsregister, p. 15) Furthermore, Ewing sarcoma patients with multifocal bone or bone marrow metastases were revealed to have a poorer prognosis than patients with lung metastases and patients with a relapse within 24 months were found to have a poorer prognosis than patients with a relapse later than 24 months after diagnosis. (Burdach & Jurgens 2002)

Disappointing survival rates stress the necessity of alternate therapeutic approaches. Especially metastatic and recurrent diseases are difficult to treat. In these cases, chemotherapy options are limited depending on prior treatment and potential impaired organ function (especially heart and kidney). A general relapse rate of 30% is unacceptable as well. (Bernstein *et al.* 2006; Potratz *et al.* 2012) Furthermore, tumors develop complex therapy resistance mechanisms. Chemotherapy-resistant cancer stem cells may give rise to new populations of tumor cells. Other tumor cells may induce drug-metabolizing enzymes or modulate signaling pathways. (Ahmed *et al.* 2014) Development of targeted therapies is necessary to improve survival rates. Especially targeting fusion protein EWS-FLI1 which is only expressed in Ewing sarcoma may be promising. Targeted therapies could also help to decrease the risk for secondary complications due to sarcoma treatment in surviving patients, such as cardiac and renal insufficiency or secondary malignancies. At least 1-2% of patients develop an acute leukemia following sarcoma treatment. (Bernstein *et al.* 2006)

Several genes such as DKK2, STEAP1 and GPR64 were found to be highly upregulated in Ewing sarcoma and associated with tumor growth, invasiveness and metastasis. (Grunewald *et al.* 2012; Hauer *et al.* 2013; Richter *et al.* 2013) EZH2 was detected to maintain an undifferentiated phenotype in Ewing sarcoma by blocking endothelial and neuro-ectodermal differentiation. (Burdach *et al.* 2009; Richter *et al.* 2009)

Recently, transgenic allo-restricted CD8-positive T cells have been generated which successfully recognize such tumor-associated target genes and thus, inhibit Ewing sarcoma growth *in vitro* and *in vivo*. (Blaeschke *et al.* 2016; Schirmer *et al.* 2016; Thiel *et al.* 2011)

It is essential for the development of targeted therapies to gain as much insight as

possible into pathogenesis of Ewing sarcoma.

1.5 Aim of this study and experimental approach

The aim of this doctoral thesis was to elucidate the role of HOX genes in pathogenesis of Ewing sarcoma. Microarray data revealed HOXD10, HOXD11 and HOXD13 to be highly upregulated in Ewing sarcoma tissues. Little is known about detailed functions of HOX genes in malignant tumors though.

One of the first aims was to find a regulatory mechanism of HOX expression in Ewing sarcoma. Ewing sarcomas are characterized by certain chromosome translocations which usually result in oncogenic fusion of EWS to FLI1. Therefore, it was examined if expression of HOXD10, HOXD11 and HOXD13 was dependent on EWS-FLI1. In development, HOX genes are usually controlled by EZH2 which in turn is also highly upregulated in Ewing sarcoma tissues. Thus, it was investigated if this regulation had been conserved in this malignant tumor. For this purpose, EWS-FLI1 and EZH2 were downregulated by siRNA interference in several Ewing sarcoma cell lines, respectively, and expression of HOXD10, HOXD11 and HOXD13 was determined using qRT-PCR.

Next aim was to gain insight into the function of these three HOX genes in pathology of Ewing sarcoma. For this purpose, each of these three HOX genes was downregulated by siRNA interference in several Ewing cell lines. In two cell lines, SK-N-MC and A-673, HOXD10, HOXD11 and HOXD13 were also constitutively suppressed by retroviral gene transfer, respectively. Effect of HOX knockdown was examined in several *in vitro* assays and extensive gene expression analysis. Among other things, proliferation, capability of endothelial tube formation and anchorage-independent growth were assessed. According to published literature, posterior HOXD genes are involved in cartilage and bone formation. Since gene expression analysis identified several genes associated with bone and cartilage formation to be downregulated after HOX knockdown, particular attention was directed to the potential of Ewing sarcoma cells to differentiate towards osteoblasts and chondrocytes depending on HOX expression. In addition, microarray analysis was implemented to identify potential downstream HOX targets.

Another doctoral student was intended for repeat experiments and confirmation of results of *in vitro* experiments in an orthotopic bone xenotransplantation model.

2 Materials and methods

2.1 Materials

2.1.1 List of manufacturers

Abbott	Wiesbaden, Germany
Abcam	Cambridge, UK
Abgent	San Diego, CA, USA
Abnova	Taipei, Taiwan
ACEA Biosciences	San Diego, CA, USA
AEG	Nuremberg, Germany
Affimetrix	High Wycombe, UK
Ambion	Austin, TX, USA
Amersham Biosciences	Piscataway, NJ, USA
Applied Biosystems (Life Technologies)	Darmstadt, Germany
ATCC	Rockyville, MD, USA
B. Braun Biotech Int.	Melsungen, Germany
Bayer HealthCare Pharmaceuticals	Leverkusen, Germany
BD (Becton, Dickinson and Company)	Heidelberg, Germany
BD Biosciences Europe	Heidelberg, Germany
Beckman Coulter	Palo Alto, CA, USA
Berthold Detection Systems	Pforzheim, Germany
Biochrom	Berlin, Germany
Biometra	Göttingen, Germany
BioRad	Richmond, CA, USA
Biowhittaker	East Rutherford, NJ, USA
Biozym	Hessisch Oldendorf, Germany
Brand	Wertheim, Germany
Branson	Dietzenbach, Germany
Carestream Health, Inc.	Stuttgart, Germany
Carl Roth GmbH & Co. KG	Karlsruhe, Germany
Cayman Chemical Company	Ann Arbor, MI, USA
Cell Signaling Technology	Frankfurt am Main, Germany
Charles River Laboratories	Wilmington, MA, USA

Clontech-Takara Bio Europe	Saint-Germain-en-Laye, France
Covance	Princeton, NJ, USA
DSMZ	Braunschweig, Germany
Eppendorf	Hamburg, Germany
Falcon	Oxnard, CA, USA
Feather	Osaka, Japan
Fermentas	St. Leon-Rot, Germany
GE Healthcare	Uppsala, Sweden
Genomed	St. Louis, MO, USA
Genzyme	Neu-Isenburg, Germany
GFL	Segnitz, Germany
GIBCO(Life Technologies GmbH)	Darmstadt, Germany
GLW	Würzburg, Germany
Greiner bio-one (Gbo)	Nürtingen, Germany
Hamilton	Bonaduz, Switzerland
Heidolph Instruments	Schwabach, Germany
Heraeus	Hanau, Germany
ImaGenes GmbH	Berlin, Germany
Implen GmbH	Munich, Germany
Invitrogen (Life Technologies)	Karlsruhe, Germany
Jackson ImmunoResearch Laboratories	West Grove, PA, USA
Josef Peske GmbH	Aindling, Germany
Kern & Sohn	Balingen, Germany
Kimberly-Clark Professional	Koblenz, Germany
Köttermann GmbH & Co KG	Uetze/Hänigsen, Germany
Laborservice	Harthausen, Germany
Leica	Wetzlar, Germany
LMS Consult (Laboratory & Medical Supplies)	Brigachtal, Germany
Lonza	Basel, Switzerland
Macherey-Nagel	Düren, Germany
Memmert	Schwabach, Germany
Merck	Darmstadt, Germany
Metabion International AG	Martinsried, Germany
Millipore	Billerica, MA, USA
Miltenyi Biotec GmbH	Bergisch Gladbach, Germany

Molecular Bio Products Inc.	San Diego, CA, USA
Nalge Nunc International	Naperville, IL, USA
Nalgene	Rochester, NY, USA
New England Biolabs	Frankfurt am Main, Germany
Nikon	Düsseldorf, Germany
PAA Laboratories GmbH	Cölbe, Germany
Pan Biotech GmbH	Aidingen, Germany
Pechiney Plastic Packaging	Menasha, WI, USA
Peqlab	Erlangen, Germany
Philips	Hamburg, Germany
Promega	Fitchburg, WI, USA
Qiagen Inc.	Valencia, CA, USA
R&D Systems	Minneapolis, MN, USA
Ratiopharm	Ulm, Germany
Roche	Mannheim, Germany
Santa Cruz Biotechnology	Heidelberg, Germany
Sarstedt	Nümbrecht, Germany
Sartorius	Göttingen, Germany
Scientific Industries	Bohemia, NY, USA
Scotsman Ice Systems	Milan, Italy
Sempermed	Vienna, Austria
Siemens	Munich, Germany
Sigma-Aldrich	St. Louis, MO, USA
Stratagene	Cedar Creek, TX, USA
Syngene	Cambridge, UK
Systec GmbH	Wettenberg, Germany
Taylor-Wharton	Mildstedt, Germany
Techlab GmbH	Braunschweig, Germany
Thermo Fisher Scientific	Ulm, Germany
Thermo Scientific GmbH	Schwerte, Germany
TKA Wasseraufbereitungssysteme	Niederelbert, Germany
TPP Techno Plastic Products AG	Trasadingen, Switzerland
Tuttnauer	PR Breda, The Netherlands
Whatman GmbH	Dassel, Germany
Zeiss	Jena, Germany

2.1.2 Instruments and equipment

Type of device		Manufacturer
Airflow		Köttermann
Autoclave	Systec 2540EL	Tuttnauer
Autoclave	Systec V95	Tuttnauer
Bacteria shaker	Certomat® BS-T	Sartorius
Camera	Coolpix 5400	Nikon
Cell counting chamber	Neubauer	Brand
Centrifuge	Multifuge 3 S-R	Heraeus
Centrifuge	Biofuge fresco	Heraeus
Centrifuge	Centrifuge 5417 R	Eppendorf
Controlled-freezing box	Mr. Frosty™ Cryo 1°C Freezing Container	Nalgene
Drying cabinet		Memmert
Flow cytometer	FACSCalibur™	BD
Freezer (-20° C)	cool vario	Siemens
Freezer (-80° C)	Hera freeze	Heraeus
Fridge (+4° C)	cool vario	Siemens
Heater		Memmert
Heating block	Thermomixer Comfort	Eppendorf
Ice flaker	AF 100	Scotsman
Incubator	Hera cell 150	Heraeus
Inverted microscope	Eclipse TS 100	Nikon
Liquid Nitrogen Tank	K Series 24K	Taylor-Wharton
Luminometer	Sirius	Berthold Detection Systems
Micropipettes	0.5-10 µl, 10-100 µl, 20-200 µl, 100-1000 µl	Eppendorf
Microscope		Leica
Microscope (fluorescence)	AxioVert 100	Zeiss
Mini Centrifuge	MCF-2360	LMS Consult
Multichannel plate	10-100 µl	Eppendorf
PCR cycler	iCycler	BioRad
Photometer	NanoPhotometer™ Pearl	Implen GmbH
Pipetting assistant	Easypet	Eppendorf

Type of device		Manufacturer
Power supplier	Standard Power Pack P25	Biometra
qRT-PCR cycler	7300 Real-Time PCR	Applied Biosystems
Real-Time Cell Analyzer	xCELLigence	ACEA Biosciences
Shaker	REAX top	Heidolph Instruments
Sterile Bench		Heraeus
Vortexer	Vortex-Genie 2	Scientific Industries
Water bath		GFL
Water purification system	TKA GenPure	TKA GmbH

2.1.3 Commonly used materials

Cryovials	Nunc
Culture plates (100 mm Ø)	Nunc
Cuvettes	Carl Roth
E-Plates (96-well)	ACEA Biosciences
Filters for cells, Cell Strainer	Falcon
Filter for solutions (0.2 µm and 0.45 µm)	Sartorius
Flasks for cell culture (75 cm² and 175 cm²)	TPP
Gloves (nitrile, latex)	Sempermed
Hybond-P PVDF membrane	GE Healthcare
Hypodermic needle (23 G)	B. Braun
Kleenex® Facial tissues	Kimberly-Clark Professional
Parafilm	Pechiney Plastic Packaging
Pasteur pipettes	Peske OHG
Petri dishes (35 x 10 mm)	Becton Dickinson
Pipettes Cellstar® (2, 5, 10 and 25 ml)	Greiner bio-one
Pipette tips (200 and 1000 µl)	Sarstedt
Pipette tips (10, 100, 200 and 1000 µl with a filter)	Molecular Bio Products
Plates for cell culture (6-well, 24-well)	BD Falcon
Plates for cell culture (12-well, 96-well)	TPP
Plates for qRT-PCR (96-well)	Applied Biosystems
Scalpels (12, 15, 20)	Feather
Tubes for cell culture (polystyrene, 15 ml)	Falcon
Tubes for cell culture (polypropylene, 15 ml and 50 ml)	Falcon

Tubes for molecular biology, Safelock (1.5 ml and 2 ml)	Eppendorf
Tubes for FACS™ (5 ml)	Falcon
Whatman paper	Whatman GmbH

2.1.4 Chemical and biological reagents

Alcian blue	Sigma-Aldrich
Alizarin red	Sigma-Aldrich
Agar	Sigma-Aldrich
Agarose	Invitrogen
Ampicillin	Merck
AmpliTaq DNA Polymerase	Invitrogen
Ammonium persulfate (APS)	Sigma-Aldrich
2-Mercaptoethanol	Sigma-Aldrich
BCP (1-bromo-3-chloropropane)	Sigma-Aldrich
Bromphenol blue	Sigma-Aldrich
Calcein AM Fluorescent Dye	BD Biosciences
DEPC (diethyl pyrocarbonate)	Sigma-Aldrich
DEPC treated water	Applied Biosystems
Deoxycholic acid	Carl Roth
Dimethylformamide	Carl Roth
dNTPs	Roche
DMEM medium	Invitrogen
DMSO (dimethyl sulfoxide)	Sigma-Aldrich
DTT (DL-Dithiothreitol)	Sigma-Aldrich
EDTA (ethylenediaminetetraacetate)	Merck
EtBr (Ethidium bromide)	BioRad
Ethanol	Carl Roth
FBS (fetal bovine serum)	Biochrom
37% formaldehyde	Merck
Gentamycin	Biochrom
Glycerol	Merck
Glycine	Merck
G418	PAA
HBSS (Hank's buffered salt solution)	Invitrogen
HCl (hydrochloric acid)	Merck

HEPES	Sigma-Aldrich
HiPerFect Transfection Reagent	Qiagen
Human IgG	Genzyme
IMDM medium	Invitrogen
Isopropanol	Carl Roth
KCl (potassium chloride)	Merck
L-glutamine	Invitrogen
Matrigel matrix	BD Biocoat
Maxima^{TM} Probe/ROX qPCR Master Mix (2x)	Fermentas
Methanol	Carl Roth
Human Methylcellulose Base Media	R&D Systems
$MgCl_2$ (magnesium chloride)	Invitrogen
NaCl (sodium chloride)	Merck
$NaHCO_3$ (sodium hydrogen carbonate)	Merck
NaN_3 (sodium azide)	Merck
NaOH (sodium hydroxide)	Merck
Nonidet-P40 (NP40)	Sigma-Aldrich
DPBS 10x (Dulbecco's phosphate buffered saline)	Invitrogen
PCR Buffer (10x)	Invitrogen
Penicillin/streptomycin	Invitrogen
Peptone	Invitrogen
PFA (paraformaldehyde)	Merck
PMSF (phenylmethanesulfonylfluoride)	Sigma-Aldrich
Polyacrylamide (30% Acrylamide/Bis)	Merck
Polybrene (hexadimethrine bromide)	Sigma-Aldrich
Propidium iodide	Sigma-Aldrich
Protease Inhibitor cocktail tablets	Roche
Proteinase K	Sigma-Aldrich
Puromycin	PAA
Ready-Load 1 kb DNA Ladder	Invitrogen
RNase A (Ribonuclease A)	Roche
RPMI 1640 medium	Invitrogen
SDS	Sigma-Aldrich
Skim milk powder	Merck
Streptavidin-agarose beads	Merck

SYBR Green Master Mix	Applied Biosystems
TEMED (N,N,N',N'-Tetramethylethan-1,2-diamin)	Sigma-Aldrich
Tris	Merck
Triton X-100	Sigma-Aldrich
Trypan blue	Invitrogen
Trypsin/EDTA	Invitrogen
Tween 20	Sigma-Aldrich

2.1.5 Commercial reagent kits

DNeasy® Blood & Tissue Kit	Qiagen
Gene Jet™ RNA Purification Kit	Fermentas
High-Capacity cDNA Reverse Transcription Kit	Applied Biosystems
MycoAlert® Mycoplasma Detection Kit	Lonza
NucleoSpin® Plasmid Kit	Macherey-Nagel
RNeasy® Mini Kit	Qiagen
StemPro® Chondrogenesis Differentiation Kit	GIBCO
StemPro® Osteogenesis Differentiation Kit	GIBCO
TaqMan Gene Expression Assays	Applied Biosystems
TRI Reagent® Solution	Ambion

2.1.6 Cell culture media

Chondrogenic differentiation medium	45 ml StemPro® Osteocyte/Chondrocyte Differentiation Basal Medium 5 ml StemPro® Chondrogenesis Supplement 5 mg gentamycin
Control growth medium for osteogenic and chondrogenic differentiation	445 ml DMEM 50 ml FBS 5 ml L-glutamine (200 mM) 12.5 mg gentamycin
Freezing medium	45 ml FBS 5 ml DMSO
Osteogenic differentiation medium	45 ml StemPro® Osteocyte/Chondrocyte Differentiation Basal Medium 5 ml StemPro® Osteogenesis Supplement 5 mg gentamycin
Standard tumor medium	500 ml RPMI 1640 55 ml FBS 50 mg gentamycin

2.1.7 Universal solutions

1x PBS	900 ml sterile water 100 ml 10x DPBS
1x Trypsin/EDTA	45 ml PBS 5 ml Trypsin/EDTA (10x)
4% formaldehyde	4% Formalin 55 mM Na2HPO4 12 mM NaH2PO4 2 H2O
70% Ethanol	35 ml 100% Ethanol 15 ml DEPC-treated water
Alcian Blue Staining Solution	1% Alcian blue in 0.1 N HCl
Alizarin Red Staining Solution	2% Alizarin red at a pH of 4.2
Calcein Stock	1 mg Calcein AM 1 ml DMSO

2.1.8 Small interfering RNAs

siRNA name	**Target sequence**
EWS-FLI1_1	5’-GCT ACG GGC AGC AGA ACC CTT-3’
EWS-FLI1_2	5’-GCA GAA CCC TTC TTA TGA CTT-3’
EZH2_7 validated	5’-AAC CAT GTT TAC AAC TAT CAA-3’
HOXD10_1	5’-CAG GGT AAC TAT TAT TGC GCA-3’
HOXD10_4	5’-CTC CTT CAC CAC CAA CAT TAA-3’
HOXD11_3	5’-CCC GTC TGA CTT CGC TAG CAA-3’
HOXD11_5	5’-CTC AAC CTC ACT GAC CGG CAA-3’
HOXD11_6	5’-TTG GCC GAG CGG ATC CTA ATA-3’
HOXD11_7	5’-AAC CGT CGT CCT GCC AGA TGA-3’
HOXD13_2	5’-ACG AAC CTA TCT GAG AGA CAA-3’
HOXD13_3	5’-GCC AGT ATA AAG GGA CTT GAA-3’
negative control siRNA	5’-AAT TCT CCG AAC GTG TCA CGT-3’
EIF2C1_2	5´-CTC CAA GAA TTG TGC AAG TAA-3´
EIF2C1_3	5´-CAG CTA CAA CTT AGA TCC CTA-3´
EIF2C2_5	5´-CAG CAC CGG CAG GAG ATC ATA-3´
EIF2C2_6	5´-CAG GCG TTA CAC GAT GCA CTT-3´

2.1.9 Oligonucleotides for retroviral gene transfer

Oligonucleotides for retroviral gene transfer each consisting of 66 bases were obtained from Metabion International AG, Martinsried, Germany.

Oligonucleotide name	Oligo sequence
HOXD10 - forward	5'-GAT CCG GGG TAA CTA TTA TTG CGC ATT CAA GAG ATG CGC AAT AAT AGT TAC CCC TTT TTT CTA GAG-3'
HOXD10 - reverse	5'-AAT TCT CTA GAA AAA AGG GGT AAC TAT TAT TGC GCA TCT CTT GAA TGC GCA ATA ATA GTT ACC CCG-3'
HOXD11 - forward	5'-GAT CCG CGT CTG ACT TCG CTA GCA ATT CAA GAG ATT GCT AGC GAA GTC AGA CGC TTT TTT CTA GAG-3'
HOXD11 - reverse	5'-AAT TCT CTA GAA AAA AGC GTC TGA CTT CGC TAG CAA TCT CTT GAA TTG CTA GCG AAG TCA GAC GCG-3'
HOXD13 - forward	5'-GAT CCG GAA CCT ATC TGA GAG ACA ATT CAA GAG ATT GTC TCT CAG ATA GGT TCC TTT TTT CTA GAG-3'
HOXD13 - reverse	5'-AAT TCT CTA GAA AAA AGG AAC CTA TCT GAG AGA CAA TCT CTT GAA TTG TCT CTC AGA TAG GTT CCG-3'
Negative control - forward	5'-GAT CCG TTC TCC GAA CGT GTC ACG TTT CAA GAG AAC GTG ACA CGT TCG GAG AAC TTT TTT CTA GAG-3'
Negative control - reverse	5'-AAT TCT CTA GAA AAA AGT TCT CCG AAC GTG TCA CGT TCT CTT GAA ACG TGA CAC GTT CGG AGA ACG-3'

2.1.10 Bacterial strain

The following bacterial strain was used for plasmid propagation. This process was necessary for HOX knockdown by retroviral gene transfer.

Bacterial strain	Genotype	Manufacturer
E. coli strain: One Shot TOP10	F- mcrA Δ(mrr-hsdRMS-mcrBC) Φ80lacZΔM15 ΔlacX74 recA1 araD139 Δ(araleu)7697 galU galK rpsL (StrR) endA1 nupG	Invitrogen

2.1.11 Primers for qRT-PCR

Depending on type of qRT-PCR, TaqMan® probe-based or SYBR® Green-based (see 2.2.7), two different kinds of primers were used.

2.1.11.1 Primers for SYBR® Green-based qRT-PCR

The concentration of primers was 900 and 250 nM, respectively.

Primer name	Sequence
pMSCVneo/pSIREN - forward	5'-GGG CAG GAA GAG GGC CTA T-3'
pMSCVneo/pSIREN - reverse	5'-GAG ACG TGC TAC TTC CAT TTG TC-3'
EWS-FLI1 - forward	5'- TAG TTA CCC ACC CAA ACT GGA T-3'
EWS-FLI1 - reverse	5'- GGG CCG TTG CTC TGT ATT CTT AC-3'
ACTB - forward	5'- GGC ATC GTG ATG GAC TCC G-3'
ACTB - reverse	5'- GCT GGA AGG TGG ACA GCG A-3'

2.1.11.2 TaqMan® Gene Expression Assays

All TaqMan® Gene Expression Assays were obtained from Applied Biosystems.

Gene	Assay ID
ATRX	Hs00230877_m1
BGLAP	Hs01587814_g1
BMP2	Hs00154192_m1
BMP4	Hs00370078_m1
COL10A1	Hs00166657_m1
COL1A1	Hs00164004_m1
COL2A1	Hs00264051_m1
EEF1D	Hs02339452_g1
EIF2C1	Hs00201864_m1
EIF2C2	Hs00293044_m1
EZH2	Hs00544830_m1
GAPDH	Hs02758991_g1
HAUS6	Hs00405942_m1
HOXD10	Hs00157974_m1
HOXD11	Hs00360798_m1
HOXD13	Hs00968515_m1
POSTN	Hs00170815_m1
RAC2	Hs01032884_m1
RUNX2	Hs01047978_m1
SMAD4	Hs00929647_m1
SOX9	Hs00165814_m1
SP7	Hs00541729_m1
SPP1	Hs00959010_m1

2.1.12 Expression vectors

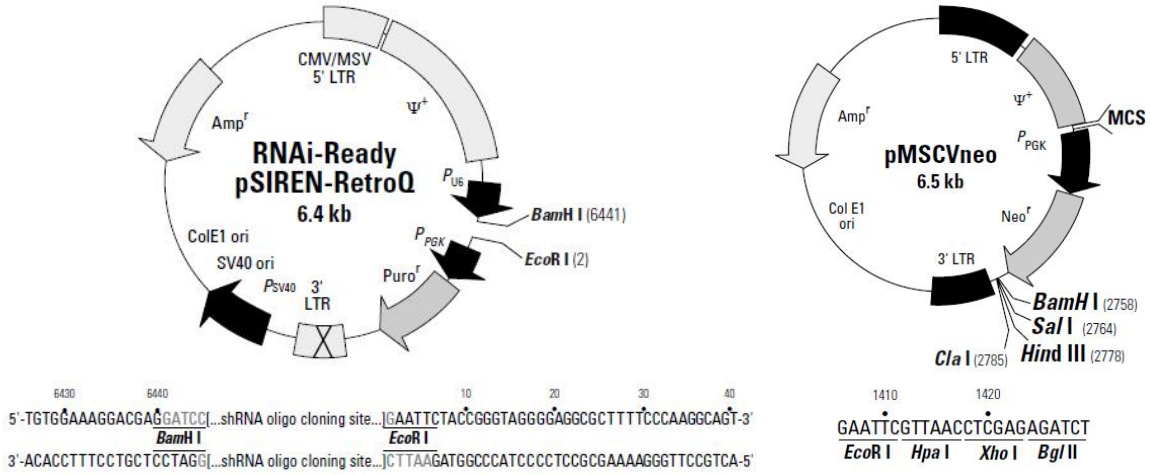

Figure 7: Maps of expression vectors.
Left panel: pSIREN vector. Constitutive HOX knockdowns in Ewing sarcoma cells were achieved by this retroviral vector which expressed expressed specific shRNAs. **Right panel:** pMSCVneo vector. MSCV Retroviral Expression System was used for introducing and expressing EWS-FLI1 in two mesenchymal stem cell lines.

2.1.13 Human cell lines

Human cell lines, except A-673, EW-7 and SB-KMS-KS1, were acquired from the German collection of Microorganisms and Cell Cultures (Leibniz Institute DSMZ, Braunschweig, Germany).

A-673 was obtained from the American Type Culture Collection (ATCC, Manassas, USA). EW-7 was kindly provided by Prof. Olivier Delattre (L'Institut National de la Santé et de la Recherche Médicale U830, Institut Curie, Paris, France). SB-KMS-KS1 is a Ewing sarcoma cell line that was established in our laboratory. L87 and V54.2 are two mesenchymal stem cell lines which were immortalized with SV40 large T-antigen. (Moosmann *et al.* 2005) PT67 is a retroviral packaging cell line which was obtained from Takara Bio Europe/Clontech.

A-673	ES cell line (type 1 translocation) A-673 was originally established from the primary tumor of a 15-year-old girl with possible rhabdomyosarcoma in 1973 . I. Roberts *et al.* (1999), however, indicated that A-673, which is also known as RMS 1598, originated from a Ewing sarcoma: chromosomal abnormalities, including the translocation t(13;11;22), and the EWS-FLI1 fusion transcript were detected, just as a p53 mutation.

EW-7	ES cell line (type 1 translocation) EW-7 derived from the primary tumor of the scapula of a Ewing sarcoma patient before chemotherapy. (Javelaud *et al.* 2000)
HOS	Osteosarcoma cell line HOS was established from the biopsy of an osteosarcoma of the distal right femur of a 13-year-old Caucasian girl before any x-ray or chemotherapy. (McAllister *et al.* 1971)
L87	Mesenchymal stem cell line L87 was derived from the bone marrow of a healthy male patient. It is a permanent Simian virus 40-transformed mesenchymal stem cell line which shows a fibroblastoid morphology. (Moosmann *et al.* 2005; Thalmeier *et al.* 1994)
MG-63	Osteosarcoma cell line MG-63 was derived from an osteogenic sarcoma of a 14-year-old Caucasian boy. (Heremans *et al.* 1978)
MHH-ES-1	ES cell line (type 2 translocation) MHH-ES-1 was established from the ascites of a 12-year-old Turkish boy with peritoneal metastasis. The primary tumor was located in the left pelvis. (Pietsch *et al.* 1989)
RD-ES	ES cell line (type 2 translocation) RD-ES was established from the primary tumor of the humerus of a 19-year-old Caucasian man in 1984 (see DSMZ datasheet, catalogue no. ACC 260).
SAOS-2	Osteosarcoma cell line SAOS-2 was established from the primary osteogenic sarcoma of an 11-year-old Caucasian girl in 1973. (Fogh & Trempe 1975)
SB-KMS-KS1	ES cell line (type 1 translocation) SB-KMS-KS1 derived from an extraosseous inguinal metastasis of a 17-year-old female patient and was established in our laboratory. The cell line was previously described as SBSR-AKS. (Richter *et al.* 2009)
SH-SY5Y	Neuroblastoma cell line SH-SY5Y is a thrice cloned (SK-N-SH > SH-SY > SH-SY5 > SH-SY5Y) subline of the neuroblastoma cell line SK-N-SH (see DSMZ datasheet, catalogue no. ACC 209). SK-N-SH was established in 1970 from the bone marrow biopsy of a 4-year-old girl with metastatic neuroblastoma. (Biedler *et al.* 1973)
SiMA	Neuroblastoma cell line SiMA was established from the adrenal tumor from a 20-month-old boy of European origin with neuroblastoma (stage III) in 1991 (see DSMZ datasheet, catalogue no. ACC 164). After treatment with two blocks of chemotherapy, a residual tumor mass of 7 x 6 x 3.5 cm was resected. (Marini *et al.* 1999)

SK-ES-1	ES cell line (type 2 translocation) SK-ES-1 was derived from the Ewing sarcoma of an 18-year-old man in 1971 (see DSMZ datasheet, catalogue no. ACC 518). Its cell surface antigens were further defined by cytotoxicity tests by Bloom in 1972. (Bloom 1972)
SK-N-MC	ES cell line (type 1 translocation) SK-N-MC was established from the biopsy of the supraorbital metastasis of a 14-year-old girl after systemic chemotherapy and radiotherapy. (Biedler *et al.* 1973) The cell line was first classified as neuroblastoma (Biedler *et al.* 1973) but is now widely regarded as having originated from the morphologically similar Askin's tumor (see DSMZ datasheet, catalogue no. ACC 203) because FLI1-EWS gene fusion in SK-N-MC was shown by Dunn *et al.* (1994). (Dunn *et al.* 1994)
TC-71	ES cell line (type 1 translocation) TC-71 was derived from a biopsy of recurrent tumor at the primary site of a 22-year-old man with metastatic Ewing sarcoma of the humerus (see DSMZ datasheet, catalogue no. ACC 516). The cell line was established in 1981 and further cytogenetically characterized by Whang-Peng *et al.* (1986).
U-2 OS	Osteosarcoma cell line U-2 OS was derived from a 15-year-old Caucasian girl with moderately differentiated osteogenic sarcoma of the tibia in 1964. (Ponten & Saksela 1967)
V54.2	Mesenchymal stem cell line V54.2 was generated from peripheral blood mononuclear cells of a healthy volunteer donor after G-CSF-mediated stem cell mobilization. It is immortalized and shows a fibroblast-like cell growth. (Conrad *et al.* 2002; Moosmann *et al.* 2005)
PT67	Retrovirus packaging cell line PT67 which was obtained from Takara Bio Europe/Clontech was used for retroviral gene transfer (see 2.2.4). Viral supernatant for transfection of Ewing sarcoma cells was harvested from these cells.

2.2 Methods

2.2.1 Cell culture

2.2.1.1 Culture of tumor cells

Ewing sarcoma cell lines were cultured in standard tumor medium, which contained RPMI, heat-inactivated fetal bovine serum and gentamycin, at 37°C and 5% CO_2 in a humidified atmosphere. Volume of the medium was 20 ml in middle-sized culture flasks (75 cm² adherence surface) and 30 ml in large-sized culture flasks (175 cm² adherence surface).

When cells grew to confluence, which was about every 3-4 days, medium was removed and cells were split 1:2 to 1:10, depending on growth rate of the individual cell lines. A-673, for example, grows much faster than SK-N-MC due to a p53 mutation.

To split the cells, medium was removed first. Then, cells were washed once with 10 ml pre-warmed 1x PBS. After that they were coated with 3-4 ml 1x trypsin and incubated at 37°C and 5% CO_2 for 2-5 minutes. Cells were detached by fresh standard tumor medium. The cell suspension was decanted into a Falcon tube which was centrifuged at 1200 rpm for 7 minutes. After that the supernatant was decanted carefully and the cell pellet was vortexed in 10 ml prewarmed 1x PBS and centrifuged at 1200 rpm for 7 minutes again. Cells were then resuspended in fresh standard tumor medium and spread in new culture flasks.

The retrovirus packaging cell line PT67 was grown at 37 °C in 8 % CO_2 in middle-sized culture flasks in a humidified atmosphere. They were cultivated in DMEM containing 10 % fetal bovine serum, 1 % L-glutamine and 100 µg/ml gentamycin.

Cell amounts were determined by use of a Neubauer counting chamber. Cell viability was assessed by trypan blue exclusion.

2.2.1.2 Cryopreservation of cells

Tumor cell lines were frozen at concentrations between 1×10^6 and 1×10^7 cells in volumes of 1-1.5 ml each. Pelleted cells were resuspended in an appropriate volume of precooled freezing medium, consisting of FBS and DMSO (see 2.1.6, page 36). Aliquots of the cell suspension were then transferred into cryovials. These cryovials were placed

into controlled freezing boxes, stored at -80°C overnight before being transferred into the liquid nitrogen freezer (-192°C) for long-term storage.

2.2.1.3 Recultivating of cryopreserved cells

Cryopreserved cells were thawed in freezing medium. Cryovials were defrozen on ice at room temperature until only small ice crystals were left inside. The content was then rapidly transferred into a 15 ml Greiner tube containing 10 ml of fresh RPMI standard tumor medium. This tube was then centrifuged at 1200 rpm for 7 minutes and the cell pellet was resuspended in 1 ml pre-warmed standard tumor medium and transferred into a middle-sized culture flask that had already contained 19 ml of this medium.

2.2.1.4 Testing for mycoplasma

Cultured cells were routinely tested for mycoplasma using MycoAlert™ Mycoplasma Detection Kit according to manufacturer's protocol (Lonza Walkersville, Inc., 2011). Briefly, 100 µl of culture supernatant was taken as the sample. MycoAlert® Reagent was added and luminescence was measured after 5 minutes. After adding MycoAlert® Substrate luminescence was measured again after another 10 minutes.

2.2.2 Transient RNA interference

Efficient siRNA transfections for effective transient gene silencing were performed using HiPerFect Transfection Reagent according to the protocol for large-scale transfection of adherent cells with siRNA in 100 mm dishes (see page 48, HiPerFect Transfection Reagent Handbook 10/2010, Qiagen).

Specific siRNAs for target genes were purchased from Qiagen, so was the negative control siRNA which is a non-silencing siRNA with no homology to any known mammalian gene. It has been shown to provide minimal nonspecific effects on gene expression and phenotype. Used siRNAs are listed in 2.1.8.

Shortly before transfection, 1-2 × 10^6 cells were seeded in 10 ml of standard tumor medium in a 100 mm culture dish. For the short time until transfection, cells were incubated under normal growth conditions, meaning 37°C and 5% CO_2 in a humidified atmosphere.

For the transfection reagent, 3.6-5 µl of 5 nM siRNA was diluted in 2 ml RPMI culture medium without serum. After adding 36 µl HiPerFect Transfection Reagent, the transfection reagent was mixed by vortexing and the samples were incubated at room temperature for 8 minutes to allow the formation of transfection complexes. After 8 minutes the transfection complexes were added drop-wise onto the cells in the 100 mm culture dishes, generating a finale volume of 12 ml per culture plate. The dishes were gently swirled to ensure uniform distribution of the transfection complexes. The cells with the transfection complexes were incubated under normal growth conditions for an appropriate time (24-72 hours).

After that RNA was isolated and gene silencing was monitored by qRT-PCR.

Triple HOX knockdown was performed analogically, just using the triple amount of siRNA, meaning 3.6-5 µl of each HOX siRNA (HOXD10, HOXD11, HOXD13) generating a final volume of 10.8-15 µl.

2.2.3 RNA isolation

For gene expression analysis by qRT-PCR, RNA from cultured cells had to be isolated. Because of organizational changes in the laboratory during this work three different methods were applied.

RNA was isolated by means of RNeasy® Mini Kit and TRI Reagent® most of the time. Gene JET™ Purification Kit was made use of for RNA isolation in the two differentiation assays (see 2.2.9.4 and 2.2.9.5).

For each of these three methods, though, cells were harvested the same way: cells in culture flasks or culture plates were washed once with PBS and then trypsinized. After the cells had detached from the dish or flask, standard tumor medium containing serum to inactivate the trypsin was added and cells were transferred into an RNase-free tube. Cells were pelleted by centrifugation (1200 rpm for 7 minutes) and the supernatant was removed.

2.2.3.1 RNeasy® Mini Kit

RNeasy® Mini Kit provides fast purification of high-quality RNA from cells, tissues and yeast using silica-membrane columns with a binding capacity of 100 µg RNA. Isolation of total RNA using this kit was performed according to the manufacturer's protocol

(Purification of Total RNA from Animal Cells Using Spin Technology, RNeasy Mini Handbook 04/2006, Qiagen).

The cell pellet was generated as described above. It was lysed in an appropriate volume of RLT Buffer, meaning 350 µl for $<5 \times 10^6$ cells and 600 µl for $>5 \times 10^6$ cells. RLT Buffer contains 10 µl β-mercaptoethanol per ml RLT. The lysate was then homogenized by vortexing. After that, the equal volume of 70% ethanol, meaning 350 µl or 600 µl, was added and mixed well with the lysate by pipetting.

Up to 700 µl of the sample, including any precipitate that may have formed, was transferred to an RNeasy spin column placed in a 2 ml collection tube. Tubes were centrifuged for 1 minute at 10,500 rpm at 4°C. Then the flow-through was discarded and 500 µl Buffer RW1 was added to the RNeasy spin column to wash the spin column membrane. Again, the tube was centrifuged for 1 minute at 10,500 rpm and the flow-through was discarded. Then, 500 µl Buffer RPE was added to the RNeasy spin column and tubes were centrifuged again for 1 minute at 10,500 rpm. After that, 300 µl of Buffer RPE was added and tubes were centrifuged again, this time for 2 minutes at 10,500 rpm. This longer centrifugation dried the spin column membrane, ensuring that no ethanol was carried over during RNA elution because residual ethanol may have interfered with downstream reactions.

In the last step the RNeasy spin column was placed in a new 1.5 ml collection tube and 40 µl RNase-free water was added directly to the spin column membrane. The tubes were centrifuged for 1 minute at 10,500 rpm; the flow-through now contained the RNA. Concentration of RNA was determined by spectrophotometric quantification before RNA was stored at -80°C.

2.2.3.2 GeneJET™ RNA Purification Kit

Gene JET™ Purification Kit also uses silica-based membrane technology in the form of a convenient spin column and works similarly as the corresponding product of Qiagen (see 2.2.3.1). Isolation of total RNA using this kit was performed according to the manufacturer's protocol (QuickProtocol™ QP15, Fermentas, 2010).

The cell pellet was generated as described above and resuspended in 600 µl of Lysis Buffer supplemented with β-mercaptoethanol. 360 µl of 96-100% ethanol was added and the lysate was mixed by vortexing. Up to 700 µl of the lysate was loaded onto one

GeneJET™ RNA Purification Column which was then centrifuged for 1 minute at 12,200 × g. After discarding the flow-through lysate loading and centrifugation were repeated. After discarding the flow-through again, 700 µl of Wash Buffer 1 was added and the tubes were centrifuged for 1 minute at 12,200 × g. The flow-through was discarded and 600 µl of Wash Buffer 2 was added. Tubes were centrifuged for 1 minute at 12,200 × g and flow-through was discarded again. After adding 250 µl of Wash Buffer 2, tubes were centrifuged for 2 minutes at 12,200 × g.

In the last step the column was transferred into a new 1.5 ml tube and 50-100 µl nuclease-free water was added. The tube was centrifuged for 1 minute at 12,200 × g; the flow-through now contained the RNA. Concentration of RNA was determined by spectrophotometric quantification before RNA was stored at -80°C.

2.2.3.3 TRI Reagent® solution

TRI Reagent® solution is a complete, ready-to-use reagent for the isolation of total RNA or the simultaneous isolation of RNA, DNA, and protein from a variety of biological samples.

Total RNA was isolated by use of TRI Reagent® solution according to the manufacturer's instructions (Manual 9738M, Revision D, Ambion, 2010).

The cell pellet, which RNA should be isolated from, was generated as described above and lysed in 1 ml TRI Reagent® solution per 5 -10 × 10^6 cells by vortexing. The homogenate was then incubated for 5 minutes at room temperature allowing nucleoprotein complexes to completely dissociate. After that, 100 µl BCP was added per 1 ml of TRI Reagent® solution, mixed well with the homogenate and incubated at room temperature for 15 minutes.

Centrifugation at 12,000 × g for 15 minutes at 4°C led to formation of three phases: an aqueous colorless phase at the top (RNA), an interphase and lower red organic phase (DNA and protein). RNA remained exclusively in the upper aqueous phase, so this phase was transferred to a fresh tube and mixed with 500 µl of isopropanol per 1 ml of TRI Reagent® solution by vortexing for 10 seconds. After incubation at room temperature for 10 minutes, the tube was centrifuged at 12,000 × g for 8 minutes at 4- 25°C. The supernatant was discarded carefully without disturbing the pellet RNA which might have formed on the side or bottom of the tube. 1 ml of 75% ethanol was

added per 1 ml TRI Reagent® before the tube was centrifuged at 7500 × g for another 5 minutes.

In the last step, after centrifugation, the ethanol was removed and the RNA pellet was briefly air dried before it was dissolved in 40-100 µl RNase-free water. Concentration of RNA was determined by spectrophotometric quantification before RNA was stored at -80°C.

2.2.4 Retrovirus-mediated stable RNA interference

Stable gene knockdowns were achieved by use of pSIREN-RetroQ retroviral vector according to manufacturer's instructions (User Manual for Retroviral Gene Transfer and Expression, Protocol No. PT3132-1, Version No. PR631543, Clontech; User Manual for Knockout™ RNAi Systems, Protocol No. 3739-1, Version No. 082812, Clontech). This plasmid shRNA expression vector contains a puromycin resistance gene for the selection of stable transfectants later on. The structure of the vector is illustrated in Figure 7 on p. 40.

2.2.4.1 Designing shRNA sequences

Small hairpin RNAs (shRNAs) behave as siRNA-like molecules capable of gene-specific silencing. They are generated using a specific oligonucleotide DNA sequence. In this work, the shRNAs were designed corresponding to the siRNA sequences with best knockdown efficiency. The control shRNA corresponds to the sequence of the negative control siRNA which had already been used for transient transfections. Two complementary oligonucleotides, a top strand and a bottom strand, were synthesized corresponding to the particular siRNA sequence for each shRNA target. A hairpin loop sequence was located between the sense and antisense sequences on each complementary strand. Synthetic oligonucleotides were obtained from Metabion international AG, Martinsried, Germany (see p. 38).

2.2.4.2 Annealing of complementary oligonucleotide strands

The two complementary oligonucleotide strands which had been mentioned above were resuspended in 1x TE Buffer to a final concentration of 100 µM each and then mixed at a ratio of 1 : 1. Under certain thermal cycler conditions which are described in

Table 1 complementary oligonucleotide strands annealed and one double strand (ds) oligonucleotide in a concentration of 50 µM was generated.

	step 1	step 2	step 3	step 4	step 5
duration	30 s	2 min	2 min	2 min	∞
temperature	95°C	72°C	37°C	25°C	4°C

Table 1: Thermal cycler conditions for annealing of the two complementary oligonucleotides.

2.2.4.3 Ligation of ds oligonucleotide into pSIREN-RetroQ vector

Annealed oligonucleotides were diluted in TE Buffer to a final concentration of 0.5 µM and ligated into the pSIREN-RetroQ vector. Ligation was achieved by mixing the linearized expression vector and the diluted annealed oligonucleotide with 10x T4 DNA Ligase Buffer, BSA, DEPC water and T4 DNA Ligase. This reagent was incubated at room temperature for 3 hours.

2.2.4.4 Transformation of pSIREN constructs into bacterial strain

pSIREN constructs were transformed into One Shot Top10 cells, an E. coli strain which is routinely used for shRNA cloning. The strain carries certain mutations which provide to generate high yields of plasmid DNA.

2.2.4.5 Isolation of plasmid DNA

Plasmid DNA was purified using NucleoSpin® Plasmid Kit according to manufacturer's instructions (Plasmid DNA purification, User Manual November 2012, Rev. 08, Macherey-Nagel). Briefly, bacterial cells were harvested and lysed. Lysate was clarified by centrifugation. Supernatant was pipetted onto a certain columns analogously to RNA isolation in 2.2.3.1 on p. 45 in which special silica membranes bind DNA. This silica membrane is washed a couple of times and finally DNA is eluted by use of a certain buffer. Correct suppressing pSIREN constructs were identified by restriction analysis and verified by sequencing.

2.2.4.6 Transfection of packaging cells by electroporation

Correct pSIREN constructs were transfected into RetroPack™ PT67 packaging cells.

PT67 is a cell line derived from a mouse fibroblast and designed for stably producing high-titer retrovirus from stably integrated genes. Transfection was achieved by means of electroporation at the capacitance of 960 µF and 270 V/0.4 cm**.** Cells were incubated on ice for 10 minutes and seeded in two cell culture flasks. Stable transfectants were selected by puromycin (2 µg puromycin/ml). After growing to confluency, which was approximately 48 hours after transfection, viral supernatant was isolated and stored at -80°C.

Preparations for retroviral infection of Ewing sarcoma cells were kindly performed by Colette Berns and PD Dr. Günther Richter.

2.2.4.7 Retroviral infection of Ewing sarcoma cell lines

Target cells were seeded into 6-well culture plates. Each well contained 3 ml standard tumor medium before it was loaded with 1-2 × 10^5 cells. Culture plates were incubated under normal growth conditions, meaning 37°C and 5% CO_2 in a humidified atmosphere, for 48 hours. Having adhered by that time, cells were incubated with 1 ml viral supernatant in the presence of 4 µg/ml polybrene for another 12-48 hours. Then, viral supernatant was removed and cells were cultured in standard tumor medium for another 24 hours before stable infectants were selected by use of puromycin (2 µg puromycin/ml standard tumor medium). At that point of time RNA was isolated and gene expression was analyzed by qRT-PCR. Stable gene knockdown was detected in comparison to negative shRNA control.

2.2.5 Isolation of genomic DNA (gDNA)

To examine genomic integration of retroviral vector constructs, total DNA from cultured cells was isolated using the DNeasy® Blood & Tissue Kit according to manufacturer's protocol (Qiagen Handbook 07/2006). Briefly, 1 - 5 x 10^6 cells were re-suspended in 200 µl 1 x PBS containing 20 µl proteinase K and transferred onto a DNA-binding membrane within the DNeasy® column. After direct cell lysis by means of specific buffers and selective binding of DNA to the membrane, samples were washed and DNA was eluted in 100 µl sterile water. DNA concentration was determined photometrically at 260 nm. To amplify integrated pSIREN-RetroQ vector-derived DNA using PCR analysis following primers and cycler conditions were used:

	step 1	step 2 (40 x)			step 3	step 4
duration	5 min	30 s	30 s	15 s	7 min	∞
temperature	94°C	94°C	58°C	72°C	72°C	4°C

Table 2: Thermal cycler conditions for amplification of pSIREN vector-derived DNA.

PCR was performed using 5 µl 10 x Rxn Buffer, 1.5 µl MgCl, 1 µl dNTPs, 0.5 µl pSIREN primer (forward and reverse), 0.3 µl AmpliTaq DNA Polymerase and 2 µl gDNA in a final volume of 50 µl per reaction. Separation of DNA fragments occurred in 1 % agarose gel by electrophoresis.

2.2.6 cDNA synthesis

Isolated RNA had to be converted into complementary DNA (cDNA) for gene expression studies by qRT-PCR. cDNA is a single-strand DNA molecule which is generated corresponding to a specific messenger RNA (mRNA) by a reverse transcriptase, an RNA-dependent DNA polymerase. The process is called reverse transcription and was performed by means of the High-Capacity cDNA Reverse Transcription Kit.

According to manufacturer's instructions (High-Capacity cDNA Reverse Transcription Kits Protocol, Part Number 4375575 Rev. E, Applied Biosystems, 06/2010) kit components had to thaw on ice first. Then 2x RT master mix was prepared from RT Buffer, dNTP Mix, RT Random Primers and MultiScribe™ Reverse Transcriptase on ice. Particular volumes of these kit components depended on required number of reactions. For one reaction, 10 µl of this master mix and 10 µl of RNA solution, consisting of 1 µg purified RNA in nuclease-free water, were mixed in an RNAse-free tube. Tubes were centrifuged to spin down the contents and to eliminate any air bubbles before they were loaded into a thermal cycler. Thermal cycler conditions for cDNA synthesis were programmed as shown in Table 3. cDNA was stored at -20°C.

	step 1	step 2	step 3	step 4
duration	10 min	120 min	5 min	∞
temperature	25°C	37°C	85°C	4°C

Table 3: Thermal cycler conditions for cDNA synthesis.

2.2.7 Quantitative Real-time PCR (qRT-PCR)

Real-time PCR was used to examine general gene expression patterns and quantify changes in gene expression levels as the amount of cDNA corresponds to the amount of cellular mRNA.

Real-time PCR is a quantification method which allows continuous measuring of specific PCR products in real time. In this work qRT-PCR was performed by means of the TaqMan® principle most of the time. SYBR Green was only used to detect EWS/FLI1 type 2 translocations (see 2.2.8) and successful genomic integration of pSIREN and pMSCVneo constructs (see 2.2.5).

2.2.7.1 TaqMan® probe-based qRT-PCR

In TaqMan® probe-based qRT-PCR oligonucleotides with a reporter fluorescent dye (fluorescein) attached to the one end and a quencher dye to the other end (primers) are hybridized to a template strand during PCR. The quencher dye suppresses the reporter dye's emission. When Taq DNA polymerase cleaves the probe because of its 5' -3' nucleolytic activity, the reporter dye is set free and the fluorescein is no longer quenched. This causes an increase in fluorescence intensity which indicates that probe-specific PCR products have been generated. (Livak *et al.* 1995)

TaqMan® probe-based gene expression assays used in this work were obtained from Applied Biosystems (see 2.1.11). As mentioned above they consist of a pair of unlabeled PCR primers and a TaqMan® probe with a fluorophore (for example FAM™ or VIC®) on the 5' end and a non-fluorescent quencher (for example MGB or TAMRA) on the 3' end.

qRT-PCR was performed by use of Maxima® Probe/ROX qPCR Master Mix (2x) which includes Maxima® Hot Start Taq DNA polymerase and dNTPs in an optimized PCR buffer and is supplemented with a ROX passive reference dye (see Product Information #K0233, Rev. 9, Fermentas). According to manufacturer's instructions (Protocol for TaqMan® Gene Expression Assays, Part Number 4333458, Rev. N, Applied Biosystems, 11/2010) qRT-PCR based analysis was carried out in 20 µl reactions in 96-well format.

A reaction master mix was prepared by mixing 10 µl of the Maxima® Probe/ROX qPCR Master Mix (2x), 1 µl of a TaqMan® Gene Expression Primer Assay and 8 µl RNase-free water per one reaction. 1 µl of cDNA template was added to 19 µl of this reaction

master mix achieving a final volume of 20 µl in each well of a 96-well reaction plate. A non-template control (NTC), i.e. only reaction master mix without cDNA template, was used to demonstrate possible contamination.

96-well plates were sealed and centrifuged briefly before they were loaded into the 7300 Real-Time PCR System of Applied Biosystems. Thermal cycler conditions for RT-PCR are shown in Table 4.

	step 1	step 2	step 3 (40x)	
duration	1 min	10 min	15 s	1 min
temperature	50°C	95°C	95°C	60°C

Table 4: Thermal cycler conditions for qRT-PCR in 7300 Real-Time PCR System of Applied Biosystems.

2.2.7.2 SYBR® Green-based qRT-PCR

SYBR® Green I is an intercalating dye that fluoresces upon binding to double-stranded DNA. Following primer-mediated replication of the target sequence during PCR, multiple molecules of SYBR® Green bind to the PCR product. The resulting DNA-dye-complex emits a strong fluorescent signal that is easily detected. The more PCR products, the stronger the fluorescent signal. (VanGuilder *et al.* 2008) SYBR® Green-based qRT-PCR was used to detect EWS/FLI1 type 2 translocations (see 2.2.8) and integration of retroviral vectors into genomic DNA (see 2.2.5) in this work.

SYBR® Green-based qRT-PCR was performed by use of Power SYBR® Green PCR Master Mix (2x) which includes SYBR® Green I Dye, AmpliTaq Gold® DNA Polymerase and dNTPs in an optimized PCR Buffer and is supplemented with a ROX passive reference dye (see Power SYBR® Green PCR Master Mix and Power SYBR® Green qRT-PCR Reagents Kit User Guide, Part Number 4367218 Rev. E, 09/2011, Applied Biosystems).

According to the manufacturer's user guide mentioned above, qRT-PCR based analysis was carried out in 96-well format.

A reaction master mix was prepared by mixing 10 µl of the Power SYBR® Green PCR Master Mix (2x), forward and reverse primer assay (0.6 µl each), 0.4 µl probe and 7.4 µl RNase-free water per one reaction. 1 µl of cDNA template was added to 19 µl of this reaction master mix achieving a final volume of 20 µl in each well of a 96-well reaction plate. A non-template control (NTC), i.e. only reaction master mix without

cDNA template, was used to demonstrate possible contamination.
96-well plates were sealed and centrifuged briefly before they were loaded into the 7300 Real-Time PCR System of Applied Biosystems. Thermal cycler conditions for qRT-PCR are shown in Table 4.

2.2.7.3 Analysis of gene expression

Gene expression was analyzed using the 2^{-ddCt} method, normalized to the standard housekeeping gene GAPDH in TaqMan®-based qRT-PCR and ACTB (β-actin) in SYBR® Green-based qRT-PCR. These two internal control genes normalize the PCRs for the amount of mRNA added to the reverse transcription reactions. (Livak & Schmittgen 2001)
Mean value and standard deviation of duplicates were illustrated by means of Microsoft Excel. Statistical significance was determined using the unpaired 2-tailed Student's t-test in Microsoft Excel; p values < 0.05 were considered statistically significant.

2.2.8 Detection of EWS-FLI1

As mentioned in 2.2.7.1 TaqMan® probe-based gene expression assays consist of a pair of primers and a TaqMan® probe with a FAM™ on the 5' end and a TAMRA non-fluorescent quencher on the 3' end. Since there was no inventoried TaqMan® Gene Expression Assay available for the detection of EWS-FLI1, primers detecting EWS (sense primer) and FLI1 (antisense primer) of the fusion transcript were custom-designed, just as a probe detecting EWS/FLI1 type 1 translocations. Custom-designed primers and probe were obtained from Applied Biosystems. Sequences are shown below.

sense primer (EWS)	5'-TAG TTA CCC ACC CAA ACT GGA T-3'
antisense primer (FLI1)	5'-GGG CCG TTG CTC TGT ATT CTT AC-3'
FAM™ probe	5'-FAM-CAG CTA CGG GCA GCA GAA CCC TTC TT-TAMRA-3'

Table 5: Primer sequences for detection of EWS-FLI1.

For detection of EWS/FLI1 type 1 translocation, a qRT-PCR master mix was prepared mixing 10 µl of Maxima® Probe/ROX qPCR Master Mix (2x) and 7.4 µl RNAse-free water with 0.6 µl of each primer (0.3 µM each) and 0.4 µl of FAM probe (0.2 µM).

1 µl cDNA template was added to 19 µl of PCR master mix, achieving a final volume of 20 µl per well in a 96-well reaction plate. 96-well plates were loaded into the 7300 Real-Time PCR System of Applied Biosystems. Gene expression was normalized to GAPDH and analyzed by using the 2^{-ddCt} method (see 2.2.7.1 and 2.2.7.3).

EWS/FLI1 type 2 translocation was detected by SYBR® Green-based qRT-PCR using above-mentioned primers and probe. Gene expression was analyzed as mentioned in 2.2.7.3.

2.2.9 In vitro assays

2.2.9.1 Proliferation assay

Cell proliferation was determined by use of the xCELLigence Real-Time Cell Analyzer according to manufacturer's instructions (The xCELLigence RTCA SP/MP instrument, Product Information, ACEA Biosciences).

This system monitors cell proliferation in real time without the use of any labels but by measuring electrical impedance across a complex system of microelectrodes integrated on the bottom of its special tissue culture plates. The principle is based on the fact that cells on top of the electrodes affect the local ionic environment, leading to an increase in the electrode impedance. The more cells attached on the electrodes, the larger the increase in the electrode impedance. Thus, electrode impedance, which is displayed as cell index values, is used to monitor proliferation (see product information mentioned above).

For this assay, 1-2 × 10^4 cells in 200 µl standard tumor medium were seeded in an E-Plate 96 in sextuplicates. The E-Plate 96 is similar to commonly used 96-well plates with the only difference that each of the 96 wells contains integral sensor electrode arrays as mentioned above. Cells were incubated at 37°C and 5% CO_2 in a humidified atmosphere up to 180 hours. Cellular impedance was measured in 4-hour intervals from the time of plating until the end of the experiment. Cell index values of sextuplicates were calculated and plotted on a graph. Gene knockdown was monitored by qRT-PCR.

In this work, SK-N-MC and A-673 pSIREN HOX cell clones were seeded in sextuplicates as described above to investigate if HOX knockdown influenced proliferation of Ewing

sarcoma cell lines.

2.2.9.2 Colony-forming cell assay

Anchorage-independent growth capacity was analyzed in the Colony-forming cell assay using Methylcellulose-based Media and a Cell Resuspension Solution. The assay is based on the ability of cells to proliferate and differentiate into colonies in a semisolid medium in response to cytokine stimulation. Methylcellulose-based Media contains methylcellulose in Iscove's Modified Dulbecco's Medium, FBS, BSA, L-glutamine and β-mercaptoethanol. Volumes of contents have been optimized for Colony-forming cell assays (see product information, Catalog Number HSC002, R&D Systems).

According to manufacturer's protocol (The Human Colony Forming Cell (CFC) Assay using Methylcellulose-based Media, Technical Information, R&D Systems), reagents were aliquoted. The assay was carried out in 35 mm culture plate format.

Aliquoted Methylcellulose Base Media and Cell Resuspension Solution, which were usually stored at -20°C, were thawed at room temperature without disturbance just before use.

5×10^3 cells were resuspended in 300 µl Cell Resuspension Solution per one approach consisting of duplicates. The Cell Solution was then mixed with 2.7 ml Methylcellulose Media by vortexing. After incubation at room temperature for 30 minutes allowing air bubbles to escape, cell mix was distributed equally to two 35 mm culture plates avoiding air bubbles while pipetting. A third 35 mm culture plate was filled with 3 ml of sterile water to provide a humidified atmosphere. Then, the three culture plates were carefully loaded into a 10 mm culture plate which was incubated under normal growth conditions, meaning 37°C and 5% CO_2. After 14 days photos were taken by use of Canon EOS 600D. Only cell lines which exhibit anchorage-independent growth were able to form colonies in these two weeks.

2.2.9.3 Endothelial cell tube formation assay

The in vitro formation of capillary-like tubes by endothelial cells on a basement membrane matrix is a powerful method to screen for factors that promote or inhibit angiogenesis. (Arnaoutova & Kleinman 2010) The basement membrane extract was derived from the EHS tumor, a murine tumor with an abundant extracellular matrix. It

forms a 3D gel at 37°C and supports cell morphogenesis, differentiation and tumor growth. (Kleinman & Martin 2005) Among others, it contains TGFβ, EGF, IGF, FGF, tPA and growth factors which occur naturally in the EHS tumor (see User Manual: BD Matrigel™ Basement Membrane Matrix, SPC-356234 Rev 6.0, BD Biosciences).

Endothelial cell tube formation was analyzed using BD Matrigel™ Basement Membrane Matrix according to manufacturer's protocol (Protocol: Endothelial Cell Tube Formation Assay, Assay Methods, BD Biosciences).

BD Matrigel™ was thawed overnight on ice at 4°C. The next day 75 µl of the liquid Matrigel™ was carefully pipetted into each well of a 96-well flat top reaction plate avoiding air bubbles. Since Matrigel™ gels immediately at 22°-35°C, the 96-well reaction plate was put on ice and pre-cooled pipets and tips were used. The culture plate was then incubated at 37°C for 30-60 minutes allowing Basement Membrane Matrix to gel.

4 - 7 x 10^4 cells in 75 µl standard tumor medium were seeded on gelled Matrix achieving a final volume of 150 µl per well.

After incubation at 37°C and 5% CO_2 in a humidified atmosphere for 24 hours, medium was carefully removed and cells were washed with 100 µl PBS per well. PBS was removed and cells were labeled by Calcein Fluorescent Dye. 100 µl Calcein in a concentration of 1 µg/ml in PBS were added per well, then culture plate was incubated in the dark at room temperature for 30 minutes before labeling solution was removed and 100 µl PBS was added again. Tube formation was analyzed by fluorescence microscopy. Images were taken by use of a Nikon Eclipse TS 100 with an attached Nikon Coolpix 5400 camera.

In this work, it was investigated if HOX knockdown influenced the angiogenesis pattern of Ewing sarcoma cell lines.

2.2.9.4 Osteogenesis differentiation assay

Potential of osteogenic differentiation of Ewing sarcoma cell lines was surveyed using the STEMPRO® Osteogenesis Differentiation Kit. This kit has been developed for the osteogenic differentiation of mesenchymal cells (MSC) in tissue-culture vessels. Consisting of a basal medium and osteogenesis supplement, it contains all reagents required for the MSCs to be committed to the osteogenesis pathway and to generate

osteocytes.

According to manufacturer's protocol (STEMPRO® Osteogenesis Differentiation Kit, Part No. A10486, Rev. 02/04/2008, GIBCO) culture media were prepared. Osteogenesis differentiation medium contained 45 ml of STEMPRO® Osteocyte/Chondrocyte Differentiation Basal Medium, 5 ml of STEMPRO® Osteogenesis Supplement and 5 mg of gentamycin. Prepared media was stored in volumes of 50 ml at 4°C in the dark.

Control growth medium contained 445 ml of DMEM medium, 50 ml of FBS, 5 ml of 200 mM L-glutamine and 12.5 mg gentamycin.

The experiment was carried out in 6-well culture plates. Cells had to be seeded in a way different from the method used in the chondrogenesis differentiation assay. A pattern of how differentiation culture plates were loaded is illustrated in Figure 8.

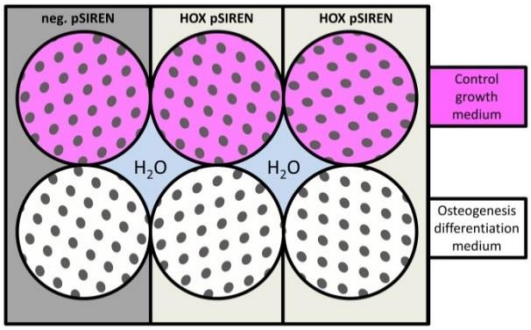

Figure 8: Pattern of 6-well culture plate for osteogenesis differentiation assay. All cells were seeded in duplicates in control growth medium in the beginning. After 24 hours of incubation medium of the lower row was replaced with differentiation medium. Cells were distributed equally in each well.

2 ml of sterile water was filled in the lacuna in the middle of the 6-well culture plate to generate a humidified atmosphere. 3 ml of control growth medium was added to each well of the plate. 4.7×10^4 cells per well were collected in 1 ml of pre-warmed selfsame medium and seeded equally by panning carefully. Allowing the cells to adhere, the culture plate was then incubated at 37°C and 5% CO_2 for 24 hours. At that point of time control growth media in the lower row was replaced with pre-warmed osteogenesis differentiation medium and incubation was continued.

Ewing sarcoma cells continued to expand as they differentiated under osteogenic conditions. Media were replaced every 3 days. After 21 days under differentiating condition, cell cultures were processed for gene expression analysis or Alizarin red staining.

Gene expression analysis

Media were removed carefully from 6-well plate. Cells were rinsed once with PBS, detached by control growth medium and pipetted into a Greiner tube. Cells were pelleted by centrifugation at 1200 rpm for 7 minutes and RNA was isolated by means

of the Gene JET™ Purification Kit (see 2.2.3.2). cDNA was synthesized and gene expression was analyzed using RT-PCR (see 2.2.6 and 2.2.7).

Alizarin red staining

Media were removed carefully from 6-well plate. Cells were rinsed once with PBS and fixed with 4% formaldehyde solution for 30 minutes. After fixation, wells were rinsed twice with sterile distilled water and stained with 2% Alizarin red solution at a pH of 4.2 for 30 minutes. After staining, wells were rinsed three times with sterile distilled water and visualized by microscopy. Alizarin red staining indicates the presence of calcific deposition of cells of the osteogenic lineage. Images were taken by use of a Nikon Eclipse TS 100 with an attached Nikon Coolpix 5400 camera.

2.2.9.5 Chondrogenesis differentiation assay

Potential of chondrogenic differentiation of Ewing sarcoma cell lines was surveyed using the STEMPRO® Chondrogenesis Differentiation Kit. Similarly to the osteogenesis differentiation kit mentioned in 2.2.9.4, this kit has been developed for the chondrogenic differentiation of mesenchymal cells (MSC) in tissue-culture vessels. Also consisting of a basal medium and chondrogenesis supplement, it contains all reagents required for the MSCs to be committed to the chondrogenesis pathway and to generate chondrocytes.

According to manufacturer's protocol (STEMPRO® Chondrogenesis Differentiation Kit, Part No. A10582, Rev. 05/22/2008, GIBCO) culture media were prepared. Chondrogenesis differentiation medium contained 45 ml of STEMPRO® Osteocyte/Chondrocyte Differentiation Basal Medium, 5 ml of STEMPRO® Chondrogenesis Supplement and 5 mg of gentamycin. Prepared media was stored in volumes of 50 ml at 4°C in the dark.

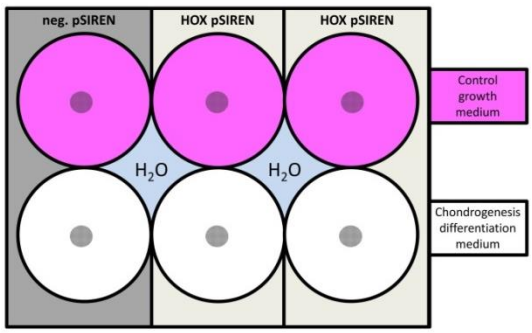

Figure 9: Pattern of 6-well culture plate for chondrogenesis differentiation assay. Cells were seeded in duplicates, in each case in 5 µl droplets. The upper row of wells was filled with control growth medium; the lower row was filled with differentiation medium right from the start.

Control growth medium, called "Attachment Medium" in manufacturer's

protocol, was the same as the one in the osteogenic differentiation assay (see p. 58).
This differentiation assay was also carried out in 6-well culture plates but wells were loaded in a method different from the one of the osteogenesis differentiation assay. Cells were not distributed equally all over each well, but seeded in 5 µl droplets instead. A pattern of how culture plates looked like is shown in Figure 9.
2 ml of sterile water was filled in the lacuna in the middle of the 6-well culture plate to generate a humidified atmosphere. Using control growth medium a cell solution of 1.6×10^7 cells/ml was prepared.
Micromass cultures were generated by seeding 5 µl droplets of this cell solution in the center of each well of a 6-well plate. Cells were then cultivated at 37°C and 5% CO_2 for 20 minutes. According to manufacturer's protocol micromass cultures should have been cultivated for two hours, this long incubation led to cell's death though. So a shorter period of incubation was chosen.
After incubation 4 ml of pre-warmed media was carefully added circularly from outside to the center of the well, avoiding the micromass culture to detach from the bottom. Control growth medium was added to the upper wells, chondrogenesis differentiation medium was added to the lower wells (see Figure 9).
Cells were cultivated at 37°C and 5% CO_2 in a humidified atmosphere. Ewing sarcoma cells continued to expand as they differentiated under chondrogenic conditions. According to manufacturer's protocol, media had to be replaced every second day. After 14 days under differentiating conditions, chondrogenic pellets were processed for gene expression analysis or Alcian blue staining.

Gene expression analysis

Media were removed carefully from 6-well plate. Cells were rinsed once with PBS, detached by control growth medium and pipetted into a Greiner tube. Cells were pelleted by centrifugation at 1200 rpm for 7 minutes and RNA was isolated by means of the Gene JET™ Purification Kit (see 2.2.3.2). cDNA was synthesized and gene expression was analyzed using qRT-PCR (see 2.2.6 and 2.2.7).

Alcian blue staining

According to manufacturer's protocol, media were removed carefully from 6-well plate. Cells were rinsed once with PBS and fixed with 4% formaldehyde solution for

30 minutes. After fixation, wells were rinsed twice with PBS and stained with 1% Alcian blue solution prepared in 0.1 N HCl for 30-60 minutes. After rinsing with 0.1 N HCl three times and adding sterile distilled water to neutralize the acidity, cells were visualized by microscopy. Images were taken by use of a Nikon Eclipse TS 100 with an attached Nikon Coolpix 5400 camera.

2.2.10 Microarray analysis

Staege *et al.* (2004) examined ES-specific gene expression patterns by means of customized high-density DNA microarrays called EOS-Hu01 and HG-U133A. Ewing sarcoma samples were compared to neuroblastoma tissue, fetal tissue as well as other normal tissue of different origins. Altogether 35,356 oligonucleotide probe sets queried a total of 25,194 gene clusters. This analysis revealed a number of genes that are upregulated and specific to the Ewing sarcoma. (Staege *et al.* 2004)

Changes in gene expression signatures after HOX knockdown by RNA interference were also determined by microarray analysis. Experiments were done as previously described (Richter *et al.* 2009) in cooperation with Dr. rer.biol.hum. Olivia Prazeres da Costa (Expression Core Facility at the Institute for Medical Microbiology, Immunology and Hygiene of the Technical University Munich, Germany). After transient siRNA transfection of EW-7 and SK-N-MC RNA was isolated by use of TRI Reagent RNA Isolation Kit (see 2.2.3.3) and quantified photometrically. Total RNA (200 ng) was amplified and labeled using Affymetrix GeneChip Whole Transcript Sense Target Labeling Kit according to manufacturer's protocol. cRNA was hybridized to Affymetrix Human Gene 1.0 ST arrays and microarray data were subsequently analyzed using different control tools to ensure representative high quality data. A detailed procedure is available at www.affymetrix.com. The whole data set is available at the Gene Expression Omnibus (GSE36100). (Edgar *et al.* 2002)

Data was kindly analyzed by PD Dr. Günther Richter who used Affimetrix software "Microarray Suite 5.0", independent one-sample t-test and Genesis software package (Sturn *et al.* 2002; Tsai *et al.* 2003). Differentially expressed genes were identified by means of significance analysis of microarrays (SAM). (Tusher *et al.* 2001) Transcripts were functionally assigned using GO-annotations (http://www.cgap.nci.nih.gov). Gene set enrichment analysis (GSEA) and pathway analyzes were done by using the

GSEA tool (http://www.broad.mit.edu/gsea). (Subramanian *et al.* 2005)

2.2.11 Statistical analysis

Data are mean values ± SEM (standard error of the mean) as indicated. Differences were analyzed by unpaired two-tailed student's t-test as indicated using Microsoft Excel, p values < 0.05 were considered statistically significant. $p < 0.05$: *, $p < 0.01$: **, $p < 0.001$: ***.

3 Results

3.1 Posterior HOXD genes are overexpressed in Ewing sarcoma

Microarray analysis demonstrated that HOXD10, HOXD11 and HOXD13 are ubiquitously expressed in different tissues at a low level. In primary Ewing sarcoma tissue, however, especially these three HOX genes are highly overexpressed in comparison to neuroblastoma and normal tissue (see Figure 10).

The upper chart of Figure 10 illustrates that HOXD10 is also expressed at a higher level in SiMA, a neuroblastoma cell line, and uterine tissue, but only to a minor degree in other tissues compared to primary Ewing sarcoma tissue. In Ewing sarcoma tissue relative expression of HOXD10 amounts to almost the 2000-fold.

Gene expression of HOXD11 in non-Ewing sarcoma tissue, however, seems to be higher than expression of HOXD10 and HOXD13 (see middle chart of Figure 10). Many tissues, especially genitalia such as ovary, uterus or prostate, but also kidney and salivary glands show an increased HOXD11 gene expression up to the 200-fold.

The lower chart of Figure 10 illustrates that HOXD13 is also expressed in prostate tissue to a higher degree (88-fold). Gene expression levels in non-Ewing sarcoma tissue are very low though (less than 10-fold) in comparison to primary Ewing sarcoma tissue where relative expression amounts up to a 2200-fold.

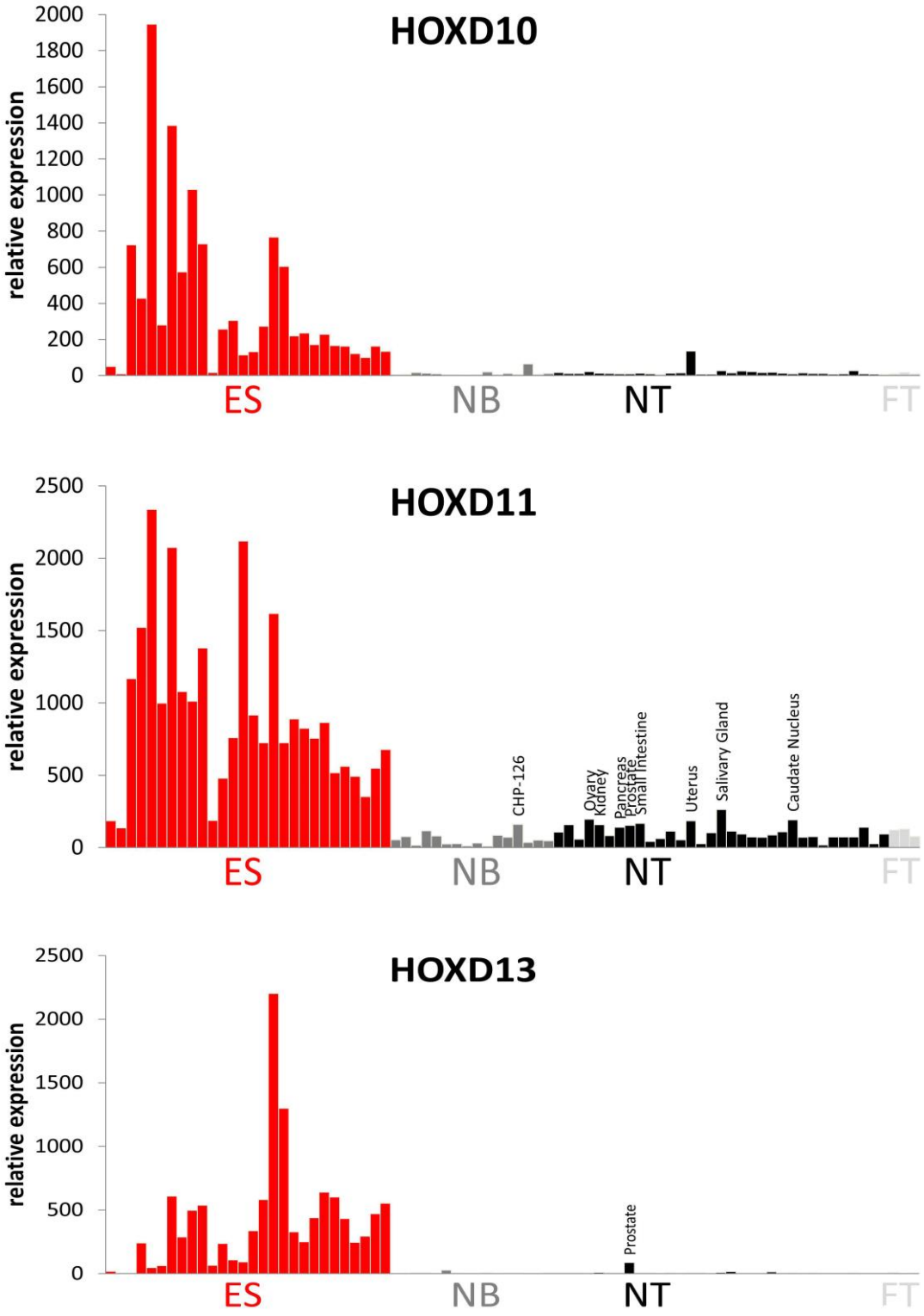

Figure 10: HOX expression in Ewing sarcoma compared to other tissue.
Microarray data show HOXD10, HOXD11 and HOXD13 expression on mRNA level in primary ES tissue samples (red) in comparison to neuroblastoma tissue (NB, dark grey), normal tissue (NT, black) and fetal tissue (FT, light grey). Gene expression of all three HOX genes is increased up to a 2000-fold in primary Ewing sarcoma tissue (ES and NB RNA were hybridized onto HG U133A arrays (Affymetrix; GSE1825, GSE15757) and compared to a published microarray study of normal tissue (GSE2361). Each bar represents the expression signal of an individual array, see von Heyking *et al.* (2016))

There are also HOX genes of the three other clusters (A, B, C) which are highly expressed in the Ewing sarcoma. Just as HOXD10, HOXD11 and HOXD13, these HOX genes are also located on the 5'-end of each cluster. More information about the HOX cluster can be found on p. 1 onwards. HOX genes with numbers 10-13 of clusters A, B and C show a ubiquitously high expression in healthy tissue, though. Figure 11 below displays that these HOX genes are not that specific for Ewing sarcoma.

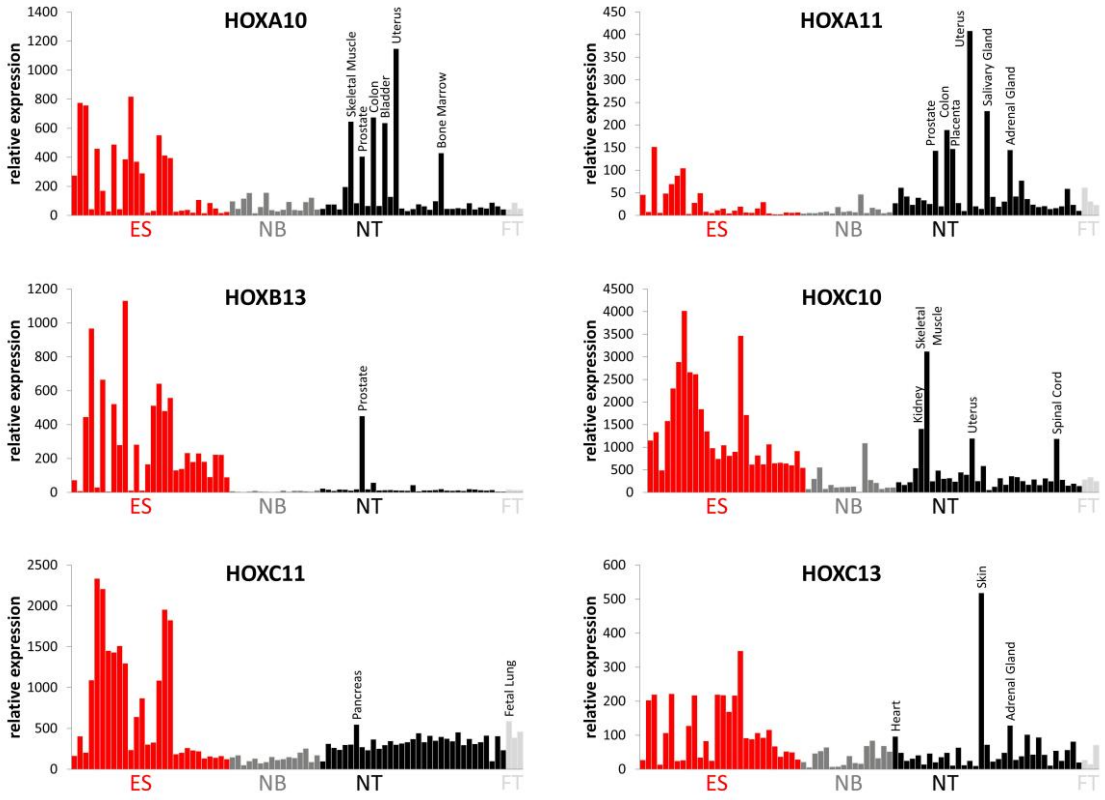

Figure 11: Expression of posterior HOX genes of other clusters than HOXD in Ewing sarcoma compared to other tissue.
Microarray data show expression of HOX genes of other clusters than HOXD on mRNA level in primary ES tissue samples (red) in comparison to neuroblastoma tissue (NB, dark grey), normal tissue (NT, black) and fetal tissue (FT, light grey).Except HOXB13, all of these genes are also highly expressed in non-Ewing sarcoma tissue and less specific than HOXD10, HOXD11 and HOXD13.

Other posterior HOX genes of the same cluster also show an expression pattern totally different from HOXD10, HOXD11 and HOXD13. Figure 12 on p. 66 illustrates that HOXD9 and HOXD12, both of them, are ubiquitously expressed to a modest degree but relative expression amounts less than a 20-fold in most tissues. In contrast to HOXD10, HOXD11 and HOXD13 they are not specific to the Ewing sarcoma.

Altogether, HOXD10, HOXD11 and HOXD13 are the three HOX genes which are most specific to the Ewing sarcoma.

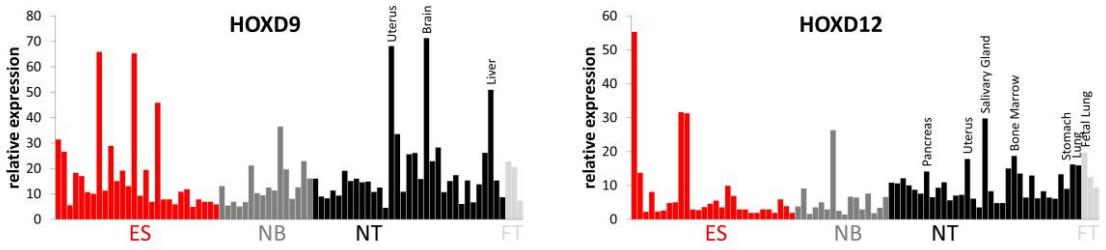

Figure 12: Expression of other posterior HOXD genes in Ewing sarcoma compared to other tissue.
Microarray data show expression of HOXD9 (left panel) and HOXD12 (right panel) on mRNA level in primary ES tissue samples (red) in comparison to neuroblastoma tissue (NB, dark grey), normal tissue (NT, black) and fetal tissue (FT, light grey).

To verify the microarray data, HOX mRNA levels of established ES lines were compared to those of other pediatric tumor cell lines by qRT-PCR using specific gene expression assays. cDNA of neuroblastoma cell lines was used, since this tumor is also considered as member of the group of small round-cell tumors, just like the Ewing sarcoma. (McManus *et al.* 1996) Four osteosarcoma cell lines were used for comparison to a different bone tumor.

Figure 13 shows that ES cell lines express HOXD11 and HOXD13 on higher mRNA levels in comparison to neuroblastoma and osteosarcoma cell lines. In detail, Ewing sarcoma

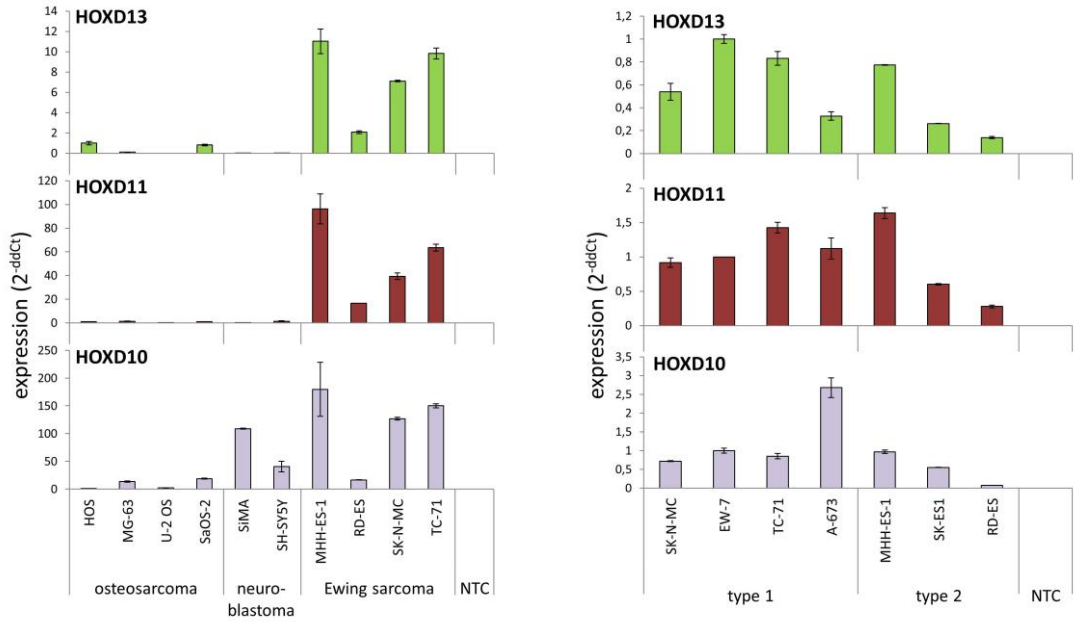

Figure 13: HOX expression in ES cell lines.
Expression of HOXD10, HOXD11 and HOXD13 was analyzed on mRNA level: mRNA levels were quantified by qRT-PCR. NTC is non-template control. Error bars represent standard deviation of duplicates. **Left panel:** HOX expression in ES cell lines in comparison to other pediatric tumor cell lines. Four ES cell lines were compared to four osteosarcoma and two neuroblastoma cell lines. **Right panel:** HOX expression in different ES cell lines. Type 1 and 2 refers to type of EWS/FLI1 translocation.

cell lines show an up to 12-fold higher HOXD13 mRNA level and even up to 100-fold higher HOXD11 mRNA level than the other two tumor entities. Osteosarcoma and neuroblastoma cell lines express HOXD11 and HOXD13 only to a small degree. ES cell lines also show an up to 180-fold higher HOXD10 mRNA level than osteosarcoma cell lines. Two neuroblastoma cell lines, however, also express HOXD10 at a considerable degree. This indicates that HOXD10 is less specific to the Ewing sarcoma but might also be an important gene in neuroblastoma as well.

The right panel of Figure 13 illustrates that all Ewing sarcoma cell lines express HOXD10, HOXD11 and HOXD13 similarly, independently from their type of EWS/FLI1 translocation (see p. 23). From all ES cell lines, RD-ES showed lowest HOX mRNA levels. SK-N-MC, EW-7 and A-673 are the three cell lines which were chosen for upcoming experiments.

3.2 HOX gene expression is not regulated by the two “main suspects”

3.2.1 HOX gene expression is not regulated by EWS-FLI1

To analyze HOX gene expression under EWS-FLI1 suppression, EWS-FLI1 was downregulated in A-673 by retroviral gene transfer. Control cells were treated with a negative control shRNA (see 2.2.4.1). For a detailed protocol of retroviral gene transfer, see 2.2.3. RNA was isolated and cDNA was synthesized.

In four other Ewing sarcoma cell lines EWS-FLI1 was knocked down using two different siRNAs (see Figure 14). Control cells were transfected with a negative control siRNA. After an appropriate period of incubation, RNA was isolated from these cells and cDNA was synthesized. Method of transient transfection is described in detail in 2.2.2. Target sequences of EWS-FLI1 siRNAs are listed in 2.1.8. EWS-FLI1 and HOX gene expression was determined on mRNA level by qRT-PCR using specific gene expression assays.

Figure 14 shows that EWS-FLI1 mRNA levels were significantly downregulated by RNA interference and retroviral gene transfer; in detail down to 24-26% in SK-N-MC, 17-37% in EW-7, 40% in TC-71, 16% in SB-KMS-KS-1 and 20% in A-673. Cells which had been transfected with a negative control siRNA served as control in each case.

In none of these five ES cell lines, HOXD10 mRNA level was influenced by EWS-FLI1 expression. HOXD11 showed a significantly lower mRNA level using EWS-FLI1 #2 siRNA

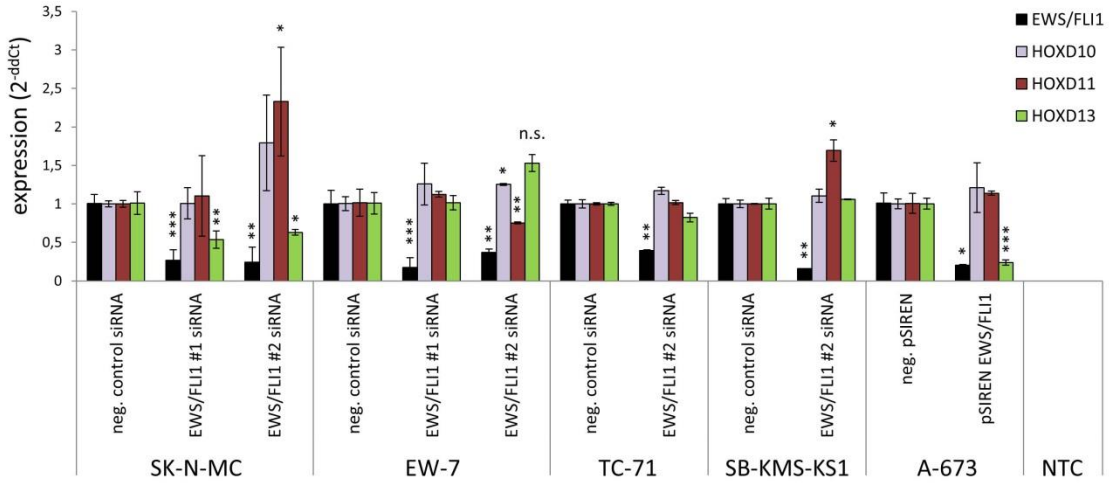

Figure 14: HOX expression after suppression of EWS-FLI1 in five ES cell lines.
SK-N-MC, EW-7, TC-71 and SB-KMS-KS-1 were transfected with two specific EWS-FLI1 siRNAs. Controls were transfected with a negative control siRNA. In A-673 EWS-FLI1 was downregulated by retroviral gene transfer, control was treated with a negative control shRNA. From all cell lines RNA was isolated, cDNA was synthesized and gene expression on mRNA level was determined by qRT-PCR using specific gene expression assays. EWS-FLI1 was downregulated to less than 40% in all cell lines. In SK-N-MC and A-673, HOXD13 was significantly downregulated under EWS-FLI1 suppression. HOXD10 and HOXD11 expression was not influenced by EWS-FLI1 mRNA level. Error bars represent standard deviation of at least duplicates. NTC is non-template control. $p < 0.05$ (*), $p < 0.01$ (**), $p < 0.001$ (***).

in EW-7. Since this result could not be verified neither using the other siRNA in EW-7 nor in any other ES cell line, this effect was rather considered as a random event. In SK-N-MC, however, HOXD13 mRNA level was significantly downregulated down to 53-63% under EWS-FLI1 suppression, irrespective of which siRNA had been used. An even stronger downregulation of HOXD13 under EWS-FLI1 suppression could be detected in A-673, in detail HOXD13 mRNA level showed a decrease down to 24%.

Altogether, EWS-FLI1 did not influence gene expression of HOXD10 and HOXD11 on mRNA level. In the two cell lines SK-N-MC and A-673, however, EWS-FLI1 suppression led to a significant downregulation of HOXD13 on mRNA level. To verify this result, it was investigated if HOX gene expression could be induced by EWS-FLI1. For this, cDNA of the fusion protein was cloned into the pMSCV Neo expression vector, another retroviral vector which was used similarly to pSIREN expression vector. For further information of pMSCV Neo expression vector, see 2.1.12. Method of retroviral gene transfer is described in detail in 2.2.3.

Two different human mesenchymal stem cell (MSC) lines were transfected with EWS-FLI1 pMSCV constructs to achieve an overexpression of the fusion protein. V54.2 is a predominantly adherent growing cell line that has been generated from peripheral

blood mononuclear cells of a healthy volunteer donor after G-CSF-mediated stem cell mobilization. It is immortalized and shows a fibroblast-like cell growth. (Conrad *et al.* 2002) L87 is a permanent Simian virus 40-transformed mesenchymal stem cell line which also shows a fibroblastoid morphology. In contrast to V54.2, this cell line was derived from the bone marrow of a healthy male patient. (Thalmeier *et al.* 1994)

In both cell lines, V54.2 and L87, ectopic EWS-FLI1 expression was induced by pMSCV constructs. By this means two stem cell clones of each cell line were generated: V54.2 #1 and #3, L87 #3 and #5. pMSCV Neo clones of both cell lines were generated by transfecting with an empty vector respectively, they served as control. Transfected cell lines were generated by Diana Löwel. Induction of ectopic EWS-FLI1 expression and HOX gene expression were determined on mRNA level by qRT-PCR using specific primers (see 2.2.8).

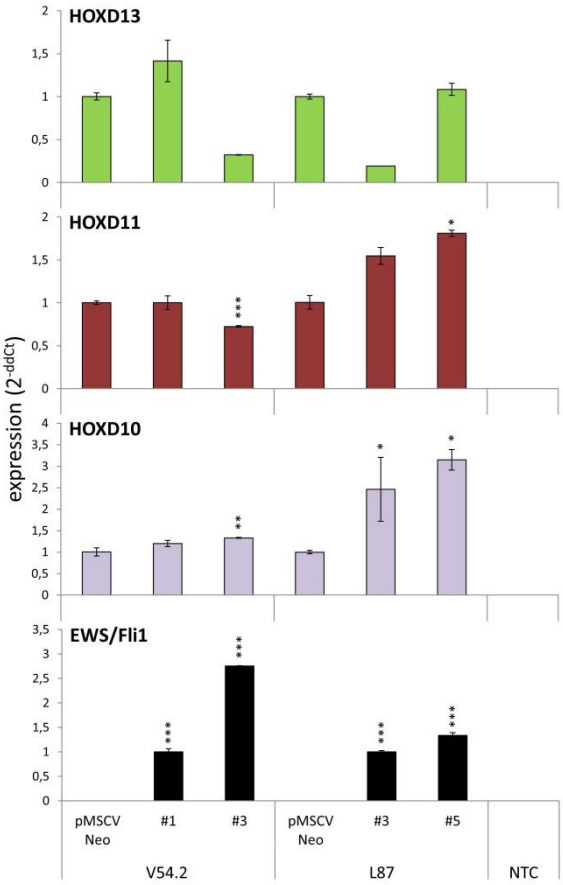

Figure 15: HOX expression in two human MSC cell lines which ectopically express EWS-FLI1.
Two human MSC cell lines, V54.2 and L87, were transfected with EWS-FLI1 pMSCV constructs, resulting in a significant ectopic EWS-FLI1 expression. Gene expression was analyzed on mRNA level by qRT-PCR. pMSCV Neo represents control which was transfected with an empty vector. NTC is non-template control. Error bars represent standard deviation of duplicates. $p < 0.05$ (*), $p < 0.01$ (**), $p < 0.001$ (***).

Figure 15 illustrates that all MSC clones of both cell lines, V54.2 and L87, express HOXD10, HOXD11 and HOXD13. Ectopic expression of EWS-FLI1 led to a 2-3-fold increase of mRNA levels of HOXD10 and HOXD11 in L87. This upregulation seemed to be dose-dependent in this cell line since strongest EWS-FLI1 induction showed highest upregulation of HOXD10 and HOXD11 expression compared to empty vector control. This induction could not be detected in V54.2, though. Here, HOXD10 and HOXD11 mRNA levels of the MSC clones differed from control in a modest way only.

All clones expressed HOXD13 on mRNA

level but in neither of the two cell lines, EWS-FLI1 expression led to a dose-dependent induction of this gene. Since EWS-FLI1 suppression led to a significant downregulation of HOXD13 on mRNA in SK-N-MC and A-673 (see Figure 14, p. 68), HOXD13 mRNA level of V54.2 #3 was expected to be higher than the one of clone #1 and HOXD13 mRNA level of L87 #3 was expected between the ones of the empty vector control and L87 clone #5.

Altogether, ectopic EWS-FLI1 expression did not induce HOXD10, HOXD11 and HOXD13 in mesenchymal stem cells. Potential regulation of HOXD13 under EWS-FLI1 suppression could not be verified by this experiment.

3.2.2 HOX gene expression is not influenced by EZH2

We previously reported that EZH2 was a highly upregulated gene in Ewing sarcoma which was required to maintain stemness and metastastic spread. It blocks endothelial and neuro-ectodermal differentiation and its suppression inhibits contact-independent growth *in vitro* and tumor growth *in vivo*. (Richter *et al.* 2009) Since histone methyltransferases usually regulate HOX gene expression (Hanson *et al.* 1999) we checked whether EZH2 regulated HOX gene expression in ES cell lines. In several ES cell lines EZH2 was downregulated by siRNA interference. Cells which had been treated with a negative control siRNA served as control. RNA was isolated and gene expression was analyzed on mRNA level by qRT-PCR. EZH2 was downregulated to values of 27-57% on mRNA level. HOX gene expression was analyzed on mRNA level as well.

Figure 16 shows reduced EZH2 mRNA levels in SK-N-MC, TC-71 and EW-7. In EW-7 HOXD11 was significantly downregulated under EZH2 suppression. This effect could not be verified in any other cell line, though, suggesting this was rather a random event. Furthermore, EZH2 mRNA levels in EW-7 were not as reduced as in other cell lines. mRNA levels of HOXD10 and HOXD13 did not change at all under EZH2 suppression. Altogether, EZH2 did not influence gene expression of HOXD10, HOXD11 and HOXD13 on mRNA level.

Furthermore, HOX gene expression was not influenced by Argonaute proteins AGO1 and AGO2. The two Argonaute proteins AGO1 and AGO2 were both downregulated down to less than 30% on mRNA level in comparison to control cells. Suppression of Argonaute proteins did not lead to any change of HOX gene expression in four Ewing

sarcoma cell lines (data not shown).

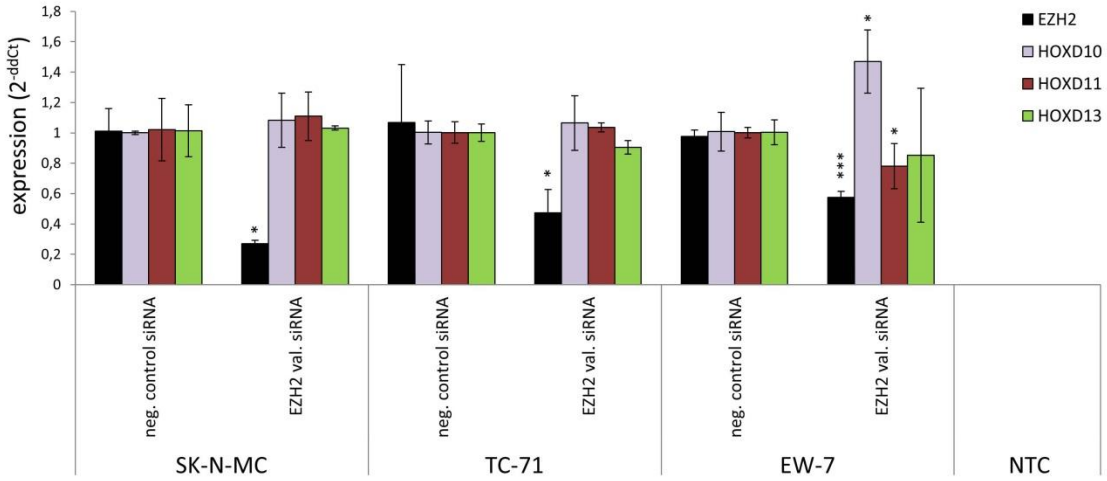

Figure 16: HOX expression after suppression of EZH2 in several ES cell lines.
Several ES cell lines were transfected with EZH2 validated siRNA. Controls were transfected with a negative control siRNA. RNA was isolated, cDNA was synthesized and gene expression on mRNA level was determined by qRT-PCR using specific gene expression assays. EZH2 knockdown did not influence HOX gene expression. Error bars represent standard deviation of at least duplicates. NTC is non-template control. $p < 0.05$ (*), $p < 0.01$ (**), $p < 0.001$ (***).

3.3 HOX gene expression is downregulated by siRNA interference

3.3.1 Transient HOX downregulation by specific siRNAs

To explore the role of HOX genes in Ewing sarcoma pathogenesis, HOXD10, HOXD11 and HOXD13 were downregulated by siRNA interference in several ES cell lines. Two siRNAs were tested in MHH-ES-1 at the beginning to determine the siRNA with better knockdown efficiency. Method of transient transfection is described in 2.2.2. Target sequences of siRNAs which were used are listed in 2.1.8. After an appropriate period of incubation, which was usually about 48 hours, RNA was isolated from culture dishes as described in 2.2.5. Gene expression was determined on mRNA level by qRT-PCR using gene specific gene expression assays (see 2.1.11.1).

Figure 17 shows HOX mRNA levels after transient transfection with specific siRNAs. siRNAs HOXD13_3 and HOXD10_4 generated a downregulation of only 65-75% of the corresponding HOX genes in MHH-ES-1 compared to those of cells that had been transfected with a negative control siRNA. Using HOXD13_2 and HOXD10_1, however, a suppression of 47-60% was possible. Thus, the two latter siRNAs were preferred for further transfection experiments with other Ewing sarcoma cell lines. In SK-N-MC and

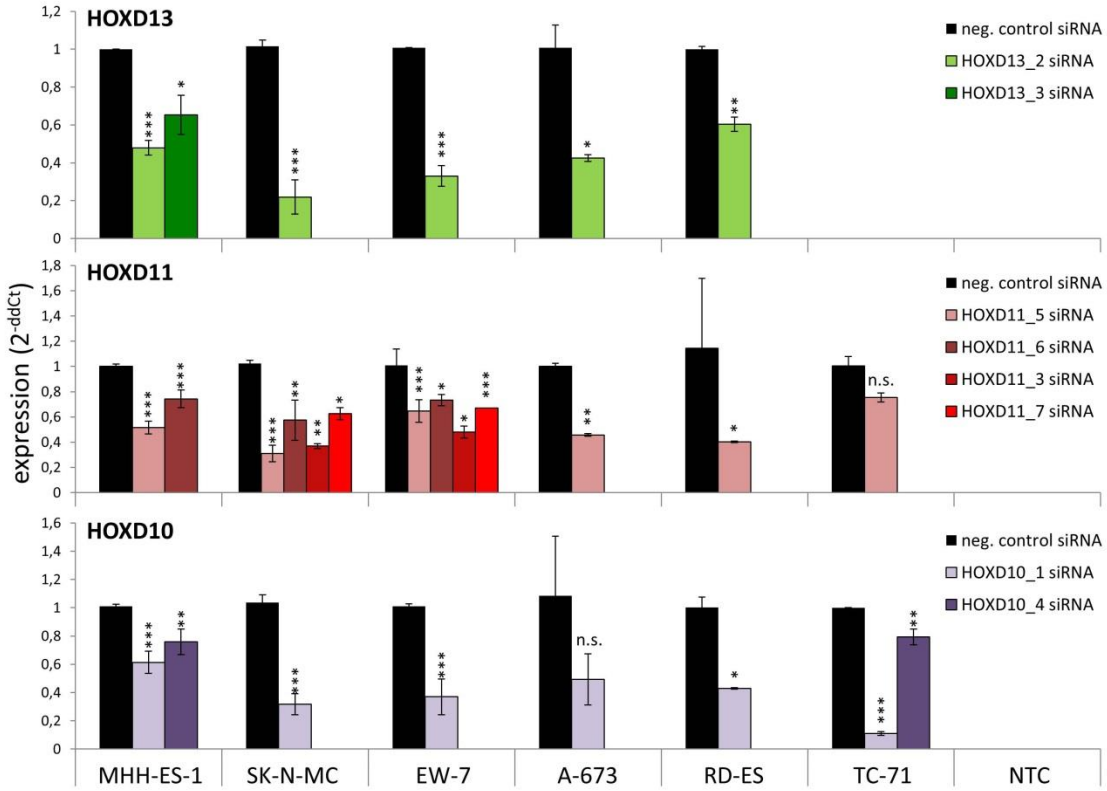

Figure 17: HOX expression after RNA interference.
Several ES cell lines were transfected with specific target siRNAs as described in 2.2.2. RNA was isolated, cDNA was synthesized and gene expression was determined by qRT-PCR using specific gene expression assays. Control was transfected with a negative control siRNA. Error bars represent standard deviation of at least quadruplicates. NTC is non-template control. $p < 0.05$ (*), $p < 0.01$ (**), $p < 0.001$ (***); n.s. not significant

EW-7, the two cell lines which were used mainly, a downregulation of 31-37% of HOXD10 and 21-33% of HOXD13 could be achieved using these two siRNAs. RNA of these transfections was also analyzed by microarray (see 3.5).

Figure 17 illustrates that HOXD11 could be suppressed to 30-51% in MHH-ES-1 and SK-N-MC using HOXD11_5 siRNA, but only to 65% in EW-7. Thus, two more siRNAs were tested. Best knockdown in two cell lines at the same time was achieved by HOXD11_3 siRNA, in detail 36% in SK-N-MC and 48% in EW-7. Altogether, all three HOX genes, HOXD10, HOXD11 and HOXD13 were significantly knocked down on mRNA level by RNA interference.

Oligonucleotides which were used for retrovirus-mediated stable RNA interference (see 2.2.3 and 0) encode the target sequences of HOXD10_1, HOXD11_3 and HOXD13_2 siRNA, respectively.

3.3.2 Triple HOX gene knockdowns

Analogically to the transfections described in 3.3.1 an attempt was made to downregulate all three HOX genes, HOXD10, HOXD11 and HOXD13, at the same time. As described in 2.2.2, the experiment was performed using the same number of cells and the same amount of media and transfection reagent. The only difference was that, instead of 3.6-5 µl of only one specific siRNA, 3.6-5 µl of each of the three HOX siRNAs was used at the same time. RNA was harvested, cDNA was synthesized and HOX gene expression was analyzed as usual.

In four Ewing sarcoma cell lines HOXD10, HOXD11 and HOXD13 could be downregulated significantly at the same time by one transfection. In SK-N-MC and A-673, for example, each of the three HOX genes was knocked down to around 34%. Downregulation of HOXD10, HOXD11 and HOXD13 was achieved more easily by these triple HOX knockdowns than by those single knockdowns mentioned previously (see Figure 17). RNA of these experiments was also used for further gene expression analysis (see chapters 3.5.3 to 3.5.5 and 3.6.2 to 3.6.3).

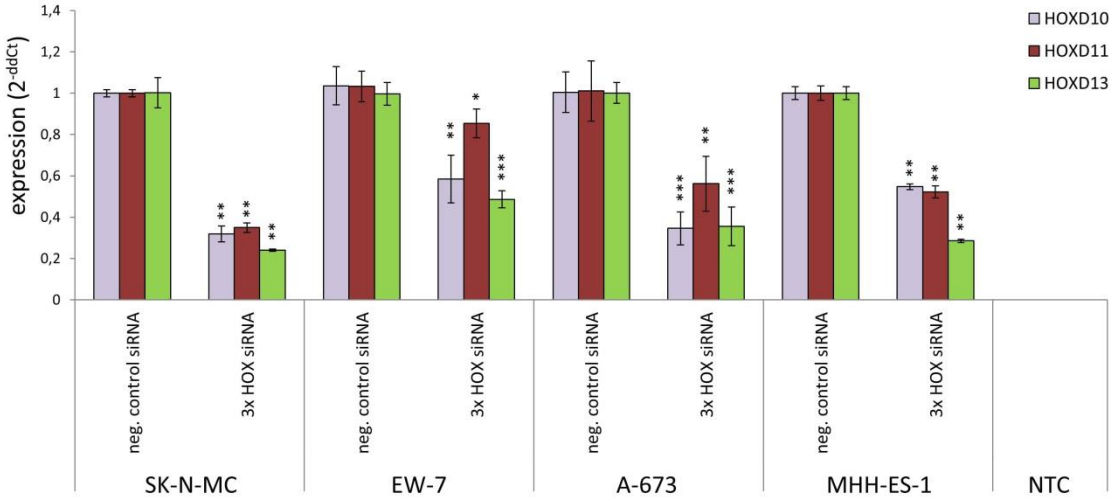

Figure 18: HOX mRNA levels after triple siRNA interference quantified by qRT-PCR.
Four ES cell lines were transfected with HOXD10_1, HOXD11_3 and HOXD13_2 siRNA at the same time. RNA was isolated, cDNA was synthesized and gene expression was determined by qRT-PCR using specific gene expression assays. Control was transfected with triple amount of negative control siRNA. Error bars represent standard deviation of duplicates. NTC is non-template control. $p < 0.05$ (*), $p < 0.01$ (**), $p < 0.001$ (***).

3.4 HOX gene expression is downregulated by retroviral gene transfer

Since gene downregulation by siRNA interference is only detectable in the range from hours to few days and some in vitro assays take a couple of weeks, Ewing sarcoma cell lines with a permanent HOX knockdown were generated. Oligonucleotides encoding the target sequences of the three HOX siRNAs with best gene knockdown efficiency (see 3.3.1) and the target sequence of the negative control siRNA, which had already been used in transient transfection experiments, were cloned into a retroviral vector system called pSIREN RetroQ. Two Ewing sarcoma cell lines were transfected with the corresponding viral supernatants. A constitutive HOX gene downregulation was mediated by a permanent expression of small hairpin RNAs. For a detailed description of small hairpin RNAs and retroviral gene transfer, see 2.2.3.

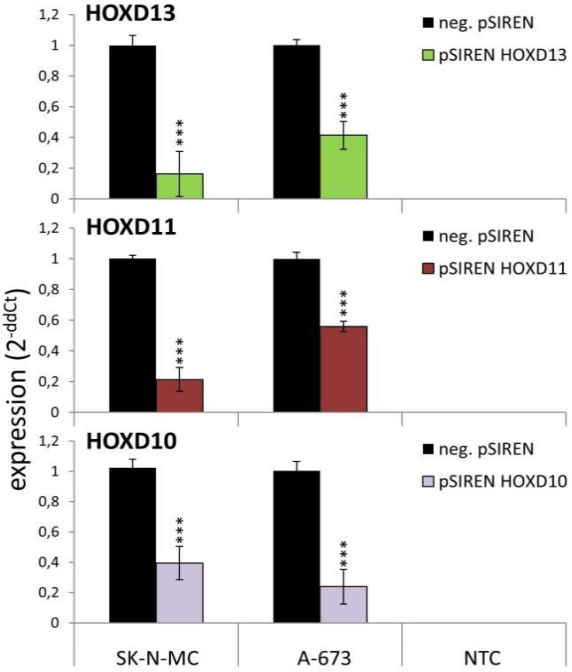

Figure 19: HOX expression on mRNA level after constitutive knock down by retroviral gene transfer.
mRNA levels of two Ewing sarcoma cell lines were determined by qRT-PCR. NTC is non-template control. Error bars represent standard deviation of at least quadruplicates. $p < 0.001$ (***).

pSIREN HOX constructs were transferred into SK-N-MC and A-673. Control cells were treated with a small hairpin RNA corresponding to the target sequence of the negative control siRNA. Stable HOX downregulation was determined by qRT-PCR using specific gene expression assays. Altogether, mRNA levels showed a significant downregulation of HOXD10 down to 29-39%, of HOXD11 down to 21-55% and of HOXD13 down to 16-41% (see Figure 19). Ewing sarcoma cell lines with stable significant downregulation of HOXD10, HOXD11 and HOXD13 were then used for several in vitro assays (see chapters 3.8 - 3.11).

3.5 Microarray analysis reveals possible downstream HOX targets

In the two Ewing sarcoma cell lines SK-N-MC and EW-7 HOXD10, HOXD11 and HOXD13 were successfully downregulated by siRNA interference (see 3.3.1). To identify possible HOX downstream targets, cDNA of SK-N-MC and EW-7 of this experiment was sent to microarray analysis (see 2.2.10).

Gene expression patterns after HOX knockdown were compared on human Gene ST arrays (Affymetrix, GSE36100).

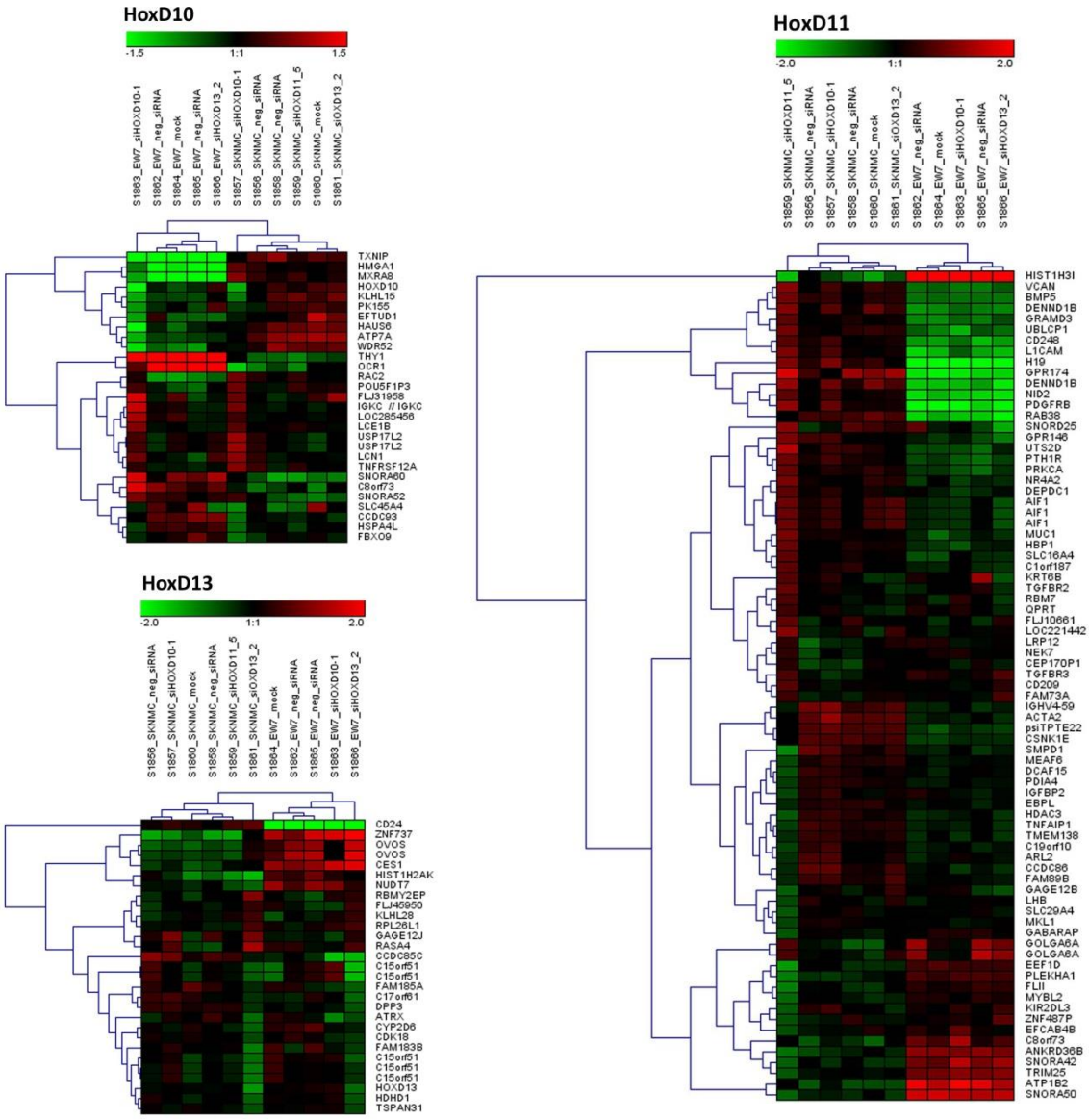

Figure 20: Microarray data of selected genes after transient HOXD10, HOXD11 and HOXD13 knockdown (GSE36100) in SK-N-MC and EW-7 cells.

Each column represents one individual array. Upper left panel shows first most significant genes of SAM analysis after HOXD10 knockdown which were identified by a fold change > ± 1.5 and a t-test $p < 0.05$. Lower left panel and right panel show most significant genes of SAM analysis after HOXD13 and HOXD11 knockdown, respectively. These genes were identified by a fold change of > ± 2 and a t-test $p < 0.05$. Control cells were treated with a neg. control siRNA, mock controls correspond to wildtype cells.

SK-N-MC and EW-7 which had been transfected with a negative siRNA served as control. Mock controls correspond to wild type cells; they were not transfected but only treated with the transfection reagent without any siRNA.

Considering a minimum linear fold change > ±1.5 78 differentially regulated genes after HOXD10 knockdown were identified, 38 of those genes were downregulated. Considering a minimum linear fold change > ±2 108 differentially regulated genes after HOXD11 knockdown were detected, 70 of those genes were downregulated. After HOXD13 knockdown 67 differentially regulated genes were identified considering a minimum linear fold change > ±2, 37 of those genes were downregulated. Differentially regulated genes after HOXD10, HOXD11 and HOXD13 knockdown didn't overlap and only a handful of these genes, however, were confirmed by qRT-PCR.

3.5.1 HOXD10 knockdown also causes a downregulation of HOXD11 in Ewing sarcoma cells

Microarray revealed a downregulation of HOXD11 after HOXD10 knockdown (detailed data not shown). To verify microarray data and also to detect a similar effect of

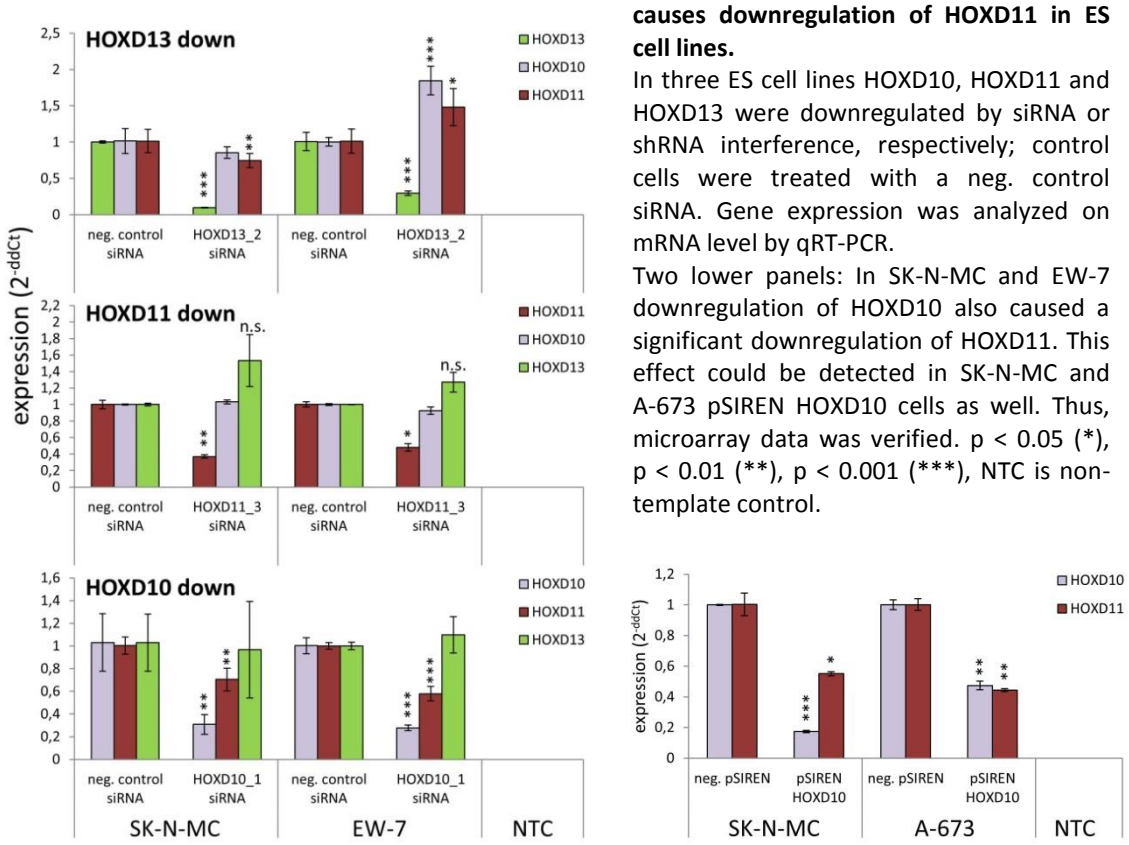

Figure 21: HOXD10 knockdown also causes downregulation of HOXD11 in ES cell lines.
In three ES cell lines HOXD10, HOXD11 and HOXD13 were downregulated by siRNA or shRNA interference, respectively; control cells were treated with a neg. control siRNA. Gene expression was analyzed on mRNA level by qRT-PCR.
Two lower panels: In SK-N-MC and EW-7 downregulation of HOXD10 also caused a significant downregulation of HOXD11. This effect could be detected in SK-N-MC and A-673 pSIREN HOXD10 cells as well. Thus, microarray data was verified. $p < 0.05$ (*), $p < 0.01$ (**), $p < 0.001$ (***), NTC is non-template control.

HOXD11 and HOXD13 knockdown, in several Ewing sarcoma cell lines HOXD10, HOXD11 and HOXD13 were downregulated to less than 30% by siRNA or shRNA interference, respectively. HOX gene expression of these cell lines was analyzed on mRNA level by qRT-PCR using specific primer assays.

Figure 21 illustrates HOX gene expression patterns after HOXD10, HOXD11 and HOXD13 knockdown, respectively. In SK-N-MC and EW-7 downregulation of HOXD10 by siRNA interference also caused a significant downregulation of HOXD11 to 58-70% (see left lower panel). This effect was also observed in SK-N-MC and A-673 pSIREN HOXD10 cells. Here HOXD11 was even downregulated to 44-55% compared to control cells (see right lower panel).

After HOXD11 downregulation HOXD10 and HOXD13 gene expression didn't differ from control cells. Results of HOXD13 downregulation were inconsistent in SK-N-MC and EW-7.

3.5.2 HOXD10 knockdown leads to an upregulation of RAC2

Microarray data revealed that in EW-7 and SK-N-MC RAC2 was significantly upregulated after HOXD10 knockdown. The protein encoded by RAC2 is a member of the RAC family of small guanosine triphosphate (GTP)-metabolizing proteins. (Didsbury *et al.* 1989) GTP-binding proteins are key regulators in signaling pathways. Associated at the plasma membrane, they function as binary switches which control multiple cellular processes. (Zohn *et al.* 1998) The RAS family consists of three isoforms RAC1-3, of which RAC2 is selectively expressed in hematopoietic cells whereas RAC1 and RAC3 are ubiquitously expressed. (Didsbury *et al.* 1989; Haataja *et al.* 1997)

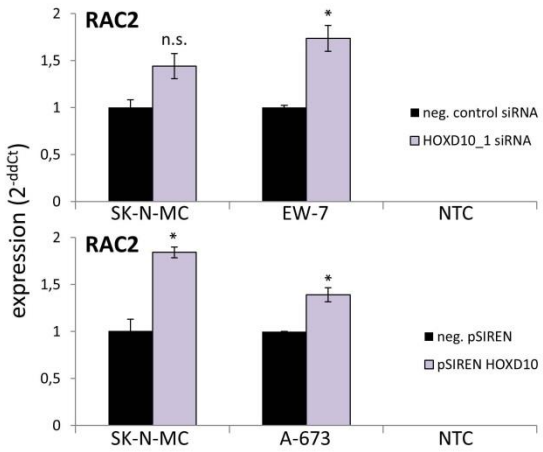

Figure 22: HOXD10 knockdown is associated with an upregulation of RAC2 in ES cell lines. HOXD10 was significantly downregulated to less than 30% by siRNA or shRNA interference. Control cells were treated with a neg. control siRNA. After HOXD10 knockdown RAC2 was significantly upregulated in three Ewing sarcoma cell lines. Gene expression was analyzed on mRNA level by qRT-PCR. Microarray result could be confirmed. $p < 0.05$ (*), not significant (n.s.), NTC is non-template control.

Figure 22 on p. 77 shows RAC2 expression on mRNA level after HOXD10 knockdown in several Ewing sarcoma cell lines. In SK-N-MC and EW-7 HOXD10 was downregulated by siRNA interference, in A-673 and also SK-N-MC HOXD10 knockdown was achieved by retroviral gene transfer. In all cell lines RAC2 expression increased after HOXD10 knockdown.

3.5.3 HOX knockdown seems to cause a downregulation of HAUS6

Microarray data revealed that HAUS6 was downregulated after transient HOXD10 knockdown in SK-N-MC and EW-7. The protein encoded by HAUS6 is a subunit of HAUS which is a critical 8-subunit protein complex that regulates centrosome and spindle integrity. It localizes to interphase centrosomes and to mitotic spindle microtubules, its disruption causes microtubule dependent fragmentation of centrosomes and destabilization of kinetochore microtubules. Just as HOX genes, HAUS is evolutionary conserved and shares homology to a similar protein complex in Drosophila called Augmin. (Lawo *et al.* 2009).

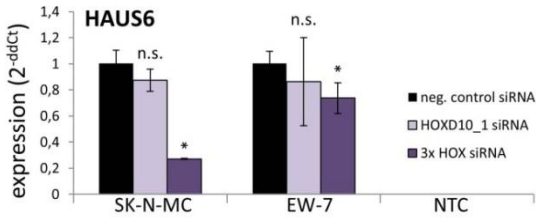

Figure 23: HOXD10 knockdown is associated with a downregulation of HAUS6.
Gene expression was analyzed on mRNA level by qRT-PCR. HAUS6 expression only changed significantly in SK-N-MC and EW-7 after triple HOX knockdown. $p < 0.05$ (*), not significant (n.s.), NTC is non-template control.

Interestingly, microarray results were only confirmed in cells in which all three HOX genes were downregulated. Figure 23 shows that, in contrast to microarray results, HOXD10 downregulation alone didn't lead to a clear downregulation of HAUS6 in SK-N-MC and EW-7. Triple HOX knockdown, however, caused a significant downregulation of this gene, 27% in SK-N-MC and 73% in EW-7. Further information about HOX gene expression of triple HOX knockdowns can be found in 3.3.2, method of transfection is described in detail in 2.2.2.

3.5.4 HOX knockdown seems to cause a downregulation of EEF1D

Microarray data also revealed that EEF1D was downregulated in SK-N-MC after transient HOXD11 knockdown using HOXD11_5 siRNA.

Figure 24 illustrates EEF1D expression on mRNA level after HOX knockdown in several

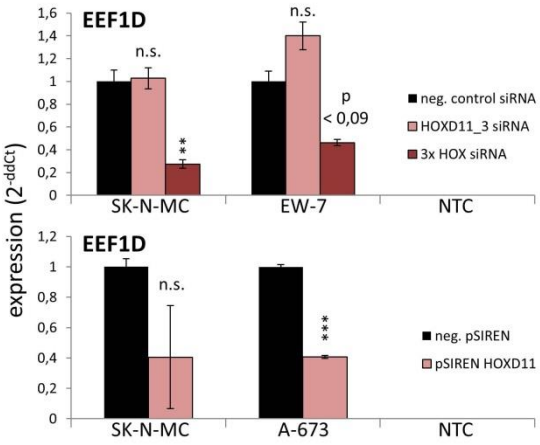

Figure 24: EEF1D expression after HOXD11 knockdown.
Gene expression was analyzed on mRNA level by qRT-PCR. Control cells were treated with a neg. control siRNA/shRNA. **Upper panel:** EEF1D expression only changed significantly in SK-N-MC and EW-7 after triple HOX knockdown. **Lower panel:** SK-N-MC and A-673 pSIREN HOXD11 cells show lower EEF1D mRNA levels than control cells. $p < 0.01$ (**), $p < 0.001$ (***), not significant (n.s.), NTC is non-template control.

Ewing sarcoma cell lines. SK-N-MC and EW-7 were transfected with HOXD11_3 siRNA. Although HOXD11 was downregulated to less than 40%, EEF1D expression didn't differ from control cells. In A-673 and SK-N-MC pSIREN HOXD11 cells, however, a downregulation of EEF1D to 40% could be detected, in A-673 this downregulation was significant ($p < 0.001$). Interestingly, analogically to HAUS6 expression (see Figure 23), a significant downregulation of EEF1D was achieved by triple HOX knockdown; EEF1D mRNA levels amounted 27% in SK-N-MC and 46% in EW-7 compared to control cells.

3.5.5 HOXD13 knockdown causes a downregulation of ATRX in Ewing sarcoma cells

ATRX is a member of the SWI2/SNF2 family of chromatin remodelers. (Picketts *et al.* 1996) It is associated with ATR-X syndrome, a severe non-progressive X-linked mental retardation with an unusal form of thalassemia. Affected boys show a typical facial appearance, severe psychomotor retardation genital and multiple other congenital abnormalities. Female carriers only have mild hematologic changes but are otherwise healthy. (Gibbons *et al.* 1995) Comparison of human and murine ATRX nucleotide sequence revealed 85% identity and thus, just as HOX genes, a high level of evolutionary conservation. (De La Fuente *et al.* 2011; Picketts *et al.* 1998) Recently ATRX also appeared more and more in the context of malignant tumors. (Berbegall *et al.* 2014; Chen *et al.* 2014; Haberler & Wohrer 2014; Marinoni *et al.* 2014) Interestingly, microarray data resulted in a downregulation of ATRX after transient HOXD13 knockdown.

Figure 25 on the following page shows ATRX expression in three Ewing sarcoma cell lines after HOXD13 knockdown. In SK-N-MC and EW-7 ATRX was downregulated to

48% and 65% after HOXD13 suppression by siRNA interference. After triple HOX knockdown ATRX expression amounted 39% and 60% compared to control cells. Reduced ATRX expression was also observed in pSIREN HOXD13 cells.

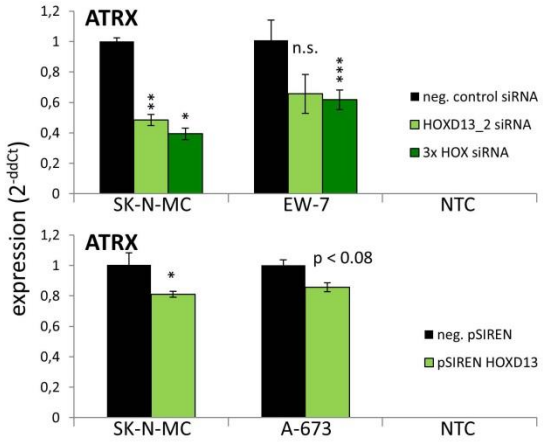

Figure 25: HOXD13 knockdown is associated with downregulation of ATRX.
Gene expression was analyzed on mRNA level by qRT-PCR. HOXD13 knockdown resulted in reduced ATRX expression, after triple HOX knockdown an even stronger downregulation of ATRX was detectable. $p < 0.05$ (*), $p < 0.01$ (**), $p < 0.001$ (***), not significant (n.s.), NTC is non-template control.

3.6 HOX genes seem to intervene in BMP signaling in ES cells

BMP signaling is, among other things, crucial for bone and cartilage formation (see 1.3). Interestingly, HOX knockdown in Ewing sarcoma cells was associated with significant downregulation of several components of the BMP pathway. Gene expression of ligands, co-factors and common BMP targets was decreased in Ewing sarcoma cells with low HOX expression.

3.6.1 BMP2 and BMP4 expression is reduced after HOX knockdown

HOXD10, HOXD11 and HOXD13 knockdown in Ewing sarcoma cells caused a significant downregulation of BMP2 and BMP4, respectively. These two BMPs do not only belong to the bone morphogenetic proteins with greatest osteogenic activity *in vitro* (Cheng *et al.* 2003) but were also revealed to be essential for cartilage formation. (Pizette & Niswander 2000)

Figure 26 illustrates BMP2 and BMP4 expression on mRNA level under HOX suppression. In SK-N-MC and A-673 HOXD10, HOXD11 and HOXD13 were successfully downregulated by retroviral gene transfer. In both cell lines, HOX knockdown was associated with significantly decreased BMP expression. In some cases BMP4 expression was not even detectable. After triple HOX knockdown in two other Ewing cell lines (MHH-ES-1 and EW-7), BMP expression was only determined in control cells (data not shown).

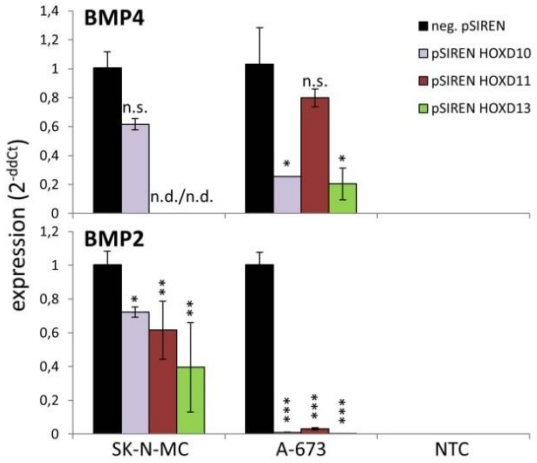

Figure 26: Decrease of BMP expression after HOX knockdown.
Gene expression was analyzed on mRNA level by qRT-PCR. Individual HOX downregulation (less than 30%) by retroviral gene transfer resulted in significantly reduced BMP2 and BMP4 expression in two ES cell lines. $p < 0.05$ (*), $p < 0.01$ (**), $p < 0.001$ (***), not significant (n.s.), not detectable (n.d.), NTC is non-template control.

3.6.2 HOX knockdown leads to downregulation of SMAD4

SMAD4 is an important component in BMP signaling. It forms complexes with R-SMADs which transfer into the nucleus where they, along with cofactors, control transcription of various target genes (see 1.3). In four Ewing sarcoma cell lines triple HOX knockdown was associated with significant decrease of SMAD4 expression.

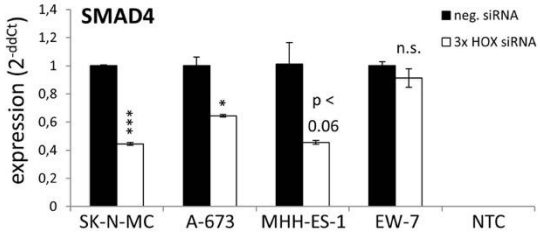

Figure 27: Decrease of SMAD4 expression under HOX suppression.
Gene expression was analyzed on mRNA level by qRT-PCR. After triple HOX knockdown by siRNA interference downregulation of SMAD4 was detectable in several ES cell lines. $p < 0.05$ (*), $p < 0.01$ (**), $p < 0.001$ (***), not significant (n.s.), not detectable (n.d.), NTC is non-template control.

Figure 27 illustrates SMAD4 expression on mRNA level under HOX suppression. HOXD10, HOXD11 and HOXD13 were successfully downregulated by siRNA interference. In three of four cell lines SMAD4 expression was significantly decreased after HOX knockdown. Gene expression in EW-7 was not significantly changed after HOX knockdown. Individual HOX knockdown did not lead to a significant change of SMAD4 expression (data not shown). Problems with downregulation of individual HOX genes due to functional redundancy, compensation mechanisms and even due to a sort of recruitment will be addressed in 4.4 (see p. 110).

3.6.3 HOX knockdown is associated with a decrease of RUNX2 expression

RUNX2 is not only the master regulator of osteoblast differentiation but also maintains a major role in terminal chondrocyte differentiation. (Ducy *et al.* 1997; Komori 2010) It is a common BMP target and also an important cofactor in BMP signaling since it was identified to physically interact with R-SMADs. (Lee *et al.* 2000; Zhang *et al.* 2000)

Figure 28 illustrates RUNX2 expression on mRNA level under HOX suppression in various ES cell lines. Triple HOX knockdown was commonly associated with a decrease of RUNX2 expression. In SK-N-MC and A-673, HOX genes were downregulated by retroviral gene transfer, respectively. RUNX2 expression was also reduced in cells with low HOXD10 expression. Osterix expression didn't change after HOX knockdown (data not shown).

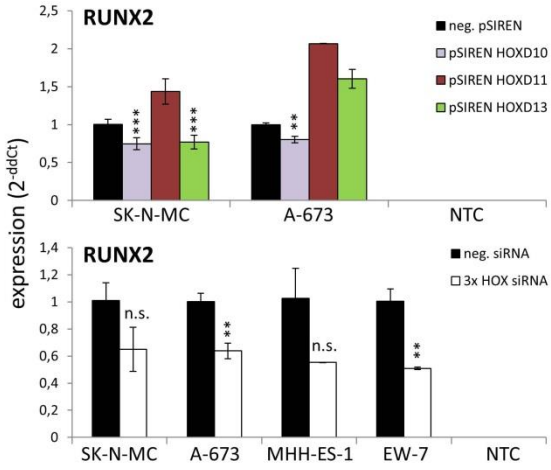

Figure 28: Decrease of RUNX2 expression under HOX suppression.
Gene expression was analyzed on mRNA level by qRT-PCR. In four ES cell lines, triple HOX knockdown was achieved by siRNA interference. In SK-N-MC and A-673, HOXD10, HOXD11 and HOXD13 were also downregulated by retroviral gene transfer, respectively. $p < 0.05$ (*), $p < 0.01$ (**), $p < 0.001$ (***), not significant (n.s.), not detectable (n.d.), NTC is non-template control.

3.6.4 Especially HOXD13 knockdown leads to reduced expression of collagen-encoding genes

Collagens are not only common targets of BMP signaling but also downstream targets of RUNX2. BMPs and RUNX2 were demonstrated to activate COL1A1 which encodes type I collagen. BMP2-induced transcription of type X collagen gene is suggested to involve cooperation of RUNX2 and SMAD proteins. (Ducy *et al.* 1997; Leboy *et al.* 2001; Lee *et al.* 2000; Volk *et al.* 1998)

Figure 29 shows collagen gene expression on mRNA level after HOX knockdown. COL1A1 expression was reduced after HOXD10, HOXD11 and HOXD13 knockdown, respectively. HOXD13 knockdown was additionally associated with a significant decrease of COL2A1 and COL10A1 expression.

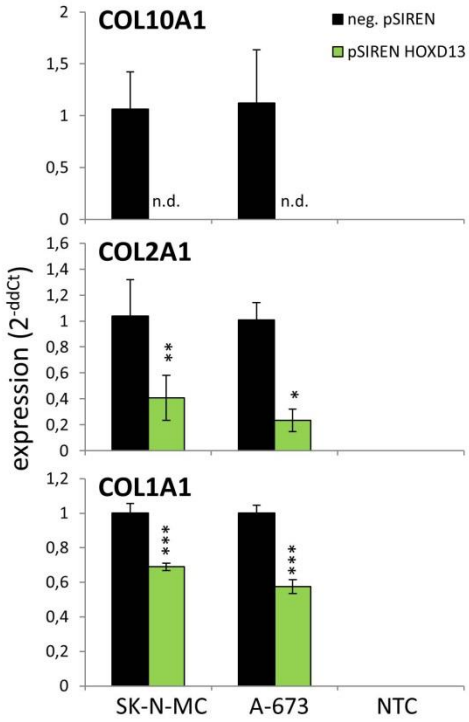

Figure 29: Decrease of expression of collagen-encoding genes after HOX knockdown.
Gene expression was analyzed on mRNA level by qRT-PCR. Especially HOXD13 downregulation (less than 30%) by retroviral gene transfer resulted in significantly reduced expression of collagen-encoding genes in two ES cell lines. Type I, type II and type X collagens were affected. COL1A1 expression was also reduced after HOXD10 and HOXD11 knockdown.
$p < 0.05$ (*), $p < 0.01$ (**), $p < 0.001$ (***), not significant (n.s.), not detectable (n.d.), NTC is non-template control.

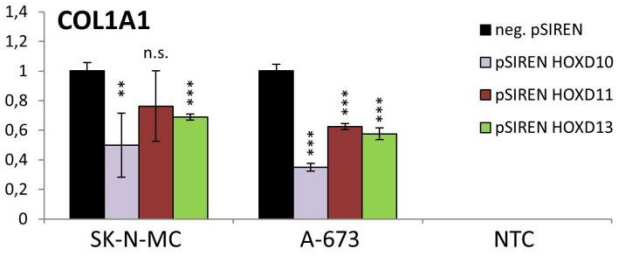

3.7 HOX genes don't influence endothelial cell tube formation

To investigate if HOX knockdown influences the angiogenesis pattern of Ewing sarcoma cell lines, the endothelial cell tube formation assay was performed using BD Matrigel™ as described in 2.2.9.1. The experiment was carried out in 96-well culture plates. 40,000-70,000 transiently transfected Ewing sarcoma cells were grown on gelled Matrix. Tube formation was analyzed by fluorescence microscopy. Images were taken by use of a Nikon Eclipse TS 100 with an attached Nikon Coolpix 5400 camera. RNA was isolated, cDNA was synthesized and HOX gene knockdown was determined on mRNA level by qRT-PCR. In those cell lines which had been treated with a specific HOX siRNA, gene expression of HOXD10, HOXD11 and HOXD13 was downregulated to less than 45%, respectively.

Figure 30 on p. 84 shows that in three Ewing sarcoma cell lines, neither downregulation of HOXD10 nor HOXD11 and HOXD13 led to a change of endothelial tube formation. Wildtypes of SK-N-MC and A-673 didn't form any endothelial tubes at all. Neither these two cell lines did after treatment with a negative control siRNA or any HOX siRNA. RD-ES wildtype shows only weak tube formation but this cell line still formed tubes after treatment with a negative control siRNA or any HOX siRNA.

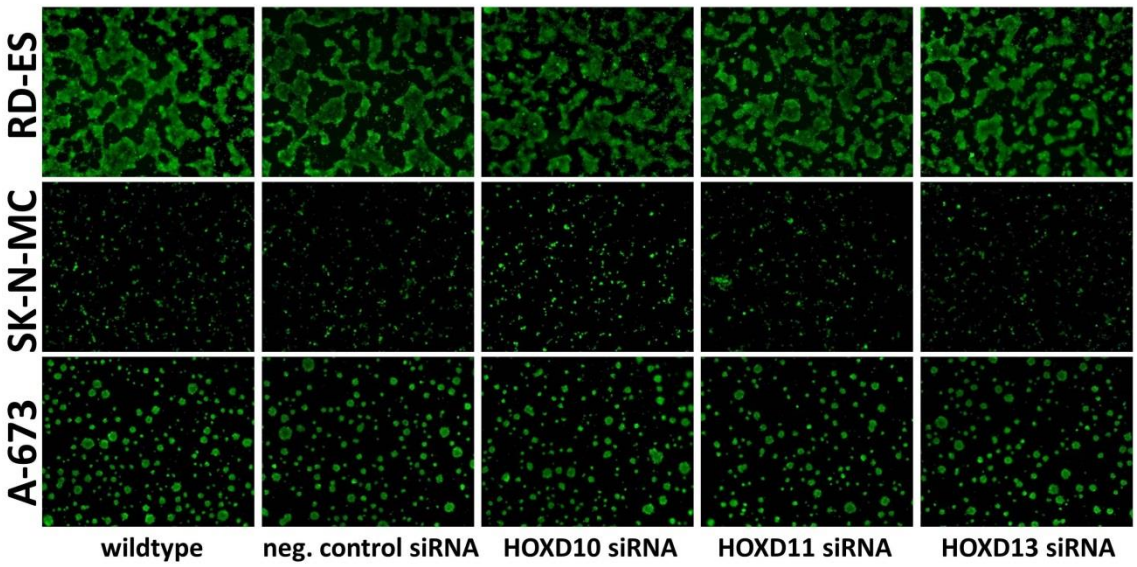

Figure 30: Endothelial cell tube formation assay.
SK-N-MC, A-673 and RD-ES were transiently transfected with specific HOX siRNAs. HOX gene expression was downregulated to less than 45%. Endothelial differentiation potential of all three cell lines did not change after transient RNA interference. Images were taken by fluorescence microscopy at 4x magnification.

3.8 HOX genes promote proliferation of Ewing sarcoma cells

To determine whether proliferation rate changes under HOX gene suppression pSIREN HOX cells of two Ewing sarcoma cell lines were seeded in particular 96-well plates. These plates contain integral sensors which measure cell proliferation according to electrode impedance. The proliferation experiment was performed by use of the xCELLigence Real-Time Cell Analyzer (see 2.2.9.1).

In SK-N-MC and A-673 HOXD10, HOXD11 and HOXD13 were downregulated by retroviral gene transfer (pSIREN cells). SK-N-MC and A-673 neg. pSIREN which were treated with a negative control siRNA served as control. Cells were seeded in hexaduplicates, respectively, and proliferation rate was determined every 4 hours for 10 days.

Figure 31 shows proliferation rates of A-673 and SK-N-MC after HOX gene knockdown. The upper panel illustrates that all A-673 pSIREN cells suffer from a decrease of proliferation rate in comparison to neg. pSIREN control cells. A-673 neg. pSIREN cells achieved a cell index value of 6 after 100 hours of incubation. A-673 pSIREN HOXD11 cells also achieved this cell index value, but not before 150 hours of incubation, cell index values of pSIREN HOXD10 and pSIREN HOXD13 cells were much lower. The lower

panel of Figure 31 shows proliferation rates of SK-N-MC pSIREN cells in comparison to neg. pSIREN cells. Altogether, all SK-N-MC cells showed lower cell index values in comparison to A-673 cells. Since A-673 possesses a p53 mutation unlike SK-N-MC, higher cell index values for A-673 are the logical consequence. Proliferation of SK-N-MC pSIREN HOXD13 and HOXD11 was delayed in comparison to neg. pSIREN control cells; this effect was significant in pSIREN HOXD13 only though. SK-N-MC pSIREN HOXD10 acted in an extraordinary and unexpected way: it achieved cell index values of 5.3 after 150 hours and thus showed a significantly higher proliferation than neg. pSIREN control cells and the two other pSIREN cells. This behavior seemed to be uncommon but correlated with the results of the colony forming assay (see p. 56). Another doctoral student was intended for the repeat experiment.

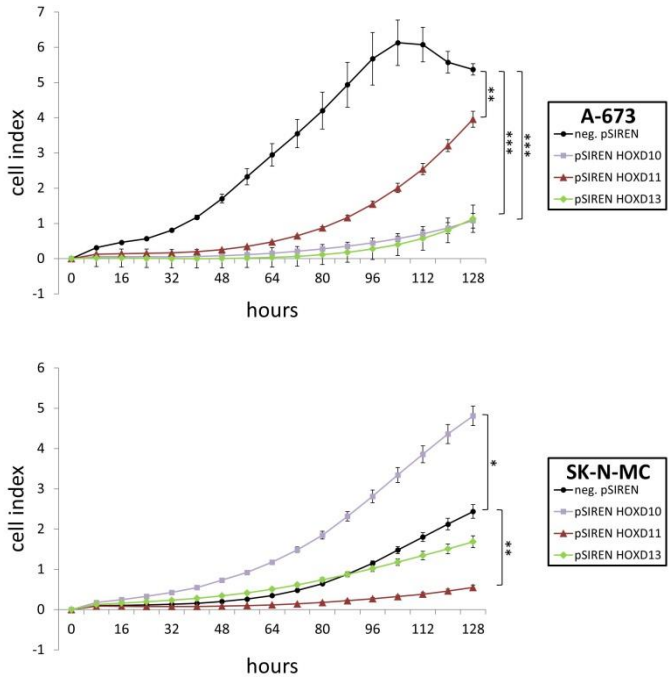

Figure 31: Decreased cell proliferation under HOX suppression.
In A-673 and SK-N-MC HOXD10, HOXD11 and HOXD13 were downregulated by retroviral gene transfer, neg. pSIREN cells were treated with a control siRNA. Cell index was determined according to change of electrode impedance by use of xCELLigence Real-Time Cell Analyzer. Upper panel: In all three A-673 pSIREN HOX cells cell index values were significantly lower than in neg. pSIREN cells. Lower panel: In SK-N-MC, proliferation rate of neg. pSIREN cells was higher than the one of pSIREN HOXD11 and HOXD13 cells. pSIREN HOXD10 cells proliferated stronger than control cells. Error bars represent standard deviation of sextuplicates. $p < 0.05$ (*), $p < 0.01$ (**), $p < 0.001$ (***).

3.9 HOX knockdown inhibits anchorage-independent growth of ES cells

A potential influence of HOX gene knockdown on anchorage-independent growth capacity of ES cells was monitored in the colony-forming assay. As described in detail in 2.2.9.2, Ewing sarcoma cells were resuspended in a certain cell resuspension solution and then mixed with methylcellulose-based media before they were distributed equally onto 35 mm culture plates. Ewing sarcoma cell clones in which HOX gene expression was downregulated by retroviral gene transfer were used: A-673 pSIREN HOXD10, pSIREN HOXD11, pSIREN HOXD13and shRNA controls, similarly

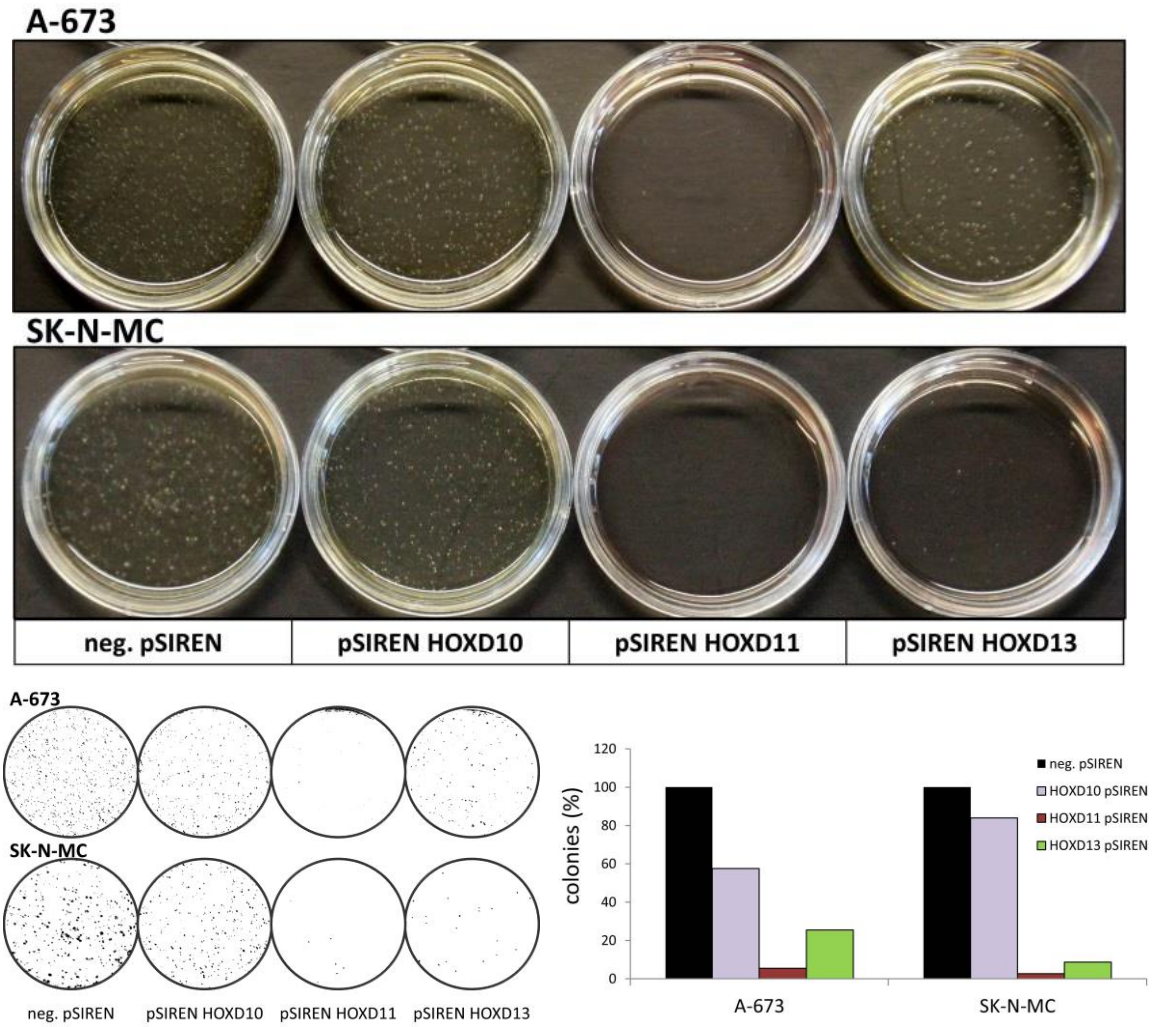

Figure 32: HOX genes promote anchorage-independent growth capacity of Ewing sarcoma cells.
Upper panel: Ewing sarcoma cell clones in which HOXD10, HOXD11 and HOXD13 were downregulated by retroviral gene transfer were seeded in methylcellulose-based media. Cells treated with a negative control siRNA served as control. After two weeks of incubation at 37°C photos were taken. **Lower panels:** Left chart illustrates virtual culture plates before counting colonies by use of Image J software. Right chart shows numbers of colonies counted. Colonies were counted manually and automatically three times. In both cell lines, pSIREN HOXD10, HOXD11 and HOXD13 cells formed fewer colonies than control cells.

experiments were performed for SK-N-MC. Cells which had been treated with a negative control siRNA, neg. pSIREN, served as control.

After two weeks of incubation at 37°C images were taken by use of Canon EOS 600D and colonies were counted manually and automatically by means of Image J software. Colonies were counted three times, altogether leading to the same result regarding descending order of cell clones. Left panel of Figure 32 shows culture plates of this experiment after two weeks of incubation at 37°C. Upper chart of the right panel illustrates virtual culture plates before counting, lower chart shows colonies counted using Image J. Altogether, all A-673 cell clones formed more colonies in comparison to the particular SK-N-MC cell clones, its p53 mutation could be the reason for this. In both cell lines neg. pSIREN control cells formed most colonies. Colonies of SK-N-MC neg. pSIREN cells were also bigger than the ones of the pSIREN cells. After HOX downregulation by retroviral gene transfer, all three cell clones, pSIREN HOXD10, pSIREN HOXD11 and pSIREN HOXD13 of A-673 and SK-N-MC, formed fewer colonies than control cells. This effect seemed to apply especially to pSIREN HOXD11 cells.

Summing up, downregulation of HOXD10, HOXD11 and HOXD13, decreased anchorage-independent growth capacity in these two Ewing sarcoma cell lines.

3.10 HOX genes promote chondrogenic differentiation in Ewing sarcoma cells

Since there are many publications which describe the role of HOX genes in limb development and bone formation (see p. 6), we investigated whether HOX gene knockdown influenced chondrogenic and osteogenic differentiation potential of Ewing sarcoma cells.

Potential of chondrogenic differentiation of Ewing sarcoma cell lines was analyzed using a special differentiation kit which had originally been developed for the chondrogenic differentiation of mesenchymal stem cells. The experiment was carried out in 6-well culture plates. SK-N-MC and A-673 were seeded out in micromass cultures and cultivated under differentiating conditions for two weeks. Ewing sarcoma cells in which HOX gene expression was downregulated by retroviral gene transfer were used: SK-N-MC or A-673 with pSIREN HOXD10, pSIREN HOXD11, pSIREN HOXD13 expression. Cells treated with a negative control shRNA (neg. pSIREN) served as

control. For a detailed description of this experiment, see 2.2.9.5.

Cells were seeded in control growth medium and in chondrogenic differentiation medium. After 14 days, cells were processed for gene expression analysis or Alcian blue staining. Gene expression was analyzed on mRNA level, comparing cells which had grown under differentiation conditions with those which had grown in control medium.

Cells in control medium grew and proliferated much better in comparison to those under differentiating conditions. Although differentiation medium was changed almost every day, a lot of SK-N-MC cells died under differentiating conditions. This especially applied to pSIREN HOX cells, however. There was no problem with neg. pSIREN cells; under differentiating conditions they formed dendritic branches (see 20x magnification, Figure 33). Figure 33 illustrates that Ewing sarcoma cells in micromass cultures, neg. pSIREN cells as well as pSIREN HOX cells, proliferated normally in control growth medium. A lot of SK-N-MC pSIREN HOX cells died under

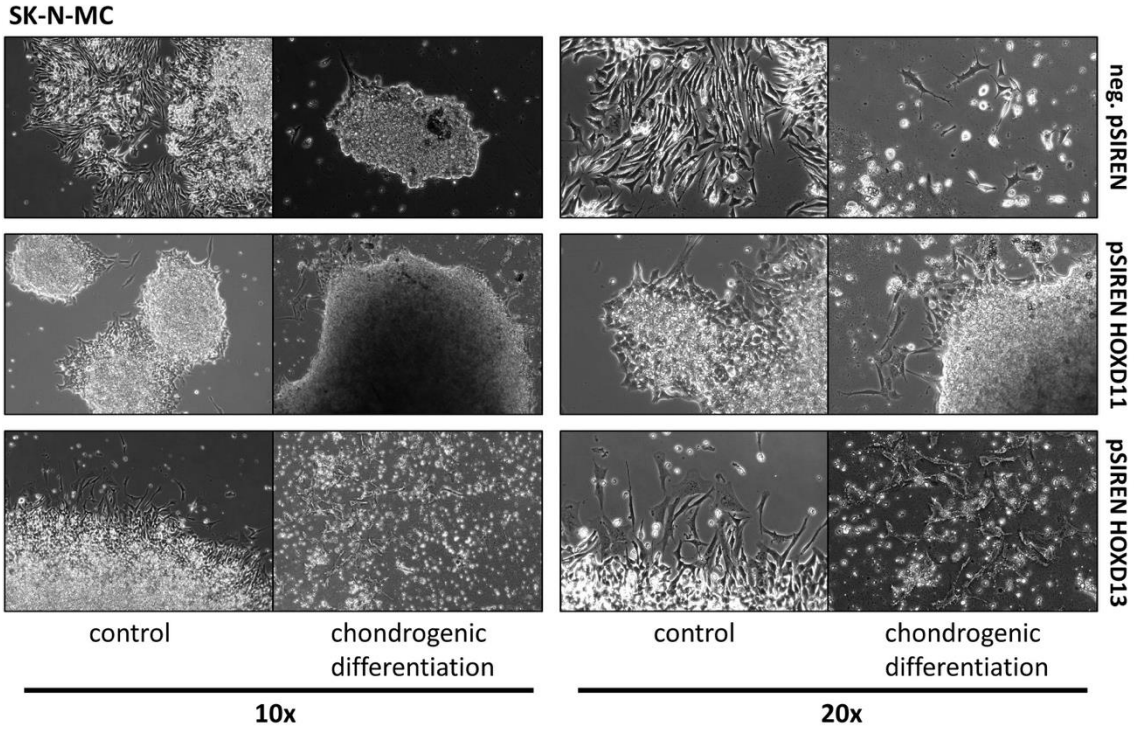

Figure 33: Ewing sarcoma cells after 14 days under chondrogenic differentiation conditions. neg. pSIREN is the control cell line which was treated with a negative control siRNA. In pSIREN HOXD11 and HOXD13 the correspondent gene was downregulated by retroviral gene transfer. A lot of cells of pSIREN HOXD11 and HOXD13 cells died under differentiating conditions. Cells grew and proliferated in control medium though, neg. pSIREN cells grew under control and differentiating conditions. Under differentiating conditions, neg. pSIREN cells formed dendritic branches. Images were taken by microscopy at 10x and 20x magnification.

differentiating conditions, this even applied more to pSIREN HOXD13 than to pSIREN HOXD11 cells (see 10x magnification). This did not apply to A-673, however; this cell line grew under differentiating conditions as well as in control medium.

The chondrogenic differentiation experiment was repeated several times. On the one hand RNA was isolated for gene expression analysis (see Figure 34), on the other hand cells were processed for Alcian blue staining. Despite several attempts and modifications of the protocol, Ewing sarcoma cells didn't dye Alcian blue positive. Neither cells which had grown under differentiation conditions, nor cells which had grown in control medium could be stained. This also seemed to be independent from HOX gene expression since neg. pSIREN as well as pSIREN HOX cells could not be stained.

For gene expression analysis, RNA was isolated using Gene JET™ Purification Kit (2.2.3.2), cDNA was synthesized as usual. Marker genes of chondrogenic differentiation like SOX9, COL2A1, COL10A1 and IHH were determined on mRNA level by qRT-PCR. Different stages of chondrogenesis with more or less typical gene signatures are described on p. 16. Figure 34 illustrates gene expression patterns of SK-N-MC and A-673 cells after 14 days under chondrogenic differentiation conditions in comparison to 14 days in control growth medium.

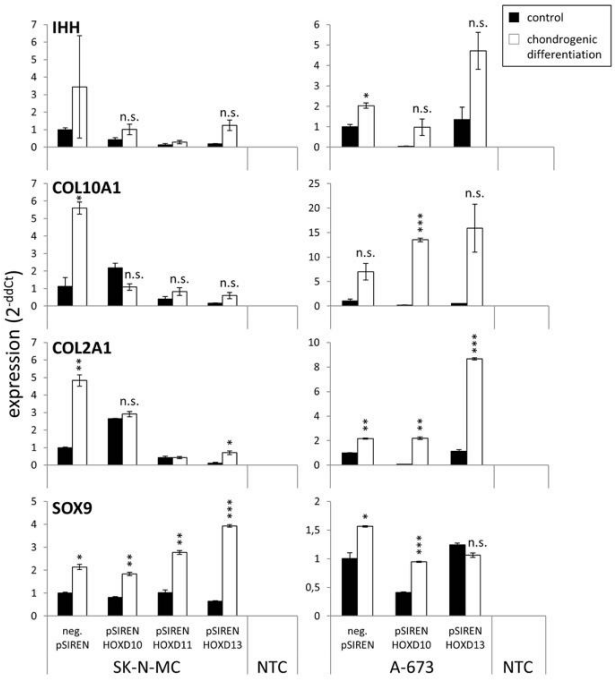

Figure 34: Gene expression analysis after 14 days under chondrogenic differentiation conditions.
After 14 days of incubation, media were removed, RNA was isolated and cDNA was synthesized. Expression of marker genes of chondrogenesis was determined on mRNA level by qRT-PCR. Control cells were incubated in control growth medium for 14 days. Chondrogenic differentiation of SK-N-MC under HOX suppression seems to have stopped at an earlier stage compared to control cells since only early markers of chondrogenesis like SOX9 and COL2A1 were upregulated. In A-673 as well, markers of late chondrogenesis were not significantly upregulated under HOX suppression. Markers of chondrogenesis: SRY (sex determining region Y)-box 9 (SOX9), collagen type II alpha I (COL2A1), collagen type X alpha I (COL10A1), indian hedgehog (IHH). NTC is non-template control. $p < 0.05$ (*), $p < 0.01$ (**), $p < 0.001$ (***), not significant (n.s.).

SK-N-MC significantly upregulated early markers of chondrogenic differentiation like SOX9 and partially COL2A1 under differentiating conditions. Even under HOX suppression, these early marker genes could be upregulated; COL2A1 only in neg. pSIREN and pSIREN HOXD13 cells though. Marker genes of later chondrogenic differentiation like COL10A1 and IHH, however, were not significantly increased in SK-N-MC under HOX suppression. This indicates that chondrogenic differentiation stopped in SK-N-MC pSIREN cells at an earlier stage than in control cells. Interestingly, mRNA levels of COL2A1, COL10A1 and IHH in pSIREN HOXD11 and pSIREN HOXD13 cells which grew in control medium were also much lower than levels in control cells.

RUNX2 was revealed to regulate late chondrocyte differentiation (see 1.2). Interestingly, RUNX2 expression significantly increased in SK-N-MC neg. pSIREN cells which had grown under differentiation conditions (data not shown). In pSIREN HOX cells, RUNX2 expression was lower than in neg. pSIREN cells. This indicates an advanced stage of chondrocyte differentiation of neg. pSIREN cells.

In A-673 marker genes of early chondrocyte differentiation, SOX9 and COL2A1, were similarly upregulated under differentiating conditions. Markers of later chondrogenic differentiation were not significantly upregulated, only pSIREN HOXD10 cells showed increased COL10A1 mRNA levels.

Gene expression analysis and observed increased cell death under differentiating conditions indicate reduced potential of chondrogenic differentiation of Ewing cells under HOX suppression.

3.11 Ewing sarcoma cells are capable of osteogenic differentiation - irrespective of HOX expression

Potential of osteogenic differentiation of Ewing sarcoma cell lines was also investigated using a special differentiation kit which had originally been developed for the osteogenic differentiation of mesenchymal stem cells. The experiment was carried out in 6-well culture plates as well but unlike the chondrogenic differentiation assay, in this experiment SK-N-MC and A-673 were distributed equally into each well of the culture plate and then cultivated under differentiating conditions for three weeks.

Cells were the same as the ones which had been used for the chondrogenic differentiation experiment. For a detailed description of this experiment and

particularly how cells were seeded in comparison to the chondrogenic differentiation assay, see 2.2.9.4.

After 21 days of incubation images were taken by microscopy (see Figure 35) and cells were processed for gene expression analysis (see Figure 36) or Alizarin red staining (see Figure 37). The experiment was repeated several times because osteogenic differentiation could be evaluated by either gene expression or Alizarin red staining.

Figure 35 shows a representative experiment with SK-N-MC. pSIREN HOXD11 and pSIREN HOXD13 cells were compared with neg. pSIREN cells. Regardless of HOX gene expression SK-N-MC cells grew and proliferated under osteogenic differentiation conditions, in contrast to chondrogenic differentiation conditions. Cells which had grown under differentiation conditions seemed to be bigger than respective control cells; this could indicate a successful differentiation. Interestingly, pSIREN HOX cells differed from neg. pSIREN cells morphologically, see 20x magnification.

For gene expression analysis RNA was isolated using Gene JET™ Purification Kit (see 2.2.3.2), cDNA was synthesized as usual. Gene expression of several marker genes of

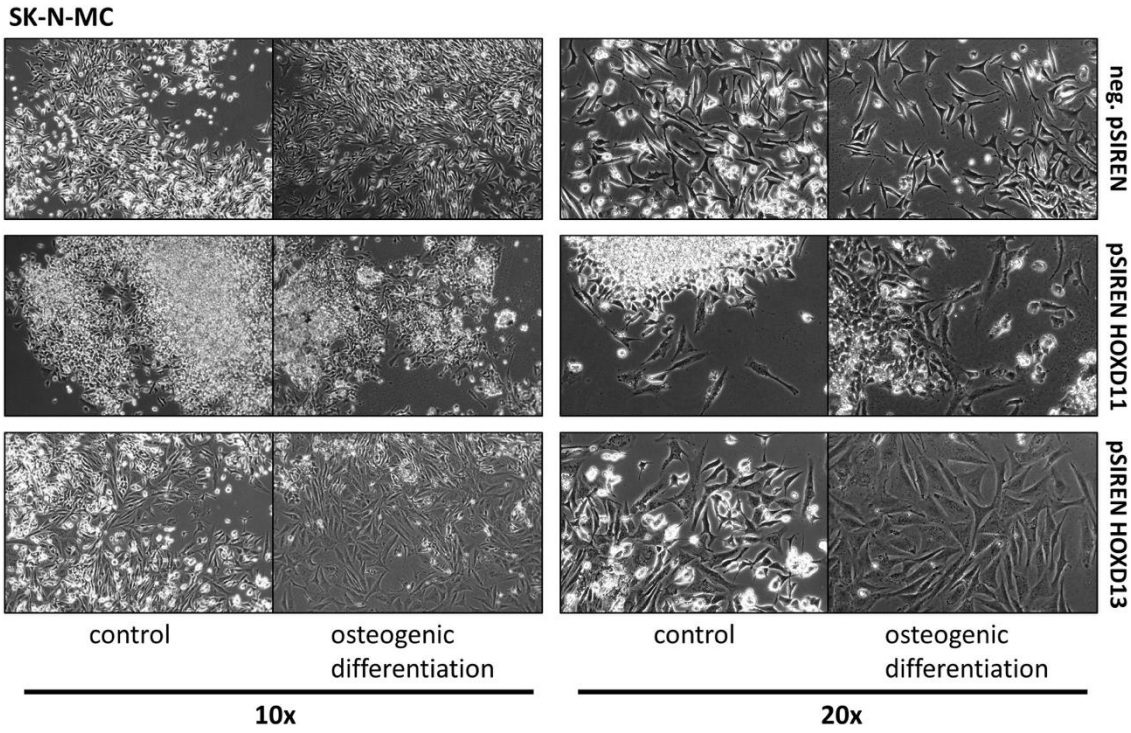

Figure 35: Ewing sarcoma cells after 21 days under osteogenic differentiation conditions. neg. pSIREN is the control cell line which was treated with a negative control siRNA. In pSIREN HOXD11 and HOXD13 the correspondent gene was downregulated by retroviral gene transfer. Regardless of HOX gene expression SK-N-MC cells grew and proliferated. Cells which had grown under osteogenic differentiation conditions seemed to be bigger than respective control cells, indicating a successful differentiation maybe. Furthermore pSIREN HOX cells differed from neg. pSIREN cells. Images were taken by microscopy at 10x and 20x magnification.

osteogenesis was analyzed on mRNA level by qRT-PCR, for example expression of BGLAP (osteocalcin), SPP1 (osteopontin), COL1A1 (collagen type I alpha I), ALPL (alkaline phosphatase), SP7 (osterix) and RUNX2 (runt-related transcription factor 2). Different stages of osteogenesis with more or less typical gene signatures are illustrated on p. 16.

In SK-N-MC and A-673 HOXD10, HOXD11 and HOXD13 had been downregulated by retroviral gene transfer, respectively. After 21 days under differentiation conditions gene expression of several osteogenic markers differed significantly from respective control cells (cells which had grown in control medium for 21 days). A specific pattern of this difference, however, was not detectable in these two cell lines (see Figure 36).

In A-673 SP7, ALPL, SPP1 and BGLAP were upregulated, mRNA levels of RUNX2 and COL1A1 were significantly lower in differentiated cells compared to control cells. In SK-N-MC only SP7, COL1A1 and BGLAP were upregulated, mRNA levels of other gene markers of osteogenesis didn't change significantly. In both cell lines gene expression pattern of pSIREN HOX cells didn't differ significantly from respective neg. pSIREN cells. Ewing sarcoma cells, regardless of HOX gene expression, seemed to be able to differentiate osteogenically. This indicates that downregulation of HOXD10, HOXD11

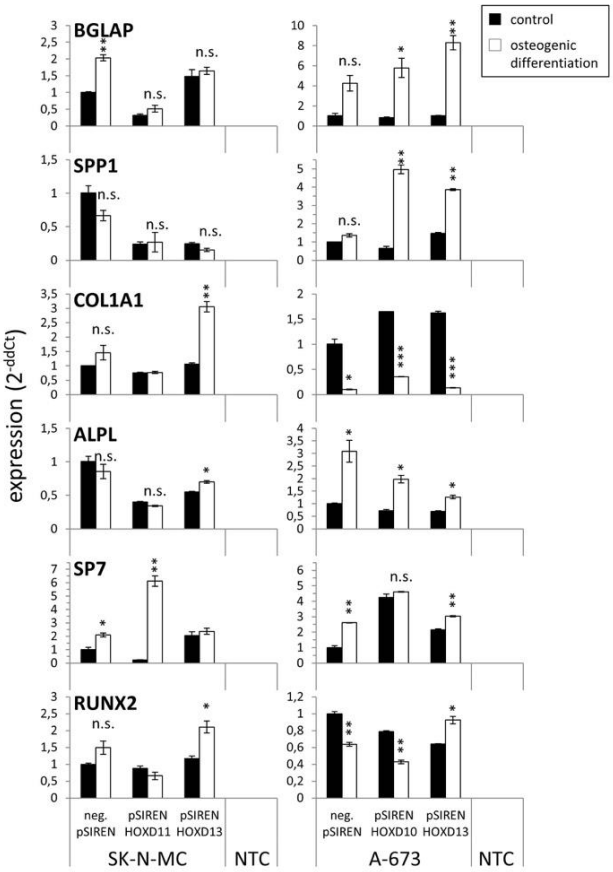

Figure 36: Gene expression analysis after 21 days under osteogenic differentiation conditions.
After 21 days of incubation, media were removed from culture plates. RNA was isolated and cDNA was synthesized. Gene expression of markers of osteogenesis was determined on mRNA level by qRT-PCR. Control cells were incubated in control growth medium for 21 days. In SK-N-MC and A-673 pSIREN HOX cells which had grown under differentiation conditions expression of several genes differed from respective control cells, a specific pattern was not detectable though. Marker genes of osteogenesis: osteocalcin (BGLAP), osteopontin (SPP1), collagen type I alpha I (COL1A1), alkaline phosphatase (ALPL), osterix (SP7), runt-related transcription factor 2 (RUNX2). NTC is non-template control. $p < 0.05$ (*), $p < 0.01$ (**), $p < 0.001$ (***), not significant (n.s.).

or HOXD13 doesn't influence osteogenic differentiation potential of Ewing sarcoma cells. This hypothesis was verified by repeating the experiment and this time analyzing differentiation of cells by Alizarin red staining. A detailed protocol of staining method can be found in 2.2.9.4.

Figure 37 shows SK-N-MC and A-673 after 21 days of incubation under osteogenic differentiation conditions. Media were removed and cells were stained with Alizarin red which usually indicates the presence of calcific deposition of cells of the osteogenic lineage. Images were taken by use of a Nikon Eclipse TS 100 with an attached Nikon Coolpix 5400 camera.

Cells which had been incubated in control medium could not be stained with Alizarin red. Figure 37 illustrates Alizarin red positivity of SK-N-MC and A-673 cells which had grown under osteogenic differentiation conditions, indicating a successful osteogenic

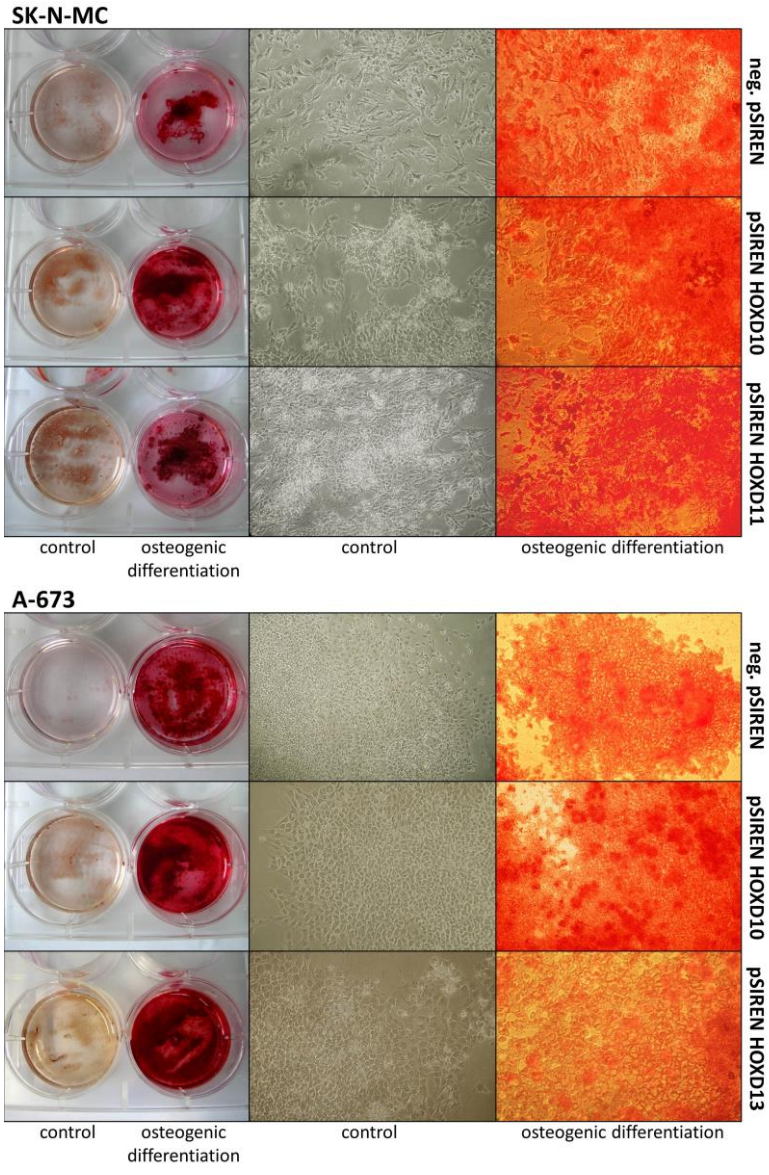

Figure 37: Alizarin red staining of Ewing sarcoma cells after 21 days of incubation under osteogenic differentiation conditions.
Left row of upper and lower panel shows top view of Alizarin red stained culture plates after 21 days of incubation under osteogenic differentiation conditions. Control cells had been incubated in control medium and were Alizarin red-negative. Images were taken by use of a Nikon Eclipse TS 100 with an attached Nikon Coolpix 5400 camera. All cells which had grown under differentiation conditions stained Alizarin red positive, indicating a successful osteogenic differentiation.
A difference between neg. pSIREN and pSIREN HOX cells was not detectable.

differentiation. A grading of Alizarin red staining, however, was indistinguishable. Regardless of HOX gene expression, cells stained Alizarin red-positive after 21 days of osteogenic differentiation conditions. A difference between neg. pSIREN cells and pSIREN HOX cells was not detectable. Thus, Alizarin red staining correlated with results of gene expression analysis.

4 Discussion

4.1 Overexpression of HOXD10, HOXD11 and HOXD13 in Ewing sarcoma

Here we present another malignant tumor with remarkable HOX gene expression. Microarray data revealed HOXD10, HOXD11 and HOXD13, all three of them, to be strongly upregulated in primary Ewing sarcoma tissue samples and Ewing sarcoma cell lines. HOXD10, HOXD11 and HOXD13 expression varies in other tissues such as normal healthy tissue and fetal tissue as well as neuroblastoma tissues; in general, these three HOX genes are detectable, but only to a very small negligible extent. According to Kessel and Gruss (1991) a certain "HOX code" defines each vertebral segment. According to this, each structure of the body, each tissue is characterized by a particular set of active HOX genes and a change of this HOX code will cause homeotic transformations, analogous to homeotic mutations in drosophila fly which were mentioned in the introduction of this doctoral thesis. (Kessel & Gruss 1991) The theory of a certain "HOX code" for each tissue is compatible with our microarray data: each tissue seems to have a particular HOX gene profile. Strong upregulation of HOXD10, HOXD10 and HOXD13, however, can only be observed in Ewing sarcoma samples. This specificity especially applies to HOXD13. Interestingly, HOXD10 expression was also detectable in neuroblastoma samples, a tumor which is derived from neural crest cells (Louis & Shohet 2015). This is interesting in this sense because currently a neural crest-derived precursor cell at the transition to mesenchymal and endothelial differentiation is assumed to be the cell of origin in Ewing sarcoma. (Staege *et al.* 2004) HOXD10 seems to be important in nervous system in general. It was shown to be involved in lumbar motor neuron patterning and spinal cord development on the one hand, and brain tumors on the other hand. (Abdel-Fattah *et al.* 2006; Lance-Jones *et al.* 2001; Lin & Carpenter 2003). Moreover, a mutation of HOXD10 is associated with Charcot-Marie-Tooth disease, a hereditary motor and sensory neuropathy. (Shrimpton *et al.* 2004)

HOX genes were initially identified to be master regulators of development, specifying the body segments along the anterior-posterior axis. (Lewis 1978; McGinnis & Krumlauf 1992) However, as already mentioned in the introduction, deregulated HOX

gene expression was observed in many different malignomas, especially in solid tumors but also in hematological neoplasias. In AML certain translocations result in leukemogenic fusion proteins consisting of HOXD11 and HOXD13 among other HOX genes, and the nucleoporin gene NUP98. NUP98 is part of a certain protein complex which controls transport from the cytoplasm into the nucleus and vice versa. It also maintains a role in transcription, cell cycle progression and mitotic spindle formation. Induction of HOX-NUP98 fusion in bone marrow cells lead to leukemic transformation with increase of white blood cells, anemia, decrease of lymphoid progenitors as well as increased proliferation of immature myeloid cells. Moleculargenetic consequences of HOX-NUP98 fusion in hematological malignancies have been investigated broadly and provided insight into pathogenesis of leukemia. (Gough *et al.* 2011) In contrast to this, mechanisms which lead to a deregulation of HOX gene expression or direct consequences of an upregulation of certain HOX genes in solid tumors are less understood. HOX genes were shown to be involved in multiple cellular processes which control cell cycle and apoptosis, adhesion and migration as well as differentiation and invasion. They are assumed to have direct effects on receptor signaling. (Shah & Sukumar 2010) However, little is known about specific HOX functions in malignant tumors, as is true for HOXD10, HOXD11 and HOXD13. Pathogenic mechanisms of HOXD10, especially in context of breast cancer, have yet been surfaced at best. HOXD10 was shown to be a direct target of miR-10b which is highly expressed in breast cancer cells. HOXD10 expression is inhibited by miR-10b; it is being lost with increasing degree of malignancy and re-expression compromises features of malignancy such as migration and progression. miR-10b, on the other hand, positively regulates cell migration and invasion and induces distant metastasis. (Carrio *et al.* 2005; Ma *et al.* 2007) Since then, upregulation of miR-10b with inhibition of HOXD10 expression has been observed in several other malignant tumors, among others in bladder cancer, brain tumors and gastrointestinal tumors. In most cases, HOXD10 seems to have an anti-tumorigenic effect since its gene expression levels were commonly low and stronger expression was associated with better differentiated, less invasive, in general less malignant phenotypes associated with better prognosis. (Carrio *et al.* 2005; Liu *et al.* 2012; Nakayama *et al.* 2013; Osborne *et al.* 1998; Sun *et al.* 2011; Wang *et al.* 2015; Xiao *et al.* 2014) Furthermore, malignomas were described

wherein HOXD10 was inactivated by hypermethylation. (Bennett *et al.* 2009; Wang *et al.* 2012)

Abate-Shen (2002) divided aberrant HOX gene expression in cancer into three different categories. In the first and most frequent category particular HOX genes are re-expressed in tumor cells. The malignant cells originate from cells which had already expressed those particular HOX genes during development, i.e. when they "were forced to" differentiate. In the second category particular HOX genes are newly expressed in tumor cells, in other words the cells of which the tumor cells are derived usually don't express these certain HOX genes during development. Only very few examples fall into this category. In the third category particular HOX genes are normally expressed in highly-differentiated tissues and corresponding tumor cells show a downregulation of these genes. (Abate-Shen 2002) Tumors with a downregulation of HOXD10 by miR-10b as mentioned earlier fall into the third category. In some cases tumors show very high levels of HOXD10 expression and HOXD10 levels are associated with invasive and proliferative phenotypes. This applies to head and neck squamous cell cancer, for example. (Sharpe *et al.* 2014) Those cases correspond to Abate-Shen's (2002) first category. Interestingly, in colorectal cancer HOXD10 expression can be very high or lost with degree of invasiveness, both is possible. (Bhatlekar *et al.* 2014; Wang *et al.* 2015)

Compared to HOXD10, HOXD11 and HOXD13 appear much less frequently in context of malignancies. As already mentioned before, HOXD11 and HOXD13, both of them, turned out to be fusion partner genes of NUP98 in hematological malignancies, such as MDS and AML with certain translocations. (Taketani *et al.* 2002) Only few cases are described, however, in which HOXD11 or HOXD13 expression is altered in solid tumors. HOXD11 was shown to be aberrantly methylated in breast cancer, ovarian cancer and malignant melanoma. (Cai *et al.* 2007; Furuta *et al.* 2006; Miyamoto *et al.* 2005) An overexpression of HOXD11 was observed in one ovarian cancer cell line and few ENT tumors (Morgan *et al.* 2010; Rodini *et al.* 2012) where HOXD11 knockdown partially impaired invasion (Sharpe *et al.* 2014). Aberrant methylation of HOXD13 was only described in malignant melanoma, glioblastomas and extrahepatic cholangiocarcinoma. (Furuta *et al.* 2006; Shinawi *et al.* 2013; Y. Shu *et al.* 2011) HOXD13 expression, in general, was determined in multiple tumor samples, its

potential functions or capacities, however, remain entirely unsolved. (Cantile *et al.* 2009)

It was already mentioned earlier that HOX genes are arranged in four clusters A - D on four different chromosomes (see p. 4-4). Within each cluster HOX genes follow a certain order from the 3' to the 5' end with genes at the 3' end being expressed not only in the more anterior parts of the body but also at an earlier moment of time than 5' end genes. According to this "spatial" and "temporal collinearity" especially caudal body parts and limbs express 5' HOX genes of all four HOX clusters. (Duboule & Morata 1994) To detect a potential similar mechanism of collinearity in Ewing sarcoma tissue, we also examined expression of posterior HOX genes of the other three clusters, i.e. gene expression of the paralogs of HOXD10, HOXD11 and HOXD13. Interestingly, some of them were also highly expressed in Ewing sarcoma samples, for example HOXB13. Altogether, however, there was also a strong expression in tissue samples which served as control. Paralogs were way less specific than respective HOXD genes. Mechanism of collinearity doesn't seem to be true here, especially since expression of posterior HOX genes was shown to be independent from tumor site. (Svoboda *et al.* 2014)

Since HOXD9 to HOXD13, all of them appear in context of limb development and they are assumed to have arisen from one ancestral HOX gene by duplication (see Figure 3, p. 4), we further examined gene expression of HOXD9 and HOXD12 in Ewing sarcoma tissue compared to normal tissue. Expression of these two genes, however, differed a lot from gene expression of other posterior HOXD genes. It could be observed ubiquitously in all tested tissues and didn't show any specificity for Ewing sarcoma. Gene expression of posterior HOX genes of other clusters (e.g. HOXB13) was more alike to HOXD10, HOXD11 and HOXD13 expression than expression of posterior HOX genes of the same cluster (i.e. HOXD9 and HOXD12). It is known, though, that HOX genes are subdivided into those 13 paralogous groups according to sequence similarity and position within the cluster and that these paralogs in turn show a functional relationship. (Maconochie *et al.* 1996)

Especially posterior HOXA and HOXD genes are related to proper limb development. Knowledge about detailed functions of particular HOX genes mainly originates from gene expression analysis during normal limb development and from multiple loss- and

gain-of-function experiments in animals. HOXA and HOXD paralogous groups were shown to be expressed similarly in the developing chick limb bud. (Nelson *et al.* 1996) They seem to function in a redundant kind of way because targeted mutations of single HOX genes and their paralogs cause similar phenotypes, respectively, whereas double mutants have synergistic defects and more severe phenotypes. (Boulet & Capecchi 2004; Fromental-Ramain *et al.* 1996) A combined tissue-specific deletion of both clusters in mice causes a severe phenotype with early arrest of limb growth. Deletion of one cluster only, i.e. HOXA or HOXD, results in way less drastic malformations. (Kmita *et al.* 2005; Zakany & Duboule 2007) Different paralogs are assumed to be responsible for different parts of the limbs; in simplified terms HOXD10 mutations especially cause malformations of the stylopod, HOXD11 mutations lead to malformations of the zeugopod whereas HOXD13 mutations especially affect the autopod. (Zakany & Duboule 1999, 2007) HOXB and HOXC genes rather don't maintain a major role in limb development. They are expressed in the developing limb bud, deletions of HOXB and HOXC cluster, however, don't cause characteristic limb malformations. (Nelson *et al.* 1996; Zakany & Duboule 2007)

Summing up, only Ewing sarcoma samples show a specific upregulation of HOXD10, HOXD11 and HOXD13. Other pediatric tumors such as osteosarcoma, rhabdomyosarcoma and neuroblastoma possess different HOX gene profiles. (Svoboda *et al.* 2014) These three HOX genes are especially associated with limb malformations. In only 50% of cases, however, Ewing sarcoma affects bones of extremities. (Bernstein *et al.* 2006) HOX gene expression can be detected in both bone and soft tissue Ewing sarcoma and it was shown to be irrespective of primary site of origin since it was equally high in all Ewing sarcomas. (Svoboda *et al.* 2014) Thus, a collinear HOX expression, which was mentioned earlier, can be eliminated in context of Ewing sarcoma. One of the categories of aberrant HOX gene expression in malignomas which were postulated by Abate-Shen (2002) may be considered. (Abate-Shen 2002)

The question whether it is a matter of re-expression or new expression of HOX genes in this case remains unanswered in this work but some ideas are given in our subsequent publication, see von Heyking *et al.* (2016).

4.2 HOX gene expression is not regulated by EZH2 in Ewing sarcoma

In drosophila homeotic gene expression is antagonistically regulated by Trithorax-group (trxG) and Polycomb-group (PcG) proteins. These proteins are associated with chromatin and modify its structure to activate or suppress transcription, respectively. (Hanson *et al.* 1999) Whereas Trithorax proteins function as an activator by removing a trimethyl group of histone H3, PcG proteins keep homeotic genes in a silent state by methylation of histone H3. (Di Croce & Helin 2013) PcG proteins were shown to function in multi-protein complexes called polycomb repressor complexes (PRC). Two of these PcG complexes have been discovered so far, PRC1 and PRC2. Common structure of a polycomb repressor complex and its function as repressor of HOX gene expression were evolutionarily conserved in flies and mammals. (Di Croce & Helin 2013; Levine *et al.* 2002) In mammals three components form PRC2: EZH2 (enhancer of zeste 2) or its homolog EZH1, SUZ12 and EED. Within this complex EZH2 exerts methyltransferase activity and maintains target genes in a silent state by methylation of lysine 27 on histone 3. (Di Croce & Helin 2013; Richter *et al.* 2009) PRC1 consists of the four core components RING1, PCGF, CBX and HPH. Several homologous proteins of each of the four components allow a high diversity. One PCGF homolog is PCGF4, also known as BMI1. (Di Croce & Helin 2013) Interestingly, EZH2 and BMI1 were shown to be highly upregulated in Ewing sarcoma tissue, both of them maintaining major roles in tumorigenesis. EZH2 was shown to maintain stemness by blocking endothelial and neuro-ectodermal differentiation. (Burdach *et al.* 2009; Richter *et al.* 2009; Svoboda *et al.* 2014) BMI1 on the other hand promotes anchorage-independent growth of Ewing sarcoma. (Douglas *et al.* 2008) Since HOX gene expression is normally regulated by PcG proteins and especially since PcG genes (EZH2, BMI1) and HOX genes, both were identified to be upregulated in Ewing sarcoma tissue, we wondered whether HOX gene expression was influenced by EZH2 expression. EZH2 was downregulated by siRNA interference and HOX gene expression was determined on mRNA level. A significant change of HOX gene expression, however, could not be observed in three Ewing sarcoma cell lines. Abate-Shen (2002) criticized that HOX genes were mostly examined on mRNA levels. Their gene products, the HOX proteins, which function as transcription factors have to be further analyzed. It can't be ruled out that aberrant HOX gene expression causes proteins with different functions or which don't function

at all. (Abate-Shen 2002) Overexpression of HOX genes in Ewing sarcoma, however, was recently found to be associated with altered epigenetic regulation. Polycomb proteins were identified to be highly upregulated suggesting a strong repression of their target genes. A lot of polycomb-regulated genes were simultaneously overexpressed though. Furthermore, polycomb target genes in Ewing sarcoma were shown to be different from those in normal tissues. With regard to its polycomb target genes, Ewing sarcoma was more similar to mesenchymal stem cells than to adult tissues. Moreover, methylation of lysine 27 on histone 3 (H3K27me3), which commonly occurs through EZH2, could not be detected across the HOXD cluster. EWS-FLI1 was assumed to interfere with the usual control of developmental transcriptional programs during stem cell differentiation. (Svoboda *et al.* 2014) These findings are compatible with our results. EZH2 knockdown didn't change HOX gene expression on mRNA level because epigenetic regulation of HOX gene expression in Ewing sarcoma is different from normal tissues. At some point of time in development of Ewing sarcoma the common regulation of HOX gene expression might have been lost.

EZH2, however, is only one of multiple polycomb-group proteins. Furthermore, HOX genes are not only regulated epigenetically. Soon after detection of HOX genes it was found out that they responded to retinoic acid, furthermore retinoic acid responsiveness decreased from 3' to 5' HOX genes. Retinoic acid was revealed to be essential during development of the central nervous system as well as limb formation. (Maden *et al.* 1996; Power *et al.* 1999) It was shown to sequentially activate HOX genes and induce differentiation of human embryonal carcinoma cells. (McGinnis & Krumlauf 1992; Simeone *et al.* 1990) Especially neuronal differentiation was promoted by retinoic acid. (Jones-Villeneuve *et al.* 1982) This phenomenon was also observed in neuroblastoma cells. Here, retinoic acid promoted growth arrest and neuronal differentiation by induction of HOXD genes, of which especially paralogous groups 8, 9, 10 and 12 seemed to be important. (Zha *et al.* 2012) Extensive research is also being done on endocrine regulation mechanisms of HOX gene expression. Influence of hormones and vitamins may not be neglected. (Daftary & Taylor 2006) Furthermore, HOX genes were recently shown to be capable of a "self-regulation" mechanism. Especially 5' HOX genes were demonstrated to be required for proper expression of

other, more anterior HOX genes in limb development. This regulation could even be achieved across different clusters, i.e. disruption of HOXA genes caused aberrant expression of anterior HOXD genes and vice versa. (Sheth *et al.* 2014) Autoregulatory mechanisms of HOX genes were already described decades ago. (Gould *et al.* 1997; Popperl & Featherstone 1992) We could also show a sort of "self-regulation" of HOX gene expression in Ewing sarcoma cells. HOXD10 knockdown also caused decrease of HOXD11 expression (see Figure 21, p. 76).

A lot of research is being done on cis-regulatory elements and their effects on HOX expression, especially in context of collinearity during development. Such regulatory elements were identified within and outside the HOX clusters. Regulatory elements which control expression of HOXD genes in limb development, however, were not detected within the HOXD cluster but in flanking genomic regions which contain only few genes. All those non-coding sequences are assumed to be capable of influencing HOX expression. (Lee *et al.* 2006; Spitz *et al.* 2001; Tschopp & Duboule 2011) Regulation of HOX gene expression by non-coding RNAs has been well established. Especially long non-coding RNA "HOTAIR" (**HO**X **A**ntisense **I**ntergenic **R**NA) was shown to control HOX gene expression on chromatin level. (Rinn *et al.* 2007) Effects of HOTAIR on HOX gene expression could recently be observed in malignomas as well. (Chakravadhanula *et al.* 2014; Heubach *et al.* 2015) Moreover, short non-coding RNAs, such as miRNAs, within the HOX clusters were identified to preferably target mRNA of more anterior, i.e. more 3' HOX genes. (Yekta *et al.* 2008) In general, other "common" regulation mechanisms such as activation by transcription factors or post-transcriptional modifications such as alternative splicing or polyadenylation have to be considered.

4.3 HOX gene expression is not regulated by EWS-FLI1

Chromosome translocations in Ewing sarcomas were already described in the early 1980s. (Turc-Carel *et al.* 1984) Soon Ewing sarcomas were discovered to be characterized by particular translocations which lead to oncogenic gene fusions. In more than 85% of cases reciprocal chromosomal translocation t (11; 22) causes a fusion between EWS and FLI1, resulting in fusion protein EWS-FLI1. Two types of translocation exist, involving two different exons of the FLI1 gene. In other, less

frequent translocations EWS is fused to ERG, ETV1, ETV4 or FEV. (Bernstein *et al.* 2006; Delattre *et al.* 1992; Sankar & Lessnick 2011) EWS-FLI1 was identified as the major driving force in pathogenesis of Ewing sarcoma because it was shown to induce genes regulating cell cycle, proliferation and DNA damage response on the one hand whereas genes associated with differentiation and cell communication are repressed. (Kauer *et al.* 2009; Riggi *et al.* 2005) We wondered whether EWS-FLI1 was also responsible for overexpression of HOXD10, HOXD11 and HOXD13 in Ewing sarcoma. In the past, at least FLI1 was shown to control HOXA10 expression in megakaryocytic differentiation. (Gosiengfiao *et al.* 2007) So we examined effects of EWS-FLI1 expression on HOX expression. We assessed that HOXD10, HOXD11 and HOXD13 expression in Ewing sarcoma cells was irrespective of type of EWS/FLI1 translocation (see right panel of Figure 13, p. 66). Then we downregulated EWS-FLI1 in four Ewing sarcoma cell lines by use of two different siRNAs. In a fifth cell line, EWS-FLI1 was knocked down by retroviral gene transfer. In some cases we achieved a downregulation to less than 20%. In two cell lines (SK-N-MC and A-673) HOXD13 expression decreased significantly under EWS-FLI1 suppression. However, this phenomenon could not be observed in the other three Ewing sarcoma cell lines. We wondered whether HOX gene expression could be induced by EWS-FLI1. Induction of EWS/FLI1 in mesenchymal progenitor cells is known to cause a transformation and generation of a tumor similar to Ewing sarcoma. (Riggi *et al.* 2005) So we transfected two human mesenchymal stem cell lines with EWS-FLI1 constructs and examined HOX gene expression on mRNA level. Since HOXD13 expression decreased under EWS-FLI1 suppression in two Ewing sarcoma cell lines, we especially expected HOXD13 to be increased after EWS-FLI1 induction. EWS-FLI1 induction was validated on mRNA level. HOX expression was already detected in mesenchymal stem cells which had been transfected with an empty vector. This expression seemed to be irrespective of origin of mesenchymal stem cell because one cell line had been generated from peripheral blood mononuclear cells after G-CSF administration; the other cell line was derived from bone marrow. Both cell lines were obtained from healthy patients. (Conrad *et al.* 2002; Thalmeier *et al.* 1994) Surprisingly, HOX expression did not increase significantly after EWS-FLI1 induction, a slight induction of HOXD10 was vaguely perceptible. HOXD13 expression, however, didn’t change under EWS-FLI1 expression. Altogether, our findings are a little

inconsistent with published literature.

Svoboda *et al.* (2014) blamed EWS/FLI1 to be responsible for the aberrant HOX gene expression in Ewing sarcoma. They described two clinically designated Ewing sarcomas without a typical EWS/FLI1 or EWS/ERG translocation. In these two tumors, an overexpression of posterior HOX genes could not be observed. Moreover, they detected a discrepancy regarding histone modifications of HOX promoters between stem cells and Ewing sarcoma cells. They generated EWS/FLI1-positive neural crest stem cells and cultivated them in differentiation conditions. A significant induction of HOXD10, HOXD11 and HOXD13 expression was determined after a couple of weeks in differentiation conditions. (Svoboda *et al.* 2014) Maybe our transfected mesenchymal stem cells have not been cultivated in differentiation conditions long enough. It is conceivable that an induction of HOX genes by EWS/FLI1 might not be observed before several weeks of incubation. Thus, this experiment was repeated. See our subsequent publication von Heyking *et al.* (2016)

HOX gene expression and possible roles in different types of stem cells were recently reviewed by Seifert *et al.* (2015). HOX genes are assumed to be actively repressed in embryonic stem cells and induced pluripotent stem cells until they commit themselves into a certain lineage. In hematopoietic stem cells and neural crest cells on the other hand, HOX gene expression can be observed and seems to indicate a certain commitment, respectively. HOXA genes, for example, are especially assumed to control the differentiation program of hematopoiesis. In mesenchymal stem cells HOX gene expression patterns vary depending on source and determine respective differentiation potential. (Seifert *et al.* 2015) Especially HOXD genes, are essential for limb development and bone formation. According to Seifert *et al.* (2015) expression of posterior HOXD genes in mesenchymal stem cells indicates a sort of commitment. HOX genes are known to dictate cell identity. (Ladam & Sagerstrom 2014) Induction of particularly HOXD10, HOXD11 and HOXD13, those HOX genes which are associated with limb and bone development, by EWS-FLI1 in Ewing sarcoma could be one reason why Ewing sarcoma is a bone tumor in the first place. (Seifert *et al.* 2015; Svoboda *et al.* 2014) This, however, raises the question why Ewing sarcoma also emerges beyond the skeletal system and why high expression of posterior HOXD genes can be observed in both bone and soft tissue Ewing sarcomas. Even though it has to be mentioned that

soft tissue tumors seem to present low expression of posterior HOXD genes a little more often than bone tumors. (Svoboda *et al.* 2014)

4.4 Microarray analysis reveals few but critical downstream targets

Most knowledge about HOX gene function was acquired by means of gain- and loss-of-function experiments in animals. Our experiments were not different from these types of experiments; we generated a loss of function by gene knockdown by siRNA interference. Since siRNA interference causes only a transient downregulation of particular genes, we generated stable transfectants with low HOX expression by retroviral gene transfer. cDNA from two cell lines in which HOX genes had been downregulated successfully was sent away for microarray analysis. Gene expression patterns after HOX knockdown were compared on human Gene ST arrays (Affymetrix, GSE36100). 70-100 differentially regulated genes were identified after HOXD10, HOXD11 and HOXD13 knockdown, respectively. A little more than half of those genes were significantly downregulated. Only very few of these genes, however, could be verified by qRT-PCR. Microarray analysis provided only little insight into possible downstream targets of HOX genes in Ewing sarcoma. However, this little insight has already given an idea how diverse HOX targets can be and especially which diverse cell processes HOX genes can intervene in.

Microarray data revealed RAC2 to be significantly upregulated after HOXD10 knockdown. The protein encoded by RAC2 is a member of the RAC family of small guanosine triphosphate (GTP)-metabolizing proteins. (Didsbury *et al.* 1989) GTP-binding proteins are key regulators in signaling pathways; associated at the plasma membrane, they function as binary switches which control multiple cellular processes. (Zohn *et al.* 1998) The RAS family consists of three isoforms RAC1-3, of which RAC2 is selectively expressed in hematopoetic cells whereas RAC1 and RAC3 are ubiquitously expressed. (Didsbury *et al.* 1989; Haataja *et al.* 1997) RAC2 was shown to be a part of the NAPDH oxidase complex of neutrophils and essential for immunity. RAC2-deficient mice suffer from impaired hematopoiesis. RAC2-deficient neutrophils exhibit impaired superoxide production as well as impaired inflammatory response; this makes mice more susceptible for bacterial and fungal infections. (A. W. Roberts *et al.* 1999) RAC2 is also assumed to maintain an important role in B-cell adhesion and

T-helper 1 cell differentiation. (Arana *et al.* 2008; Li *et al.* 2000) Lane *et al.* (2012) demonstrated RAC signaling to be essential for normal bone development. RAC2 is also supposed to influence osteoclastogenesis, although RAC1 seems to be the more important player. (Y. Wang *et al.* 2008) Especially the two latter findings are interesting in context of Ewing sarcoma. Furthermore, RAC2 was shown to promote tumor growth, angiogenesis, invasion and metastasis in three tumor entities (lung cancer, melanoma, neuroblastoma). (Joshi *et al.* 2014) In our case, RAC2 expression was upregulated after HOXD10 knockdown. Thus, RAC2 expression should be further examined in Ewing sarcoma cells. Low RAC2 expression might be a hint at impaired immune response and bone development in Ewing sarcoma.

Another gene which was differentially regulated after HOX knockdown is ATRX. HOXD13 downregulation caused a significant decrease of ATRX expression (see 3.5.5, p. 79). ATRX belongs to the SWI2/SNF2 family of chromatin remodelers. (Picketts *et al.* 1996) ATRX, just like HOX genes, has been highly evolutionarily conserved. Nucleotide sequence revealed 85% identity between mice and humans. (De La Fuente *et al.* 2011; Picketts *et al.* 1998) It is associated with ATR-X syndrome, a severe non-progressive X-linked mental retardation which is associated with an unusal form of thalassemia. (Gibbons *et al.* 1995) ATR-X syndrome patients also suffer from multiple skeletal deformities and short stature. Thus, ATRX expression was further examined in early developing cartilage. ATRX expression could be observed in chondrocytes throughout the cartilage growth plate. Loss of ATRX, however, did not affect viability, growth or growth plate morphology; only minor defects of ossification were detectable. (Solomon *et al.* 2009) Mice with targeted loss of ATRX in limb mesenchyme on the other hand developed shortened and smaller digits. This suggested ATRX function to be more important in mesenchymal precursor cells than in differentiated chondrocytes. (Solomon *et al.* 2013) HOX genes are also known to be essential for proper limb development. (Goff & Tabin 1997; Kmita *et al.* 2005; Zakany & Duboule 2007) Potential relationships between HOX genes and ATRX in limb development, bone formation and especially in development of malignant bone tumors like Ewing sarcoma should be further elucidated.

Moreover, ATRX dosage seems to be critical for neuronal development. ATRX expression usually increases during neuronal differentiation. Loss of ATRX was

associated with size reduction and hypocellularity of cortex and hippocampus. Fewer neurons were prone to migrate and cell death rates were increased whereas proliferation was unaffected. ATRX overexpression in transgenic mice, on the other hand, was associated with multiple neurodevelopmental defects and in general, increased mortality. (Berube *et al.* 2002; Berube *et al.* 2005) Members of the Ewing family of tumors display different degrees of neuroglial differentiation. Whereas classic Ewing sarcoma is poorly differentiated, peripheral primitive neuroectodermal tumors appear better differentiated and more mature. Neural differentiation is indicated by expression of neural marker genes such as NSE, S100 or HNK-1. (Bernstein *et al.* 2006; Lizard-Nacol *et al.* 1989) Ewing cell lines were shown to be capable of neural differentiation after treatment with certain agents such as butylated hydroxyanisole (BHA). (Cavazzana *et al.* 1987; Richter *et al.* 2009) EWS/FLI1 was demonstrated to be responsible for the primitive neuroectodermal phenotype of this tumor family. It upregulates genes associated with neural crest development and differentiation; these genes are repressed upon inhibition of EWS-FLI1. (Hu-Lieskovan *et al.* 2005; Tirode *et al.* 2007) EWS-FLI1 induction in neuroblastoma cells changed their neural differentiation programs. Cells, in presence of EWS-FLI1, undergo parasympathetic differentiation like Ewing sarcoma cells instead of the sympathetic differentiation program of neuroblastoma cells. (Rorie *et al.* 2004; Tirode *et al.* 2007) ATRX expression should be further examined in Ewing cell lines, especially focusing on the question if neural differentiation potential of Ewing cells is related to ATRX expression.

Recently, ATRX appeared more and more in context of malignancies, for example osteosarcoma, glioma, neuroblastoma, melanoma, gastrointestinal tumors and prostate cancer. In these tumors ATRX expression is often lost, sometimes due to mutations, and in that case, patients have reduced survival. (Berbegall *et al.* 2014; Chen *et al.* 2014; Haberler & Wohrer 2014; Je *et al.* 2012; Marinoni *et al.* 2014; Qadeer *et al.* 2014) Certain functions of ATRX seem to be notably critical in pathogenesis of malignant tumors. Various mechanisms how ATRX maintains genomic stability have been reported. Lack of ATRX led to hypersensitivity to replication stress. On the one hand, ATRX was shown to be required for checkpoint activation and replication restart, further it was even demonstrated to be recruited to sites of DNA damage. (Leung *et al.* 2013) ATRX seems to be especially responsible for structural integrity of telomere

regions. ATRX knockdown in embryonic stem cells causes a telomere dysfunction. Increased telomere fusions and accumulating DNA damage can be observed. (Watson *et al.* 2013; Wong *et al.* 2010) Conserving the telomere regions is especially critical for indefinite proliferation of tumor cells. Some tumor cells are equipped with a telomerase which saves the telomeric DNA. Other tumor cells use a mechanism called "alternative lengthening of telomeres" pathway which is commonly associated with loss of ATRX. (Lovejoy *et al.* 2012) Moreover, ATRX was revealed to be required for proper mitosis. Loss of ATRX resulted in a prolonged prometaphase, chromatid cohesion and defective chromosome segregation. (Ritchie *et al.* 2008) ATRX was also identified to regulate X chromosome inactivation. (Sarma *et al.* 2014) Lastly, ATRX is capable of intervening in endocrine and metabolic signaling. Deletion of ATRX in embryonic nervous system and anterior pituitary of mice led to reduced growth and life span. (Watson *et al.* 2013)

HOXD13 knockdown caused a significant downregulation of ATRX in Ewing sarcoma cells (see 3.5.5, p. 79). Thus, strong HOXD13 expression is assumed to be associated with strong ATRX expression in Ewing sarcoma. Ewing sarcoma is a highly malignant bone tumor which surprisingly exhibits low mitotic and proliferative activity despite poor differentiation and partially extensive necrosis. (Freyschmidt *et al.* 2010) It should be further examined whether strong ATRX expression correlates with genomic stability in Ewing sarcoma cells. It is possible that ATRX expression guarantees a consistent and stable proliferation and growth despite low rates.

We suggest RAC2 and ATRX to be possible downstream targets of HOXD10 and HOXD13. Altogether, changes of gene expression seemed to be more remarkable after triple HOX knockdown though. Thus, posterior HOXD gene expression could be reduced to one third (see 3.3.2, p. 73). Interestingly, ATRX expression was even lower after triple HOX knockdown than after HOXD13 knockdown only (see Figure 25, p. 80).

Microarray data revealed two more genes to be differentially expressed after HOX knockdown. HAUS6 and EEF1D were downregulated after HOXD10 and HOXD11 knockdown, respectively. However, this could not be verified by qRT-PCR. Single HOXD10 and HOXD11 knockdown didn't lead to a clear downregulation of HAUS6 and EEF1D. But after triple HOX knockdown, gene expression on the mRNA level was significantly reduced (see p. 78). This phenomenon equally applied to HAUS6 and

EEF1D expression and resembled the phenomenon of ATRX expression which was even lower after triple HOX knockdown than after HOXD13 knockdown only.

HAUS6 encodes a subunit of a multiprotein complex called HAUS. Just like HOX genes, this protein complex is assumed to have been evolutionarily conserved because it shares homology to a similar protein complex in drosophila called Augmin. HAUS consists of eight subunits and regulates centrosome and spindle integrity. It localizes to interphase centrosomes and to mitotic spindle microtubules, its disruption causes microtubule dependent fragmentation of centrosomes and destabilization of kinetochore microtubules. (Lawo *et al.* 2009) Interestingly, a lot of tumor cells have multiple centrosomes. Although this usually leads to formation of multipolar mitotic spindles and chromosome segregation defects, such tumor cells can divide successfully because they can cluster multiple centrosomes into two spindle poles. Microtubule formation via the multiprotein complex Augmin was found to be necessary for this centrosome clustering in tumor cells. (Leber *et al.* 2010) Triple HOX knockdown led to a significant downregulation of HAUS6. Thus, HAUS6 expression should be further examined in Ewing sarcoma cells. It would be interesting to know if and how many cells in Ewing sarcomas contain multiple centrosomes. If true, function of HAUS multiprotein complex might be important in pathogenesis of Ewing sarcoma.

EEF1D expression decreased significantly after triple HOX knockdown. EEF1D encodes a subunit of the elongation factor 1 complex. Mediating the elongation step of mRNA translation, elongation factors are critical for efficient protein synthesis. Loading aminoacyl tRNAs onto the ribosome occurs under hydrolysis of GTP. EEF1D functions as a guanine nucleotide exchange protein and replaces GDP by GTP. (Cormier *et al.* 1993; Morales *et al.* 1992) EEF1D could be important in the context of Ewing sarcoma. EEF1D expression was revealed to be oncogenic. EEF1D overexpression by transfection caused a transformation of embryonic fibroblast cells. Anchorage-independent growth and the potential to grow as tumors in mice were observed. Blocking EEF1D translation, however, decreased this oncogenic potential and led to suppression of anchorage-independent growth and tumorigenesis. (Joseph *et al.* 2002; Lei *et al.* 2002) Furthermore, higher levels of EEF1D expression in malignant tumors such as medulloblastoma and esophageal carcinoma were associated with lymph node metastases, advanced stages and in general poorer prognosis for patients. (De Bortoli

et al. 2006; Ogawa *et al.* 2004) Involvement of translation factors in tumorigenesis was already reported 20 years ago. Multiple translation factors were identified to intervene in cell growth, proliferation and apoptosis and thus, be crucial in cancer development. (Thornton *et al.* 2003) Different phases of translation, initiation and elongation, both may be affected. Multiple translation initiation factors were reported to be differentially expressed in malignant tumors, but also elongation factors were revealed to function as oncogenes. (Spilka *et al.* 2013; Tatsuka *et al.* 1992) In our studies, triple HOX knockdown caused a significant decrease of EEF1D expression on mRNA level. It is conceivable that HOX genes might intervene in the process of translation in Ewing sarcoma, especially since this capability had already been described for other HOX genes. (Topisirovic *et al.* 2005)

Altogether, microarray data revealed only few possible downstream targets of HOX genes. However, some of them were reported to have crucial functions which might be important for pathogenesis of Ewing sarcoma. RAC2 signaling controls immune response and bone development. (Lane *et al.* 2012; A. W. Roberts *et al.* 1999) The chromatin remodeler ATRX is associated with limb development and skeletal deformities, just as neuronal differentiation. (Berube *et al.* 2005; Solomon *et al.* 2009; Solomon *et al.* 2013) ATRX, HAUS6 and EEF1D are assumed to intervene in fundamental cellular processes such as mitosis, microtubule formation and translation and all of these genes already appeared in the context of malignant tumors.

However, inconsistency verifying those genes of microarray analysis by qRT-PCR should be addressed briefly. As already mentioned in the introduction, HOX genes are assumed to have arisen from one ancestral HOX gene cluster by duplication and divergence. They are subdivided into 13 paralogous groups according to similarity in the homeobox region and position within the cluster. (Maconochie *et al.* 1996) Krumlauf (1992) already suggested that HOX genes of paralogous groups, i.e. HOX genes with the same numbers, might be partially redundant and capable of compensating each other's functions. (Krumlauf 1992) Few years later rescue mechanisms in case of loss of function among paralogous HOX genes were initially described. (Zakany *et al.* 1996) Indeed HOXD10, HOXD11, HOXD13 aren't paralogs, however, paralogs 9 - 13 are considered to originate from the same ancestral HOX gene by duplication (see Figure 3, p. 4). Thus, a potential redundancy of information

can't be denied. Targeted disruption of HOXD10, HOXD11 and HOXD13, respectively, results in different phenotypes of limb malformations though. Depending on which one of the three HOX genes is dysfunctional, stylopod, zeugopod or autopod are affected. HOXD13 mutations, for example, are associated with synpolydactyly whereas HOXD11 seems to be more responsible for the zeugopod since mice lacking HOXA11 and HOXD11 don't have radius and ulna. (Davis *et al.* 1995; Muragaki *et al.* 1996; Zakany & Duboule 1996) It has to be mentioned though that compound mutations of posterior HOX genes cause more severe phenotypes. Digit malformations which occur in absence of HOXD11 - HOXD13 are more complex than those due to simple HOXD13 mutations. Mice with targeted HOXD11 disruption practically don't have any digit malformations, those only occur in simultaneous absence of HOXD13 function. (Delpretti *et al.* 2012; Zakany & Duboule 1996) These findings indicate a prevalent role of HOXD13. The functional hierarchy of HOX genes and the theory of a sort of "posterior prevalence" have already been described decades ago. According to this, HOXD13 is supposed to be functionally dominant over the more anterior HOXD10 and HOXD11 when all three of them are being expressed simultaneously. (Duboule 1994; Duboule & Morata 1994) A certain HOXD13 mutation was even shown to disrupt the function of other posterior HOXD genes although expression of those genes was unaffected. (Bruneau *et al.* 2001) Maconochie *et al.* (1996) suggested the possibility of a sort of recruitment of HOX genes. In case of absence of one HOX gene another which is usually not involved might be recruited.

Since redundant and additive functions of posterior HOXD genes in limb development were documented, Salsi *et al.* (2008), on the other hand, considered the identification of target genes regulated exclusively by a single HOX protein as improbable. Instead, expression of genes which were bound by HOXD13 *in vivo* was assumed to be controlled by other posterior HOX proteins as well. (Salsi *et al.* 2008) These data are consistent with our microarray results and gene expression analysis. Only few downstream targets of HOXD10, HOXD11 and HOXD13, respectively, revealed by microarray data could be verified by qRT-PCR. Significantly differential expression of those genes, however, was observed after triple HOX knockdown. Interestingly, triple HOX knockdowns in Ewing sarcoma cells were successful at the first attempt in comparison to individual HOX knockdowns. Especially HOXD11 knockdown seemed to

be successful more often under simultaneous HOXD13 knockdown. According to this, a prevalent role of HOXD13 in Ewing sarcoma cells is conceivable, just as a sort of compensation through other HOX genes in absence of one.

4.5 HOX knockdown impairs proliferation and anchorage-independent growth of Ewing sarcoma cells

HOXD10, HOXD11 and HOXD13 expression was downregulated by siRNA interference to examine the function of HOX genes in Ewing sarcoma. We investigated the ability of Ewing sarcoma cells to form capillary-like structures depending on HOX expression. We used two Ewing sarcoma cell lines which are known not to be able to form endothelial tubes *in vitro* and a third cell line which is known to be competent to do so. HOX knockdown did not influence capability of endothelial tube formation. SK-N-MC and A-673 didn't form capillary-like structures after HOX knockdown either; RD-ES still did so, even under HOX suppression (see p. 84). Thus, capability of forming endothelial tubes in vitro was irrespective of HOX expression. According to published literature we had expected a different result at least for HOXD10 knockdown. Especially HOXD10 overexpression was revealed to maintain a non-angiogenic phenotype of endothelial cells by blocking angiogenesis *in vivo*. When implanted into mice, those cells with HOXD10 overexpression failed to form new vessels. (Myers *et al.* 2002) According to this, HOXD10 knockdown should have enabled Ewing sarcoma cells to form capillary-like structures.

Ewing sarcoma cells may not be equated with endothelial cells, though. The tissue-specific context of cell origin may not be neglected.

Since transient siRNA interference only had temporary effects, stable transfectants with low HOX expression were generated by retroviral gene transfer. Those were especially necessary for experiments which required 2 - 3 weeks of incubation. First, we measured proliferation rates of Ewing sarcoma cells depending on HOX gene expression. We assessed a decrease of proliferation under HOX suppression. In A-673, a cell line which possesses a p53 mutation (see p. 40), cell indices of all pSIREN HOX cells were significantly lower than control cells. This result was mostly verified in a second cell line (SK-N-MC). Here, cell indices of pSIREN HOXD11 and HOXD13 were lower than control cells; in case of HOXD13 this decrease was significant. Surprisingly,

SK-N-MC pSIREN HOXD10 cells overgrew the culture plate. It has to be mentioned though that HOX expression was not monitored at exactly that point of time. A normal or even overexpression of HOXD10 cannot be ruled out. It may-be questioned whether proliferation of cells with p53 mutation suffers more from HOX knockdown than cells with normal p53 function. A regulation of p53 expression through HOX genes was at least observed in breast cancer. (Chu *et al.* 2004) Repeat experiments after confirmation of successful HOX downregulation were done by another doctoral student and led to similar results. That way we could confirm that HOX genes promoted growth of Ewing sarcoma cells. (von Heyking *et al.* 2016) It is commonly known that HOX genes are capable of controlling cell proliferation and apoptosis, also in malignant tumors. Several HOX genes, although from other clusters, were shown to promote proliferation in various tumors such as hepatocellular carcinoma, gynecological tumors and renal cancer, this partially occurs via cyclin E1 and cyclin-dependent kinase 2. (Lee *et al.* 2015; Li *et al.* 2015; Liu *et al.* 2015) Moreover, it has been known for quite some time that HOX genes control developmental cell death via multiple death and survival pathways. Body parts, for example, are patterned by activation of localized cell death. A deletion in the coding sequence of HOXA13 which causes hypodactyly is associated with an increase in cell death as well. (Alonso 2002; Arya & White 2015; Post & Innis 1999) HOXD genes in general were revealed to particularly regulate cell cycle genes in neuroblastoma. (Zha *et al.* 2012) In head and neck cancer cells, HOXD10 and HOXD11 knockdown impaired proliferation and invasion. HOXD10 overexpression was identified to give head and neck squamous carcinoma cells a proliferative and migratory advantage. (Hakami *et al.* 2014; Sharpe *et al.* 2014) Cell cycle analysis might provide further insight into how HOXD10, HOXD11 and HOXD13 influence proliferation in Ewing sarcoma cells. Assessing cell death depending on HOX expression, for example by measuring certain apoptosis markers could be useful as well.

Results from proliferation assay were consistent with results from the second experiment, the colony-forming assay. The experiment measured ability of cells to proliferate and differentiate into colonies in a semisolid medium in response to cytokine stimulation. In two Ewing cell lines, pSIREN HOX cells formed fewer colonies than control cells (see Figure 32, p. 86); this especially applied to pSIREN HOXD11 and

HOXD13 cells. Results from colony-forming assay indicate an inhibition of anchorage-independent growth capacity under HOX suppression and suggest a prevalent role of HOXD11 and HOXD13 since downregulation of these two genes led to most remarkable results.

Already 30 years ago, *in vitro* anchorage-independent growth of tumor cells was suggested to correlate with the ability to form metastases *in vivo*. (Cifone & Fidler 1980) Since then colony-forming capacity has not only been linked with tumor cell aggressiveness *in vitro* such as tumorigenic and metastatic potentials but has also served as an indicator for *in vitro* transformation. (Mori *et al.* 2009) According to this, especially HOXD11 and HOXD13 knockdown reduced metastatic potential of Ewing sarcoma cells. This function was at least described for several paralogs of HOXD10, HOXD11 and HOXD13. HOXB13, for example, was revealed to mediate invasiveness of ovarian cancer and breast cancer cells; HOXA10 overexpression in ovarian cancer was in turn associated with poorer prognosis. (Li *et al.* 2009; Shah *et al.* 2013; Yamashita *et al.* 2006) Cervical cancer cells were less invasive after HOXC10 downregulation by siRNA interference. (Zhai *et al.* 2007) Strong and progressive HOXC13 overexpression was particularly observed in metastatic melanoma. (Cantile *et al.* 2012) These data indicate a role of posterior HOX genes in metastasis and progression of malignant tumors. Our *in vitro* experiments so far could be complemented with an invasion assay for example. An appropriate *in vivo* experiment might have more significance though. Invasiveness and tumor growth depending on HOX expression, for example, could be further examined by injection of A-673 pSIREN HOX cells into mice. According to our *in vitro* experiments, tumors generated by injection of pSIREN HOX cells are expected to be smaller, less invasive and in general less prone to metastasize in comparison to tumors generated by A-673 neg. pSIREN cells. Metastasis is in general a critical event in tumor progression. For patients with Ewing sarcoma, metastasis is the most unfavorable prognostic factor, it compromises survival rates massively. (Bernstein *et al.* 2006) So far, several genes such as DKK2, EZH2 and GPR64 have been identified to promote metastatic spread in Ewing sarcoma. (Hauer *et al.* 2013; Richter *et al.* 2013; Richter *et al.* 2009) It is essential to find out more about the key drivers of metastasis in Ewing sarcoma. Then, maybe in near future, a potential targeted therapy could be developed and prognosis of these patients could be improved.

4.6 HOX genes control genes related to BMP signaling and are critical for chondrogenic differentiation of Ewing sarcoma cells

Bone morphogenetic proteins were originally identified to induce ectopic bone and cartilage formation when cortical bone matrix was implanted in muscle and subcutaneous tissue of rodents. (Reddi & Anderson 1976; Urist & Strates 2009) Since then, BMPs were revealed to be critical for various processes in embryonic development such as neural patterning, skeletal development, limb patterning and organogenesis (kidney, lung, gut). (Hogan 1996) These days recombinant BMPs are even used therapeutically. Especially patients with non-union fractures and fibrotic diseases seem to benefit from this therapy. (Ali & Brazil 2014) Their involvement in the development of the skeletal system seems to be the most important function of bone morphogenetic proteins, since most BMPs were demonstrated to be capable of inducing cartilage and bone formation. (Carreira *et al.* 2014) This ectopic cartilage and bone develops accordingly to endochondral bone formation in limb development (see 1.2). (Tsumaki & Yoshikawa 2005)

HOXD10, HOXD11 and HOXD13 are highly upregulated in primary Ewing sarcoma tissue and Ewing sarcoma cell lines (see 3.1). HOX knockdown was associated with a significant downregulation of BMP2 and BMP4 on mRNA level (see 3.6.1). BMP2 and BMP4 do not only belong to the bone morphogenetic proteins with greatest osteogenic activity *in vitro* (Cheng *et al.* 2003) but were also revealed to be essential for cartilage formation. In the developing chick limb bud BMP2 expression can be detected in mesenchyme surrounding early cartilage condensations whereas BMP4 is expressed in the perichondrium of the cartilage elements. Ectopic BMP2 and BMP4 overexpression in the developing limb bud, respectively, led to dramatic increase of volume of cartilage elements. Increase in the amount of cartilage matrix and in the number of chondrocytes probably occurred through increased recruitment of precursor cells. (D. Duprez *et al.* 1996) Treatment with BMP antagonist noggin, on the other hand, inhibited cartilage formation due to failure of mesenchymal condensations and blocked chondrogenic differentiation. This suggests BMPs regulate initial steps of chondrogenesis. (Pizette & Niswander 2000) However, BMP2, but not BMP4, was reported to be crucial for chondrocyte proliferation and maturation during

endochondral bone formation. (B. Shu *et al.* 2011) On the other hand, BMP2- and BMP4-deficient mouse embryos, both die soon after conception, or rather before any chondrogenesis is initiated. (Winnier *et al.* 1995; Zhang & Bradley 1996)

Posterior HOXD genes are also expressed in the developing limb bud mesenchyme. Their expression domains are located in perichondral regions of cartilage growth and overlap with BMP expression domains. (Dolle & Duboule 1989; D. Duprez *et al.* 1996) Especially HOXD13 and BMP2 were identified to be expressed in overlapping regions and both were shown to be regulated by the same factors, one of them being retinoic acid. (Francis *et al.* 1994) Moreover, HOXD11 and HOXD13 expression was demonstrated to be activated by BMP2 in limb development. (D. M. Duprez *et al.* 1996) Misexpression of HOXD11 and HOXD13 in developing limb bud affected early cartilage condensation phase and bone growth, respectively. Respective long bones were shortened. (Goff & Tabin 1997) Posterior HOXD genes are considered to be critical in controlling growth and differentiation of mesenchymal stem cells to chondrocytes. Their expression can be detected during both, condensation and chondrogenesis. Treatment with oligodeoxynucleotides complementary to HOXD10, HOXD11 and HOXD13, respectively, inhibited chondrogenesis in vitro. (Jung & Tsonis 1998)

In two Ewing sarcoma cell lines, HOXD10, HOXD11 and HOXD13 were significantly downregulated by retroviral gene transfer, respectively. Potential of chondrogenic differentiation depending on HOX expression was assessed by means of a certain commercial kit (see 2.1.5). Cells had been seeded in droplets and incubated in a certain differentiation medium. Altogether, increased cell death was observed by microscopy during incubation in differentiation medium; this especially applied to pSIREN HOX cells and thus, indicated difficulties with chondrogenic differentiation of respective Ewing sarcoma cells (see p. 88). In general, SK-N-MC cells seemed to be more affected than A-673 cells. This was only a microscopic observation though. Rate of apoptosis or markers of induced cell death were not determined. In contrast to other Ewing cell lines, A-673 is known to possess a p53 mutation (see 2.1.13, p. 40). Thus, it might also have a growth advantage under differentiation conditions. Successful chondrogenic differentiation was intended to be confirmed by positive Alcian blue staining. Alcian blue usually stains proteoglycans produced by chondrocytes. After two weeks of

incubation in chondrogenic differentiation medium, however, no Alcian blue-positive material was detected in Ewing cell droplets. This equally applied to control cells and pSIREN HOX cells. The experiment was repeated several times including modifications of the staining protocol. All attempts remained Alcian blue-negative. The STEMPRO® Chondrogenesis Differentiation Kit was originally developed for chondrogenic differentiation of mesenchymal stem cells. It can be discussed whether tumor cells are equally qualified for this commercial kit as mesenchymal stem cells. However, Ewing sarcoma cells may not have differentiated far enough towards chondrocytes and thus, there were just no proteoglycans to be stained. It can't be excluded though that Alcian blue staining was not successful due to general problems with this technique. That's why cells of another experiment were processed for gene expression analysis. Markers of early and late chondrogenesis were determined on mRNA level by qRT-PCR. Especially control cells upregulated late chondrogenic markers such as COL10A1 and IHH, but also RUNX2 which is known to maintain a major role in terminal chondrocyte differentiation. (Komori 2010) In contrast to this, Ewing sarcoma cells with low HOX expression only showed significant increase of SOX9 and partially COL2A1. These are markers of early chondrogenesis. Especially SOX9 expression is critical for commitment and differentiation of mesenchymal cells toward the chondrogenic lineage. (Akiyama *et al.* 2002; Akiyama *et al.* 2005) SOX9 and two other SOX genes (SOX5 and SOX6) were shown to activate markers for early chondrogenesis and suppress markers for hypertrophic chondrocytes and osteoblasts at the same time. (Lefebvre *et al.* 2001; Lefebvre & Smits 2005) Especially SOX9 overexpression suppresses terminal differentiation of hypertrophic chondrocytes and inhibits endochondral bone formation. (Kim *et al.* 2011) Altogether, qRT-PCR results of Ewing sarcoma cells with low HOX expression indicated an earlier arrest in chondrogenic differentiation compared to control cells. It might have been useful though to determine other markers of chondrogenesis as well. Especially SPP1, IBSP and MMP13 are only expressed by terminal hypertrophic chondrocytes, for example. (Komori 2010) However, results of gene expression analysis corresponded to increased cell death of pSIREN HOX cells in differentiation medium which had been observed microscopically. We assume that Ewing sarcoma cells with low HOX expression are less capable of chondrogenic differentiation and thus, more prone to apoptosis in differentiation

medium than control cells. This especially applied to cell line SK-N-MC, and less to A-673 which possesses a p53 mutation (see p. 40). The discrepancy between the two cell lines is consistent with published literature. Ewing sarcoma cells have been known to be capable of differentiation for almost 30 years. Cavazzana *et al.* (1987), for example, demonstrated neural differentiation of Ewing cells after treatment with cyclic AMP and TPA. (Cavazzana *et al.* 1987) Tirode *et al.* (2007) analyzed differentiation potential of Ewing cells especially upon EWS-FLI1-silencing. They discovered that EWS-FLI1-silenced cells converged towards mesenchymal stem cells and were more competent to differentiate along several lineages. Especially adipogenic, osteogenic and chondrogenic differentiation were facilitated upon EWS-FLI1 suppression. However, various Ewing cell lines exhibited various differentiation potential. For example, A-673 was demonstrated to differentiate along the adipogenic pathway whereas SK-N-MC was not capable of this at all. Furthermore, they also reported on difficulties of Ewing cells to differentiate towards chondrocytes. (Tirode *et al.* 2007) According to our results, these difficulties were more considerable under HOX suppression. Briefly, we observed decreased BMP expression under HOX suppression; on the other hand chondrogenic differentiation of Ewing cells with low HOX expression was affected.

BMP signaling generally occurs via SMAD and non-SMAD signaling pathways (see 1.3). In the SMAD pathway (see Figure 6 on p. 20), the signal is transduced via R-SMADs, which form a complex with Co-SMAD SMAD4. This complex in turn transfers into the nucleus and controls transcription of various target genes. (Massague *et al.* 2005; Shi & Massague 2003) One of these target genes is RUNX2. (Lee *et al.* 2000) Interestingly, in several Ewing sarcoma cell lines triple HOX knockdown was associated with a significant decrease of SMAD4 and RUNX2 expression on mRNA level. Individual knockdowns of HOXD10, HOXD11 and HOXD13 did not lead to significant changes of SMAD4 and RUNX2 expression (see p. 82).

SMAD4 is not only a crucial component in both, TGFβ and BMP signaling but was also revealed to maintain critical functions in endochondral bone formation. (Massague *et al.* 2005) Mice with a conditional deletion of SMAD4 in the limb mesenchyme had severe skeletal defects due to failure of precartilaginous mesenchymal condensation and increased apoptosis. In absence of SMAD4, SOX9 expression initiates normally but

fails to maintain its level or expand its territory. (Lim *et al.* 2015) Furthermore, targeted disruption of SMAD4 in chondrocytes led to disorganization of the cartilage growth plate and affected mice had a short stature. (Zhang *et al.* 2005) SMAD4 is considered to be essential for bone homeostasis as well since, among other things, bone mineral density and osteoblast function were also reduced in mutant mice. (Tan *et al.* 2007) SMAD4 expression is also required for proper osteoclast function. (Tasca *et al.* 2015) Effects of SMAD4 expression in context of malignant diseases has recently become focus of current research as well. On the one hand, SMAD4 was reported to maintain a tumor-promoting role in hepatocellular carcinoma; on the other hand, it was shown to function as a tumor suppressor, particularly in pancreatic cancer. (Hernanda *et al.* 2014; Xia *et al.* 2015)

Interactions of HOX proteins with SMADs were initially reported in 1999. Especially HOXC8 was reported to interact with all kinds of SMAD proteins: R-SMADs, Co-SMAD and I-SMADs. As a reaction to BMP stimulation, HOXC8, for example, interacts with SMAD1 (R-SMAD) and thus, activates transcription osteopontin and other genes associated with bone formation. Interaction of HOXC8 with SMAD6 (I-SMAD) on the other hand, inhibits BMP signaling in the nucleus. Interaction of HOXC8 with SMAD4 was also observed. (Bai *et al.* 2000; Liu *et al.* 2004; Shi *et al.* 1999) Most HOX proteins were revealed to interact with SMAD proteins. Group 13 HOX proteins were identified to modulate transcriptional activation functions of R-SMADs. HOXD13, for example, was shown to bind to SMAD1 and SMAD5. SMADs, in turn, were discovered to prevent HOX proteins from binding to DNA. HOXD10 activity, for example, is opposed by SMAD1 and SMAD6. (Li *et al.* 2006; Williams *et al.* 2005)

We observed a significant decrease of SMAD4 expression after triple HOX knockdown in Ewing sarcoma cells. SMAD4, the Co-SMAD, is one of the most important components of BMP signaling even if in individual cases, SMADs were reported to activate target genes without formation of a complex with SMAD4. (He *et al.* 2006) Since HOX knockdown significantly affected SMAD4 expression in Ewing sarcoma cells and HOX-SMAD interactions are well-described, further experiments in this context should be aimed at. HOX-SMAD interactions in malignant tumors can’t be excluded. The activation of osteopontin expression in response to HOX-SMAD interactions which was mentioned earlier, for example, could be crucial in tumor progression.

Osteopontin is considered to be an important mediator of tumor metastasis. (Wai & Kuo 2008) Interestingly, osteopontin expression, in turn, was also significantly decreased after HOX knockdown in three of four Ewing cell lines (data not shown).

As already mentioned, HOX knockdown in Ewing cells was not only associated with decreased BMP and SMAD4 expression but also with reduced RUNX2 levels (see Figure 28 on p. 82). RUNX2 is a common target of BMP signaling. (Lee *et al.* 2000) BMP signaling occurs via SMAD signaling on the one hand, on the other hand via non-SMAD signaling pathways such as MAP kinase cascades. However, both, SMAD and non-SMAD pathways were revealed to converge at RUNX2 gene. (Chen *et al.* 2012; Lee *et al.* 2002) RUNX2 is the master regulator of osteoblast differentiation. However, BMP signaling is considered to be required for the RUNX2-dependent induction of the osteoblast phenotype. (Phimphilai *et al.* 2006) RUNX2 activates various bone matrix protein genes such as osteocalcin, osteopontin, bone sialoprotein and type I collagen (encoded by COL1A1). (Ducy *et al.* 1997) Interestingly, HOX knockdown in Ewing sarcoma cells was commonly associated with significantly decreased expression of collagen-encoding genes. COL1A1 expression was reduced after HOXD10, HOXD11 and HOXD13 knockdown, respectively. HOXD13 knockdown also led to reduced COL2A1 and COL10A1 mRNA levels (see Figure 29 on p. 83). Especially COL1A1 expression was documented to be upregulated by HOXD13. (Villavicencio-Lorini *et al.* 2010)

RUNX2 null mice completely lack bone formation and die shortly after birth. (Komori *et al.* 1997) RUNX2 haploinsufficiency is associated with cleidocranial dysplasia (CCD). This autosomal dominant inherited syndrome is characterized by defective intramembranous and endochondral bone formation. Patients, among other things, present with failed closure of the fontanelles, abortive clavicles and short stature. (Mundlos *et al.* 1997) RUNX2 is known to interact with SMAD proteins in vitro and *in vivo*. SMADs are considered to enhance transactivation ability of RUNX2. In one patient with CCD, a nonsense mutation was identified which led to a shortened RUNX2 protein. Since this protein failed to bind SMADs, pathogenesis of cleidocranial dysplasia is suggested to be related to impaired SMAD signaling. (Zhang *et al.* 2000) Since then, RUNX2-SMAD cooperation has been examined especially in context of bone formation induced by bone morphogenetic proteins. Osteogenic activity of BMP2, for example, was discovered to be mediated by structural coupling of RUNX2

and SMAD proteins. These complexes induce commitment to the osteoblast-like phenotype and osteoblast differentiation of mesenchymal stem cells. (Javed *et al.* 2008) On the other hand, RUNX2-deficient mice also exhibit impaired chondrocyte differentiation besides their lack of bone formation. (Komori *et al.* 1997) RUNX2-SMAD interactions were also detected during chondrocyte maturation. BMP2-induced transcription of type X collagen gene is suggested to involve cooperation of RUNX2 and SMAD proteins. (Leboy *et al.* 2001)

According to this, RUNX2 seems to have three major functions in BMP signaling (see Figure 6 on p. 20). On the one hand, it functions as a cofactor and interacts with SMAD proteins; on the other hand, it promotes late chondrogenic differentiation and induces osteogenic differentiation of mesenchymal stem cells. (Ducy *et al.* 1997; Komori 2010; Zhang *et al.* 2000) Besides decreased gene expression levels of BMP2, BMP4 and SMAD4, we first observed difficulties with chondrogenic differentiation of Ewing sarcoma cells with low HOX expression. However, we also examined potential of osteogenic differentiation of Ewing sarcoma cells. Again, we used a certain commercial kit which was originally developed for osteogenic differentiation of mesenchymal stem cells (see p. 36). Since HOX knockdown was associated with a decrease of RUNX2 expression and RUNX2 is considered to be the master regulator of osteogenesis, we expected potential of osteogenic differentiation to be impaired in Ewing sarcoma cells with low HOX expression. Surprisingly, two cell lines were capable of terminal osteogenic differentiation irrespective of HOX gene expression (see p. 93). Ewing sarcoma cells are known to be competent to differentiate along the osteogenic lineage, especially upon EWS-FLI1 silencing. EWS-FLI1-silenced cells were shown to be able to exhibit characteristic features of osteocytes and produce calcified matrix. (Tirode *et al.* 2007) We observed similar results. Unexpectedly however, there was no significant difference between Ewing sarcoma cells with low HOX expression and control cells. All cells which had been incubated in osteogenic differentiation medium differentiated into mature osteoblasts irrespective of HOX gene expression. Degree of differentiation was assessed by gene expression analysis and Alizarin red staining in two separate experiments. Results of both experiments were consistent though. Calcified matrix which is commonly produced by mature osteoblasts was positively stained by Alizarin Red (see Figure 37, p. 93). Upregulation of osteoblast-specific

marker genes such as osteocalcin (BGLAP) and osteopontin (SPP1) indicated a successful differentiation. Decreased RUNX2 levels were interestingly apparent in A-673 cells which had grown in differentiation medium. Komori (2010), however, already mentioned that RUNX2 expression had to be downregulated for differentiation in mature osteoblasts which formed mature bone. (Komori 2010) Osteogenic marker genes were differentially expressed in individual Ewing cells but eventually, all Ewing cells reached a terminal stage of osteogenic differentiation because calcified matrix was detected in each culture plate with differentiation medium. Since HOX knockdown was associated with a significant decrease of RUNX2 expression, especially Ewing cells with low HOX expression were expected to produce less calcified bone matrix. On closer inspection, however, RUNX2 expression was significantly reduced after triple HOX knockdown only. Individual knockdown of HOXD10, HOXD11 and HOXD13 did not lead to decreased RUNX2 expression. Thus, RUNX2 dosage might have been sufficient for proper differentiation of Ewing sarcoma cells into osteoblasts.

Problems with downregulation of individual genes due to functional redundancy, compensation mechanisms and even due to a sort of recruitment of HOX genes were already addressed in 4.4 (see p. 110). Compound mutations of posterior HOX genes were demonstrated to cause more severe phenotypes than simple HOX gene mutations. (Delpretti *et al.* 2012; Zakany & Duboule 1996) Compensation mechanisms of HOX genes can't be excluded in Ewing sarcoma. Targeting HOXD10, HOXD11 and HOXD13 in Ewing sarcoma cells at the same time would certainly provide more insights. It remains unclear whether Ewing cells were still competent to differentiate towards mature osteoblasts in absence of all three HOX genes. For osteogenic differentiation, cells have to be incubated in differentiation medium for three weeks. Triple HOX knockdown, however, was achieved by siRNA interference which is known to have transient effects only. Generation of Ewing cells with a permanent triple HOX knockdown by retroviral gene transfer – if it is possible at all - could be extremely challenging.

In contrast to RUNX2, BMP2 and BMP4 expression was significantly reduced after individual HOX knockdown of Ewing sarcoma cells. In general, results of our chondrogenic and osteogenic differentiation assays are consistent with published literature. Treatment with BMP antagonist Noggin, for example, was shown to only

inhibit chondrogenesis of a mesodermal stem cell line. Osteogenic differentiation, however, was unaffected. (Nifuji *et al.* 2004)

Besides being a common BMP target, RUNX2 was also demonstrated to act downstream of HOX genes in both, cartilage and bone formation. It was revealed to be a direct transcriptional target of HOXD13; furthermore it can be induced by other posterior HOX genes such as HOXD11. (Gross *et al.* 2012; Lee *et al.* 2000; Villavicencio-Lorini *et al.* 2010) Mice with a certain HOXD13 mutation (mouse mutant synpolydactyly homolog; spdh) which results in a loss of function did not only show strongly reduced levels of RUNX2 expression but also differences in the expression of BMP4 and osteopontin. (Villavicencio-Lorini *et al.* 2010) We made similar observations in Ewing sarcoma cells with low HOX expression.

RUNX proteins are known to be involved in tumorigenesis and have already been mentioned in connection with Ewing sarcoma as well. There are three different RUNX genes in mammals, RUNX1, RUNX2 and RUNX3, each of them having a tissue-specific expression pattern. (Ito *et al.* 2015) RUNX1 is mainly expressed in hematopoietic cells and mutations resulting in a loss or impairment of function are associated with different types of leukemia. (Ichikawa *et al.* 2013) RUNX3 inactivation can be observed in various solid tumors. However, RUNX3 is also considered to have oncogenic functions. (Chuang & Ito 2010) In Ewing sarcoma, for example, RUNX3 suppression led to reduced cell growth. (Bledsoe *et al.* 2014) RUNX2 expression can be observed in malignant bone tumors. Altered RUNX2 expression is considered to be critical in osteosarcoma development and its overexpression was identified to correlate with poor response to chemotherapy. (Martin *et al.* 2011; Sadikovic *et al.* 2010) In Ewing sarcoma, osteoblast differentiation is blocked by binding of EWS-FLI1 to RUNX2. That way, the tumor is maintained in an undifferentiated state. (Li *et al.* 2010) Interestingly, RUNX2 expression is especially found in tumors which metastasize primarily to bone such as prostate and breast cancer. Altogether, RUNX2 expression seems to be linked to increased invasion, growth and metastasis of tumors. (Nagaraja *et al.* 2006; Zeng & Xu 2015; Zhang *et al.* 2015) It was revealed to upregulate multiple oncogenic target genes responsible for metastasis, proliferation and osteolysis. (Sun *et al.* 2015) Among other things, RUNX2 was demonstrated to modulate RANKL expression which induces the differentiation of osteoclasts. (Bar-Shavit 2007; Kitazawa *et al.* 2008)

Osteoclast-mediated bone resorption, in turn, also occurs in osteolytic bone metastases. (Mundy 2002) Besides RUNX2, intact BMP-SMAD signaling, particularly sufficient SMAD4 expression, was also revealed to be critical for proper osteoclastogenesis. Increased BMP2 signaling was reported to promote osteoclast differentiation. (Jensen *et al.* 2010; Tasca *et al.* 2015) According to this, HOX knockdown in Ewing sarcoma cells was associated with downregulation of genes which are especially important for bone resorption and metastasis. Furthermore, capability of colony formation which is considered to correlate with the ability to form metastases *in vivo* was reduced in Ewing sarcoma cells with low HOX expression. (Cifone & Fidler 1980)

A major part of this thesis is based on gene expression analysis. However, HOX knockdown in Ewing sarcoma cells was linked to reduced gene expression of several important components of BMP signaling. On the one hand, we observed a significant downregulation of ligands, BMP2 and BMP4, and the common mediator which interacts with all SMAD proteins, SMAD4. On the other hand, expression of several genes which are known to be common targets of BMP signaling was decreased, in detail RUNX2, all kinds of collagen-encoding genes and osteopontin. Furthermore, chondrogenic differentiation, a process which is regulated by BMPs and HOX genes, was impaired under HOX suppression. Osteogenic differentiation was surprisingly unaffected. This may be explained by sufficient RUNX2 dosage due to induction via other pathways involving the non-SMAD signaling pathway or others such as FGF or WNT signaling. (Komori 2011) Despite intact osteogenic differentiation, we assume HOXD10, HOXD11 and HOXD13 may alter BMP signaling in Ewing sarcoma. Alterations of BMP signaling have already been detected in various tumors. BMPs were revealed to be involved in the regulation of several cellular functions of tumors cells such as cell growth and death, migration, invasion and especially bone metastasis. (Hardwick *et al.* 2008; Ye *et al.* 2009; Ye *et al.* 2007)

HOX genes were reported to be both, activators and targets of BMP signaling. Interactions of HOX proteins with SMADs were already mentioned earlier. Besides these interactions, HOX genes were documented to activate BMP promoters. HOXD13 and HOXA13, for example, induced BMP4 expression. (Suzuki *et al.* 2003; Villavicencio-Lorini *et al.* 2010) In mice with the synpolydactyly homolog (spdh) mutation, HOX

genes were demonstrated to regulate BMP expression before RUNX2 is expressed. (Albrecht *et al.* 2002) Villavicencio-Lorini *et al.* (2010) therefore suggested that the effect of HOX proteins on RUNX2 was especially promoted by the regulation of BMPs by HOX genes. (Villavicencio-Lorini *et al.* 2010) In contrast, BMPs were demonstrated to control initiation of HOX expression in various animals. BMP2, for example, induced HOXD11 and HOXD13 in the developing chick limb, whereas BMP4 regulated HOX expression in a certain frog. (D. M. Duprez *et al.* 1996; Wacker *et al.* 2004) Changes of HOX gene expression were also observed during BMP-induced ectopic bone formation. (Iimura *et al.* 1994) Functions of BMPs and HOX proteins in development are closely related. BMPs and HOX proteins are considered to cooperate to fulfill common tasks. (Li & Cao 2006) Both of them, for example, are involved in various processes associated with limb development which, among other things, include limb patterning, chondrogenesis and apoptosis. (Li & Cao 2003)

Their loss of function was shown to affect early mesenchymal condensation, chondrocyte differentiation and bone growth, the latter probably being limited because of defective cartilage growth plates. (De Luca *et al.* 2001; Francis *et al.* 1994; Goff & Tabin 1997; Gross *et al.* 2012; Kuss *et al.* 2014; Kuss *et al.* 2009; Pizette & Niswander 2000) BMP and HOX misexpression was related to similar phenotypes. Association of synpolydactyly with mutations of posterior HOXD genes is well-known. (Muragaki *et al.* 1996; Zakany & Duboule 1996) Interestingly, ectopic BMP2 expression also caused formation of supernumerary fingers. (D. M. Duprez *et al.* 1996)

Bone morphogenetic proteins induce ectopic bone and cartilage formation, which develops analogically to endochondral bone formation in limb development (see 1.2). (Reddi & Anderson 1976; Tsumaki & Yoshikawa 2005; Urist & Strates 2009) HOX genes were identified to control the ossification pattern of bones. (Villavicencio-Lorini *et al.* 2010) Interestingly, Ewing sarcoma preferably arises from the diaphyseal portion of long bones where endochondral ossification is commonly initiated. In that place blood vessels invade into the cartilage and bone collar is formed from the surrounding perichondrium. (Bernstein *et al.* 2006; Long & Ornitz 2013)

4.7 Assumed role of HOX genes in pathogenesis of Ewing sarcoma

HOX knockdown in Ewing sarcoma cells was associated with a decrease of proliferation and capability of colony formation *in vitro*. We therefore suppose that HOXD10, HOXD11 and HOXD13 positively regulate growth and metastasis of Ewing sarcoma.

Gene expression analysis after HOX knockdown revealed a significant downregulation of genes associated with BMP signaling. Gene expression of ligands, cofactors and transcriptional targets of this pathway such as RUNX2 and collagens were significantly reduced. Furthermore, Ewing cells with low HOX expression failed to differentiate into chondrocytes. However, BMP signaling is not only known to be involved in cartilage and bone formation but also in tumorigenesis. We assume HOXD10, HOXD11 and HOXD13 alter BMP signaling in Ewing sarcoma and thus, may substantially contribute to its phenotype. This thesis is primarily based on gene expression analysis and *in vitro* experiments. Results were substantiated in a subsequent thesis work employing a preclinical mouse model.

4.8 Clinical implications and future perspectives

This thesis provided first indications for the role of HOXD10, HOXD11 and HOXD13 in Ewing sarcoma. A potential positive regulation of tumor growth and metastasis by HOX genes was verified in a mouse model by another doctoral student. Molecular mechanisms of how HOX genes may contribute to tumor growth and metastatic spread of Ewing sarcoma have to be further elucidated.

Ewing sarcoma cells with low HOX expression failed to differentiate into chondrocytes. Triple HOX knockdown was associated with a significant decrease of RUNX2 expression which commonly induces differentiation of mesenchymal stem cells into osteoblasts and promotes late chondrogenic differentiation. (Komori 2010) Application of pSIREN HOX cells into mice demonstrated changes of tumor phenotype changes depending on HOX expression. It not clear at the moment, however, which role RUNX2 exactly maintains in tumorigenesis of Ewing sarcoma. In contrast to RUNX3 which can be detected in all Ewing sarcoma cells, RUNX2 expression is only found in 73% of specimens. (Bledsoe *et al.* 2014) In osteosarcoma, for example, RUNX2 expression was associated with increased invasion and RUNX2 overexpression correlated with poor response to chemotherapy. (Sadikovic *et al.* 2010; Zeng & Xu 2015) Since tumors due

to application of pSIREN HOX cells into mice were less invasive (von Heyking *et al.* 2016), clinical studies could address the question if prognosis of patients correlates with HOX expression in tumor tissue.

Since several components of BMP signaling were differentially expressed after HOX knockdown, we assume that HOXD10, HOXD11 and HOXD13 alter BMP signaling in Ewing sarcoma. This hypothesis, however, has to be confirmed by further experiments. For example, it should be examined if HOX proteins really activate BMP promoters in Ewing sarcoma. If they do so, it is important to obtain information about the detailed function of BMPs in this tumor.

Finally, according to our results, expression of HOXD10, HOXD11 and HOXD13 didn't seem to be influenced by EWS-FLI1 and EZH2. But subsequent analysis revealed their critical regulation via DKK2. (von Heyking *et al.* 2016)

5 Summary

Ewing sarcoma is the second most frequent primary bone tumor in children and young adults. It is characterized by certain chromosome translocations which lead to an oncogenic gene fusion. Chromosomal translocation t (11; 22), which involves EWS and FLI1, is the most common translocation and can be detected in more than 85% of Ewing sarcomas. In the last 40 years survival rates have been improving, numbers are still frustrating though. In case of metastasis, survival rates decrease severely and only amount to 28%.

HOX genes form a subgroup of the family of homeobox genes which are characterized by a common DNA sequence called “homeobox” encoding the “homeodomain”, a certain 60-amino-acid long polypeptide segment. HOX genes are highly conserved across evolution. Controlling the patterning along the anterior-posterior axis during embryonic development of all animals, they are regarded as master regulators of development. In humans, there are 39 HOX genes arranged in four HOX clusters A-D. HOXD genes do not only affect chondrogenesis but also bone condensation and growth. Posterior HOXD genes are especially involved in limb development including limb anterior-posterior asymmetry. Downstream HOX targets include transcription factors and members of signaling pathways such as BMPs but also genes which directly regulate cellular processes. That way, HOX genes intervene in cell proliferation, differentiation, apoptosis, cell adhesion and migration. Alterations of HOX expression are associated with malformations and malignant tumors.

This thesis shows for the first time that HOX genes play an important role in pathogenesis of Ewing sarcoma. HOXD10, HOXD11 and HOXD13 are strongly overexpressed in primary Ewing sarcoma as well as in established Ewing sarcoma cell lines. These genes were not only demonstrated to positively regulate growth and metastasis but also promote chondrogenic differentiation of established Ewing sarcoma cell lines.

RNA interference-mediated knock down of these genes led to a decrease of proliferation and capability of colony formation *in vitro*. Ewing cells with low HOX expression failed to differentiate into chondrocytes and died. Osteogenic differentiation, however, was not affected.

Gene expression analysis after HOX knockdown revealed a significant downregulation

of genes associated with BMP signaling. Gene expression of ligands (BMP2, BMP4), cofactors (SMAD4) and transcriptional targets of this pathway such as RUNX2 and collagens were significantly reduced after HOX knockdown. BMP signaling is not only known to be involved in cartilage and bone formation but also in tumorigenesis. Results indicate BMP signaling might be altered in Ewing sarcoma.

Furthermore, microarray analysis showed into which diverse cell processes HOX genes can intervene. Expression of GTP-binding protein RAC2, chromatin remodeler ATRX, HAUS6 which is part of a protein complex which regulates centrosome and spindle integrity, EEF1D which is a subunit of elongation factor complex 1 critical for efficient protein synthesis was significantly changed after HOX knockdown. These genes are, among other things, involved in controlling immune response, bone and limb development, just as neuronal differentiation. They are assumed to intervene in fundamental cellular processes such as mitosis, microtubule formation and translation and all of these genes already appeared in the context of malignant tumors.

Promoting proliferation, metastasis and chondrogenesis in Ewing sarcoma HOXD10, HOXD11 and HOXD13 substantially contribute to its malignant phenotype.

Disappointing survival rates of Ewing sarcoma patients stress the necessity of alternate therapeutic approaches. These results provide a potential point of attack for a targeted therapy.

6 Zusammenfassung

Das Ewing-Sarkom ist der zweithäufigste Knochentumor bei Kindern und jungen Erwachsenen. Es ist durch den Nachweis bestimmter Chromosomentranslokationen charakterisiert, die zur Bildung einer onkogenen Genfusion führen. Die Chromosomentranslokation t (11; 22) verursacht eine Fusion von EWS und FLI1 und ist die häufigste Translokation, sie kann in mehr als 85% der Ewing-Sarkome nachgewiesen werden. In den letzten 40 Jahren haben sich die Überlebensraten verbessert, die Zahlen sind aber immer noch enttäuschend. Im Falle einer Metastasierung sinkt die Überlebensrate massiv und beträgt nur noch 28%.

HOX-Gene gehören zur Familie der Homöobox-Gene, die durch eine bestimmte DNA-Sequenz gekennzeichnet sind, die „Homöobox“ genannt wird. Diese DNA-Sequenz codiert für ein ca. 60 Aminosäuren langes Polypeptid, das „Homöodomäne“ genannt wird. HOX-Gene sind in der Evolution hoch konserviert. HOX-Gene werden als Hauptregulatoren der Entwicklung angesehen, weil sie in der Embryonalentwicklung aller Lebewesen für die Strukturierung entlang der anteriorposterioren Achse verantwortlich sind. Im Menschen existieren 39 HOX-Gene, die in vier Clustern A-D angeordnet sind. HOXD-Gene beeinflussen nicht nur die Chondrogenese, sondern auch die Knochenkondensation und das Knochenwachstum. Posteriore HOXD-Gene spielen vor allem in der Entwicklung der Gliedmaßen eine entscheidende Rolle. Insbesondere sind sie auch verantwortlich für die Asymmetrie entlang der anteriorposterioren Achse. Unter den Zielgenen der HOX-Proteine sind neben Transkriptionsfaktoren, Bestandteile von Signalkaskaden wie z. B. die BMPs, auch Gene, die zelluläre Vorgänge direkt steuern. Auf diese Weise können HOX-Gene die Proliferation, Differenzierung, Apoptose, Adhäsion und Migration von Zellen beeinflussen. Eine Veränderung der Genexpression von HOX-Genen kann Fehlbildungen und malignen Tumore verursachen.

Diese Dissertation zeigt erstmals, dass HOX-Gene eine wichtige Rolle in der Pathogenese des Ewing-Sarkoms spielen. HOXD10, HOXD11 und HOXD13 sind stark überexprimiert in primärem Ewing-Sarkom-Gewebe und etablierten Ewing-Sarkom-Zelllinien. Diese drei Gene hatten nicht nur einen positiven Einfluss auf das Wachstum und die Metastasierung von Ewing-Sarkom-Zellen, sondern induzierten *in vitro* auch eine chondrogene Differenzierung der Tumorzellen.

Das Ausschalten von HOXD10, HOXD11 und HOXD13 mittels siRNA führte einerseits zu einer Abnahme der Proliferationsrate, andererseits verringerte sich die Fähigkeit der Tumorzellen im Colony formation-Assay Kolonien zu bilden. Außerdem konnten Ewing-Zellen mit niedriger HOX-Expression schlechter chondrogen differenzieren und starben vermehrt unter Differenzierungskonditionen. Die osteogene Differenzierung dieser Zellen war nicht eingeschränkt.

In den Genexpressionsanalysen nach HOX-Knockdown zeigte sich eine signifikante Herunterregulation von Genen, die mit der BMP-Signalkaskade assoziiert sind. Die Genexpression von Liganden (BMP2, BMP4), Cofaktoren (SMAD4) und Zielgene dieses Signalwegs wie z. B. RUNX2 und Kollagene, war nach HOX-Knockdown signifikant verringert. Der BMP-Signalweg spielt nicht nur in der Knorpel- und Knochenbildung eine Rolle, sondern auch in der Tumorgenese. Die Ergebnisse deuten auf einen möglicherweise veränderten BMP-Signalweg im Ewing-Sarkom hin.

Microarray-Daten lieferten einen Anhaltspunkt, wie viele verschiedene Zellvorgänge HOX-Gene beeinflussen können. Die Genexpression vom GTP-bindenden Protein RAC2, dem Chromatin-Remodeler ATRX, HAUS6, das ein Teil eines Proteinkomplexes ist, der die Zentrosomen- und Spindelintegrität kontrolliert, sowie EEF1D, das eine Untereinheit des Elongationsfaktorenkomplex 1 darstellt, der entscheidend für eine effiziente Proteinsynthese ist, waren nach HOX-Knockdown signifikant verändert. Diese Gene sind unter anderem in der Immunantwort, in der Knochen- und Gliedmaßenentstehung sowie der neuronalen Differenzierung involviert. Es wird angenommen, dass diese Gene entscheidende Zellvorgänge wie z. B. die Mitose, die Mikrotubuli-Bildung sowie die Translation steuern. Außerdem wurden all diese Gene bereits im Zusammenhang mit malignen Tumoren beschrieben.

Indem HOXD10, HOXD11 und HOXD13 die Proliferation, Metastasierung und Chondrogenese des Ewing-Sarkoms positiv beeinflussen, tragen sie maßgeblich zu dessen malignem Phänotyp bei. Aufgrund der enttäuschenden Überlebensraten sind dringend alternative Therapieverfahren erforderlich. Die Ergebnisse dieser Dissertation liefern einen Angriffspunkt für eine mögliche zielgerichtete Therapie.

7 References

Abate-Shen, C. (2002). Deregulated homeobox gene expression in cancer: cause or consequence? *Nat Rev Cancer, 2*(10), 777-785.

Abdel-Fattah, R., Xiao, A., Bomgardner, D., Pease, C. S., Lopes, M. B., & Hussaini, I. M. (2006). Differential expression of HOX genes in neoplastic and non-neoplastic human astrocytes. *J Pathol, 209*(1), 15-24.

Ahmed, A. A., Zia, H., & Wagner, L. (2014). Therapy resistance mechanisms in Ewing's sarcoma family tumors. *Cancer Chemother Pharmacol, 73*(4), 657-663.

Akbas, G. E., & Taylor, H. S. (2004). HOXC and HOXD gene expression in human endometrium: lack of redundancy with HOXA paralogs. *Biol Reprod, 70*(1), 39-45.

Akiyama, H., Chaboissier, M. C., Martin, J. F., Schedl, A., & de Crombrugghe, B. (2002). The transcription factor Sox9 has essential roles in successive steps of the chondrocyte differentiation pathway and is required for expression of Sox5 and Sox6. *Genes Dev, 16*(21), 2813-2828.

Akiyama, H., Kim, J. E., Nakashima, K., Balmes, G., Iwai, N., Deng, J. M., Zhang, Z., Martin, J. F., Behringer, R. R., Nakamura, T., & de Crombrugghe, B. (2005). Osteo-chondroprogenitor cells are derived from Sox9 expressing precursors. *Proc Natl Acad Sci U S A, 102*(41), 14665-14670.

Alberts, B., Johnson, A., Lewis, J., Morgan, D., Raff, M., Roberts, K., & Walter, P. (2014). *Molecular Biology of the Cell* (Sixth ed.). New York, US and Milton Park, Abingdon, UK: Garland Science, Taylor & Francis Group.

Albrecht, A. N., Kornak, U., Boddrich, A., Suring, K., Robinson, P. N., Stiege, A. C., Lurz, R., Stricker, S., Wanker, E. E., & Mundlos, S. (2004). A molecular pathogenesis for transcription factor associated poly-alanine tract expansions. *Hum Mol Genet, 13*(20), 2351-2359.

Albrecht, A. N., Schwabe, G. C., Stricker, S., Boddrich, A., Wanker, E. E., & Mundlos, S. (2002). The synpolydactyly homolog (spdh) mutation in the mouse -- a defect in patterning and growth of limb cartilage elements. *Mech Dev, 112*(1-2), 53-67.

Ali, I. H., & Brazil, D. P. (2014). Bone morphogenetic proteins and their antagonists: current and emerging clinical uses. *British Journal of Pharmacology, 171*(15), 3620-3632.

Alonso, C. R. (2002). Hox proteins: sculpting body parts by activating localized cell death. *Curr Biol, 12*(22), R776-778.

Aono, A., Hazama, M., Notoya, K., Taketomi, S., Yamasaki, H., Tsukuda, R., Sasaki, S., & Fujisawa, Y. (1995). Potent ectopic bone-inducing activity of bone morphogenetic protein-4/7 heterodimer. *Biochem Biophys Res Commun, 210*(3), 670-677.

Apiou, F., Flagiello, D., Cillo, C., Malfoy, B., Poupon, M. F., & Dutrillaux, B. (1996). Fine mapping of human HOX gene clusters. *Cytogenet Cell Genet, 73*(1-2), 114-115.

Arana, E., Vehlow, A., Harwood, N. E., Vigorito, E., Henderson, R., Turner, M., Tybulewicz, V. L., & Batista, F. D. (2008). Activation of the small GTPase Rac2 via the B cell receptor regulates B cell adhesion and immunological-synapse formation. *Immunity, 28*(1), 88-99.

Arnaoutova, I., & Kleinman, H. K. (2010). In vitro angiogenesis: endothelial cell tube formation on gelled basement membrane extract. *Nat Protoc, 5*(4), 628-635.

Arya, R., & White, K. (2015). Cell death in development: Signaling pathways and core mechanisms. *Seminars in Cell & Developmental Biology, 39*(0), 12-19.

Baffa, R., Fassan, M., Volinia, S., O'Hara, B., Liu, C. G., Palazzo, J. P., Gardiman, M., Rugge, M., Gomella, L. G., Croce, C. M., & Rosenberg, A. (2009). MicroRNA expression profiling of human metastatic cancers identifies cancer gene targets. *J Pathol, 219*(2), 214-221.

Bai, S., Shi, X., Yang, X., & Cao, X. (2000). Smad6 as a transcriptional corepressor. *J Biol Chem, 275*(12), 8267-8270.

Bar-Shavit, Z. (2007). The osteoclast: a multinucleated, hematopoietic-origin, bone-resorbing osteoimmune cell. *J Cell Biochem, 102*(5), 1130-1139.

Bennett, L. B., Schnabel, J. L., Kelchen, J. M., Taylor, K. H., Guo, J., Arthur, G. L., Papageorgio, C. N., Shi, H., & Caldwell, C. W. (2009). DNA hypermethylation accompanied by transcriptional repression in follicular lymphoma. *Genes Chromosomes Cancer, 48*(9), 828-841.

Berbegall, A. P., Villamon, E., Tadeo, I., Martinsson, T., Canete, A., Castel, V., Navarro, S., & Noguera, R. (2014). Neuroblastoma after childhood: prognostic relevance of segmental chromosome aberrations, ATRX protein status, and immune cell infiltration. *Neoplasia, 16*(6), 471-480.

Bernstein, M., Kovar, H., Paulussen, M., Randall, R. L., Schuck, A., Teot, L. A., & Juergens, H. (2006). Ewing's sarcoma family of tumors: current management. *Oncologist, 11*(5), 503-519.

Berube, N. G., Jagla, M., Smeenk, C., De Repentigny, Y., Kothary, R., & Picketts, D. J. (2002). Neurodevelopmental defects resulting from ATRX overexpression in transgenic mice. *Hum Mol Genet, 11*(3), 253-261.

Berube, N. G., Mangelsdorf, M., Jagla, M., Vanderluit, J., Garrick, D., Gibbons, R. J., Higgs, D. R., Slack, R. S., & Picketts, D. J. (2005). The chromatin-remodeling protein ATRX is critical for neuronal survival during corticogenesis. *J Clin Invest, 115*(2), 258-267.

Bhatlekar, S., Addya, S., Salunek, M., Orr, C. R., Surrey, S., McKenzie, S., Fields, J. Z., & Boman, B. M. (2014). Identification of a developmental gene expression signature, including HOX genes, for the normal human colonic crypt stem cell niche: overexpression of the signature parallels stem cell overpopulation during colon tumorigenesis. *Stem Cells Dev, 23*(2), 167-179.

Biedler, J. L., Helson, L., & Spengler, B. A. (1973). Morphology and growth, tumorigenicity, and cytogenetics of human neuroblastoma cells in continuous culture. *Cancer Res, 33*(11), 2643-2652.

Blaeschke, F., Thiel, U., Kirschner, A., Thiede, M., Rubio, R. A., Schirmer, D., Kirchner, T., Richter, G. H., Mall, S., Klar, R., Riddell, S., Busch, D. H., Krackhardt, A., Grunewald, T. G., & Burdach, S. (2016). Human HLA-A*02:01/CHM1+ allo-restricted T cell receptor transgenic CD8+ T Cells specifically inhibit Ewing sarcoma growth in vitro and in vivo. *Oncotarget*.

Bledsoe, K. L., McGee-Lawrence, M. E., Camilleri, E. T., Wang, X., van Wijnen, A. J., Oliveira, A. M., & Westendorf, J. J. (2014). RUNX3 Facilitates Growth of Ewing Sarcoma Cells. *J Cell Physiol*.

Bloom, E. T. (1972). Further definition by cytotoxicity tests of cell surface antigens of human sarcomas in culture. *Cancer Res, 32*(5), 960-967.

Bouba, I., Siomou, E., Stefanidis, C. J., Emmanouilidou, A., Galidi, A., Hatzi, E., Markoula, S., Mitsioni, A., Siamopoulou, A., & Georgiou, I. (2009). Absence of mutations in the HOXA11 and HOXD11 genes in children with congenital renal malformations. *Pediatr Nephrol, 24*(8), 1569-1572.

Boulet, A. M., & Capecchi, M. R. (2002). Duplication of the Hoxd11 gene causes alterations in the axial and appendicular skeleton of the mouse. *Dev Biol, 249*(1), 96-107.

Boulet, A. M., & Capecchi, M. R. (2004). Multiple roles of Hoxa11 and Hoxd11 in the formation of the mammalian forelimb zeugopod. *Development, 131*(2), 299-309.

Bruneau, S., Johnson, K. R., Yamamoto, M., Kuroiwa, A., & Duboule, D. (2001). The mouse Hoxd13(spdh) mutation, a polyalanine expansion similar to human type II synpolydactyly (SPD), disrupts the function but not the expression of other Hoxd genes. *Dev Biol, 237*(2), 345-353.

Burdach, S., & Jurgens, H. (2002). High-dose chemoradiotherapy (HDC) in the Ewing family of tumors (EFT). *Critical Reviews in Oncology/Hematology, 41*(2), 169-189.

Burdach, S., Jurgens, H., Peters, C., Nurnberger, W., Mauz-Korholz, C., Korholz, D., Paulussen, M., Pape, H., Dilloo, D., & Koscielniak, E. (1993). Myeloablative radiochemotherapy and hematopoietic stem-cell rescue in poor-prognosis Ewing's sarcoma. *J Clin Oncol, 11*(8), 1482-1488.

Burdach, S., Nurnberger, W., Laws, H. J., Engel, B. C., Dirksen, U., Krauth, K., Pape, H., Kahn, T., Korholz, D., Gadner, H., Gobel, U., & Jurgens, H. (1996). Myeloablative therapy, stem cell rescue and gene transfer in advanced Ewing tumors. *Bone Marrow Transplantation, 18 Suppl 1*, S67-68.

Burdach, S., Plehm, S., Unland, R., Dirksen, U., Borkhardt, A., Staege, M. S., Muller-Tidow, C., & Richter, G. H. (2009). Epigenetic maintenance of stemness and malignancy in peripheral neuroectodermal tumors by EZH2. *Cell Cycle, 8*(13), 1991-1996.

Burdach, S., van Kaick, B., Laws, H. J., Ahrens, S., Haase, R., Korholz, D., Pape, H., Dunst, J., Kahn, T., Willers, R., Engel, B., Dirksen, U., Kramm, C., Nurnberger, W., Heyll, A., Ladenstein, R., Gadner, H., Jurgens, H., & Go el, U. (2000). Allogeneic and autologous stem-cell transplantation in advanced Ewing tumors. An update after long-term follow-up from two centers of the European Intergroup study EICESS. Stem-Cell Transplant Programs at Dusseldorf University Medical Center, Germany and St. Anna Kinderspital, Vienna, Austria. *Annals of Oncology, 11*(11), 1451-1462.

Cai, L. Y., Abe, M., Izumi, S., Imura, M., Yasugi, T., & Ushijima, T. (2007). Identification of PRTFDC1 silencing and aberrant promoter methylation of GPR150, ITGA8 and HOXD11 in ovarian cancers. *Life Sci, 80*(16), 1458-1465.

Cantile, M., Franco, R., Tschan, A., Baumhoer, D., Zlobec, I., Schiavo, G., Forte, I., Bihl, M., Liguori, G., Botti, G., Tornillo, L., Karamitopoulou-Diamantis, E., Terracciano, L., & Cillo, C. (2009). HOX D13 expression across 79 tumor tissue types. *Int J Cancer, 125*(7), 1532-1541.

Cantile, M., Schiavo, G., Franco, R., Cindolo, L., Procino, A., D'Armiento, M., Facchini, G., Terracciano, L., Botti, G., & Cillo, C. (2011). Expression of lumbosacral HOX genes, crucial in kidney organogenesis, is systematically deregulated in clear cell kidney cancers. *Anticancer Drugs, 22*(5), 392-401.

Cantile, M., Scognamiglio, G., Anniciello, A., Farina, M., Gentilcore, G., Santonastaso, C., Fulciniti, F., Cillo, C., Franco, R., Ascierto, P. A., & Botti, G. (2012). Increased HOX C13 expression in metastatic melanoma progression. *J Transl Med, 10*, 91.

Cao, D., Jin, C., Ren, M., Lin, C., Zhang, X., & Zhao, N. (2009). The expression of Gli3, regulated by HOXD13, may play a role in idiopathic congenital talipes equinovarus. *BMC Musculoskelet Disord, 10*, 142.

Carpenter, E. M., Goddard, J. M., Davis, A. P., Nguyen, T. P., & Capecchi, M. R. (1997). Targeted disruption of Hoxd-10 affects mouse hindlimb development. *Development, 124*(22), 4505-4514.

Carreira, A. C., Alves, G. G., Zambuzzi, W. F., Sogayar, M. C., & Granjeiro, J. M. (2014). Bone Morphogenetic Proteins: Structure, biological function and therapeutic applications. *Archives of Biochemistry and Biophysics, 561*(0), 64-73.

Carrio, M., Arderiu, G., Myers, C., & Boudreau, N. J. (2005). Homeobox D10 induces phenotypic reversion of breast tumor cells in a three-dimensional culture model. *Cancer Res, 65*(16), 7177-7185.

Cavazzana, A. O., Miser, J. S., Jefferson, J., & Triche, T. J. (1987). Experimental evidence for a neural origin of Ewing's sarcoma of bone. *Am J Pathol, 127*(3), 507-518.

Chakravadhanula, M., Ozols, V. V., Hampton, C. N., Zhou, L., Catchpoole, D., & Bhardwaj, R. D. (2014). Expression of the HOX genes and HOTAIR in atypical teratoid rhabdoid tumors and other pediatric brain tumors. *Cancer Genet, 207*(9), 425-428.

Chen, G., Deng, C., & Li, Y. P. (2012). TGF-beta and BMP signaling in osteoblast differentiation and bone formation. *Int J Biol Sci, 8*(2), 272-288.

Chen, X., Bahrami, A., Pappo, A., Easton, J., Dalton, J., Hedlund, E., Ellison, D., Shurtleff, S., Wu, G., Wei, L., Parker, M., Rusch, M., Nagahawatte, P., Wu, J., Mao, S., Boggs, K., Mulder, H., Yergeau, D., Lu, C., Ding, L., Edmonson, M., Qu, C., Wang, J., Li, Y., Navid, F., Daw, N. C., Mardis, E. R., Wilson, R. K., Downing, J. R., Zhang, J., & Dyer, M. A. (2014). Recurrent somatic structural variations contribute to tumorigenesis in pediatric osteosarcoma. *Cell Rep, 7*(1), 104-112.

Cheng, H., Jiang, W., Phillips, F. M., Haydon, R. C., Peng, Y., Zhou, L., Luu, H. H., An, N., Breyer, B., Vanichakarn, P., Szatkowski, J. P., Park, J. Y., & He, T. C. (2003). Osteogenic activity of the fourteen types of human bone morphogenetic proteins (BMPs). *J Bone Joint Surg Am, 85-A*(8), 1544-1552.

Choudhry, S., Deshpande, A., Qiao, L., Beckman, K., Sen, S., & Baskin, L. S. (2012). Genome-wide DNA methylation profiling of CpG islands in hypospadias. *J Urol, 188*(4 Suppl), 1450-1455.

Chu, M. C., Selam, F. B., & Taylor, H. S. (2004). HOXA10 regulates p53 expression and matrigel invasion in human breast cancer cells. *Cancer Biol Ther, 3*(6), 568-572.

Chuang, L. S., & Ito, Y. (2010). RUNX3 is multifunctional in carcinogenesis of multiple solid tumors. *Oncogene, 29*(18), 2605-2615.

Cifone, M. A., & Fidler, I. J. (1980). Correlation of patterns of anchorage-independent growth with in vivo behavior of cells from a murine fibrosarcoma. *Proc Natl Acad Sci U S A, 77*(2), 1039-1043.

Conrad, C., Gottgens, B., Kinston, S., Ellwart, J., & Huss, R. (2002). GATA transcription in a small rhodamine 123(low)CD34(+) subpopulation of a peripheral blood-derived CD34(-)CD105(+) mesenchymal cell line. *Exp Hematol, 30*(8), 887-895.

Cormier, P., Osborne, H. B., Morales, J., Bassez, T., Minella, O., Poulhe, R., Belle, R., & Mulner-Lorillon, O. (1993). Elongation factor 1 contains two homologous guanine-nucleotide exchange proteins as shown from the molecular cloning of beta and delta subunits. *Nucleic Acids Res, 21*(3), 743.

Daftary, G. S., & Taylor, H. S. (2006). Endocrine regulation of HOX genes. *Endocrine Reviews, 27*(4), 331-355.

Davis, A. P., & Capecchi, M. R. (1994). Axial homeosis and appendicular skeleton defects in mice with a targeted disruption of hoxd-11. *Development, 120*(8), 2187-2198.

Davis, A. P., Witte, D. P., Hsieh-Li, H. M., Potter, S. S., & Capecchi, M. R. (1995). Absence of radius and ulna in mice lacking hoxa-11 and hoxd-11. *Nature, 375*(6534), 791-795.

De Bortoli, M., Castellino, R. C., Lu, X. Y., Deyo, J., Sturla, L. M., Adesina, A. M., Perlaky, L., Pomeroy, S. L., Lau, C. C., Man, T. K., Rao, P. H., & Kim, J. Y. (2006). Medulloblastoma outcome is adversely associated with overexpression of EEF1D, RPL30, and RPS20 on the long arm of chromosome 8. *BMC Cancer, 6*, 223.

de la Cruz, C. C., Der-Avakian, A., Spyropoulos, D. D., Tieu, D. D., & Carpenter, E. M. (1999). Targeted disruption of Hoxd9 and Hoxd10 alters locomotor behavior, vertebral identity, and peripheral nervous system development. *Dev Biol, 216*(2), 595-610.

De La Fuente, R., Baumann, C., & Viveiros, M. M. (2011). Role of ATRX in chromatin structure and function: implications for chromosome instability and human disease. *Reproduction, 142*(2), 221-234.

De Luca, F., Barnes, K. M., Uyeda, J. A., De-Levi, S., Abad, V., Palese, T., Mericq, V., & Baron, J. (2001). Regulation of growth plate chondrogenesis by bone morphogenetic protein-2. *Endocrinology, 142*(1), 430-436.

Delattre, O., Zucman, J., Melot, T., Garau, X. S., Zucker, J. M., Lenoir, G. M., Ambros, P. F., Sheer, D., Turc-Carel, C., & Triche, T. J. (1994). The Ewing family of tumors--a subgroup of small-round-cell tumors defined by specific chimeric transcripts. *New England Journal of Medicine, 331*(5), 294-299.

Delattre, O., Zucman, J., Plougastel, B., Desmaze, C., Melot, T., Peter, M., Kovar, H., Joubert, I., de Jong, P., & Rouleau, G. (1992). Gene fusion with an ETS DNA-binding domain caused by chromosome translocation in human tumours. *Nature, 359*(6391), 162-165.

Delpretti, S., Zakany, J., & Duboule, D. (2012). A function for all posterior Hoxd genes during digit development? *Dev Dyn, 241*(4), 792-802.

Deutsches Kinderkrebsregister. Jahresbericht 2013/2014.

Di Croce, L., & Helin, K. (2013). Transcriptional regulation by Polycomb group proteins. *Nature Structural & Molecular Biology, 20*(10), 1147-1155.

Didsbury, J., Weber, R. F., Bokoch, G. M., Evans, T., & Snyderman, R. (1989). rac, a novel ras-related family of proteins that are botulinum toxin substrates. *J Biol Chem, 264*(28), 16378-16382.

Dobbs, M. B., Gurnett, C. A., Pierce, B., Exner, G. U., Robarge, J., Morcuende, J. A., Cole, W. G., Templeton, P. A., Foster, B., & Bowcock, A. M. (2006). HOXD10 M319K mutation in a family with isolated congenital vertical talus. *J Orthop Res, 24*(3), 448-453.

Dockhorn-Dworniczak, B., Schafer, K. L., Dantcheva, R., Blasius, S., van Valen, F., Burdach, S., Winkelmann, W., Jurgens, H., & Bocker, W. (1994). [Molecular genetic detection of t(11;22)(q24;12) translocation in Ewing sarcoma and malignant peripheral neuroectodermal tumors]. *Pathologe, 15*(2), 103-112.

Dolle, P., & Duboule, D. (1989). Two gene members of the murine HOX-5 complex show regional and cell-type specific expression in developing limbs and gonads. *EMBO J, 8*(5), 1507-1515.

Douglas, D., Hsu, J. H., Hung, L., Cooper, A., Abdueva, D., van Doorninck, J., Peng, G., Shimada, H., Triche, T. J., & Lawlor, E. R. (2008). BMI-1 promotes ewing sarcoma tumorigenicity independent of CDKN2A repression. *Cancer Res, 68*(16), 6507-6515.

Duboule, D. (1994). *Guidebook to the Homeobox Genes* (1st ed.): A Sambrook and Tooze Publication at Oxford University Press.

Duboule, D., & Morata, G. (1994). Colinearity and functional hierarchy among genes of the homeotic complexes. *Trends Genet, 10*(10), 358-364.

Duchman, K. R., Gao, Y., & Miller, B. J. (2015). Prognostic factors for survival in patients with Ewing's sarcoma using the surveillance, epidemiology, and end results (SEER) program database. *Cancer Epidemiol, 39*(2), 189-195.

Ducy, P., Zhang, R., Geoffroy, V., Ridall, A. L., & Karsenty, G. (1997). Osf2/Cbfa1: a transcriptional activator of osteoblast differentiation. *Cell, 89*(5), 747-754.

Dunn, T., Praissman, L., Hagag, N., & Viola, M. V. (1994). ERG gene is translocated in an Ewing's sarcoma cell line. *Cancer Genetics and Cytogenetics, 76*(1), 19-22.

Duprez, D., Bell, E. J., Richardson, M. K., Archer, C. W., Wolpert, L., Brickell, P. M., & Francis-West, P. H. (1996). Overexpression of BMP-2 and BMP-4 alters the size and shape of developing skeletal elements in the chick limb. *Mech Dev, 57*(2), 145-157.

Duprez, D. M., Kostakopoulou, K., Francis-West, P. H., Tickle, C., & Brickell, P. M. (1996). Activation of Fgf-4 and HoxD gene expression by BMP-2 expressing cells in the developing chick limb. *Development, 122*(6), 1821-1828.

Edgar, R., Domrachev, M., & Lash, A. E. (2002). Gene Expression Omnibus: NCBI gene expression and hybridization array data repository. *Nucleic Acids Res, 30*(1), 207-210.

Erselius, J. R., Goulding, M. D., & Gruss, P. (1990). Structure and expression pattern of the murine Hox-3.2 gene. *Development, 110*(2), 629-642.

Ewing, J. (1972). Classics in oncology. Diffuse endothelioma of bone. James Ewing. Proceedings of the New York Pathological Society, 1921. *CA: A Cancer Journal for Clinicians, 22*(2), 95-98.

Fogh, J., & Trempe, G. (1975). New human tumor cell lines. In J. Fogh (Ed.), *Human Tumor Cells In Vitro*. New York and London: Plenum Press.

Foronda, D., de Navas, L. F., Garaulet, D. L., & Sanchez-Herrero, E. (2009). Function and specificity of Hox genes. *Int J Dev Biol, 53*(8-10), 1404-1419.

Foster, J. W., Dominguez-Steglich, M. A., Guioli, S., Kwok, C., Weller, P. A., Stevanovic, M., Weissenbach, J., Mansour, S., Young, I. D., & Goodfellow, P. N. (1994). Campomelic dysplasia and autosomal sex reversal caused by mutations in an SRY-related gene. *Nature, 372*(6506), 525-530.

Francis, P. H., Richardson, M. K., Brickell, P. M., & Tickle, C. (1994). Bone morphogenetic proteins and a signalling pathway that controls patterning in the developing chick limb. *Development, 120*(1), 209-218.

Freyschmidt, J., Ostertag, H., & Jundt, G. (2010). Knochentumoren mit Kiefertumoren: Klinik, Radiologie, Pathologie (Vol. 3. Auflage, pp. 444-474). Dordrecht Heidelberg London New York: Springer-Verlag.

Fromental-Ramain, C., Warot, X., Messadecq, N., LeMeur, M., Dolle, P., & Chambon, P. (1996). Hoxa-13 and Hoxd-13 play a crucial role in the patterning of the limb autopod. *Development, 122*(10), 2997-3011.

Fu, Y., Li, F., Zhao, D. Y., Zhang, J. S., Lv, Y., & Li-Ling, J. (2014). Interaction between Tbx1 and Hoxd10 and connection with TGFbeta-BMP signal pathway during kidney development. *Gene, 536*(1), 197-202.

Furuta, J., Nobeyama, Y., Umebayashi, Y., Otsuka, F., Kikuchi, K., & Ushijima, T. (2006). Silencing of Peroxiredoxin 2 and aberrant methylation of 33 CpG islands in putative promoter regions in human malignant melanomas. *Cancer Res, 66*(12), 6080-6086.

Garcia-Barcelo, M. M., Wong, K. K., Lui, V. C., Yuan, Z. W., So, M. T., Ngan, E. S., Miao, X. P., Chung, P. H., Khong, P. L., & Tam, P. K. (2008). Identification of a HOXD13 mutation in a VACTERL patient. *Am J Med Genet A, 146A*(24), 3181-3185.

Gehring, W. J., Affolter, M., & Burglin, T. (1994). Homeodomain proteins. *Annu Rev Biochem, 63*, 487-526.

Gerard, M., Zakany, J., & Duboule, D. (1997). Interspecies exchange of a Hoxd enhancer in vivo induces premature transcription and anterior shift of the sacrum. *Dev Biol, 190*(1), 32-40.

Giard, D. J., Aaronson, S. A., Todaro, G. J., Arnstein, P., Kersey, J. H., Dosik, H., & Parks, W. P. (1973). In vitro cultivation of human tumors: establishment of cell lines derived from a series of solid tumors. *J Natl Cancer Inst, 51*(5), 1417-1423.

Gibbons, R. J., Picketts, D. J., Villard, L., & Higgs, D. R. (1995). Mutations in a putative global transcriptional regulator cause X-linked mental retardation with alpha-thalassemia (ATR-X syndrome). *Cell, 80*(6), 837-845.

Goff, D. J., & Tabin, C. J. (1997). Analysis of Hoxd-13 and Hoxd-11 misexpression in chick limb buds reveals that Hox genes affect both bone condensation and growth. *Development, 124*(3), 627-636.

Goodman, F. R., Mundlos, S., Muragaki, Y., Donnai, D., Giovannucci-Uzielli, M. L., Lapi, E., Majewski, F., McGaughran, J., McKeown, C., Reardon, W., Upton, J., Winter, R. M., Olsen, B. R., & Scambler, P. J. (1997). Synpolydactyly phenotypes correlate with size of expansions in HOXD13 polyalanine tract. *Proc Natl Acad Sci U S A, 94*(14), 7458-7463.

Gosiengfiao, Y., Horvat, R., & Thompson, A. (2007). Transcription factors GATA-1 and Fli-1 regulate human HOXA10 expression in megakaryocytic cells. *DNA Cell Biol, 26*(8), 577-587.

Gough, S. M., Slape, C. I., & Aplan, P. D. (2011). NUP98 gene fusions and hematopoietic malignancies: common themes and new biologic insights. *Blood, 118*(24), 6247-6257.

Gould, A., Morrison, A., Sproat, G., White, R. A., & Krumlauf, R. (1997). Positive cross-regulation and enhancer sharing: two mechanisms for specifying overlapping Hox expression patterns. *Genes Dev, 11*(7), 900-913.

Grier, D. G., Thompson, A., Kwasniewska, A., McGonigle, G. J., Halliday, H. L., & Lappin, T. R. (2005). The pathophysiology of HOX genes and their role in cancer. *J Pathol, 205*(2), 154-171.

Gross, S., Krause, Y., Wuelling, M., & Vortkamp, A. (2012). Hoxa11 and Hoxd11 regulate chondrocyte differentiation upstream of Runx2 and Shox2 in mice. *PLoS One, 7*(8), e43553.

Grunewald, T. G., Diebold, I., Esposito, I., Plehm, S., Hauer, K., Thiel, U., da Silva-Buttkus, P., Neff, F., Unland, R., Muller-Tidow, C., Zobywalski, C., Lohrig, K., Lewandrowski, U., Sickmann, A., Prazeres da Costa, O., Gorlach, A., Cossarizza, A., Butt, E., Richter, G. H., & Burdach, S. (2012). STEAP1 is associated with the invasive and oxidative stress phenotype of Ewing tumors. *Mol Cancer Res, 10*(1), 52-65.

Gu, Z. D., Chen, X. M., Zhang, W., Gu, J., & Chen, K. N. (2007). [Expression of 39 HOX genes in esophageal cancer cell lines]. *Zhonghua Wei Chang Wai Ke Za Zhi, 10*(4), 365-367.

Haataja, L., Groffen, J., & Heisterkamp, N. (1997). Characterization of RAC3, a novel member of the Rho family. *J Biol Chem, 272*(33), 20384-20388.

Haberler, C., & Wohrer, A. (2014). Clinical Neuropathology practice news 2-2014: ATRX, a new candidate biomarker in gliomas. *Clin Neuropathol, 33*(2), 108-111.

Hakami, F., Darda, L., Stafford, P., Woll, P., Lambert, D. W., & Hunter, K. D. (2014). The roles of HOXD10 in the development and progression of head and neck squamous cell carcinoma (HNSCC). *Br J Cancer, 111*(4), 807-816.

Han, J. A., Kim, J. Y., & Kim, J. I. (2014). Analysis of gene expression in cyclooxygenase-2-overexpressed human osteosarcoma cell lines. *Genomics Inform, 12*(4), 247-253.

Hansen, S. L., Dosanjh, A., Young, D. M., Boudreau, N., & Hoffman, W. Y. (2006). Hemangiomas and homeobox gene expression. *J Craniofac Surg, 17*(4), 767-771.

Hanson, R. D., Hess, J. L., Yu, B. D., Ernst, P., van Lohuizen, M., Berns, A., van der Lugt, N. M., Shashikant, C. S., Ruddle, F. H., Seto, M., & Korsmeyer, S. J. (1999). Mammalian Trithorax and polycomb-group homologues are antagonistic regulators of homeotic development. *Proc Natl Acad Sci U S A, 96*(25), 14372-14377.

Hardwick, J. C., Kodach, L. L., Offerhaus, G. J., & van den Brink, G. R. (2008). Bone morphogenetic protein signalling in colorectal cancer. *Nat Rev Cancer, 8*(10), 806-812.

Hauer, K., Calzada-Wack, J., Steiger, K., Grunewald, T. G., Baumhoer, D., Plehm, S., Buch, T., Prazeres da Costa, O., Esposito, I., Burdach, S., & Richter, G. H. (2013). DKK2 mediates osteolysis, invasiveness, and metastatic spread in Ewing sarcoma. *Cancer Res, 73*(2), 967-977.

He, W., Dorn, D. C., Erdjument-Bromage, H., Tempst, P., Moore, M. A., & Massague, J. (2006). Hematopoiesis controlled by distinct TIF1gamma and Smad4 branches of the TGFbeta pathway. *Cell, 125*(5), 929-941.

Heldin, C. H., Miyazono, K., & ten Dijke, P. (1997). TGF-beta signalling from cell membrane to nucleus through SMAD proteins. *Nature, 390*(6659), 465-471.

Heremans, H., Billiau, A., Cassiman, J. J., Mulier, J. C., & de Somer, P. (1978). In vitro cultivation of human tumor tissues. II. Morphological and virological characterization of three cell lines. *Oncology, 35*(6), 246-252.

Hernanda, P. Y., Chen, K., Das, A. M., Sideras, K., Wang, W., Li, J., Cao, W., Bots, S. J., Kodach, L. L., de Man, R. A., Ijzermans, J. N., Janssen, H. L., Stubbs, A. P., Sprengers, D., Bruno, M. J., Metselaar, H. J., Ten Hagen, T. L., Kwekkeboom, J., Peppelenbosch, M. P., & Pan, Q. (2014). SMAD4 exerts a tumor-promoting role in hepatocellular carcinoma. *Oncogene*.

Heubach, J., Monsior, J., Deenen, R., Niegisch, G., Szarvas, T., Niedworok, C., Schulz, W. A., & Hoffmann, M. J. (2015). The long noncoding RNA HOTAIR has tissue and cell type-dependent effects on HOX gene expression and phenotype of urothelial cancer cells. *Mol Cancer, 14*(1), 108.

Hogan, B. L. (1996). Bone morphogenetic proteins: multifunctional regulators of vertebrate development. *Genes Dev, 10*(13), 1580-1594.

Holland, P. W. (2013). Evolution of homeobox genes. *Wiley Interdiscip Rev Dev Biol, 2*(1), 31-45.

Hu-Lieskovan, S., Zhang, J., Wu, L., Shimada, H., Schofield, D. E., & Triche, T. J. (2005). EWS-FLI1 fusion protein up-regulates critical genes in neural crest development and is responsible for the observed phenotype of Ewing's family of tumors. *Cancer Res, 65*(11), 4633-4644.

Hu, J., Gray, C. A., & Spencer, T. E. (2004). Gene expression profiling of neonatal mouse uterine development. *Biol Reprod, 70*(6), 1870-1876.

Hu, X., Chen, D., Cui, Y., Li, Z., & Huang, J. (2013). Targeting microRNA-23a to inhibit glioma cell invasion via HOXD10. *Sci Rep, 3*, 3423.

Ichikawa, M., Yoshimi, A., Nakagawa, M., Nishimoto, N., Watanabe-Okochi, N., & Kurokawa, M. (2013). A role for RUNX1 in hematopoiesis and myeloid leukemia. *International Journal of Hematology, 97*(6), 726-734.

Iimura, T., Oida, S., Takeda, K., Maruoka, Y., & Sasaki, S. (1994). Changes in homeobox-containing gene expression during ectopic bone formation induced by bone morphogenetic protein. *Biochem Biophys Res Commun, 201*(2), 980-987.

Israel, D. I., Nove, J., Kerns, K. M., Kaufman, R. J., Rosen, V., Cox, K. A., & Wozney, J. M. (1996). Heterodimeric bone morphogenetic proteins show enhanced activity in vitro and in vivo. *Growth Factors, 13*(3-4), 291-300.

Ito, Y., Bae, S. C., & Chuang, L. S. (2015). The RUNX family: developmental regulators in cancer. *Nat Rev Cancer, 15*(2), 81-95.

Izpisua-Belmonte, J. C., Falkenstein, H., Dolle, P., Renucci, A., & Duboule, D. (1991). Murine genes related to the Drosophila AbdB homeotic genes are sequentially expressed during development of the posterior part of the body. *EMBO J, 10*(8), 2279-2289.

Javed, A., Bae, J. S., Afzal, F., Gutierrez, S., Pratap, J., Zaidi, S. K., Lou, Y., van Wijnen, A. J., Stein, J. L., Stein, G. S., & Lian, J. B. (2008). Structural coupling of Smad and Runx2 for execution of the BMP2 osteogenic signal. *J Biol Chem, 283*(13), 8412-8422.

Javed, A., Chen, H., & Ghori, F. Y. (2010). Genetic and transcriptional control of bone formation. *Oral Maxillofac Surg Clin North Am, 22*(3), 283-293, v.

Javelaud, D., Wietzerbin, J., Delattre, O., & Besancon, F. (2000). Induction of p21Waf1/Cip1 by TNFalpha requires NF-kappaB activity and antagonizes apoptosis in Ewing tumor cells. *Oncogene, 19*(1), 61-68.

Je, E. M., An, C. H., Yoo, N. J., & Lee, S. H. (2012). Expressional and mutational analysis of ATRX gene in gastric, colorectal and prostate cancers. *APMIS, 120*(6), 519-520.

Jensen, E. D., Pham, L., Billington, C. J., Jr., Espe, K., Carlson, A. E., Westendorf, J. J., Petryk, A., Gopalakrishnan, R., & Mansky, K. (2010). Bone morphogenic protein 2 directly enhances differentiation of murine osteoclast precursors. *J Cell Biochem, 109*(4), 672-682.

Johnson, D., Kan, S. H., Oldridge, M., Trembath, R. C., Roche, P., Esnouf, R. M., Giele, H., & Wilkie, A. O. (2003). Missense mutations in the homeodomain of HOXD13 are associated with brachydactyly types D and E. *Am J Hum Genet, 72*(4), 984-997.

Jones-Villeneuve, E. M., McBurney, M. W., Rogers, K. A., & Kalnins, V. I. (1982). Retinoic acid induces embryonal carcinoma cells to differentiate into neurons and glial cells. *J Cell Biol, 94*(2), 253-262.

Joseph, P., Lei, Y. X., Whong, W. Z., & Ong, T. M. (2002). Oncogenic potential of mouse translation elongation factor-1 delta, a novel cadmium-responsive proto-oncogene. *J Biol Chem, 277*(8), 6131-6136.

Joshi, S., Singh, A. R., Zulcic, M., Bao, L., Messer, K., Ideker, T., Dutkowski, J., & Durden, D. L. (2014). Rac2 controls tumor growth, metastasis and M1-M2 macrophage differentiation in vivo. *PLoS One, 9*(4), e95893.

Jung, J. C., & Tsonis, P. A. (1998). Role of 5' HoxD genes in chondrogenesis in vitro. *Int J Dev Biol, 42*(4), 609-615.

Kanzler, B., Viallet, J. P., Le Mouellic, H., Boncinelli, E., Duboule, D., & Dhouailly, D. (1994). Differential expression of two different homeobox gene families during mouse tegument morphogenesis. *Int J Dev Biol, 38*(4), 633-640.

Kappen, C., Schughart, K., & Ruddle, F. H. (1989). Organization and expression of homeobox genes in mouse and man. *Ann N Y Acad Sci, 567*, 243-252.

Karsenty, G., Kronenberg, H. M., & Settembre, C. (2009). Genetic control of bone formation. *Annual Review of Cell and Developmental Biology, 25*, 629-648.

Kauer, M., Ban, J., Kofler, R., Walker, B., Davis, S., Meltzer, P., & Kovar, H. (2009). A molecular function map of Ewing's sarcoma. *PLoS One, 4*(4), e5415.

Kawabata, M., Imamura, T., & Miyazono, K. (1998). Signal transduction by bone morphogenetic proteins. *Cytokine Growth Factor Rev, 9*(1), 49-61.

Kessel, M., & Gruss, P. (1991). Homeotic transformations of murine vertebrae and concomitant alteration of Hox codes induced by retinoic acid. *Cell, 67*(1), 89-104.

Kim, E. K., & Choi, E. J. (2010). Pathological roles of MAPK signaling pathways in human diseases. *Biochim Biophys Acta, 1802*(4), 396-405.

Kim, Y., Murao, H., Yamamoto, K., Deng, J. M., Behringer, R. R., Nakamura, T., & Akiyama, H. (2011). Generation of transgenic mice for conditional overexpression of Sox9. *Journal of Bone and Mineral Metabolism, 29*(1), 123-129.

Kitazawa, R., Mori, K., Yamaguchi, A., Kondo, T., & Kitazawa, S. (2008). Modulation of mouse RANKL gene expression by Runx2 and vitamin D3. *J Cell Biochem, 105*(5), 1289-1297.

Kjosness, K. M., Hines, J. E., Lovejoy, C. O., & Reno, P. L. (2014). The pisiform growth plate is lost in humans and supports a role for Hox in growth plate formation. *J Anat, 225*(5), 527-538.

Kleinman, H. K., & Martin, G. R. (2005). Matrigel: basement membrane matrix with biological activity. *Semin Cancer Biol, 15*(5), 378-386.

Kmita, M., Tarchini, B., Zakany, J., Logan, M., Tabin, C. J., & Duboule, D. (2005). Early developmental arrest of mammalian limbs lacking HoxA/HoxD gene function. *Nature, 435*(7045), 1113-1116.

Komori, T. (2010). Regulation of bone development and extracellular matrix protein genes by RUNX2. *Cell Tissue Res, 339*(1), 189-195.

Komori, T. (2011). Signaling networks in RUNX2-dependent bone development. *J Cell Biochem, 112*(3), 750-755.

Komori, T., Yagi, H., Nomura, S., Yamaguchi, A., Sasaki, K., Deguchi, K., Shimizu, Y., Bronson, R. T., Gao, Y. H., Inada, M., Sato, M., Okamoto, R., Kitamura, Y., Yoshiki, S., & Kishimoto, T. (1997). Targeted disruption of Cbfa1 results in a complete lack of bone formation owing to maturational arrest of osteoblasts. *Cell, 89*(5), 755-764.

Kondo, T., Dolle, P., Zakany, J., & Duboule, D. (1996). Function of posterior HoxD genes in the morphogenesis of the anal sphincter. *Development, 122*(9), 2651-2659.

Koyama, E., Yasuda, T., Minugh-Purvis, N., Kinumatsu, T., Yallowitz, A. R., Wellik, D. M., & Pacifici, M. (2010). Hox11 genes establish synovial joint organization and phylogenetic characteristics in developing mouse zeugopod skeletal elements. *Development, 137*(22), 3795-3800.

Krumlauf, R. (1992). Evolution of the vertebrate Hox homeobox genes. *Bioessays, 14*(4), 245-252.

Krumlauf, R. (1994). Hox genes in vertebrate development. *Cell, 78*(2), 191-201.

Kuss, P., Kraft, K., Stumm, J., Ibrahim, D., Vallecillo-Garcia, P., Mundlos, S., & Stricker, S. (2014). Regulation of cell polarity in the cartilage growth plate and perichondrium of metacarpal elements by HOXD13 and WNT5A. *Dev Biol, 385*(1), 83-93.

Kuss, P., Villavicencio-Lorini, P., Witte, F., Klose, J., Albrecht, A. N., Seemann, P., Hecht, J., & Mundlos, S. (2009). Mutant Hoxd13 induces extra digits in a mouse model of synpolydactyly directly and by decreasing retinoic acid synthesis. *J Clin Invest, 119*(1), 146-156.

Ladam, F., & Sagerstrom, C. G. (2014). Hox regulation of transcription: more complex(es). *Dev Dyn, 243*(1), 4-15.

Lance-Jones, C., Omelchenko, N., Bailis, A., Lynch, S., & Sharma, K. (2001). Hoxd10 induction and regionalization in the developing lumbosacral spinal cord. *Development, 128*(12), 2255-2268.

Lane, S. W., De Vita, S., Alexander, K. A., Karaman, R., Milsom, M. D., Dorrance, A. M., Purdon, A., Louis, L., Bouxsein, M. L., & Williams, D. A. (2012). Rac signaling in osteoblastic cells is required for normal bone development but is dispensable for hematopoietic development. *Blood, 119*(3), 736-744.

Lawo, S., Bashkurov, M., Mullin, M., Ferreria, M. G., Kittler, R., Habermann, B., Tagliaferro, A., Poser, I., Hutchins, J. R., Hegemann, B., Pinchev, D., Buchholz, F., Peters, J. M., Hyman, A. A., Gingras, A. C., & Pelletier, L. (2009). HAUS, the 8-subunit human Augmin complex, regulates centrosome and spindle integrity. *Curr Biol, 19*(10), 816-826.

Leber, B., Maier, B., Fuchs, F., Chi, J., Riffel, P., Anderhub, S., Wagner, L., Ho, A. D., Salisbury, J. L., Boutros, M., & Kramer, A. (2010). Proteins required for centrosome clustering in cancer cells. *Sci Transl Med, 2*(33), 33ra38.

Leboy, P., Grasso-Knight, G., D'Angelo, M., Volk, S. W., Lian, J. V., Drissi, H., Stein, G. S., & Adams, S. L. (2001). Smad-Runx interactions during chondrocyte maturation. *J Bone Joint Surg Am, 83-A Suppl 1*(Pt 1), S15-22.

Lee, A. P., Koh, E. G., Tay, A., Brenner, S., & Venkatesh, B. (2006). Highly conserved syntenic blocks at the vertebrate Hox loci and conserved regulatory elements within and outside Hox gene clusters. *Proc Natl Acad Sci U S A, 103*(18), 6994-6999.

Lee, J. Y., Hur, H., Yun, H. J., Kim, Y., Yang, S., Kim, S. I., & Kim, M. H. (2015). HOXB5 Promotes the Proliferation and Invasion of Breast Cancer Cells. *Int J Biol Sci, 11*(6), 701-711.

Lee, K. S., Hong, S. H., & Bae, S. C. (2002). Both the Smad and p38 MAPK pathways play a crucial role in Runx2 expression following induction by transforming growth factor-beta and bone morphogenetic protein. *Oncogene, 21*(47), 7156-7163.

Lee, K. S., Kim, H. J., Li, Q. L., Chi, X. Z., Ueta, C., Komori, T., Wozney, J. M., Kim, E. G., Choi, J. Y., Ryoo, H. M., & Bae, S. C. (2000). Runx2 is a common target of transforming growth factor beta1 and bone morphogenetic protein 2, and cooperation between Runx2 and Smad5 induces osteoblast-specific gene expression in the pluripotent mesenchymal precursor cell line C2C12. *Mol Cell Biol, 20*(23), 8783-8792.

Lefebvre, V., Behringer, R. R., & de Crombrugghe, B. (2001). L-Sox5, Sox6 and Sox9 control essential steps of the chondrocyte differentiation pathway. *Osteoarthritis and Cartilage, 9, Supplement 1*(0), S69-S75.

Lefebvre, V., Li, P., & de Crombrugghe, B. (1998). A new long form of Sox5 (L-Sox5), Sox6 and Sox9 are coexpressed in chondrogenesis and cooperatively activate the type II collagen gene. *EMBO J, 17*(19), 5718-5733.

Lefebvre, V., & Smits, P. (2005). Transcriptional control of chondrocyte fate and differentiation. *Birth Defects Research Part C: Embryo Today: Reviews, 75*(3), 200-212.

Lei, Y. X., Chen, J. K., & Wu, Z. L. (2002). Blocking the translation elongation factor-1 delta with its antisense mRNA results in a significant reversal of its oncogenic potential. *Teratog Carcinog Mutagen, 22*(5), 377-383.

Leung, J. W., Ghosal, G., Wang, W., Shen, X., Wang, J., Li, L., & Chen, J. (2013). Alpha thalassemia/mental retardation syndrome X-linked gene product ATRX is required for proper replication restart and cellular resistance to replication stress. *J Biol Chem, 288*(9), 6342-6350.

Levine, M., & Hoey, T. (1988). Homeobox proteins as sequence-specific transcription factors. *Cell, 55*(4), 537-540.

Levine, S. S., Weiss, A., Erdjument-Bromage, H., Shao, Z., Tempst, P., & Kingston, R. E. (2002). The core of the polycomb repressive complex is compositionally and functionally conserved in flies and humans. *Mol Cell Biol, 22*(17), 6070-6078.

Lewis, E. B. (1978). A gene complex controlling segmentation in Drosophila. *Nature, 276*(5688), 565-570.

Li, B., Jin, H., Yu, Y., Gu, C., Zhou, X., Zhao, N., & Feng, Y. (2009). HOXA10 is overexpressed in human ovarian clear cell adenocarcinoma and correlates with poor survival. *International Journal of Gynecological Cancer, 19*(8), 1347-1352.

Li, B., Yu, H., Zheng, W., Voll, R., Na, S., Roberts, A. W., Williams, D. A., Davis, R. J., Ghosh, S., & Flavell, R. A. (2000). Role of the guanosine triphosphatase Rac2 in T helper 1 cell differentiation. *Science, 288*(5474), 2219-2222.

Li, Q., Ding, C., Chen, C., Zhang, Z., Xiao, H., Xie, F., Lei, L., Chen, Y., Mao, B., Jiang, M., Li, J., Wang, D., & Wang, G. (2014). miR-224 promotion of cell migration and invasion by targeting Homeobox D 10 gene in human hepatocellular carcinoma. *J Gastroenterol Hepatol, 29*(4), 835-842.

Li, X., & Cao, X. (2003). BMP signaling and HOX transcription factors in limb development. *Front Biosci, 8*, s805-812.

Li, X., & Cao, X. (2006). BMP signaling and skeletogenesis. *Ann N Y Acad Sci, 1068*, 26-40.

Li, X., McGee-Lawrence, M. E., Decker, M., & Westendorf, J. J. (2010). The Ewing's sarcoma fusion protein, EWS-FLI, binds Runx2 and blocks osteoblast differentiation. *J Cell Biochem, 111*(4), 933-943.

Li, X., Nie, S., Chang, C., Qiu, T., & Cao, X. (2006). Smads oppose Hox transcriptional activities. *Exp Cell Res, 312*(6), 854-864.

Li, Y., Yang, X. H., Fang, S. J., Qin, C. F., Sun, R. L., Liu, Z. Y., Jiang, B. Y., Wu, X., & Li, G. (2015). HOXA7 stimulates human hepatocellular carcinoma proliferation through cyclin E1/CDK2. *Oncol Rep, 33*(2), 990-996.

Liao, C. G., Kong, L. M., Zhou, P., Yang, X. L., Huang, J. G., Zhang, H. L., & Lu, N. (2014). miR-10b is overexpressed in hepatocellular carcinoma and promotes cell proliferation, migration and invasion through RhoC, uPAR and MMPs. *J Transl Med, 12*(1), 234.

Lim, J., Tu, X., Choi, K., Akiyama, H., Mishina, Y., & Long, F. (2015). BMP-Smad4 signaling is required for precartilaginous mesenchymal condensation independent of Sox9 in the mouse. *Dev Biol, 400*(1), 132-138.

Lin, A. W., & Carpenter, E. M. (2003). Hoxa10 and Hoxd10 coordinately regulate lumbar motor neuron patterning. *J Neurobiol, 56*(4), 328-337.

Lin, J., Teo, S., Lam, D. H., Jeyaseelan, K., & Wang, S. (2012). MicroRNA-10b pleiotropically regulates invasion, angiogenicity and apoptosis of tumor cells resembling mesenchymal subtype of glioblastoma multiforme. *Cell Death Dis, 3*, e398.

Lin, Y. W., Slape, C., Zhang, Z., & Aplan, P. D. (2005). NUP98-HOXD13 transgenic mice develop a highly penetrant, severe myelodysplastic syndrome that progresses to acute leukemia. *Blood, 106*(1), 287-295.

Liu, Y. J., Zhu, Y., Yuan, H. X., Zhang, J. P., Guo, J. M., & Lin, Z. M. (2015). Overexpression of HOXC11 homeobox gene in clear cell renal cell carcinoma induces cellular proliferation and is associated with poor prognosis. *Tumour Biol, 36*(4), 2821-2829.

Liu, Z., Shi, W., Ji, X., Sun, C., Jee, W. S., Wu, Y., Mao, Z., Nagy, T. R., Li, Q., & Cao, X. (2004). Molecules mimicking Smad1 interacting with Hox stimulate bone formation. *J Biol Chem, 279*(12), 11313-11319.

Liu, Z., Zhu, J., Cao, H., Ren, H., & Fang, X. (2012). miR-10b promotes cell invasion through RhoC-AKT signaling pathway by targeting HOXD10 in gastric cancer. *Int J Oncol, 40*(5), 1553-1560.

Livak, K. J., Flood, S. J., Marmaro, J., Giusti, W., & Deetz, K. (1995). Oligonucleotides with fluorescent dyes at opposite ends provide a quenched probe system useful for detecting PCR product and nucleic acid hybridization. *PCR Methods Appl, 4*(6), 357-362.

Livak, K. J., & Schmittgen, T. D. (2001). Analysis of relative gene expression data using real-time quantitative PCR and the 2(-Delta Delta C(T)) Method. *Methods, 25*(4), 402-408.

Lizard-Nacol, S., Lizard, G., Justrabo, E., & Turc-Carel, C. (1989). Immunologic characterization of Ewing's sarcoma using mesenchymal and neural markers. *Am J Pathol, 135*(5), 847-855.

Long, F., & Ornitz, D. M. (2013). Development of the endochondral skeleton. *Cold Spring Harb Perspect Biol, 5*(1), a008334.

Louis, C. U., & Shohet, J. M. (2015). Neuroblastoma: molecular pathogenesis and therapy. *Annual Review of Medicine, 66*, 49-63.

Lovejoy, C. A., Li, W., Reisenweber, S., Thongthip, S., Bruno, J., de Lange, T., De, S., Petrini, J. H., Sung, P. A., Jasin, M., Rosenbluh, J., Zwang, Y., Weir, B. A., Hatton, C., Ivanova, E., Macconaill, L., Hanna, M., Hahn, W. C., Lue, N. F., Reddel, R. R., Jiao, Y., Kinzler, K., Vogelstein, B., Papadopoulos, N., & Meeker, A. K. (2012). Loss of ATRX, genome instability, and an altered DNA damage response are hallmarks of the alternative lengthening of telomeres pathway. *PLoS Genet, 8*(7), e1002772.

Ma, L., Teruya-Feldstein, J., & Weinberg, R. A. (2007). Tumour invasion and metastasis initiated by microRNA-10b in breast cancer. *Nature, 449*(7163), 682-688.

Maconochie, M., Nonchev, S., Morrison, A., & Krumlauf, R. (1996). Paralogous Hox genes: function and regulation. *Annu Rev Genet, 30*, 529-556.

Maden, M., Gale, E., Kostetskii, I., & Zile, M. (1996). Vitamin A-deficient quail embryos have half a hindbrain and other neural defects. *Curr Biol, 6*(4), 417-426.

Malik, S., & Grzeschik, K. H. (2008). Synpolydactyly: clinical and molecular advances. *Clin Genet, 73*(2), 113-120.

Marini, P., MacLeod, R. A., Treuner, C., Bruchelt, G., Bohm, W., Wolburg, H., Schweizer, P., & Girgert, R. (1999). SiMa, a new neuroblastoma cell line combining poor prognostic cytogenetic markers with high adrenergic differentiation. *Cancer Genetics and Cytogenetics, 112*(2), 161-164.

Marinoni, I., Kurrer, A. S., Vassella, E., Dettmer, M., Rudolph, T., Banz, V., Hunger, F., Pasquinelli, S., Speel, E. J., & Perren, A. (2014). Loss of DAXX and ATRX are associated with chromosome instability and reduced survival of patients with pancreatic neuroendocrine tumors. *Gastroenterology, 146*(2), 453-460 e455.

Martin, J. W., Zielenska, M., Stein, G. S., van Wijnen, A. J., & Squire, J. A. (2011). The Role of RUNX2 in Osteosarcoma Oncogenesis. *Sarcoma, 2011*, 282745.

Massague, J., Seoane, J., & Wotton, D. (2005). Smad transcription factors. *Genes Dev, 19*(23), 2783-2810.

McAllister, R. M., Gardner, M. B., Greene, A. E., Bradt, C., Nichols, W. W., & Landing, B. H. (1971). Cultivation in vitro of cells derived from a human osteosarcoma. *Cancer, 27*(2), 397-402.

McGinnis, W. (1994). A century of homeosis, a decade of homeoboxes. *Genetics, 137*(3), 607-611.

McGinnis, W., & Krumlauf, R. (1992). Homeobox genes and axial patterning. *Cell, 68*(2), 283-302.

McGinnis, W., Levine, M. S., Hafen, E., Kuroiwa, A., & Gehring, W. J. (1984). A conserved DNA sequence in homoeotic genes of the Drosophila Antennapedia and bithorax complexes. *Nature, 308*(5958), 428-433.

McKie, J., & Radomisli, T. (2010). Congenital vertical talus: a review. *Clin Podiatr Med Surg, 27*(1), 145-156.

McManus, A. P., Gusterson, B. A., Pinkerton, C. R., & Shipley, J. M. (1996). The molecular pathology of small round-cell tumours--relevance to diagnosis, prognosis, and classification. *J Pathol, 178*(2), 116-121.

Merrill, R. A., Ahrens, J. M., Kaiser, M. E., Federhart, K. S., Poon, V. Y., & Clagett-Dame, M. (2004). All-trans retinoic acid-responsive genes identified in the human SH-SY5Y neuroblastoma cell line and their regulated expression in the nervous system of early embryos. *Biol Chem, 385*(7), 605-614.

Misra, M., Shah, V., Carpenter, E., McCaffery, P., & Lance-Jones, C. (2009). Restricted patterns of Hoxd10 and Hoxd11 set segmental differences in motoneuron subtype complement in the lumbosacral spinal cord. *Dev Biol, 330*(1), 54-72.

Miyamoto, K., Fukutomi, T., Akashi-Tanaka, S., Hasegawa, T., Asahara, T., Sugimura, T., & Ushijima, T. (2005). Identification of 20 genes aberrantly methylated in human breast cancers. *Int J Cancer, 116*(3), 407-414.

Miyazono, K., Kamiya, Y., & Morikawa, M. (2010). Bone morphogenetic protein receptors and signal transduction. *J Biochem, 147*(1), 35-51.

Miyazono, K., Maeda, S., & Imamura, T. (2005). BMP receptor signaling: transcriptional targets, regulation of signals, and signaling cross-talk. *Cytokine Growth Factor Rev, 16*(3), 251-263.

Montavon, T., & Soshnikova, N. (2014). Hox gene regulation and timing in embryogenesis. *Seminars in Cell & Developmental Biology, 34*, 76-84.

Moosmann, S., Hutter, J., Moser, C., Krombach, F., & Huss, R. (2005). Milieu-Adopted in vitro and in vivo Differentiation of Mesenchymal Tissues Derived from Different Adult Human CD34-Negative Progenitor Cell Clones. *Cells Tissues Organs, 179*(3), 91-101.

Morales, J., Cormier, P., Mulner-Lorillon, O., Poulhe, R., & Belle, R. (1992). Molecular cloning of a new guanine nucleotide-exchange protein, EF1 delta. *Nucleic Acids Res, 20*(15), 4091.

Morgan, R., Plowright, L., Harrington, K. J., Michael, A., & Pandha, H. S. (2010). Targeting HOX and PBX transcription factors in ovarian cancer. *BMC Cancer, 10*, 89.

Mori, S., Chang, J. T., Andrechek, E. R., Matsumura, N., Baba, T., Yao, G., Kim, J. W., Gatza, M., Murphy, S., & Nevins, J. R. (2009). Anchorage-independent cell growth signature identifies tumors with metastatic potential. *Oncogene, 28*(31), 2796-2805.

Mugford, J. W., Sipila, P., Kobayashi, A., Behringer, R. R., & McMahon, A. P. (2008). Hoxd11 specifies a program of metanephric kidney development within the intermediate mesoderm of the mouse embryo. *Dev Biol, 319*(2), 396-405.

Muller, M., Affolter, M., Leupin, W., Otting, G., Wuthrich, K., & Gehring, W. J. (1988). Isolation and sequence-specific DNA binding of the Antennapedia homeodomain. *EMBO J, 7*(13), 4299-4304.

Mundlos, S., Otto, F., Mundlos, C., Mulliken, J. B., Aylsworth, A. S., Albright, S., Lindhout, D., Cole, W. G., Henn, W., Knoll, J. H., Owen, M. J., Mertelsmann, R., Zabel, B. U., & Olsen, B. R. (1997). Mutations involving the transcription factor CBFA1 cause cleidocranial dysplasia. *Cell, 89*(5), 773-779.

Mundy, G. R. (2002). Metastasis to bone: causes, consequences and therapeutic opportunities. *Nat Rev Cancer, 2*(8), 584-593.

Muragaki, Y., Mundlos, S., Upton, J., & Olsen, B. R. (1996). Altered growth and branching patterns in synpolydactyly caused by mutations in HOXD13. *Science, 272*(5261), 548-551.

Myers, C., Charboneau, A., Cheung, I., Hanks, D., & Boudreau, N. (2002). Sustained expression of homeobox D10 inhibits angiogenesis. *Am J Pathol, 161*(6), 2099-2109.

Nagaraja, G. M., Othman, M., Fox, B. P., Alsaber, R., Pellegrino, C. M., Zeng, Y., Khanna, R., Tamburini, P., Swaroop, A., & Kandpal, R. P. (2006). Gene expression signatures and biomarkers of noninvasive and invasive breast cancer cells: comprehensive profiles by representational difference analysis, microarrays and proteomics. *Oncogene, 25*(16), 2328-2338.

Nakayama, I., Shibazaki, M., Yashima-Abo, A., Miura, F., Sugiyama, T., Masuda, T., & Maesawa, C. (2013). Loss of HOXD10 expression induced by upregulation of miR-10b accelerates the migration and invasion activities of ovarian cancer cells. *Int J Oncol, 43*(1), 63-71.

Nelson, C. E., Morgan, B. A., Burke, A. C., Laufer, E., DiMambro, E., Murtaugh, L. C., Gonzales, E., Tessarollo, L., Parada, L. F., & Tabin, C. (1996). Analysis of Hox gene expression in the chick limb bud. *Development, 122*(5), 1449-1466.

Niemeyer, C., & Rössler, J. (2013). Krebserkrankungen. In B. Koletzko (Ed.), *Kinder- und Jugendmedizin* (Vol. 14. Auflage, pp. 315-318). Berlin, Heidelberg: Springer-Verlag.

Nifuji, A., Kellermann, O., & Noda, M. (2004). Noggin inhibits chondrogenic but not osteogenic differentiation in mesodermal stem cell line C1 and skeletal cells. *Endocrinology, 145*(7), 3434-3442.

Ogawa, K., Utsunomiya, T., Mimori, K., Tanaka, Y., Tanaka, F., Inoue, H., Murayama, S., & Mori, M. (2004). Clinical significance of elongation factor-1 delta mRNA expression in oesophageal carcinoma. *Br J Cancer, 91*(2), 282-286.

Osborne, J., Hu, C., Hawley, C., Underwood, L. J., O'Brien, T. J., & Baker, V. V. (1998). Expression of HOXD10 gene in normal endometrium and endometrial adenocarcinoma. *J Soc Gynecol Investig, 5*(5), 277-280.

Otting, G., Qian, Y. Q., Muller, M., Affolter, M., Gehring, W., & Wuthrich, K. (1988). Secondary structure determination for the Antennapedia homeodomain by nuclear magnetic resonance and evidence for a helix-turn-helix motif. *EMBO J, 7*(13), 4305-4309.

Otto, F., Thornell, A. P., Crompton, T., Denzel, A., Gilmour, K. C., Rosewell, I. R., Stamp, G. W., Beddington, R. S., Mundlos, S., Olsen, B. R., Selby, P. B., & Owen, M. J. (1997). Cbfa1, a candidate gene for cleidocranial dysplasia syndrome, is essential for osteoblast differentiation and bone development. *Cell, 89*(5), 765-771.

Pareyson, D. (1999). Charcot-marie-tooth disease and related neuropathies: molecular basis for distinction and diagnosis. *Muscle Nerve, 22*(11), 1498-1509.

Patterson, L. T., Pembaur, M., & Potter, S. S. (2001). Hoxa11 and Hoxd11 regulate branching morphogenesis of the ureteric bud in the developing kidney. *Development, 128*(11), 2153-2161.

Pearson, J. C., Lemons, D., & McGinnis, W. (2005). Modulating Hox gene functions during animal body patterning. *Nature Reviews Genetics, 6*(12), 893-904.

Phimphilai, M., Zhao, Z., Boules, H., Roca, H., & Franceschi, R. T. (2006). BMP signaling is required for RUNX2-dependent induction of the osteoblast phenotype. *J Bone Miner Res, 21*(4), 637-646.

Picketts, D. J., Higgs, D. R., Bachoo, S., Blake, D. J., Quarrell, O. W., & Gibbons, R. J. (1996). ATRX encodes a novel member of the SNF2 family of proteins: mutations point to a common mechanism underlying the ATR-X syndrome. *Hum Mol Genet, 5*(12), 1899-1907.

Picketts, D. J., Tastan, A. O., Higgs, D. R., & Gibbons, R. J. (1998). Comparison of the human and murine ATRX gene identifies highly conserved, functionally important domains. *Mamm Genome, 9*(5), 400-403.

Pietsch, T., Göttert, E., Feickert, H. J., Riehm, H., Blin, N., & Kovacs, G. (1989). MHH-ES-1, A new Ewing sarcoma cell line. *Cancer Genetics and Cytogenetics, 38*(2), 167.

Pizette, S., & Niswander, L. (2000). BMPs are required at two steps of limb chondrogenesis: formation of prechondrogenic condensations and their differentiation into chondrocytes. *Dev Biol, 219*(2), 237-249.

Ponten, J., & Saksela, E. (1967). Two established in vitro cell lines from human mesenchymal tumours. *Int J Cancer, 2*(5), 434-447.

Popperl, H., & Featherstone, M. S. (1992). An autoregulatory element of the murine Hox-4.2 gene. *EMBO J, 11*(10), 3673-3680.

Post, L. C., & Innis, J. W. (1999). Altered Hox expression and increased cell death distinguish Hypodactyly from Hoxa13 null mice. *Int J Dev Biol, 43*(4), 287-294.

Potratz, J., Dirksen, U., Jurgens, H., & Craft, A. (2012). Ewing sarcoma: clinical state-of-the-art. *Pediatric Hematology and Oncology, 29*(1), 1-11.

Power, S. C., Lancman, J., & Smith, S. M. (1999). Retinoic acid is essential for Shh/Hoxd signaling during rat limb outgrowth but not for limb initiation. *Dev Dyn, 216*(4-5), 469-480.

Puthiyaveetil, A. G., Reilly, C. M., Pardee, T. S., & Caudell, D. L. (2013). Non-homologous end joining mediated DNA repair is impaired in the NUP98-HOXD13 mouse model for myelodysplastic syndrome. *Leuk Res, 37*(1), 112-116.

Qadeer, Z. A., Harcharik, S., Valle-Garcia, D., Chen, C., Birge, M. B., Vardabasso, C., Duarte, L. F., & Bernstein, E. (2014). Decreased expression of the chromatin remodeler ATRX associates with melanoma progression. *J Invest Dermatol, 134*(6), 1768-1772.

Raza-Egilmez, S. Z., Jani-Sait, S. N., Grossi, M., Higgins, M. J., Shows, T. B., & Aplan, P. D. (1998). NUP98-HOXD13 gene fusion in therapy-related acute myelogenous leukemia. *Cancer Res, 58*(19), 4269-4273.

Reddi, A. H., & Anderson, W. A. (1976). Collagenous bone matrix-induced endochondral ossification hemopoiesis. *J Cell Biol, 69*(3), 557-572.

Reddy, S. D., Ohshiro, K., Rayala, S. K., & Kumar, R. (2008). MicroRNA-7, a homeobox D10 target, inhibits p21-activated kinase 1 and regulates its functions. *Cancer Res, 68*(20), 8195-8200.

Redline, R. W., Hudock, P., MacFee, M., & Patterson, P. (1994). Expression of AbdB-type homeobox genes in human tumors. *Lab Invest, 71*(5), 663-670.

Richter, G. H., Fasan, A., Hauer, K., Grunewald, T. G., Berns, C., Rossler, S., Naumann, I., Staege, M. S., Fulda, S., Esposito, I., & Burdach, S. (2013). G-Protein coupled receptor 64 promotes invasiveness and metastasis in Ewing sarcomas through PGF and MMP1. *J Pathol, 230*(1), 70-81.

Richter, G. H., Plehm, S., Fasan, A., Rossler, S., Unland, R., Bennani-Baiti, I. M., Hotfilder, M., Lowel, D., von Luettichau, I., Mossbrugger, I., Quintanilla-Martinez, L., Kovar, H., Staege, M. S., Muller-Tidow, C., & Burdach, S. (2009). EZH2 is a mediator of EWS/FLI1 driven tumor growth and metastasis blocking endothelial and neuro-ectodermal differentiation. *Proc Natl Acad Sci U S A, 106*(13), 5324-5329.

Riggi, N., Cironi, L., Provero, P., Suva, M. L., Kaloulis, K., Garcia-Echeverria, C., Hoffmann, F., Trumpp, A., & Stamenkovic, I. (2005). Development of Ewing's sarcoma from primary bone marrow-derived mesenchymal progenitor cells. *Cancer Res, 65*(24), 11459-11468.

Rinn, J. L., Kertesz, M., Wang, J. K., Squazzo, S. L., Xu, X., Brugmann, S. A., Goodnough, L. H., Helms, J. A., Farnham, P. J., Segal, E., & Chang, H. Y. (2007). Functional demarcation of active and silent chromatin domains in human HOX loci by noncoding RNAs. *Cell, 129*(7), 1311-1323.

Ritchie, K., Seah, C., Moulin, J., Isaac, C., Dick, F., & Berube, N. G. (2008). Loss of ATRX leads to chromosome cohesion and congression defects. *J Cell Biol, 180*(2), 315-324.

Roberts, A. W., Kim, C., Zhen, L., Lowe, J. B., Kapur, R., Petryniak, B., Spaetti, A., Pollock, J. D., Borneo, J. B., Bradford, G. B., Atkinson, S. J., Dinauer, M. C., & Williams, D. A. (1999). Deficiency of the hematopoietic cell-specific Rho family GTPase Rac2 is characterized by abnormalities in neutrophil function and host defense. *Immunity, 10*(2), 183-196.

Roberts, I., Wienberg, J., Nacheva, E., Grace, C., Griffin, D., & Coleman, N. (1999). Novel method for the production of multiple colour chromosome paints for use in karyotyping by fluorescence in situ hybridisation. *Genes Chromosomes Cancer, 25*(3), 241-250.

Rodini, C. O., Xavier, F. C., Paiva, K. B., De Souza Setubal Destro, M. F., Moyses, R. A., Michaluarte, P., Carvalho, M. B., Fukuyama, E. E., Tajara, E. H., Okamoto, O. K., & Nunes, F. D. (2012). Homeobox gene expression profile indicates HOXA5 as a candidate prognostic marker in oral squamous cell carcinoma. *Int J Oncol, 40*(4), 1180-1188.

Rorie, C. J., Thomas, V. D., Chen, P., Pierce, H. H., O'Bryan, J. P., & Weissman, B. E. (2004). The Ews/Fli-1 fusion gene switches the differentiation program of neuroblastomas to Ewing sarcoma/peripheral primitive neuroectodermal tumors. *Cancer Res, 64*(4), 1266-1277.

Rossi Degl'Innocenti, D., Castiglione, F., Buccoliero, A. M., Bechi, P., Taddei, G. L., Freschi, G., & Taddei, A. (2007). Quantitative expression of the homeobox and integrin genes in human gastric carcinoma. *Int J Mol Med, 20*(4), 621-629.

Sadikovic, B., Thorner, P., Chilton-Macneill, S., Martin, J. W., Cervigne, N. K., Squire, J., & Zielenska, M. (2010). Expression analysis of genes associated with human osteosarcoma tumors shows correlation of RUNX2 overexpression with poor response to chemotherapy. *BMC Cancer, 10*, 202.

Salsi, V., Ferrari, S., Gorello, P., Fantini, S., Chiavolelli, F., Mecucci, C., & Zappavigna, V. (2014). NUP98 fusion oncoproteins promote aneuploidy by attenuating the mitotic spindle checkpoint. *Cancer Res, 74*(4), 1079-1090.

Salsi, V., Vigano, M. A., Cocchiarella, F., Mantovani, R., & Zappavigna, V. (2008). Hoxd13 binds in vivo and regulates the expression of genes acting in key pathways for early limb and skeletal patterning. *Dev Biol, 317*(2), 497-507.

Sankar, S., & Lessnick, S. L. (2011). Promiscuous partnerships in Ewing's sarcoma. *Cancer Genet, 204*(7), 351-365.

Sarma, K., Cifuentes-Rojas, C., Ergun, A., Del Rosario, A., Jeon, Y., White, F., Sadreyev, R., & Lee, J. T. (2014). ATRX directs binding of PRC2 to Xist RNA and Polycomb targets. *Cell, 159*(4), 869-883.

Schirmer, D., Grunewald, T. G., Klar, R., Schmidt, O., Wohlleber, D., Rubio, R. A., Uckert, W., Thiel, U., Bohne, F., Busch, D. H., Krackhardt, A. M., Burdach, S., & Richter, G. H. (2016). Transgenic antigen-specific, HLA-A*02:01-allo-restricted cytotoxic T cells recognize tumor-associated target antigen STEAP1 with high specificity. *Oncoimmunology, 5*(6), e1175795.

Scott, M. P. (1992). Vertebrate homeobox gene nomenclature. *Cell, 71*(4), 551-553.

Seifert, A., Werheid, D. F., Knapp, S. M., & Tobiasch, E. (2015). Role of Hox genes in stem cell differentiation. *World J Stem Cells, 7*(3), 583-595.

Sekar, P., Bharti, J. N., Nigam, J. S., Sharma, A., & Soni, P. B. (2014). Evaluation of p53, HoxD10, and E-Cadherin Status in Breast Cancer and Correlation with Histological Grade and Other Prognostic Factors. *J Oncol, 2014*, 702527.

Shah, N., Jin, K., Cruz, L. A., Park, S., Sadik, H., Cho, S., Goswami, C. P., Nakshatri, H., Gupta, R., Chang, H. Y., Zhang, Z., Cimino-Mathews, A., Cope, L., Umbricht, C., & Sukumar, S. (2013). HOXB13 mediates tamoxifen resistance and invasiveness in human breast cancer by suppressing ERalpha and inducing IL-6 expression. *Cancer Res, 73*(17), 5449-5458.

Shah, N., & Sukumar, S. (2010). The Hox genes and their roles in oncogenesis. *Nat Rev Cancer, 10*(5), 361-371.

Shah, V., Drill, E., & Lance-Jones, C. (2004). Ectopic expression of Hoxd10 in thoracic spinal segments induces motoneurons with a lumbosacral molecular profile and axon projections to the limb. *Dev Dyn, 231*(1), 43-56.

Sharpe, D. J., Orr, K. S., Moran, M., White, S. J., McQuaid, S., Lappin, T. R., Thompson, A., & James, J. A. (2014). POU2F1 activity regulates HOXD10 and HOXD11 promoting a proliferative and invasive phenotype in head and neck cancer. *Oncotarget, 5*(18), 8803-8815.

Shepherd, J. C., McGinnis, W., Carrasco, A. E., De Robertis, E. M., & Gehring, W. J. (1984). Fly and frog homoeo domains show homologies with yeast mating type regulatory proteins. *Nature, 310*(5972), 70-71.

Sheth, R., Bastida, M. F., Kmita, M., & Ros, M. (2014). "Self-regulation," a new facet of Hox genes' function. *Dev Dyn, 243*(1), 182-191.

Shi, X., Yang, X., Chen, D., Chang, Z., & Cao, X. (1999). Smad1 interacts with homeobox DNA-binding proteins in bone morphogenetic protein signaling. *J Biol Chem, 274*(19), 13711-13717.

Shi, Y., & Massague, J. (2003). Mechanisms of TGF-beta signaling from cell membrane to the nucleus. *Cell, 113*(6), 685-700.

Shinawi, T., Hill, V. K., Krex, D., Schackert, G., Gentle, D., Morris, M. R., Wei, W., Cruickshank, G., Maher, E. R., & Latif, F. (2013). DNA methylation profiles of long- and short-term glioblastoma survivors. *Epigenetics, 8*(2), 149-156.

Shrimpton, A. E., Levinsohn, E. M., Yozawitz, J. M., Packard, D. S., Jr., Cady, R. B., Middleton, F. A., Persico, A. M., & Hootnick, D. R. (2004). A HOX gene mutation in a family with isolated congenital vertical talus and Charcot-Marie-Tooth disease. *Am J Hum Genet, 75*(1), 92-96.

Shu, B., Zhang, M., Xie, R., Wang, M., Jin, H., Hou, W., Tang, D., Harris, S. E., Mishina, Y., O'Keefe, R. J., Hilton, M. J., Wang, Y., & Chen, D. (2011). BMP2, but not BMP4, is crucial for chondrocyte proliferation and maturation during endochondral bone development. *J Cell Sci, 124*(Pt 20), 3428-3440.

Shu, Y., Wang, B., Wang, J., Wang, J. M., & Zou, S. Q. (2011). Identification of methylation profile of HOX genes in extrahepatic cholangiocarcinoma. *World J Gastroenterol, 17*(29), 3407-3419.

Simeone, A., Acampora, D., Arcioni, L., Andrews, P. W., Boncinelli, E., & Mavilio, F. (1990). Sequential activation of HOX2 homeobox genes by retinoic acid in human embryonal carcinoma cells. *Nature, 346*(6286), 763-766.

Slape, C., Chung, Y. J., Soloway, P. D., Tessarollo, L., & Aplan, P. D. (2007). Mouse embryonic stem cells that express a NUP98-HOXD13 fusion protein are impaired in their ability to differentiate and can be complemented by BCR-ABL. *Leukemia, 21*(6), 1239-1248.

Slape, C., Lin, Y. W., Hartung, H., Zhang, Z., Wolff, L., & Aplan, P. D. (2008). NUP98-HOX translocations lead to myelodysplastic syndrome in mice and men. *J Natl Cancer Inst Monogr*(39), 64-68.

Smits, P., Li, P., Mandel, J., Zhang, Z., Deng, J. M., Behringer, R. R., de Crombrugghe, B., & Lefebvre, V. (2001). The transcription factors L-Sox5 and Sox6 are essential for cartilage formation. *Dev Cell, 1*(2), 277-290.

Solomon, L. A., Li, J. R., Berube, N. G., & Beier, F. (2009). Loss of ATRX in chondrocytes has minimal effects on skeletal development. *PLoS One, 4*(9), e7106.

Solomon, L. A., Russell, B. A., Watson, L. A., Beier, F., & Berube, N. G. (2013). Targeted loss of the ATR-X syndrome protein in the limb mesenchyme of mice causes brachydactyly. *Hum Mol Genet, 22*(24), 5015-5025.

Spilka, R., Ernst, C., Mehta, A. K., & Haybaeck, J. (2013). Eukaryotic translation initiation factors in cancer development and progression. *Cancer Letters, 340*(1), 9-21.

Spitz, F., Gonzalez, F., Peichel, C., Vogt, T. F., Duboule, D., & Zakany, J. (2001). Large scale transgenic and cluster deletion analysis of the HoxD complex separate an ancestral regulatory module from evolutionary innovations. *Genes Dev, 15*(17), 2209-2214.

Staege, M. S., Hutter, C., Neumann, I., Foja, S., Hattenhorst, U. E., Hansen, G., Afar, D., & Burdach, S. E. (2004). DNA microarrays reveal relationship of Ewing family tumors to both endothelial and fetal neural crest-derived cells and define novel targets. *Cancer Res, 64*(22), 8213-8221.

Sturn, A., Quackenbush, J., & Trajanoski, Z. (2002). Genesis: cluster analysis of microarray data. *Bioinformatics, 18*(1), 207-208.

Subramanian, A., Tamayo, P., Mootha, V. K., Mukherjee, S., Ebert, B. L., Gillette, M. A., Paulovich, A., Pomeroy, S. L., Golub, T. R., Lander, E. S., & Mesirov, J. P. (2005). Gene set enrichment analysis: a knowledge-based approach for interpreting genome-wide expression profiles. *Proc Natl Acad Sci U S A, 102*(43), 15545-15550.

Sun, L., Yan, W., Wang, Y., Sun, G., Luo, H., Zhang, J., Wang, X., You, Y., Yang, Z., & Liu, N. (2011). MicroRNA-10b induces glioma cell invasion by modulating MMP-14 and uPAR expression via HOXD10. *Brain Res, 1389*, 9-18.

Sun, S.-S., Zhang, L., Yang, J., & Zhou, X. (2015). Role of runt-related transcription factor 2 in signal network of tumors as an inter-mediator. *Cancer Letters, 361*(1), 1-7.

Suzuki, M., Ueno, N., & Kuroiwa, A. (2003). Hox proteins functionally cooperate with the GC box-binding protein system through distinct domains. *J Biol Chem, 278*(32), 30148-30156.

Svoboda, L. K., Harris, A., Bailey, N. J., Schwentner, R., Tomazou, E., von Levetzow, C., Magnuson, B., Ljungman, M., Kovar, H., & Lawlor, E. R. (2014). Overexpression of HOX genes is prevalent in Ewing sarcoma and is associated with altered epigenetic regulation of developmental transcription programs. *Epigenetics, 9*(12), 1613-1625.

Taketani, T., Taki, T., Shibuya, N., Ito, E., Kitazawa, J., Terui, K., & Hayashi, Y. (2002). The HOXD11 gene is fused to the NUP98 gene in acute myeloid leukemia with t(2;11)(q31;p15). *Cancer Res, 62*(1), 33-37.

Tan, X., Weng, T., Zhang, J., Wang, J., Li, W., Wan, H., Lan, Y., Cheng, X., Hou, N., Liu, H., Ding, J., Lin, F., Yang, R., Gao, X., Chen, D., & Yang, X. (2007). Smad4 is required for maintaining normal murine postnatal bone homeostasis. *J Cell Sci, 120*(Pt 13), 2162-2170.

Tasca, A., Stemig, M., Broege, A., Huang, B., Davydova, J., Zwijsen, A., Umans, L., Jensen, E. D., Gopalakrishnan, R., & Mansky, K. C. (2015). Smad 1/5 and Smad 4 Expression Are Important for Osteoclast Differentiation. *J Cell Biochem*.

Tatsuka, M., Mitsui, H., Wada, M., Nagata, A., Nojima, H., & Okayama, H. (1992). Elongation factor-1 alpha gene determines susceptibility to transformation. *Nature, 359*(6393), 333-336.

Thalmeier, K., Meissner, P., Reisbach, G., Falk, M., Brechtel, A., & Dormer, P. (1994). Establishment of two permanent human bone marrow stromal cell lines with long-term post irradiation feeder capacity. *Blood, 83*(7), 1799-1807.

Thiel, U., Pirson, S., Muller-Spahn, C., Conrad, H., Busch, D. H., Bernhard, H., Burdach, S., & Richter, G. H. (2011). Specific recognition and inhibition of Ewing tumour growth by antigen-specific allo-restricted cytotoxic T cells. *Br J Cancer, 104*(6), 948-956.

Thornton, S., Anand, N., Purcell, D., & Lee, J. (2003). Not just for housekeeping: protein initiation and elongation factors in cell growth and tumorigenesis. *J Mol Med (Berl), 81*(9), 536-548.

Tirode, F., Laud-Duval, K., Prieur, A., Delorme, B., Charbord, P., & Delattre, O. (2007). Mesenchymal stem cell features of Ewing tumors. *Cancer Cell, 11*(5), 421-429.

Topisirovic, I., Kentsis, A., Perez, J. M., Guzman, M. L., Jordan, C. T., & Borden, K. L. (2005). Eukaryotic translation initiation factor 4E activity is modulated by HOXA9 at multiple levels. *Mol Cell Biol, 25*(3), 1100-1112.

Tsai, C. A., Chen, Y. J., & Chen, J. J. (2003). Testing for differentially expressed genes with microarray data. *Nucleic Acids Res, 31*(9), e52.

Tschopp, P., & Duboule, D. (2011). A regulatory 'landscape effect' over the HoxD cluster. *Dev Biol, 351*(2), 288-296.

Tsumaki, N., & Yoshikawa, H. (2005). The role of bone morphogenetic proteins in endochondral bone formation. *Cytokine Growth Factor Rev, 16*(3), 279-285.

Turc-Carel, C., Philip, I., Berger, M. P., Philip, T., & Lenoir, G. M. (1984). Chromosome study of Ewing's sarcoma (ES) cell lines. Consistency of a reciprocal translocation t(11;22)(q24;q12). *Cancer Genetics and Cytogenetics, 12*(1), 1-19.

Tusher, V. G., Tibshirani, R., & Chu, G. (2001). Significance analysis of microarrays applied to the ionizing radiation response. *Proc Natl Acad Sci U S A, 98*(9), 5116-5121.

Tuzel, E., Samli, H., Kuru, I., Turkmen, S., Demir, Y., Maralcan, G., & Guler, C. (2007). Association of hypospadias with hypoplastic synpolydactyly and role of HOXD13 gene mutations. *Urology, 70*(1), 161-164.

Urist, M. R., & Strates, B. S. (2009). The classic: Bone morphogenetic protein. *Clin Orthop Relat Res, 467*(12), 3051-3062.

van der Hoeven, F., Zakany, J., & Duboule, D. (1996). Gene transpositions in the HoxD complex reveal a hierarchy of regulatory controls. *Cell, 85*(7), 1025-1035.

VanGuilder, H. D., Vrana, K. E., & Freeman, W. M. (2008). Twenty-five years of quantitative PCR for gene expression analysis. *Biotechniques, 44*(5), 619-626.

Vardhini, N. V., Rao, P. J., Murthy, P. B., & Sudhakar, G. (2014). HOXD10 expression in human breast cancer. *Tumour Biol, 35*(11), 10855-10860.

Villavicencio-Lorini, P., Kuss, P., Friedrich, J., Haupt, J., Farooq, M., Turkmen, S., Duboule, D., Hecht, J., & Mundlos, S. (2010). Homeobox genes d11-d13 and a13 control mouse autopod cortical bone and joint formation. *J Clin Invest, 120*(6), 1994-2004.

Volk, S. W., Luvalle, P., Leask, T., & Leboy, P. S. (1998). A BMP responsive transcriptional region in the chicken type X collagen gene. *J Bone Miner Res, 13*(10), 1521-1529.

von Heyking, K., Roth, L., Ertl, M., Schmidt, O., Calzada-Wack, J., Neff, F., Lawlor, E. R., Burdach, S., & Richter, G. H. (2016). The posterior HOXD locus: Its contribution to phenotype and malignancy of Ewing sarcoma. *Oncotarget, 7(27)*, 41767-41780.

Wacker, S. A., McNulty, C. L., & Durston, A. J. (2004). The initiation of Hox gene expression in Xenopus laevis is controlled by Brachyury and BMP-4. *Dev Biol, 266*(1), 123-137.

Wai, P. Y., & Kuo, P. C. (2008). Osteopontin: regulation in tumor metastasis. *Cancer Metastasis Rev, 27*(1), 103-118.

Wang, L., Chen, S., Xue, M., Zhong, J., Wang, X., Gan, L., Lam, E. K., Liu, X., Zhang, J., Zhou, T., Yu, J., Jin, H., & Si, J. (2012). Homeobox D10 gene, a candidate tumor suppressor, is downregulated through promoter hypermethylation and associated with gastric carcinogenesis. *Mol Med, 18*, 389-400.

Wang, L. L., Fu, W. N., Li-Ling, J., Li, Z. G., Li, L. Y., & Sun, K. L. (2008). HOXD13 may play a role in idiopathic congenital clubfoot by regulating the expression of FHL1. *Cytogenet Genome Res, 121*(3-4), 189-195.

Wang, Y., Lebowitz, D., Sun, C., Thang, H., Grynpas, M. D., & Glogauer, M. (2008). Identifying the relative contributions of Rac1 and Rac2 to osteoclastogenesis. *J Bone Miner Res, 23*(2), 260-270.

Wang, Y. F., Li, Z., Zhao, X. H., Zuo, X. M., Zhang, Y., Xiao, Y. H., Li, J., & Peng, Z. H. (2015). MicroRNA-10b is upregulated and has an invasive role in colorectal cancer through enhanced Rhoc expression. *Oncol Rep, 33*(3), 1275-1283.

Warot, X., Fromental-Ramain, C., Fraulob, V., Chambon, P., & Dolle, P. (1997). Gene dosage-dependent effects of the Hoxa-13 and Hoxd-13 mutations on morphogenesis of the terminal parts of the digestive and urogenital tracts. *Development, 124*(23), 4781-4791.

Warren, S. T. (1997). Polyalanine expansion in synpolydactyly might result from unequal crossing-over of HOXD13. *Science, 275*(5298), 408-409.

Watson, L. A., Solomon, L. A., Li, J. R., Jiang, Y., Edwards, M., Shin-ya, K., Beier, F., & Berube, N. G. (2013). Atrx deficiency induces telomere dysfunction, endocrine defects, and reduced life span. *J Clin Invest, 123*(5), 2049-2063.

Wellik, D. M., Hawkes, P. J., & Capecchi, M. R. (2002). Hox11 paralogous genes are essential for metanephric kidney induction. *Genes Dev, 16*(11), 1423-1432.

Whang-Peng, J., Triche, T. J., Knutsen, T., Miser, J., Kao-Shan, S., Tsai, S., & Israel, M. A. (1986). Cytogenetic characterization of selected small round cell tumors of childhood. *Cancer Genetics and Cytogenetics, 21*(3), 185-208.

Williams, T. M., Williams, M. E., Heaton, J. H., Gelehrter, T. D., & Innis, J. W. (2005). Group 13 HOX proteins interact with the MH2 domain of R-Smads and modulate Smad transcriptional activation functions independent of HOX DNA-binding capability. *Nucleic Acids Res, 33*(14), 4475-4484.

Winnier, G., Blessing, M., Labosky, P. A., & Hogan, B. L. (1995). Bone morphogenetic protein-4 is required for mesoderm formation and patterning in the mouse. *Genes Dev, 9*(17), 2105-2116.

Wong, L. H., McGhie, J. D., Sim, M., Anderson, M. A., Ahn, S., Hannan, R. D., George, A. J., Morgan, K. A., Mann, J. R., & Choo, K. H. (2010). ATRX interacts with H3.3 in maintaining telomere structural integrity in pluripotent embryonic stem cells. *Genome Res, 20*(3), 351-360.

Worch, J., Matthay, K. K., Neuhaus, J., Goldsby, R., & DuBois, S. G. (2010). Ethnic and racial differences in patients with Ewing sarcoma. *Cancer, 116*(4), 983-988.

Wuelling, M., & Vortkamp, A. (2011). Chondrocyte proliferation and differentiation. *Endocrine Development, 21*, 1-11.

Xia, X., Wu, W., Huang, C., Cen, G., Jiang, T., Cao, J., Huang, K., & Qiu, Z. (2015). SMAD4 and its role in pancreatic cancer. *Tumour Biol, 36*(1), 111-119.

Xiao, H., Li, H., Yu, G., Xiao, W., Hu, J., Tang, K., Zeng, J., He, W., Zeng, G., Ye, Z., & Xu, H. (2014). MicroRNA-10b promotes migration and invasion through KLF4 and HOXD10 in human bladder cancer. *Oncol Rep, 31*(4), 1832-1838.

Xu, B., Geerts, D., Bu, Z., Ai, J., Jin, L., Li, Y., Zhang, H., & Zhu, G. (2014). Regulation of endometrial receptivity by the highly expressed HOXA9, HOXA11 and HOXD10 HOX-class homeobox genes. *Hum Reprod, 29*(4), 781-790.

Xue, M., Fang, Y., Sun, G., Zhuo, W., Zhong, J., Qian, C., Wang, L., Wang, L., Si, J., & Chen, S. (2013). IGFBP3, a transcriptional target of homeobox D10, is correlated with the prognosis of gastric cancer. *PLoS One, 8*(12), e81423.

Yamashita, T., Tazawa, S., Yawei, Z., Katayama, H., Kato, Y., Nishiwaki, K., Yokohama, Y., & Ishikawa, M. (2006). Suppression of invasive characteristics by antisense introduction of overexpressed HOX genes in ovarian cancer cells. *Int J Oncol, 28*(4), 931-938.

Yang, L., Tsang, K. Y., Tang, H. C., Chan, D., & Cheah, K. S. (2014). Hypertrophic chondrocytes can become osteoblasts and osteocytes in endochondral bone formation. *Proc Natl Acad Sci U S A, 111*(33), 12097-12102.

Ye, L., Bokobza, S. M., & Jiang, W. G. (2009). Bone morphogenetic proteins in development and progression of breast cancer and therapeutic potential (review). *Int J Mol Med, 24*(5), 591-597.

Ye, L., Lewis-Russell, J. M., Kyanaston, H. G., & Jiang, W. G. (2007). Bone morphogenetic proteins and their receptor signaling in prostate cancer. *Histology and Histopathology, 22*(10), 1129-1147.

Yekta, S., Tabin, C. J., & Bartel, D. P. (2008). MicroRNAs in the Hox network: an apparent link to posterior prevalence. *Nature Reviews Genetics, 9*(10), 789-796.

Yu, X., Li, Z., Shen, J., Wu, W. K., Liang, J., Weng, X., & Qiu, G. (2013). MicroRNA-10b promotes nucleus pulposus cell proliferation through RhoC-Akt pathway by targeting HOXD10 in intervetebral disc degeneration. *PLoS One, 8*(12), e83080.

Zakany, J., & Duboule, D. (1996). Synpolydactyly in mice with a targeted deficiency in the HoxD complex. *Nature, 384*(6604), 69-71.

Zakany, J., & Duboule, D. (1999). Hox genes in digit development and evolution. *Cell Tissue Res, 296*(1), 19-25.

Zakany, J., & Duboule, D. (2007). The role of Hox genes during vertebrate limb development. *Curr Opin Genet Dev, 17*(4), 359-366.

Zakany, J., Gerard, M., Favier, B., & Duboule, D. (1997). Deletion of a HoxD enhancer induces transcriptional heterochrony leading to transposition of the sacrum. *EMBO J, 16*(14), 4393-4402.

Zakany, J., Gerard, M., Favier, B., Potter, S. S., & Duboule, D. (1996). Functional equivalence and rescue among group 11 Hox gene products in vertebral patterning. *Dev Biol, 176*(2), 325-328.

Zakany, J., Kmita, M., & Duboule, D. (2004). A dual role for Hox genes in limb anterior-posterior asymmetry. *Science, 304*(5677), 1669-1672.

Zeltser, L., Desplan, C., & Heintz, N. (1996). Hoxb-13: a new Hox gene in a distant region of the HOXB cluster maintains colinearity. *Development, 122*(8), 2475-2484.

Zeng, H., & Xu, X. (2015). RUNX2 RNA interference inhibits the invasion of osteosarcoma. *Oncol Lett, 9*(6), 2455-2458.

Zha, Y., Ding, E., Yang, L., Mao, L., Wang, X., McCarthy, B. A., Huang, S., & Ding, H. F. (2012). Functional dissection of HOXD cluster genes in regulation of neuroblastoma cell proliferation and differentiation. *PLoS One, 7*(8), e40728.

Zhai, Y., Kuick, R., Nan, B., Ota, I., Weiss, S. J., Trimble, C. L., Fearon, E. R., & Cho, K. R. (2007). Gene expression analysis of preinvasive and invasive cervical squamous cell carcinomas identifies HOXC10 as a key mediator of invasion. *Cancer Res, 67*(21), 10163-10172.

Zhang, H., & Bradley, A. (1996). Mice deficient for BMP2 are nonviable and have defects in amnion/chorion and cardiac development. *Development, 122*(10), 2977-2986.

Zhang, J., Tan, X., Li, W., Wang, Y., Wang, J., Cheng, X., & Yang, X. (2005). Smad4 is required for the normal organization of the cartilage growth plate. *Dev Biol, 284*(2), 311-322.

Zhang, X., Akech, J., Browne, G., Russell, S., Wixted, J. J., Stein, J. L., Stein, G. S., & Lian, J. B. (2015). Runx2-Smad signaling impacts the progression of tumor-induced bone disease. *Int J Cancer, 136*(6), 1321-1332.

Zhang, Y. W., Yasui, N., Ito, K., Huang, G., Fujii, M., Hanai, J., Nogami, H., Ochi, T., Miyazono, K., & Ito, Y. (2000). A RUNX2/PEBP2alpha A/CBFA1 mutation displaying impaired transactivation and Smad interaction in cleidocranial dysplasia. *Proc Natl Acad Sci U S A, 97*(19), 10549-10554.

Zhao, X., Sun, M., Zhao, J., Leyva, J. A., Zhu, H., Yang, W., Zeng, X., Ao, Y., Liu, Q., Liu, G., Lo, W. H., Jabs, E. W., Amzel, L. M., Shan, X., & Zhang, X. (2007). Mutations in HOXD13 underlie syndactyly type V and a novel brachydactyly-syndactyly syndrome. *Am J Hum Genet, 80*(2), 361-371.

Zhou, X., von der Mark, K., Henry, S., Norton, W., Adams, H., & de Crombrugghe, B. (2014). Chondrocytes Transdifferentiate into Osteoblasts in Endochondral Bone during Development, Postnatal Growth and Fracture Healing in Mice. *PLoS Genetics, 10*(12), e1004820.

Zohn, I. M., Campbell, S. L., Khosravi-Far, R., Rossman, K. L., & Der, C. J. (1998). Rho family proteins and Ras transformation: the RHOad less traveled gets congested. *Oncogene, 17*(11 Reviews), 1415-1438.

Zuscik, M. J., Hilton, M. J., Zhang, X., Chen, D., & O'Keefe, R. J. (2008). Regulation of chondrogenesis and chondrocyte differentiation by stress. *J Clin Invest, 118*(2), 429-438.

8 Publication

Parts of this doctoral thesis have already been published.

von Heyking K, Roth L, Ertl M, Schmidt O, Calzada-Wack J, Neff F, Lawlor ER, Burdach S, Richter GH. The posterior HOXD locus: Its contribution to phenotype and malignancy of Ewing sarcoma. *Oncotarget*. 2016.

9 Appendices

9.1 List of figures

9.2 List of tables

9.3 Amino acids and their codes

Table was adopted from Alberts *et al.* (2014, p. T: 1).

1-letter code	3-letter code	amino acid	codon
A	Ala	Alanine	GCA GCC GCG GCU
C	Cys	Cysteine	UGC UGU
D	Asp	Aspartic acid	GAC GAU
E	Glu	Glutamic acid	GAA GAG
F	Phe	Phenylalanine	UUC UUU
G	Gly	Glycine	GGA GGC GGG GGU
H	His	Histidine	CAC CAU
I	Ile	Isoleucine	AUA AUC AUU
K	Lys	Lysine	AAA AAG
L	Leu	Leucine	UUA UUG CUA CUC CUG CUU
M	Met	Methionine	AUG
N	Asn	Asparagine	AAC AAU
P	Pro	Proline	CCA CCC CCG CCU
Q	Gln	Glutamine	CAA CAG
R	Arg	Arginine	AGA AGG CGA CGC CGG CGU
S	Ser	Serine	AGC AGU UCA UCC UCG UCU
T	Thr	Threonine	ACA ACC ACG ACU
V	Val	Valine	GUA GUC GUG GUU
W	Trp	Tryptophan	UGG
Y	Tyr	Tyrosine	UAC UAU

10 Acknowledgements

An dieser Stelle möchte ich mich bei allen bedanken, die zum Gelingen dieser Doktorarbeit beigetragen haben.

Mein besonderer Dank gilt:
Herrn Prof. Dr. Stefan Burdach und Herrn PD Dr. Günther Richter für die Möglichkeit, meine Promotion am Forschungszentrum für krebskranke Kinder der TU München durchzuführen, für die Überlassung eines so interessanten und anspruchsvollen Themas sowie für das mir entgegengebrachte Vertrauen sowie für ihre Unterstützung und Begleitung der Arbeit, die größtenteils von der Else Kröner-Fresenius-Stiftung finanziert wurde.
Herrn Prof. Rummeny für die Übernahme des Prüfungsvorsitzes und für die Organisation des Prüfungsverfahrens.
Stephanie Plehm für die Vorarbeiten und die Einarbeitung.
Kristina von Heyking für die Einarbeitung, Unterstützung sowie die kritische und hilfreiche Durchsicht dieser Arbeit.
Laura Roth, die sich um das Mausmodell des Projekts gekümmert hat, weil es mir meine Tierliebe unmöglich machte.
Colette Berns für die Übernahme von einigen experimentellen Arbeiten und die mir auch bei manchem Dreisatz auf die Sprünge geholfen hat.
Franziska Blaeschke und Uwe Thiel, die immer einen Jägermeister für mich übrig hatten.

Und natürlich Cem, der mit mir um Mitternacht noch ins Labor marschiert ist, um die PCR-Maschine auszuschalten.
Nicht zuletzt meiner Familie, vor allem meiner Mutter und Winfried, die immer an mich geglaubt und mich unterstützt haben.